

Padova, 31 December 2015

Dear Editor,

please find enclosed the revised manuscript cp-2015-116 by Giusberti et al. entitled "Variability in climate and productivity during the Paleocene/Eocene Thermal Maximum in the western Tethys (Forada section)". We have really appreciated the comments from reviewers and we have strictly followed their suggestions. Most of the observations regarding text, figures and tables have been accepted and the text has been modified accordingly. All parts with changes in the text are highlighted in red color in the marked up manuscript version.

We appreciated the opportunity to improve the paper based on the reviewers' comments and look forward to hearing from the Editor about a final decision concerning the acceptance of this manuscript for publication.

The most relevant changes in the manuscript are listed below:

- The title has been changed (as requested by reviewers);
- Introduction. Introduction has been shortened, moving part of it in a new paragraph (par. 4.4) entitled "Clues from Forada on PETM climate change" at the end of the Discussion;
- Removal of par. 2.2.1. Paleocene-Eocene benthic foraminifera ecology. In place of 2.2.1, following reviewer 2 suggestion, we provided a new table (Table 1) summarizing the ecology of the most common taxa at Forada, only based on published literature. We also discussed some aspects of the ecology of taxa as *Osangularia*, *Eobigenerina* and *Karrerulina* in par. 4.3.2;
- Titles of several paragraph of Chapter 4 have been modified, according to reviewer's 2 request.
- The Fig. S.1 (Supplementary) is now Text Fig. 4. Figure 1 of the original manuscript became Fig. 10, as consequence of the moving of part of the Introduction to the new par. 4.4. at the end of Discussion;
- Conclusions have been modified into bullet points;
- Specific answers to main issues/comments of both reviewers (reported below) are now included in the text and are clearly recognizable in the marked up manuscript version.

I would be pleased to give you any further information that you might request.

Luca Giusberti on the behalf of the co-authors

Authors answers to referee #1 (R. Speijer)

MAIN ISSUES

4212, 13-15: point out to what extent these extraction methods may or may not interfere with foraminiferal preservation in these deposits, notably %F.

In pyrite-lean sediments the use of H₂O₂ solution may not significantly alter foram residues; however, it will corrode pyrite-filled shells. Experimental studies demonstrate that “H₂O₂ is an unsuitable chemical for extracting delicate CaCO₃ and pyritized microfossils because of the damage and dissolution it causes” (Kennedy & Coe 2014 - Journal of Micropalaeontology). This is in agreement with earlier as well as own experimental observations. Note that when all radiolarians are calcified this calcite must have come from a carbonate source, probably from within the rock unit and it is not unlikely that in a hemipelagic setting the most fragile foraminifera and/or nannos provided this calcite.

The authors are aware of the problems concerning the extraction methods of forams with pyrite-filled shells, but the tests in the Forada samples are not pyrite filled, and invariably filled by calcite. None of the examined samples yielded foraminifera preserved with pyrite infilling, or replaced by pyrite. Moreover, the samples with the lowest content of CaCO₃ (e.g., clays of basal Clay Marl Unit) were treated with diluted H₂O₂ (10%), in order to avoid possible additional breakage of tests. We will add a sentence in the paragraph ‘Material and Methods’, in which we will give details about the state of preservation of foraminifera at Forada. We do not fully respond to the comment on %F (fragmentation index) in this paper, because these data (and preparations) have been discussed in Luciani et al. (2007), and we just cite them here.

Part 2.2.1. It is not quite clear how the ecological overview is assembled. It seems as if the present data are already included in this overview, as “We allocated the taxa to the categories recolonizers (R1,R2) and opportunistics (O1, O2), based on their abundance pattern in the studied and other PETM sections”. Does this mean that the observed patterns of Forada are include to allocate the taxa to the various ecologic groups? If so, then this is not a correct procedure as it may lead to circular reasoning once the data are being interpreted. It would be helpful to add a table with included PETM localities from which these patterns are derived. (also note that ‘opportunist’ is the correct noun to the adjective ‘opportunistic’).

Having re-read the manuscript in light of comments by referee #1 and #2 on paragraph 2.2.1 (the benthic ecology overview), we appreciated their concern, and also agree with the reviewers that the paragraph is too long. We thus decided to eliminate the entire paragraph 2.2.1 and with it any reference to taxa ecology as inferred from the Forada record (e.g., the clustering into the categories R1, R2, O1, O2). Part of these aspects will be also discussed in the Discussion paragraph. In place of paragraph 2.2.1, following referee (1 and 2) suggestions, we will provide a new table (Table 1) summarizing the ecology of the most common taxa at Forada, based on published literature.

4216, 11: *Osangularia - I'd like to caution for ecologic interpretations at generic level, especially when the reference taxa are many millions years younger or older, such as the OAE2 data referred to*

here. Mid-Cretaceous benthic foram communities were quite different from those of the early Paleogene and ecologic affinities at generic level (in as far as these can be generalized at all) are likely to have been different. For instance modern *Lenticulina* is a deep water taxon and *Oridorsalis* a cold water taxon (Murray, 2006). Both were, however, common inhabitants of early Paleogene (sub)tropical shelves (numerous data from Egypt, Tunisia, Tanzania). Extrapolations from the Recent or Mid-Cretaceous to the Paleogene (as for microhabitats pointed out in 4218, 11-18) should be avoided, especially if there is no information included from the early Paleogene itself, like for *Osangularia*.

We never meant - and in fact did not - draw any ecological interpretation for the genus *Osangularia* by quoting those OAEs papers. We just reported them as information. We just use the general information on test shape (disc-shaped, biconvex, trochospiral, keeled), to infer that fossil and extant *Osangularia* most probably were epifaunal, preferring stable, oligotrophic, well oxygenated environments (e.g. Murray, 2006; Alegret et al., 2003; Alegret, 2007). For this reason, we found it of some interest to see peaks in abundance of small *Osangularia*, coinciding with the doubtlessly stressed environment of the basal CIE in the Forada section, and therefore note that peaks of *Osangularia* occur within Cretaceous OAEs. We also note that Boscolo Galazzo et al. (2013) found small-size *Osangularia* (Plate II fig. 13 in Boscolo Galazzo et al., 2013) within organic-rich levels immediately following the Middle Eocene Climatic Optimum in the Alano section. A peak in abundance of small *Osangularia* has been observed in the basal PETM at Contessa Section, as highlighted for the first time in the present manuscript, and representatives of the genus *Osangularia* (*Osangularia* spp.) behaved opportunistically in the PETM of the Tethyan Alamedilla section (Alegret et al., 2009). We thus, in fact, are making the same point as the reviewer – that one cannot always assume that environmental preferences of morpho-taxa were constant over time. We will explain this better in the text. A specific assignment of basal PETM osangulariids at Forada (and Contessa section) was not possible because of their very small size and sub-optimal state of preservation. We will add a sentence in the text to that effect.

4218, 11: the above point could be addressed here, as this problem does not only concern microhabitats, but ecologic traits in general.

The paragraph will be deleted and substituted with Table 1 (explained above). The specific case of *Osangularia* will be briefly discussed in the proper section of the paper (Discussion, paragraph 4.3.2.).

4219, 13: Results. I consider it a missed opportunity that the authors do not include a statistical evaluation on such a great data set. This would allow for an objective subdivision of the main patterns and by plotting the results (e.g. PCA, DCA) in cross plots this will almost certainly provide a graphic synthesis of the faunal evolution across the PETM. Now only frequency plots and a summary of highlights in a table are provided. These data deserve better than that.

We thank the reviewer for the suggestion, but we do not agree that a full statistical analysis would (in this case) actually add to the interpretation of the assemblages. Multivariate statistical analysis is highly suitable to document subtle patterns which are not clearly discerned in the raw data, especially when

many taxa are involved. In this case, however, an objective subdivision of the faunal assemblages is possible using the raw data at Forada, because of the rapid stratigraphic succession of biotic events, and abrupt and pronounced changes in species abundance.

4221, 9: *As an individual Zoophycos often spans several dm of sediment and bioturbates 1000s of years of sedimentation, it is worthwhile to add (from Giusberti et al. 2007?) to what extent these bioturbations may or may not have affected the foraminiferal sequence.*

All micropaleontological (benthic and planktic foraminifera and calcareous nannofossils) and geochemical evidence (mineralogy, stable isotopes, etc.) published on the Forada PETM concur in indicating that the foraminiferal sequence was virtually unaffected by significant disturbance (we found no evidence of "mixing" of different biotic and abiotic signals or "anomalous" signals). We stress that samples collected for micropaleontological and geochemical analysis of the PA I interval of Giusberti et al. (2007) and samples from the rest of the section were carefully collected avoiding, where possible, the portions of rock containing clear evidence of the above-mentioned ichnofossils, and other traces as *Planolites*, *Thalassinoides*, etc. In the specific case of the Pa I interval ("Assemblage B" of the present manuscript), the entire block of the uppermost portion of Paleocene (ca. 20 cm) was removed during sampling in the field, and sliced in the laboratory into subsamples of ca. 3 cm thick, checking carefully the integrity of the sediment, and lack of (bio)disturbance. We are well aware of the fact that hemipelagic Scaglia sediments in "normal conditions" are always bioturbated (e.g., mottling). To what extent bioturbation affected Scaglia sediments in general is beyond the scope of present paper, because a proper and reliable evaluation will be possible only through an extensive ichnological analysis. We underline that, based on the comment of the reviewer, almost the 100% of published sections should undergo a ichnological revision/approach in order to test the reliability of micropaleontological and geochemical datasets. We will insert a sentence (in par. 2.2) explaining that we, to the extent possible, excluded bioturbated materials, and have found no evidence for bioturbation-effects in data published on the Forada section.

4226, 19: "surface waters were oligotrophic" whereas 4227, 4 "indicates oligo-mesotrophic surface waters"

Previously published data on Forada calcareous plankton (Agnini et al., 2007, Luciani et al., 2007) indicate "oligotrophic" conditions in surface waters (see text and Figure 8) at Forada, whereas our data based on benthic forams suggest oligo-mesotrophic waters. It is explained in the text at 4.2.1. We removed from the text (pag. 4227, line 3) the misleading sentence "in agreement with data on calcareous plankton)".

4222, 12: *are these clays (probably shales; also in other places in the text), truly laminated, resulting from a lack of bioturbation (e.g., laminae with different composition, mostly caused by lack of oxygen) or are they just fissile (homogeneous composition) from reorientation of clay minerals through compaction as is a normal feature in shales? Some image support of the laminations (cf. Nicolo et al. 2010) could significantly strengthen the interpretation. Without this, skepticism will remain.*

Clays in the lowermost decimeters of the CMU are not shales (as described in detail in Giusberti et al., 2007). The only shales occurring in the entire Scaglia sequence of the region are the black shales of the upper Cenomanian OAE2 Bonarelli level. Clays of basal PETM at Forada present primary lamination, but they are not "fissile", in strict analogy to what Rodriguez-Tovar et al. (2011) described for the basal siliciclastic unit of PETM at Zumaia section (Spain). We interpreted such lamination as consequence of the lack of bioturbators in the strongly stressed conditions of basal PETM, conform Nicolo et al. (2010). Besides high temperatures, changes in food availability and dysoxia of interstitial water pores, as well as low-pH sea-floor conditions, may have played a significant role in excluding macrobenthic fauna in this early phase of PETM. Deep-sea organisms are highly sensitive to even modest but rapid pH changes (Seibold and Walsh, 2001; *Science*, 294, 319–320) that have been shown to be harmful even for infaunal deep-sea communities (Barry et al., 2004; *Journal of Oceanography*, 60, 759–766). Usually, the Paleogene Scaglia Rossa is mottled (greenish flames in reddish-brownish sediments), indicative of activity of macrobenthics in the sediments. In the investigated section, mottling completely disappears only within the basal-most, laminated greenish clays of CMU, and gradually reappears (as thin reddish "flames") at the Assemblage D-E transition. We will ensure that this description of sediment is clear in the revised version.

4228, 20: *It would perhaps be worthwhile here to add a section on extinction rate within this particular sequence. I have the impression that considering the inclusion of the fine size fraction here, leads to a (much?) lower extinction rate than the 40% or more that is usually mentioned.*

The proportion of Paleocene cosmopolitan "extinction" species expressed relative to the total of benthic foraminifera at Forada is quite low (ca. 10%), clearly related to the huge number of Bolivinacea dominating the fine size fraction used for this study (>63 μ m). Note that many extinction taxa are epifaunal morphotypes, commonly larger than 125 μ m, as also noted elsewhere. Similarly low percentages (12-15%) of cosmopolitan extinction taxa have been recorded in Scaglia sediments of the Contessa section (Giusberti et al., 2009) and at ODP Site 690 by Thomas (2003), where infaunal morphotypes (buliminids and uniserial calcareous taxa) are abundant/dominant in the >63 μ m fraction. We will add a sentence in the text to clarify this, and we will move Fig. S1 from Supplementary material to the text.

4228, 22-25: *note that a very similar dead zone is observed at Dababiya (Ernst et al. 2006), but relating this to a rise of the CCD and lysocline up into the continental shelves of the Tethys seems quite unlikely. So the question that comes up is, up to what shallow depths could a rise of the CCD still account for the effects observed? Is that indeed up to 1000-1500 m or perhaps even shallower?*

With this paper the paleobathymetry of the Forada section is refined, and our dataset points out a fully bathyal paleodepth. We thus argue that the CCD was raised up to 1000-1500 m in the Tethys (see also tables in Thomas, 1998); we cannot say anything about Tethyan shelves. This interpretation is consistent to what has been observed at Tethyan sites with similar paleodepths (Egger et al., 2005; 2009; Alegret et al., 2009; Giusberti et al., 2009), and with the 2 km CCD raise estimated in the south

Atlantic (Zachos et al., 2005). As far as the black clay is concerned, the problem of its interpretation has been stressed in the text, as also previously in Giusberti et al., (2007). In much shallower, coastal/mid shelfal sites, carbonate may be not preserved due to local eutrophic conditions with oxidation of organic matter leading to waters corrosive to carbonate (similar to circumstances in present-day eutrophied shelves/estuaries), which may well have been the case in the Egyptian sections, but that is not relevant to this manuscript.

Minor issues:

This paper is about much more than the benthic foram record as it integrates data from earlier studies on Forada. In order to maximize readership the title could be improved accordingly, e.g. by adding a term like 'integrated' or alike.

We thank the reviewer for the suggestion and will follow his advice modifying the title of the paper.

The introduction is quite long and detailed. Some parts can certainly be preserved for the discussion instead of elaborating them in the introduction.

We agree in part with the reviewer and will try to modify the introduction accordingly, but we do not agree that all the introductory text should be included in the discussion, because it is introductory in nature and interferes with the line of discussion in the discussion section. We moved part of introduction to a new paragraph (par. 4.4) entitled "Clues from Forada on PETM climate change" at the end of the Discussion.

4208, 18: *First records of anoxia related to the PETM along the Tethyan continental margins: Gavrilov et al. 1997 – Lithology and Mineral Resources; Speijer et al. 1997 – Geology).*

Ok. We will add these references and Benjamini (1992).

4215, 22: *Note that G. subglobosa is a common to abundant component (up to 20%) in Paleocene neritic deposits at Dababiya (and Aweina,...), Egypt. It returns within PETM DQB 3 (10-15%), together with various buliminids and Tappanina selmensis (Ernst et al. 2006), under improving, but probably fluctuating seafloor oxygenation. In this shelf setting (as elsewhere in Egypt) G. subglobosa is not part of the first colonizers though (due to severe anoxia persisting after a (nearly) 'dead zone'.*

Ok. We will add such reference in the Table 1 summarizing the ecology of benthic foraminiferal taxa. It is well possible that *G. subglobosa*, like *T. selmensis*, originated at shallower depths and migrated into the deep sea after the BFEE, because the taxon is at most deep-water sites absent in the Paleocene, or present only rarely in the very latest Paleocene (Thomas & Shackleton, 1996).

4226, 3: *indicate at what depth ranges the modern OMZ is observed. Under high productivity zones with a similar export production in warmer oceans the OMZ is likely to have been more expanded.*

Ok, but this varies very strongly by oceans.

4227, 5: add references for “seasonal to periodical increases in primary productivity” leading to “high faunal diversity” at middle bathyal depths.

Ok, we will add as references: Fontanier et al. (2006a) Seasonal variability of benthic foraminiferal faunas at 1000 m depth in the bay of Biscay. *Journal of Foraminiferal Research*, 36, 1, 61–76; Fontanier et al. (2006b) Stable oxygen and carbon isotopes of live benthic foraminifera from the Bay of Biscay: Microhabitat impact and seasonal variability. *Marine Micropaleontology* 58, 159– 183; Fontanier et al. (2014) Living (stained) deep-sea foraminifera off Hachinohe (NE JAPAN, Western Pacific): environmental interplay in oxygen-depleted ecosystems. *Journal of Foraminiferal Research*, 44, 3, p. 281–299. We will add also Gooday (2003).

4232, 20-22: is this similar to modern dust supply from the Sahara to the Atlantic? This proposal needs some referencing.

Ok. Relevant citations are reported in line 4232 7-9. We will report them also where indicated by the reviewer.

4234, 15: indicate that 800 ky after the end of CMU deposition is well beyond the top of the studied interval. This also reminds of the extended (650 kyr) humid period, starting at the onset of the PETM, observed at Site 401 (Bornemann et al., 2014).

Ok. We will add in the text a sentence including the suggested reference.

Fig. 8: meaning of texts not quite clear: e.g. what is meant by “Coccolithus-Toweius dominated assemblage. No Coccolithus-No Toweius assemblage dominated by Zygr., Sphen. and Octol.”? Similar in other boxes.

We will modify both text and figures as follows: Assemblage dominated by *Coccolithus* and *Toweius*. After the removal of *Coccolithus* and *Toweius*, the assemblage is dominated by *Zygrablithus*, *Sphenolithus* and *Octolithus*.

Table S1: note that Schulte et al. 2011 (Chem. Geol.) provided additional data and an update on fluvial discharge during the PETM at Dababiya, relative to the paper by Ernst et al. 2006.

The reference of Schulte et al. 2011 will be added in Table S1 (now Table S3).

Technical issues:

4208, 10: too much ‘profound’ (rather bombastic).

Ok. We will remove "profound" from line 10. We will also substitute at lines 6-7 "profound shallowing of the calcite compensation depth" with "severe shallowing of the calcite compensation depth" (already adopted in Giusberti et al., 2007).

4208, 20: spelling 'Pälike'

Ok

4209, 14: spelling 'Collinson'

Ok

4213, 13 and elsewhere: please use infaunal/epifaunal terminology consistently. Here and there the terms 'morphotype/morphogroup/morphology' are used. As for most taxa the preferred microhabitat is unknown, one of these terms should always be added to infaunal/epifaunal. Also note that 'epibenthic' and 'endobenthic' have been proposed as preferable terms to denote 'epifaunal' and 'infaunal' microhabitats (Walker & Miller 1992 - Palaios). One last terminological nitpicking: I'm not sure whether the term 'agglutinant' as noun or adjective is appropriate in English (as it is in Dutch). Native English speaking workers generally use 'agglutinated' or 'arenaceous' (taxa).

Ok. We will make the terminology uniform as suggested. As far as epifaunal versus epibenthic etc., we are aware of the Walker & Miller 1992, but we prefer the still widely used infaunal and epifaunal terms, and prefer the more extensive discussion of this topic in Jorissen et al., 1995, 2007. We will substitute, as requested, agglutinant with agglutinated.

4215, 21: spelling 'Giusberti'

Ok

4231,27: spelling of 'sibaiyaensis'. Also note that a very similar *Acarinina* acme (80-90%) is observed in most PETM sections in Egypt, where it was also linked to enhanced nutrient availability (Guasti & Speijer 2007, GSA SP424), in contrast to the – then - widely held (open ocean) view that the acme resulted from oligotrophy.

Ok, we will correct the specific name. The significance of *Acarinina* acme at Forada has been previously stressed (comparing the African record and citing Guasti, 2005 and Ernst et al., 2006) in the paper of Luciani et al. 2007. We will add the suggested reference in our text. Note, however, that *Acarinina* acmes occur widely in open ocean (e.g., Site 690; various papers by Kelly et al.), and have been also linked to carbonate over-saturation.

4234, 27: add 'atmospheric' (CO2)

Ok

Fig. 1: The Svalbard Archipelago includes the main island Spitsbergen. Iceland probably slipped into the text erroneously as it did not yet exist back then.

Ok

Fig. 3: CF has no unit and it's not clear what is meant here. Here and there in the text reference is made to wght%. Specify this at least clearly in the caption. Reference only to Hancock & Dickens (2005) is insufficient.

Ok. We will specify in the caption: "The weight percent of the >63 μm size fraction relative to the weight of the bulk sample (coarse fraction, CF) was calculated for the Forada samples following Hancock and Dickens (2005)".

Fig. 4: Please clearly specify that N/g for the radiolarians refers to the amount of radiolarians relative to the weight of the washed residue >125 micron (N/g often refers to the number of microfossils relative to the weight of the dry sediment).

Thank you very much for this remark. We realized that there was a mistake in the original plot (X axis) of the original figure (Fig. 10) from Giusberti et al. (2007). We will modify the figure and we will add the sentence suggested. We will use "number" of radiolarians (instead of "amount of radiolarians"), the word 'amount' is incorrect use of English.

Fig. 5: "Bulimina spp." should not include other genera. Buliminids? Buliminacea? At any rate specify usage of the grouping chosen.

We will substitute "Bulimina" with "other buliminids", explaining in the caption what is included.

References: In a separate upload various errors (probably not exhaustive) are highlighted in yellow in the reference list: misspellings, non-abbreviated journals, missing initials, Palaeo3 being consistently indicated as Palaeo2. Doi numbers are given for a minor part of Elsevier and Science papers I'd personally plea for consistency in the usage (all or nothing).

Ok. We will remove all the doi throughout the references and we will correct the errors/mistakes (see also answer to reviewer #2).

Authors answers to referee #2 (N. Mancin)

MAIN ISSUES/SPECIFIC COMMENTS

1) Title: it is not fully indicative of the work here presented because the Authors combine new high resolution benthic foraminiferal results with published calcareous plankton, mineralogical and biomarker data to document climatic and environmental changes across the PETM. I suggest to change the title accordingly.

We thank both reviewers for the suggestion and we will follow their advice modifying the title.

2) Introduction. This paragraph is very long and too condensed. I suggest to reduce it. Some parts could be preserved for the discussion sections (e.g. from 4208-line 26 to 4209-line 26).

We agree with the reviewer and will try to modify the introduction accordingly, but see note above about including too much material in the discussion.

3) Materials and methods. - Subparagraph 2.2.1: I fully agree with Speijer's comment about how the ecological overview has been assembled. Please give more details of your explanation. Moreover, this subparagraph is too long and descriptive making it dull reading. I suggest to synthesize the benthic foraminiferal ecology into two tables deleting the descriptive parts. Some suggestions: the first table could report the main ecological preferences and microhabitats of the most common taxa recorded in the studied section; for each benthic taxon the table could include a first column with the known paleo-depth range, a second column with the mode of life (deep or shallow infauna and epifauna), a third column with the food supply (quantity, quality and periodicity), a fourth column with the oxygenation, a fifth column with the type of substrate and eventually a sixth column with other remarks. The second table could report the grouping taxa (R1, R2, O1, O2) and their occurrence in coeval records from the studied Forada section to other land sections or oceanic sites. Both tables should include a last column with the most relevant reference papers used to infer the ecological preferences. The descriptive parts (only when strictly necessary to the discussions) could be available as supplementary material.

Having re-read the manuscript in light of the comments by referee #1 and #2 on paragraph 2.2.1 (the benthic ecology overview), we appreciate their concern. We also agree with the reviewers that the paragraph is too long. We thus propose to eliminate the entire paragraph 2.2.1, and with it any reference to taxa ecology as inferred from the Forada's record (e.g., the clustering into the categories R1, R2, O1, O2). We propose to discuss part of these aspects in the Discussion paragraph. In place of paragraph 2.2.1, following the referees' suggestion, we will provide a table summarizing the ecology of the most common taxa at Forada based on published literature.

4) Conclusions: this paragraph could be significantly streamlined omitting a few generic statements and organising it into point bullets reporting only the main concluding remarks.

We will modify this part into bullet points.

5) *References: the references list is consistent and updated, but some references cited in the text are missing or incorrectly reported in the reference list (e.g. different year of publication), conversely some references reported in the reference list are absent in the text. Please see below in the “Technical corrections” for further details. Moreover, some references in the reference list do not follow the guide of the CPD (non-abbreviated journals, missing Author’ initials, misspellings). The reference list should be carefully checked, completed and corrected accordingly.*

Ok. Please note that in some cases the journals are not abbreviated because they do not occur in the ISI Journal Title Abbreviations Index. In any case, we will carefully check the entire reference list.

Technical corrections

- 4206-line 14 and elsewhere: *The term “agglutinant” is not fully appropriated, maybe “agglutinated or arenaceous”. Please correct throughout the MS accordingly.*

Ok, we agree. We will substitute agglutinant with agglutinated.

- 4207-line13: “*Roehl*” please replace with “*Röhl*”.

Ok

- 4207-line 23: “*Dickens et al. 1995*” in the ref. list is reported as “*Dickens et al. 1997*”, please correct/uniform.

Ok

- 4208-line 7: “*Zachos et al. 2005*” in the ref. list is indicated as “*Zachos et al. 2015*”, please correct/uniform or add.

Ok

- 4208-line 10: “*The profound paleoceanographic:*” new item.

See response to reviewer 1 for the same comment.

- 4208-line 16: *Boscolo-Galazzo et al. 2014* is missing from the ref. list.

Ok

- 4208-line 20 ”*Paelike*” please replace with “*Pälkile*”.

Ok

- 4209-line 7: “*Krauss*” in the ref. list is cited as “*Kraus*”, please uniform.

Ok

- 4209-line 29 “*Sluijs et al. 2007*”, is it 2007a or 2007b?

Ok. It is *Sluijs et al. 2007a*.

- 4212- line 22: “*Foster et al. 2013*” is missing in the ref. list. Please add it.

Ok

- 4213-line 20: “*Hayward et al. 2012*” is missing in the ref. list. Please add the ref.

Ok

- 4214-line 2: “: based on their abundance pattern in the studied and other PETM sections” please add some reference paper to support this sentence.

Ok. As stated above, the subparagraph 2.2.1 will be removed and the information presented in a Table.

- 4215-line 21: “*Alegret et al. 2011*” is reported in the ref. list as “*Alegret et al. 2010*”. Please correct or add the missing ref.

Ok. The correct citation is *Alegret et al. (2010)*.

- 4216-line 1: “*Ishman & Domack 1994*” is missing in the ref. list. Please add the ref.

Ok

- 4216-line 29: “*Steineck & Thomas, 1996*” is missing in the ref. list. Please add it.

Ok

- 4218-line10: “*Mancin et al. 2014*” please replace with “*Mancin et al. 2013*”.

Ok.

- 4218-lines 11 to 18: “Caution is needed:” I would move this sentence at the beginning of the subparagraph dealing with the foraminiferal ecology.

We will move it at the end of the previous paragraph as our intention would be that of eliminate paragraph 2.2.1

- 4218-line29: “Roehl” please replace with “Röhl”

Ok.

- 4220-line 11 and elsewhere: *The AA use the terms “morphotypes, morphogroups and morphologies”. Please uniform throughout the MS.*

Ok.

- 4221-line5: “opportunists” please replace with “opportunistic taxa”.

Ok.

- 4225-line1: *I suggest to change in “Discussion” removing “environmental reconstruction” because redundant.*

Ok, we agree.

- 4225-line13: *Please change in “Alegret et al. 2009a”.*

Ok.

- 4225-line 20: *I suggest to change the subtitle in “Environmental reconstruction during the late Paleocene”.*

We agree.

- 4225-line 21: *Please change in “The Belluno Basin deep-sea environment (Assemblage A)”*

We will change it as suggested.

- 4226-line6: “Jorissen et al., 1995” is missing in the ref. list. Please add it.

Ok.

- 4226-line 11: “Fontanier et al 2005” is reported in the ref. list as “Fontanier et al. 2008”. Please correct or add the missing reference.

Ok. The correct citation in the ref. list is Fontanier et al., 2005.

- 4227-line 4: previously you said the surface waters were “oligotrophic” and now “oligo-mesotrophic”. What is the correct one?

See answer to reviewer 1.

- 4227-line 9: Please change in “The precursor climate change (Assemblage B)”.

Ok.

- 4228-line 20: I suggest to change in “Climate and marine life during the PETM”.

Ok.

- 4229-line 2: Both the references “Higgs et al, 1994 and van Santvoort et al. 1996” are missing in the ref. list. Please add these references.

Ok

- 4229-line 11: I suggest to change in “The early peak PETM (Assemblages C and D).

Ok

- 4229-lines 16 and 19: “Zachos et al. 2005” in the ref. list is indicated as “Zachos et al. 2015”. Please correct/uniform or add.

Ok

- 4231-line 16: I suggest to change in “The core of the CIE and Recovery (assemblages E and F)”.

Ok

- 4235-line 15 “de-oxygenation” this term is not proper. Please replace with “scarce oxygenation” or “sub-oxic conditions”.

We disagree – the term deoxygenation is used widely in the literature of recent oceanic environments – see e.g., <http://www.oceanscientists.org/index.php/topics/ocean-deoxygenation>.

- 4237 to 4258 References. The following references are reported in the ref. list but they are missing in the text: Fenero et al, 2012 Hess & Jorissen, 2009 John et al., 2012 Jones & Manning, 1994 Ortiz et al., 2011 Pearson & Thomas, 2015 Sluijs et al., 2009 Sluijs et al., 2008 Smith et al., 2007 Thomas et al., 1999 Winguth et al., 2010 Zeebe et al., 2009.

We will provide appropriate corrections removing references missing in the text.

- 4262 *caption of Figure 3. Is F-index from Luciani et al 2010 or 2007 as previously said in the text? Please uniform.*

Ok. The correct citation is Luciani et al., 2007.

- 4263 *caption of Figure 4. Is F-index from Luciani et al 2010 or 2007 as previously said in the text? Please uniform.*

Ok. The correct citation is Luciani et al., 2007.

- 4264 *Caption of Figure 5. Bulimina spp. should group only different species of the genus Bulimina and not other similar genera as Buliminella etc. Please replace Bulimina spp. with “buliminids”.*

Ok. See answer to reviewer 1.

1 **Variability in climate and productivity during the**
2 **Paleocene/Eocene Thermal Maximum in the western Tethys**
3 **(Forada section)**

5 **L. Giusberti¹, F. Boscolo Galazzo¹, and E. Thomas^{2,3}**

7 [1] Department of Geosciences, University of Padova, Via Gradenigo 6, 35131 Padova, Italy;
8 [2] Department of Geology and Geophysics, Yale University, 210 Whitney Avenue, New Haven CT
9 06511, USA
10 [3] Department of Earth and Environmental Sciences, Earth and Environmental Sciences, Wesleyan
11 University, 265 Church Street, Middletown, CT 06459, USA

13 Correspondence to: L. Giusberti (luca.giusberti@unipd.it)

15 **Abstract**

17 The Forada section (northeastern Italy) provides a continuous, expanded deep-sea record of the
18 Paleocene/Eocene thermal maximum (PETM) in the central-western Tethys. We combine a new, high
19 resolution, benthic foraminiferal assemblage record with published calcareous plankton, mineralogical
20 and biomarker data to document climatic and environmental changes across the PETM, highlighting
21 the benthic foraminiferal extinction event (BEE). The onset of the PETM, occurring ~30 kyr after a
22 precursor event, is marked by a thin, black, barren clay layer, possibly representing a brief pulse of
23 anoxia and carbonate dissolution. The BEE occurred within the 10 cm interval including this layer.
24 During the first 3.5 kyr of the PETM, several agglutinated recolonizing taxa show rapid species
25 turnover, indicating a highly unstable, CaCO_3 -corrosive environment. Calcareous taxa reappeared after
26 this interval, and the next ~ 9 kyr were characterized by rapid alternation of peaks in abundance of
27 various calcareous and **agglutinated** recolonizers. These observations suggest that synergistic stressors,
28 including deep water CaCO_3 -corrosiveness, low oxygenation, and high environmental instability
29 caused the extinction. Combined faunal and biomarker data (BIT index, higher plant *n*-alkane average
30 chain length) and the high abundance of the mineral chlorite suggest that erosion and weathering

increased strongly at the onset of the PETM, due to an overall wet climate with invigorated hydrological cycle, which led to storm flood-events carrying massive sediment discharge into the Belluno Basin. This interval was followed by the core of the PETM, characterized by four precessionally paced cycles in $\text{CaCO}_3\%$, hematite%, $\delta^{13}\text{C}$, abundant occurrence of opportunistic benthic foraminiferal taxa, as well as calcareous nannofossil and planktonic foraminiferal taxa typical of high productivity environments, radiolarians, and lower $\delta\text{D}_{n\text{-alkanes}}$. We interpret these cycles as reflecting alternation between an overall arid climate, characterized by strong winds and intense upwelling, **and** an overall humid climate, with abundant rains and high sediment delivery (including refractory organic carbon) from land. Precessionally paced marl-limestone couplets occur throughout the recovery interval of the CIE and up to ten meters above it, suggesting that these wet-dry cycles persisted, though at declining intensity, after the peak PETM. Enhanced climate extremes at mid-latitudes might have been a direct response to the massive CO_2 input in the ocean atmosphere system at the Paleocene-Eocene transition, and may have had a primary role in restoring the Earth system to steady state.

45

46 1 Introduction

47 The Paleocene-Eocene Thermal Maximum (PETM) has over the last twenty four years attracted
48 intensive study by the scientific community, as one of the most dramatic and rapid climatic disruptions
49 of the Cenozoic (e.g., Kennett and Stott, 1991; Zachos et al., 2001; Sluijs et al., 2007a; McInerney and
50 Wing, 2011; Littler et al., 2014). During the PETM (~55.6 Ma), the Earth's surface temperature
51 increased by $\sim 5^\circ\text{C}$ in a few thousand years (McInerney and Wing, 2011; Dunkley-Jones et al., 2013;
52 Zeebe et al., 2014; Bowen et al., 2015), and remained high for 100 to 170-200 kyr (e.g., **Röhl** et al.,
53 2007; Giusberti et al., 2007; Murphy et al., 2010). The PETM is recognized in terrestrial and marine
54 settings by a negative carbon isotope excursion (CIE; e.g., Kennett and Stott, 1991; Bowen et al.,
55 2004), with variable magnitude ranging from $\sim 2\text{--}4.5\text{\textperthousand}$ in marine carbonates (e.g., Thomas and
56 Shackleton, 1996; Bains et al., 1999; Thomas et al., 2002; Zachos et al., 2006; Handley et al., 2008;
57 McCarren et al., 2008) to $4\text{--}7\text{\textperthousand}$ in marine and terrestrial organic carbon and leaf waxes (e.g., Kaiho et
58 al., 1996; Bowen et al., 2004, 2015; Pagani et al., 2006a; Smith et al., 2007; Handley et al., 2008;
59 McCarren et al., 2008). This CIE is attributed to a massive, rapid input of isotopically light carbon into
60 the ocean-atmosphere system, which destabilized the global carbon cycle and led to rapid and extreme

61 global warming (e.g., Dickens et al., 1997; Thomas and Shackleton, 1996; Pagani et al., 2006b;
62 Panchuk et al., 2008; Dickens, 2011; DeConto et al., 2012). Both the source(s) of the carbon and the
63 triggering mechanism(s) of the emissions are still strongly debated (e.g., Meissner et al., 2014), in part
64 because the pattern and size of the CIE does not necessarily simply reflect the size and isotopic
65 signature of the carbon input, but is affected by **biotic and** sedimentary processes (e.g., Kirtland Turner
66 and Ridgwell, 2013). Despite these debates, the onset of the CIE is an outstanding global correlation
67 tool (McInerney and Wing, 2011; Stassen et al., 2012b), formally used to define the base of the Eocene
68 (Aubry et al., 2007).

69 The carbon cycle perturbation of the PETM led to acidification of surface ocean waters (Penman
70 et al., 2014) and **severe** shallowing of the calcite compensation depth (CCD; Zachos et al., 2005; Kelly
71 et al., 2010; Hönisch et al., 2012). Widespread carbonate dissolution coincided with the base of the CIE
72 (e.g., Thomas and Shackleton, 1996; Thomas, 1998; Hancock and Dickens, 2005; McCarren et al.,
73 2008). The **profound** paleoceanographic changes affected primary and export productivity (e.g.,
74 Thomas, 2007; Winguth et al., 2012; Ma et al., 2014), which in general increased in marginal basins
75 and along continental margins, but decreased in open oceans (e.g., Gibbs et al., 2006; Stoll et al., 2007;
76 Speijer et al., 2012). The higher ocean temperatures may have led to increased remineralization of
77 organic matter in the oceans due to increased metabolic rates (John et al., 2013, 2014; Boscolo Galazzo
78 et al., 2014; **Ma et al., 2014**). The combination of increased remineralization, higher temperatures and
79 increased ocean stratification led to a decrease of oxygen levels in bottom waters regionally, especially
80 along continental margins (including the Arctic Ocean) and in the Atlantic Ocean (e.g., **Benjamini,**
81 **1992; Speijer et al., 1992; Gavrilov et al., 1997**; Thomas, 2007; Chun et al., 2010; Speijer et al., 2012;
82 Winguth et al., 2012; **Nagy et al., 2013**; Wieczorek et al., 2013; Dickson et al., 2014; **Pälike** et al.,
83 2014; Post et al., 2016), while Oxygen Minimum Zones in open oceans expanded globally (Zhou et al.,
84 2014), including at Forada (Luciani et al., 2007).

85 The increased primary productivity in marginal basins has been linked to increased influx of nutrients
86 from the continents, caused by increased erosion and weathering due to intensification of the
87 hydrological cycle, because precipitation is correlated to globally-averaged surface temperatures (e.g.,
88 Pierrehumbert, 2002). A widespread increase in kaolinite in PETM sediments has been related to the
89 global increase in precipitation and intensity of chemical weathering (e.g., Robert and Chamley, 1991;
90 Robert and Kennett, 1994; Kaiho et al., 1996; Gibson et al., 2000), as also suggested by Os-isotope
91 evidence (Ravizza et al., 2001; Wieczorek et al., 2013). However, reconstruction of hydrological

92 changes from clay mineral assemblages is complex, and additional evidence is needed (Thiry, 2000;
93 Schmitz and Pujalte 2003; 2007; Egger et al., 2003; 2005; Handley et al., 2012).

94 The severe climatic perturbations of the PETM profoundly affected terrestrial and marine
95 ecosystems, triggering faunal and floral radiations and migrations (e.g., Kelly et al., 1996; Bralower,
96 2002; Gingerich, 2003; Wing et al., 2005; [Sluijs et al., 2007a](#); Jaramillo et al., 2010; McInerney and
97 Wing, 2011). Deep-sea benthic foraminifera experienced the most severe extinction of the Cenozoic,
98 the benthic foraminiferal extinction event (BEE) (Thomas, 1989, 1990, 1998; Kennett and Stott, 1991;
99 Thomas and Shackleton, 1996; Alegret et al., 2009a, b; 2010). The BEE was rapid (<10 kyr; Thomas,
100 1989, 2003, 2007), and wiped out the Cretaceous bathyal and abyssal “Velasco-type fauna” (Berggren
101 and Aubert, 1975; Tjalsma and Lohmann, 1983; Thomas, 1998, 2007), marking a significant step
102 towards the establishment of modern benthic foraminiferal fauna (Thomas, 2007). The extinction was
103 far less severe in shelf environments (Gibson et al., 1993; Speijer, 2012; Stassen et al., 2015).

104 The cause of this global extinction remains under debate, because neither anoxia nor higher or
105 lower productivity, nor carbonate dissolution occurred globally at bathyal to abyssal depths in the deep
106 sea, the largest habitat on Earth (e.g., Thomas, 2003, 2007; Alegret et al., 2010), and benthic
107 foraminifera are highly efficient dispersers (Alve and Goldstein, 2003). The link between the
108 environmental changes during the PETM and the benthic foraminiferal extinction event thus remains
109 poorly understood. A common obstacle to perform detailed high-resolution studies of the PETM in
110 deep-sea sediments is the fact that many records are condensed or discontinuous, especially across the
111 few thousand years (Zeebe et al., 2014) of the onset of the carbon isotope excursion. The Forada
112 section (northeastern Italy) represents an outstanding exception in that it contains an expanded deep-sea
113 record of the PETM, which has been extensively studied because of its continuity and cyclostratigraphy
114 (Agnini et al., 2007; Giusberti et al., 2007; Luciani et al., 2007; Tipple et al., 2011; Dallanave et al.,
115 2012). Carbonate dissolution is less severe at Forada than in many other sections, with calcareous
116 benthic foraminifera present for most of the interval characterized by the CIE (> 4 m; Giusberti et al.,
117 2007). Given the limited number globally of complete and expanded deep-sea PETM sections, the
118 Forada section represents an invaluable opportunity to investigate the environmental impacts of the
119 PETM and repercussions on deep-sea fauna.

120 We provide a high-resolution benthic foraminiferal record for the Forada section, in order to
121 reconstruct the progression (tempo and mode) of environmental and biotic changes during the PETM.
122 These data allow us to reconstruct the environmental disruption and the benthic foraminiferal response

123 to PETM warming in detail, and document the community recovery. Benthic foraminiferal data are
124 integrated with sedimentological and geochemical data (Giusberti et al., 2007; Tipple et al., 2011), and
125 data on calcareous plankton communities (Agnini et al., 2007; Luciani et al., 2007), providing perhaps
126 the most complete reconstruction across the PETM in Europe to date.

127 We pay homage to research by Italian researchers (Di Napoli Alliata et al., 1970; Braga et al.,
128 1975), who first described the benthic foraminiferal turnover across the Paleocene-Eocene transition in
129 Italy.

130

131 2 Materials and methods

132 2.1 The Forada section

133 The Forada section (46.036083°N, 12.063975°E) is exposed along the Forada creek, ~ 2 km east of
134 the village of Lentiai (Fig. 1) in the Venetian Pre-Alps (NE Italy). It consists of ca. 62 m of Scaglia
135 Rossa, pink-reddish limestones and marly limestones, locally rhythmically bedded, and encompassing
136 the Upper Cretaceous through the lower Eocene (Fornaciari et al., 2007; Giusberti et al., 2007). The
137 upper Paleocene–lower Eocene succession is interrupted by the clay marl unit (CMU; Giusberti et al.,
138 2007), which marks the PETM and correlates with clay-rich units on other continental margins (e.g.,
139 Schmitz et al., 2001; Crouch et al., 2003; John et al., 2008; Nicolo et al., 2010). The investigated
140 interval has been subdivided into four sub-intervals based on the $\delta^{13}\text{C}$ record in bulk rock (Giusberti et
141 al., 2007). From bottom to top, these are the pre-CIE, the main CIE, the CIE recovery and post-CIE
142 (Fig. 2). The main CIE (Giusberti et al., 2007; Figs. 2, 3) occurs in the >3 m-thick CMU, within which
143 are recorded the short-lived occurrences of the calcareous plankton “excursion taxa” (Kelly et al., 1996,
144 1998) and the BEE (Agnini et al., 2007; Giusberti et al., 2007; Luciani et al., 2007). Sedimentation
145 rates in the CMU were five times higher than in the upper Paleocene, indicating increased continental
146 weathering and run-off, which led to increased sediment influx in the Belluno Basin (Giusberti et al.,
147 2007).

148

149 2.2 Benthic foraminifera

150 Benthic foraminiferal assemblages were studied in 54 samples from the same set studied by
151 Luciani et al. (2007) across an ~11 meter-thick interval straddling the PETM (-467 to +591.5 cm; Fig.

152 2), which reflects \sim 800 kyr (Giusberti et al., 2007). In this study the planktic foraminifera
153 fragmentation index (F Index) of Luciani et al. (2007) is used as a proxy for dissolution (Figs. 2, 3)
154 (Hancock and Dickens, 2005). The sample spacing for benthic foraminiferal assemblage analysis was
155 determined based on biostratigraphic and cyclostratigraphic data (Agnini et al., 2007; Giusberti et al.,
156 2007; Luciani et al., 2007). A sampling interval of 3–5 cm was used across the onset of the CIE (-42.5
157 to + 50 cm interval), a 25 cm sample interval over the main CIE (from +75 to 335 cm). Below -42.5 cm
158 and above 335 cm we adopted a spacing between 20 and 50 cm. Samples were collected excluding, to
159 the extent possible, bioturbated material. Further selection and removal of bioturbated material was
160 carried out in the laboratory before sample processing. Data previously collected from the Forada
161 section indicate that significant bioturbation effects are not present (e.g., Agnini et al., 2007; Giusberti
162 et al., 2007; Luciani et al., 2007).

163 Foraminifera were extracted from the indurated marls and limestones using the “cold acetolyse”
164 technique of Lirer (2000), following Luciani et al. (2007). Soft marly and clayey samples (mostly from
165 the CMU interval) were disaggregated using a 10–30% solution of hydrogen peroxide. The samples
166 with the lowest content of CaCO_3 (e.g., clays of basal CMU) were treated with diluted hydrogen
167 peroxide (10%), in order to prevent possible additional breakage of tests (especially of planktic
168 foraminifera). For more details on the comparison between the two methods of preparation (cold
169 acetolyse versus hydrogen peroxide), we refer to Luciani et al. (2007).

170 The quantitative study of benthic foraminifera was based on representative splits (using a micro-
171 splitter Jones, Geneq Inc.) of approximately 200–400 individuals $>63 \mu\text{m}$ and $<500 \mu\text{m}$ (Table S1). The
172 use of the small-size fraction is time-consuming and presents difficulties in taxonomic determination,
173 but we preferred to avoid the loss of small taxa, which are important for paleoecological investigations
174 (e.g., Thomas 1985; Boscolo Galazzo et al., 2013; 2015), especially directly after the BEE when small
175 species are dominant (Thomas, 1998; Foster et al., 2013). Between 0 and -222 cm (uppermost
176 Paleocene), the fraction $\geq 125 \mu\text{m}$ of at least 1/4 of the residue was carefully scanned for large
177 specimens of the extinction taxa, here labeled “Cosmopolitan Extinction Taxa” (CET) (see Thomas,
178 1998, 2003). These CET records have been treated qualitatively (Fig. 4). The extinction taxa include:
179 *Anomalinoides rubiginosus*, *Angulogavelinella avnimelechi*, *Aragonia velascoensis*, *Bolivinoides*
180 *delicatulus*, *Cibicidoides dayi*, *C. hyphalus*, *C. velascoensis*, *Clavulina amorpha*, *Clavulinoides*
181 *trilatera*, *Clavulinoides globulifera*, *Coryphostoma midwayensis*, *Dorothia beloides*, *D. bulletta*, *D.*
182 *pupa*, *D. retusa*, *Neoeponides megastoma*, *Gavelinella beccariiformis*, *Gyroidinoides globosus*, *G.*

183 *quadratus*, *Marsonella indentata*, *Neoflabellina jarvisi*, *N. semireticulata*, *Nuttallinella florealis*,
184 *Osangularia velascoensis*, *Paralabamina hillebrandti*, *Pullenia coryelli*, *Remesella varians* (e.g.,
185 Beckmann, 1960; Von Hillebrandt, 1962; Tjalsma and Lohmann, 1983; Speijer et al., 1996; Thomas,
186 1998), each of which is present at Forada.

187 We identified most common taxa at the species level (Table S2). Taxa with high morphological
188 variability and/or variable preservation were identified at generic or higher taxonomic level. Specimens
189 of the most representative taxa were imaged using the SEM at the C.U.G.A.S. (Centro Universitario
190 Grandi Apparecchiature Scientifiche) of Padova University (Plates 1-4). Relative abundances of the
191 taxa and taxon-groups, along with faunal indices such as the calcareous-agglutinated ratio, the infaunal-
192 epifaunal ratio, and bi-triserial percentage were calculated (Figs. 2, 5-7 and Fig. S1). The absolute
193 abundance (N/g: number of benthic foraminifera per gram-bulk dried sediment) was calculated for both
194 the ≥ 63 and ≥ 500 μm fractions. Faunal diversity indices (Species diversity and Fisher- α ; Fig. 2) were
195 calculated using the PAST package (Hammer et al., 2001). Segments belonging to tubular/branched
196 agglutinated forms (e.g., *Rhizammina*, *Rhabdammina*, *Bathysiphon*) were counted, but excluded from
197 calculations because there is no reliable method to convert the abundance of multiple fragments into
198 that of single individuals (Ernst et al., 2006).

199 We assigned species to epifaunal and infaunal morphotypes by comparing their test morphology to
200 the morphotypes in Corliss (1985), Jones and Charnock (1985), Corliss and Chen (1988), Kaminski
201 and Gradstein, (2005), Hayward et al. (2012), and Mancin et al. (2013). However, caution is needed in
202 applying taxonomic uniformitarianism due to our limited knowledge of the biology and ecology of the
203 highly diverse living species. Even for many living species, the relation between test morphology and
204 microhabitat has not been directly observed, but is extrapolated from data on other taxa (e.g., Jorissen,
205 1999). The assignment of modern foraminifera to microhabitats based on their morphology may be
206 accurate only about 75% (Buzas et al., 1993): comparisons between past and recent environments thus
207 need careful evaluation, and cross correlation between benthic foraminiferal and other proxy data. The
208 ecology as evaluated from the literature (Table 1) is shown for selected benthic foraminiferal taxa from
209 the PETM interval at Forada.

210

211 **2.3 Age model**

212 The age model used for calculating the longevity of benthic foraminiferal assemblages (see below)
213 follows Luciani et al. (2007), with the lower Eocene chronology based on the cyclostratigraphic age
214 model of Giusberti et al. (2007; [Fig. 3](#)). The duration of each precessional cycle has been assumed to be
215 21 kyr. Sedimentological and geochemical parameters oscillate cyclically within the main CIE, in at
216 least five complete precessional cycles ([Figs. 2, 3](#)). The CIE recovery interval is composed of six
217 distinct, precessional marly-limestone couplet cycles ([Fig. 3](#)). The recognition of eleven cycles in the
218 combined CIE and recovery interval implies an estimate of the total duration of the CIE of ca. 230 kyr
219 ([Fig. 3](#)). Giusberti et al. (2007) and Röhl et al. (2007) disagree on the duration of the main CIE and
220 recovery interval (179±17 kyr and 231±22 kyr, respectively). The main difference between these two
221 chronologies is the assignment of different numbers of precessional cycles within the main body and
222 recovery interval (Tipple et al. 2011). A ${}^3\text{He}$ -based chronology for Site 1266 (Walvis Ridge) suggests a
223 total PETM duration of 234 +48/-34 kyr (Murphy et al., 2010), in line with the age model of Giusberti
224 et al. (2007).

225 [Lithological cycles have not been firmly identified in the Paleocene part of the section](#), and
226 sedimentation rates are interpolated between the base of the PETM at ± 0 cm and the lowest occurrence
227 of the calcareous nannofossil *Discoaster multiradiatus* at ca.-12.5 m (Giusberti et al., 2007), using a
228 duration of the time between these events of 1.238 Myr (Westerhold et al., 2007). In this age model, the
229 investigated portion of Forada section spans ca. 800 kyr.

230

231 3 Results

232 Benthic foraminiferal assemblages are generally dominated by calcareous hyaline taxa (85-90%;
233 [Fig. 2](#)), but agglutinated taxa significantly increase in abundance within the CMU (25-90%; [Fig. 2](#)).
234 Infaunal taxa strongly dominate the assemblage throughout the studied interval (~80%). Faunal
235 diversity is fairly high, particularly in the upper Paleocene ([Fig. 2](#)), and preservation is generally
236 moderate, though poor within the lowermost centimeters of the Eocene. [Most foraminiferal tests at](#)
237 [Forada are recrystallized, and totally or partially filled with calcite.](#)

238 Composition and abundance of the assemblages change prominently across the ca. 11 m-thick
239 interval investigated ([Figs. 2, 5-7](#)) coeval with the geochemical signature of the PETM, and broadly
240 coincident with the main lithological changes. We recognized six successive benthic foraminiferal

241 assemblages (labeled A to F; [Figs. 2, 5-8](#)), mainly based on changes in abundance of the taxa listed in
242 Table 1. Assemblages A and B are characteristic of the dominantly reddish calcareous marls **mottled by**
243 **greenish "flames"** of the uppermost Paleocene, separated by the thin, barren clay layer from
244 Assemblages C, D and E, which occur in the first half of the main excursion of the CIE (lowermost
245 Eocene), within the CMU (**basal green laminated clays overlaid by mottled reddish clays**, marly clays
246 and marls). Assemblage F characterizes the marls of the upper half of the CMU, as well as the CIE
247 recovery interval and the overlying post-excursion interval of reddish limestone–marl couplets
248 (Giusberti et al., 2007).

249 **3.1.1 Assemblage A: the upper Paleocene fauna**

250 Assemblage A (-467.5 to -37.5 cm, estimated duration >430 kyr) has a high diversity, with
251 abundant infaunal taxa (ca. 70-80%; [Fig. 2](#)). Small bolivinids (<125 μ m) of the *Bolivinoides crenulata*
252 group (Plate 3, [Figs. 7-9](#)), and smooth-walled *Bolivina* spp. together comprise 50-60% of the > 63 μ m
253 fauna ([Fig. 5](#)), with *Siphogenerinoides brevispinosa* (~10%) and **other buliminids** less common ([Figs.](#)
254 [5, 6](#)). Epifaunal morphotypes are mainly represented by small cibicidids (10%), *Anomalinoides* spp.
255 (5%) and *Cibicidoides* spp. (usually <5%; [Fig. 5](#)). Rare taxa include reussellids, angulogerinids,
256 nodosariids, dentalinids, gyroidinids, valvalabaminids and unilocular hyaline taxa ([Fig. S1](#)).
257 Agglutinated taxa are mainly represented by *Spiroplectammina spectabilis*, *Trochamminoides* spp.,
258 *Paratrocchamminoides* spp., *Reophax* spp. and *Subreophax* spp. The Paleocene Cosmopolitan
259 Extinction Taxa (CET; Plate 1) are not a major component of the assemblage >63 μ m (<10%; [Fig. 6](#)),
260 but are common to abundant in the size fraction >125 μ m (>20%). Many of these have large, heavily
261 calcified tests. The most common taxa include *Gavelinella beccariiformis*, *Pullenia coryelli* and
262 *Coryphostoma midwayensis* ([Table S1](#)). CET such as *Clavulinoides globulifera*, *Cibicidoides dayi* and
263 *Cibicidoides velascoensis* are common in the >500 μ m size fraction, together with trochamminids and
264 large lituolids (Plate 1, [Figs. 19, 6-8](#); Plate 4, [Figs. 7, 8, 14, 20](#)). The latter occur up to the top of the
265 Paleocene, but are absent in the Eocene. At -261.5 cm, the Cosmopolitan Extinction Taxa (CET) peak
266 at 15%, their maximum abundance in the studied section ([Fig. 6](#)). At the same level, peaks of large,
267 stout, heavily calcified taxa (e.g., *Cibicidoides* and anomalinids) co-occur with agglutinated taxa
268 (*Glomospira*, *Spiroplectammina* and *Haplophragmoides*, [Figs. 6, 7](#)), whereas small, thin-walled forms
269 such as bolivinids, *Siphogenerinoides brevispinosa* and cibicids decline markedly in relative abundance

270 (Figs. 5-7). Faunal density (N/g), diversity and the percentage abundance of infaunal morphotypes
271 decrease (Fig. 2), as do $\delta^{13}\text{C}$ and $\text{CaCO}_3\%$, whereas the planktonic foraminiferal fragmentation index
272 (F Index) increases significantly (Fig. 2). The upper boundary of this assemblage is defined by the
273 increase in abundance of the **opportunistic taxa** *Tappanina selmensis* and *Siphogenerinoides*
274 *brevispinosa*, marking the onset of Assemblage B.

275 **3.1.2 Assemblage B: the pre-CIE Paleocene fauna**

276 Assemblage B occurs at -31 to 0 cm, estimated duration \sim 34 kyr. At about -20 cm the lithology
277 shifts from reddish to greenish marls with *Zoophycos* and *Chondrites* (intervals Pa I and II of Giusberti
278 et al., 2007). In this assemblage, *Siphogenerinoides brevispinosa* and *Tappanina selmensis* increase in
279 relative abundance compared to Assemblage A (>10% at \sim 27 and -12 cm; Figs. 6, 7). Between the
280 two peaks of *S. brevispinosa* (at about \sim 20 cm; Figs. 6, 7), there is a transient negative carbon isotope
281 excursion of about 1‰, a drop in CaCO_3 from 60 to 40%, a decline in the coarse fraction to 2%, and a
282 peak in the F-Index (85-90%; Figs. 2, 3). Small and thin-walled taxa such as bolivinids, cibicidids and
283 *S. brevispinosa* decrease markedly in relative abundance, whereas big, heavily calcified taxa (e.g.,
284 Cosmopolitan Extinction Taxa, *Cibicidoides* spp., *Nuttallides truempyi*) and agglutinated forms
285 increase (Figs. 5-7). In addition, faunal density drops, as does the percentage of infaunal taxa (from
286 90% to 50%), and diversity increases (Fig. 2). From -4.5 cm upwards, the preservation of benthic
287 foraminifera deteriorates, while the F Index reaches 100% (Figs. 2, 3). At -1.5 cm preservation worsens
288 and most bi-triserial taxa decline in abundance drastically, whereas benthic foraminiferal absolute
289 abundance and $\text{CaCO}_3\%$ both decrease (Fig. 2). Faunal diversity peaks, and anomalinids, *Cibicidoides*
290 spp., *N. truempyi*, *O. umbonatus* as well as agglutinated forms increase markedly in relative abundance
291 (Figs. 2, 5, 6). In the uppermost Paleocene sample, we see the highest occurrence of most CET (Figs. 4,
292 6). Few CET (e.g., *Aragonina velascoensis*) disappear below this sample (Fig. 4). These are generally
293 rare, occurring discontinuously throughout the Paleocene, even in large samples of residue $>125\text{ }\mu\text{m}$
294 (Fig. 4). The uppermost occurrence of the CET defines the upper boundary of this assemblage, at the
295 base of the black clay layer.

296 **3.1.3 The black clay**

297 The lowermost Eocene is a thin, black clay layer (0 to +0.3 cm), slightly enriched in organic
298 carbon, and carbonate-free (Giusberti et al., 2007; [Figs. 3, 8](#)). This clay marks the base of the CMU,
299 and contains a few specimens only, agglutinated benthic foraminifera of the genera *Haplophragmoides*
300 and *Recurvoides* (10 specimens in 22 g washed sediment). It probably was deposited over less than a
301 millennium, in view of its small thickness and place within the precessionally paced cycles in the
302 PETM.

303 3.1.4 Assemblage C: basal CIE agglutinated fauna

304 We label this lowermost Eocene interval (lowermost 10 cm of laminated green clays of CMU;
305 estimated duration ~3.5 kyr) the BFDI (i.e., benthic foraminiferal dissolution interval), sediment with
306 low CaCO₃ wt % (~15%), and the most negative $\delta^{13}\text{C}$ values in bulk carbonate (-2‰). Assemblage C is
307 dominated by agglutinated taxa (about 90%; [Fig. 2](#)) with badly preserved and deformed tests. Tests of
308 calcareous-hyaline forms are rare, partially dissolved and fragmented. Assemblage C has minimum
309 values of faunal density (<5), diversity, and wt% coarse fraction ([Fig. 2](#)). Infaunal morphotypes have
310 their lowest abundance (ca. 36%; [Figs. 2, 6](#)). Agglutinated foraminifera are mainly represented by
311 *Eobigenerina variabilis* (25%; [Plate 1, Figs. 2, 3](#)), *Haplophragmoides* spp. (20%), *Glomospira* spp.
312 (15%), *Saccamina* spp. (10%) and *Spiroplectammina navarroana* (~ 8%; [Plate 2, Fig. 6](#)). In its upper
313 part, Assemblage C has high abundances of *Karrerulina* spp. (~20%; *K. conversa*; [Plate 2, Fig. 4](#)) and
314 *Ammobaculites agglutinans* (10%; [Plate 2, Fig. 1](#)). The latter taxa occur at relatively high abundance in
315 the overlying assemblages, up to ~+50-70 cm ([Figs. 6, 7](#)). The upper boundary of this assemblage is
316 defined by the first substantial recovery of hyaline taxa (>50%).

317 3.1.5 Assemblage D: lowermost CIE fauna

318 In Assemblage D (+10 to +35 cm, lithologically characterized by laminated green clays; estimated
319 duration ~9 kyr), calcareous-hyaline forms are consistently present and badly preserved, with dominant
320 taxa having dwarfed and thin-walled tests, e.g., *Globocassidulina subglobosa* (25%), *Tappanina*
321 *selmensis* (20%), and *Osangularia* spp. (~11%; [Figs. 6, 7; Plate 2, Figs. 13-16](#)). **A specific assignment**
322 **of basal PETM osangulariids at Forada is not possible because of their very small size and poor state of**
323 **preservation.** From +30 cm upwards, relative abundances of *G. subglobosa* and *Osangularia* spp.
324 drastically decline, whereas *T. selmensis* reaches its maximum abundance (ca. 33%; [Figs. 6, 7](#)). Minor
325 components are "other buliminids" group (up to 10% at the top of the Assemblage; see [Fig. 5](#) and [Fig.](#)

326 5- related caption), *Pleurostomella* spp., *Oridorsalis umbonatus*, anomalinids and stilostomellids (Figs.
327 5, 6 and Fig. S1). Agglutinated forms remain abundant, up to 50%. At +20 cm, calcified radiolarians
328 become abundant, dominating the microfossil association up to +2 m above the base of CMU (Luciani
329 et al., 2007; Figs. 3, 8). Within the interval of Assemblage D, $\delta^{13}\text{C}$ shifts from -2 to -1‰, and the
330 CaCO_3 wt% recovers to ~40%, despite strong dilution with terrigenous sediments (Fig. 3). The upper
331 boundary of this assemblage is defined by the consistent decrease of *T. selmensis* (to <5%).

332 3.1.6 Assemblage E: main CIE fauna I

333 In this interval (+35 to +185 cm; lithologically characterized by green and reddish clays and marls;
334 estimated duration ca. 42 kyr) benthic foraminiferal preservation improves, and calcareous-hyaline
335 forms dominate the assemblages again (Fig. 2). *Siphogenerinoides brevispinosa* is consistently present
336 again, with two peaks up to 20% (Figs. 6, 7). *Pleurostomella* spp. increase to up to >10%, and
337 *Bolivinoides crenulata* and smooth-walled *Bolivina* spp. to up to 30 - 40% (Figs. 5, 6). Calcareous-
338 hyaline epifaunals such as cibicids and anomalinids reappear at <5% (Fig. 5). Faunal density and
339 diversity gradually increase upwards, whereas agglutinated taxa markedly decrease in abundance
340 (<20%) at ~+70 cm (Fig. 2). The upper boundary of this assemblage is defined by the marked drop in
341 relative abundance of *S. brevispinosa* (to <5%).

342 3.1.7 Assemblage F: main CIE fauna II, CIE recovery and post CIE fauna

343 Assemblage F characterizes the upper half of the CMU (reddish marls), from about +185 cm up to
344 its top (+337.5 cm), and the overlying interval (red marly limestone couplets) up to +649 cm; estimated
345 total duration > 281 kyr). The relative abundance of *Siphogenerinoides brevispinosa* is low (<5%),
346 whereas *Bulimina tuxpamensis* and *Nuttallides truempyi* increase in abundance, respectively to 5 and
347 10%, and show cyclical variations in relative abundance (Figs. 6, 7). Pleurostomellids (~10%), "other
348 buliminids" group (~10%; Fig. 5), cibicids (~10%), *Oridorsalis umbonatus* (~5%), stilostomellids
349 (~5%) and *Abyssammina* spp. (~5%) are common (Figs. 5, 6). Relative abundance of infaunal taxa
350 (mostly bolivinids) and faunal density (N/g) returns to their Paleocene values (75-80%; Fig. 2).
351 Diversity increases (simple diversity up to 60, Fisher- α diversity up to 20; Fig. 2) but remains lower
352 than in the Paleocene. All faunal indices show cyclical variation (Fig. 2), as do the relative abundance
353 of benthic foraminifera, and planktic foraminiferal and calcareous nannofossil assemblages (Agnini et

354 al., 2007; Luciani et al., 2007). In the lower third of the interval in which this assemblage occurs, just
355 above the CMU (ca. +337.5 cm), the relative and absolute abundance of radiolarians decrease markedly
356 and **agglutinated** taxa such as *Glomospira* spp., *Eobigenerina variabilis* and *Karrerulina* spp. slightly
357 increase in relative abundance (~+2-3%) (Figs. 2, 3, 6, 7).

358

359 **4 Discussion**

360 **4.1 Paleodepth of the Forada section**

361 Based on benthic foraminifera in the >125 μ m size fraction, Giusberti et al. (2007) suggested a
362 paleodepth between 600 and 1000 meters for the Forada section. Our data on the >63 μ m size fraction
363 suggest a somewhat greater paleodepth, i.e., upper lower bathyal, between 1000 and 1500 meters (van
364 Morkhoven et al., 1986). Representatives of the bathyal and abyssal Velasco-type fauna (Berggren and
365 Aubert, 1975), such as *Aragonia velascoensis*, *Cibicidoides velascoensis*, *Gyroidinoides globosus*,
366 *Nuttallides truempyi*, *Nuttallinella florealis*, *Osangularia velascoensis* and *Gavelinella beccariiformis*
367 are common at Forada. The faunas across the uppermost PETM interval and higher are similar to the
368 PETM-fauna in the upper abyssal Alamedilla section (Souther Spain; Alegret et al., 2009a) and at
369 Walvis Ridge at 1500 m paleodepth (Thomas and Shackleton, 1996; Thomas, 1998). *Abyssammina*
370 spp. and *Nuttallides truempyi* (upper depth limit at 1000 and 300 m respectively; Van Morkhoven et
371 al., 1986; Speijer and Schmitz, 1998) increase in abundance by more than a factor of 2 during the
372 PETM at Forada, as typical for PETM deep-sea benthic foraminiferal records (e.g., Thomas, 1998;
373 Thomas and Shackleton, 1996; Thomas, 2007; Alegret et al., 2009a, 2011; Giusberti et al., 2009). In
374 these deliberations we excluded the bolivinids, because we consider that their high abundance is due to
375 the “delta depression effect” (see below).

376 **4.2 Environmental reconstruction during the late Paleocene**

377 **4.2.1 The Belluno Basin Paleocene deep-sea environment (Assemblage A)**

378 Throughout most of the investigated section, infauna strongly dominate over epifauna, mainly
379 due to the high abundances of bolivinids (Figs. 2, 5). Such dominance of bolivinids is common in
380 lower and middle Eocene hemipelagic Scaglia sediments in the Belluno basin (Agnini et al., 2009;
381 Boscolo Galazzo et al., 2013). Presently, bolivinids are common along continental margins, and at

382 bathyal depths, at the interception of the oxygen minimum zone (OMZ) with the seafloor, typically
383 between 200 and 1000 m in modern oceans (Levin, 2003). High abundances of bolivinids commonly
384 correlate with high organic matter flux and/or oxygen depletion (e.g., Murray, 1991; Gooday, 1994;
385 Bernhard and Sen Gupta, 1999; Schmiedl et al., 2000; Thomas et al., 2000; Jorissen et al., 1995, 2007;
386 Thomas, 2007). We see high abundances of such taxa typically at greater depths than usual in regions
387 with significant organic matter input from rivers, the so-called “delta-depression” effect first described
388 in the Gulf of Mexico (Pflum and Frerichs, 1976; Jorissen et al., 2007). Such lateral inputs of organic
389 matter thus result in (partial) decoupling between the food supply to the benthos and local primary
390 productivity (e.g., Fontanier et al., 2005; Arndt et al., 2013).

391 At Forada, there is neither geochemical nor sedimentological evidence for persistent suboxic
392 conditions at the sea-floor (Giusberti et al., 2007), and the high benthic foraminiferal faunal diversity
393 likewise does not indicate low oxygen conditions. The upper Paleocene calcareous plankton is
394 dominated by morozovellids indicating oligotrophic surface water conditions (Luciani et al., 2007; Fig.
395 8). The calcareous nannofossil assemblage is dominated by the generalist taxa *Toweius* and
396 *Coccolithus*, with high percentages of *Sphenolithus* and *Fasciculithus* (Agnini et al., 2007; Fig. 8),
397 supporting that surface waters were oligotrophic. We thus think that environments in the Belluno
398 Basin, close to a continental margin (Agnini et al., 2007), were characterized by the “delta depression
399 effect”, in which hemipelagic sedimentation incorporated significant laterally transported terrigenous
400 organic matter to serve as food for the benthos (e.g., Fontanier et al., 2008; Arndt et al., 2013).
401 The occurrence of large, epifaunal (> 500 µm) species (Assemblage A and B), has been related to an
402 optimum food supply, but also to very low food supply, since a lack of food keeps individuals from
403 reproducing successfully and leads to continued test-growth (Boltovskoy et al., 1991; Thomas and
404 Gooday, 1996).

405 Overall, Assemblage A, indicates oligo-mesotrophic surface waters, with bolivinids probably
406 exploiting refractory, laterally advected organic matter. The high faunal diversity suggests that seasonal
407 to periodical increases in primary productivity may have occurred (e.g., Gooday, 2003; Fontanier et al.,
408 2006a, 2006b, 2014), allowing a species-rich, highly diverse infauna and epifauna to inhabit the sea-
409 floor, and co-occur with the bolivinids in the sedimentary record.

410 At Forada, the relative abundance of Paleocene Cosmopolitan Extinction Taxa (CET) is low
411 (average <10%; Fig. 6), due to the large number of Bolivinacea dominating the fine size fraction used

412 for this study (>63 μ m). Many CET (Plate 1) are epifaunal morphotypes, commonly larger than 125
413 μ m, as also noted elsewhere (e.g., Giusberti et al., 2009). Similarly low percentages (12-15%) of CET
414 have been recorded in Scaglia sediments of the Contessa section (Giusberti et al., 2009) and at ODP
415 Site 690 by Thomas (2003), where infaunal morphotypes (buliminids and uniserial calcareous taxa) are
416 abundant in the >63 μ m fraction.

417

418 4.2.2 The precursor warming event (Assemblage B)

419 The onset of Assemblage B, about 34 kyr before the onset of the CIE (~30 cm), is marked by
420 increase in relative abundance of opportunistic taxa such as *Tappanina selmensis* and
421 *Siphogenerinoides brevispinosa* (Figs. 6, 7; Table 1). The arrival of *Tappanina selmensis*, an upper
422 bathyal to outer shelf species in the Maastrichtian (Frenzel, 2000), at greater depths might indicate
423 warming of deep waters before the beginning of the PETM, as also reflected in the migration of warm-
424 water planktonic species to high southern latitudes (Thomas and Shackleton, 1996; Table 1). The
425 benthic foraminiferal changes roughly coincided with a significant increase in acarininids% (planktonic
426 foraminifera, >50%), likely indicating warming of surface waters (Luciani et al., 2007; Fig. 8). The
427 foraminiferal assemblages hence suggest warming throughout the water column, and increased surface
428 nutrient availability and deep-water food availability, whereas no changes in productivity in calcareous
429 nannofossils are recorded (Agnini et al., 2007; Luciani et al., 2007; Fig. 8). The foraminiferal evidence
430 for warming is associated with an increase in $\delta D_{n\text{-alkanes}}$ and TEX_{86} values (Fig. 9), suggesting increased
431 aridity and sea surface temperature prior to the onset of the CIE (Tipple et al., 2011).

432 Multiple proxies thus indicate that climatic and oceanographic conditions started to change ~30
433 kyr before the onset of the CIE, pointing to a PETM precursor event, reflected by a <5-cm thick
434 dissolution interval at ~22 cm, coinciding with a negative shift in bulk $\delta^{13}\text{C}$ (-1‰; Figs. 2, 3). Within
435 this interval dissolution-sensitive benthic foraminifera (e.g., *S. brevispinosa* and small bolivinids)
436 markedly decrease in abundance, while more robust and agglutinated taxa increase (Figs. 2, 5-8), as
437 does the F-Index of planktic foraminifera (to ~ 85-90%; Luciani et al., 2007; Fig. 3). This dissolution
438 level may thus reflect a brief episode of rising lysocline/CCD (<5 kyr) in response to a precursory
439 emission of isotopically light carbon (Bowen et al., 2015). Similar precursor events have been observed
440 worldwide (e.g., Sluijs et al., 2007b; 2011; Secord et al., 2010; Kraus et al., 2013; Garel et al., 2013;

441 Bornemann et al., 2014; Bowen et al., 2015), indicating that disturbance of the global carbon cycle
442 started before the PETM, as potentially also reflected in the occurrence of hyperthermals in the
443 Paleocene (Thomas et al., 2000; Cramer et al., 2003; Coccioni et al., 2012).

444 At the top of Assemblage B (uppermost 4.5 cm), just prior to the onset of the CIE, carbonate
445 preservation declined markedly, as reflected in F-Index, $\text{CaCO}_3\%$, and foraminiferal preservation. In
446 this interval, representing the “burndown” layer (BL; e.g., Thomas and Shackleton, 1996; Thomas et
447 al., 1999; Giusberti et al., 2007; [Figs. 4, 7, 8](#)), CET remained present. Dissolution in the upper BL
448 removed most thin, dissolution-prone calcareous tests (e.g., *Siphogenerinoides brevispinosa* and small
449 bolivinids), concentrating the more heavily calcified and the agglutinated taxa (included CET; [Fig. 5-](#)
450 [7](#)). Benthic foraminiferal assemblages in the topmost Paleocene at Forada thus cannot be interpreted
451 with confidence due to the severe dissolution.

452 **4.3 Climate and marine life during the PETM**

453 **4.3.1 The black clay: a desert below the CCD**

454 This very thin, carbonate-free interval is somewhat enigmatic. The virtually barren sediment may
455 have been deposited during the maximum rise of the CCD, under environmental conditions so
456 unfavorable that benthic life was excluded, a "dead-zone" (*sensu* Harries and Kauffman, 1990) during
457 the earliest phase of the PETM. Geochemical redox indices in the black clay and the underlying and
458 overlying samples suggest persistently oxygenated bottom waters (Giusberti et al., 2007), but may
459 reflect diagenesis during re-oxygenation of bottom waters after a short period of anoxia, as commonly
460 observed for Mediterranean sapropels (Higgs et al., 1994; van Santvoort et al., 1996). The presence of the
461 thin black clay without microfossils thus is highly suggestive of a brief pulse of anoxia, as supported by
462 a single peak value of organic carbon (0.6 wt %; Giusberti et al., 2007). The high value of biogenic
463 barium (3151 ppm) in the black clay ([Fig. 3](#)), despite the fact that barite is generally not preserved
464 under anoxic conditions (Paytan and Griffith, 2007; Paytan et al., 2007) may represent reprecipitation at
465 the oxic/anoxic sediment interface after dissolution under anoxic conditions (Giusberti et al., 2007),
466 and/or high rates of organic remineralization in the water column, during which the barite forms (Ma et
467 al., 2014).

468 **4.3.2 The early peak PETM (Assemblages C and D)**

469 The 10 cm of sediment directly overlying the Paleocene/Eocene boundary (i.e. the base of the CIE;
470 **Figs. 7, 8**) was deposited in strongly CaCO_3 –corrosive waters, **below the lysocline and** close to or
471 below the CCD. The rapid rise of the CCD/lysocline during the PETM is a predicted consequence of
472 massive input of carbon (CO_2 or CH_4) in the ocean-atmosphere system on a millennial timescale (e.g.,
473 Dickens et al., 1997; Thomas, 1998; Zachos et al., 2005; Zeebe et al., 2009, 2014; Hoenisch et al.,
474 2012). The carbonate dissolution at Forada is consistent with observations at many other deep-sea sites
475 (e.g., Schmitz et al., 1997; Thomas, 1998; Zachos et al., 2005; Kelly et al., 2010). The benthic
476 foraminiferal extinction event (BEE) at Forada (i.e., **corresponding to** the BB1/BB2 zonal boundary
477 of Berggren and Miller, 1989) occurs within this 10 cm-thick interval, between the top of the CET-
478 bearing burndown layer and the base of Assemblage D, where benthic calcareous taxa reappear (**Figs.**
479 **4, 7, 8**). The concentration of CET **in the burndown layer**, and the reappearance of calcareous hyaline
480 taxa only 10 cm above the onset of the PETM at Forada, confirms that the CET extinction occurred
481 over 3.5 kyr or less in the central western Tethys, **similar to evaluations of this timing from carbon**
482 **cycle modeling (Zeebe et al., 2014)**.

483 Sediment just above the black clay, reflecting a first slight deepening of the CCD, contains a low
484 diversity, fauna of mostly **agglutinated**, dwarfed (close to 63 μm **in diameter**) benthic foraminifera, and
485 calcareous nannofossils with signs of dissolution, with planktic foraminifera virtually absent (Agnini et
486 al., 2007; Luciani et al., 2007; **Fig. 8**). This first wave of benthic pioneers recolonized the sea-floor
487 during the peak-CIE, in CaCO_3 -undersaturated waters, and reflects a highly stressed environment
488 (Assemblage C; **Figs. 6-8**). **Among the pioneers, *Eobigenerina variabilis* is peculiar of the PETM of**
489 **the Forada section (Figs. 6, 7). *Eobigenerina* is a recently erected genus in the Textulariopsidae,**
490 **including non-calcareous species previously assigned to *Bigenerina* (Cetean et al., 2011), and it is**
491 **known to behave opportunistically during Cretaceous Oceanic Anoxic Event 2 (OAE2; Table 1). A**
492 **major component of the upper part of Assemblage C is *Karrerulina conversa* (Fig. 7). The species**
493 **dominates the lowermost Eocene deposits in the Polish Carpathians (Bąk, 2004), commonly occurring in**
494 **the Paleocene-Eocene of the Central North Sea and Labrador margin, and in Morocco (Kaminski and**
495 **Gradstein, 2005). Modern *Karrerulina* (e.g., *K. apicularis*=*K. conversa*) live in oligotrophic abyssal**
496 **plains, with well-oxygenated bottom and interstitial waters (Table 1). However, the test morphology of**
497 ***Karrerulina*, combined with its abundant occurrence in the doubtless stressed environment of the basal**
498 **PETM at Forada and Zumaia (Table 1), suggests that this genus may also act opportunistically.**

499 After ca. 4 kyr, a further deepening of CCD allowed a consistent increase in abundance of benthic
500 calcareous taxa (ca. 50%; Assemblage D; **Fig. 2**), coinciding with the lowermost recovery of bulk
501 carbonate $\delta^{13}\text{C}$ values, from $-2\text{\textperthousand}$ to $-1\text{\textperthousand}$ (Giusberti et al., 2007; Tipple et al., 2011; **Fig. 7**). These
502 calcareous recolonizers included dwarfed and thin-walled forms of *G. subglobosa*, *Tappanina*
503 *selmensis*, *Osangularia* spp. and *Oridorsalis umbonatus* (**Figs. 6, 7**). A similar peak in small
504 *Osangularia* also occurs in the basal PETM at Contessa Section, as documented for the first time in the
505 present paper (**Fig. S2**). Representatives of the genus *Osangularia* (*Osangularia* spp.) behaved
506 opportunistically in the PETM of the Tethyan Alamedilla section (Alegret et al., 2009a). Moreover,
507 Boscolo Galazzo et al. (2013) found small-size *Osangularia* within organic-rich levels immediately
508 following the Middle Eocene Climatic Optimum in the Alano section (in northeastern Italy). During the
509 Cretaceous OAEs *Osangularia* spp. opportunistically repopulated the sea floor during short-term re-
510 oxygenation phases (see references in Table 1). Although *Osangularia* is generally referred to as
511 preferring stable well oxygenated environments (e.g., Murray, 2006; Alegret et al., 2003), we suggest
512 that some extinct species of this genus could actually behave as opportunist and recolonizer.

513 Assemblage D contains almost equal abundances of calcareous and **agglutinated** taxa, indicating
514 that factors other than bottom water CaCO_3 concentration were controlling faunal variability within this
515 assemblage (**Figs. 6, 7**). Possibly, strongly enhanced runoff and sediment delivery can explain the
516 abundance of agglutinated taxa (40-60%), such as *Glomospira* spp. (e.g., Arreguín-Rodríguez et al.,
517 2013, 2014), above the first 10 cm of the CMU. We thus recognize a rapid succession of recolonizer
518 taxa during the first 12 kyr of the CIE (Assemblages C-D). The small size of both the **agglutinated** and
519 hyaline recolonizers is indicative of r-strategist species which reproduce quickly and can thus quickly
520 repopulate stressed environments, as soon as conditions improve slightly (e.g., Koutsoukos et al., 1990;
521 Thomas, 2003). The rapid pace at which different populations of recolonizers succeeded each other
522 indicates a highly unstable environment, with marked fluctuations in the amount, timing and quality of
523 the food reaching the sea floor. Sediment deposition during this interval may have occurred in rapid
524 pulses, e.g., following intense rainstorms, carrying refractory organic matter to the deep-sea
525 environment. Pauses between events may have allowed the benthic foraminifera to recolonize the
526 sediment, profiting of the abundance of food. This is consistent with calcareous nannofossil
527 assemblages showing an increase in *Ericsonia* and declines in abundance of *Sphenolithus*, *Octolithus*,
528 *Zygrablithus* and *Fasciculithus*, indicating an unstable and nutrient rich upper water column (Agnini et

529 al., 2007; **Fig. 8**). Archaeal biomarkers show a large influx of terrestrial, soil-derived organic matter
530 (Branched and Isoprenoid Tetraethers or BIT Index) from the onset of the PETM up to ~+10 cm
531 (Tipple et al., 2011). Higher plant *n*-alkane average chain length (ACL) decreased immediately after
532 the onset of the CIE, consistent with increased humidity (**Fig. 9**; Tipple et al., 2011). The abundance of
533 the clay mineral chlorite indicates enhanced physical erosion (Robert and Kennett, 1994) during
534 deposition of the lower 50 cm of the CMU, rapidly decreasing upward (**Fig. S3**).

535 The greenish marly clays containing Assemblages C and D show primary lamination, indicating
536 that macrobenthic invertebrates were absent, as at Dee and Mead Stream sections (New Zealand;
537 Nicolo et al., 2010), and Zumaya (Spain; Rodriguez-Tovar et al., 2011). The presence of benthic
538 foraminifera, however, indicates that bottom and pore waters were not permanently anoxic. Pore waters
539 may have become dysoxic periodically due to high temperatures, decomposing organic matter and
540 possibly enhanced water column stratification, leading to the absence of metazoans and stressed
541 benthic foraminiferal assemblages. **Low-pH sea-floor conditions may have also played a significant**
542 **role in excluding macrobenthic fauna in this early phase of PETM at Forada. Deep-sea animals are**
543 **highly sensitive to even modest but rapid pH changes (Seibel and Walsh, 2001), which are harmful**
544 **even for infaunal deep-sea communities (Barry et al., 2004).**

545 **4.3.3 The core of the CIE and Recovery (Assemblages E, F)**

546 The benthic foraminiferal assemblage changes significantly from Assemblage D to assemblage E,
547 coinciding with the gradual reappearing of mottling (as thin reddish “flames” in the green sediment).
548 Bolivinids return as a major faunal component (50%), and **agglutinated taxa** decrease in abundance.
549 Peaks of tapered elongate calcareous forms, including *Siphogenerinoides brevispinosa*, “**other**
550 **buliminids” group**, pleurostomellids and stiliostomellids, replace the recolonizers (Figs. 5, 6). These
551 groups could have been **functioned as** opportunistic taxa, able to flourish when food supply was
552 periodically high (e.g., **Table 1**). Coinciding with Assemblage E, planktic foraminifera return to be a
553 significant component of the microfossil assemblage (e.g., Luciani et al., 2007; **Fig. 8**), while
554 radiolarians remain abundant throughout the CMU (Giusberti et al., 2007; Luciani et al., 2007). The
555 planktic foraminiferal assemblage is dominated by acarininids, with a double peak of the excursion
556 species *Acarinina sibaiyaensis* and *A. africana*, which, combined with the high percentages of the
557 nannofossil *Ericsonia*, indicate warm and eutrophic surface waters (e.g., Ernst et al., 2006; Guasti and
558 Speijer, 2007; Agnini et al., 2007; Luciani et al., 2007; **Fig. 8**).

559 Detrital hematite sharply increased in concentration at the onset of Assemblage E (Giusberti et al.,
560 2007; Dallanave et al., 2010; 2012; **Fig. 3**). Hematite forms in soils under warm and dry conditions, and
561 an increase of hematite in marine sediments is considered indicative of an arid climate over the
562 adjoining land, **with** increased wind strength (Larrasoña et al., 2003; Zhang et al., 2007; Itambi et al.,
563 2009), or humid to subhumid climates with seasonal drying (Torrent et al., 2006). It is delivered to the
564 deep-sea environment through river runoff or as aeolian dust (e.g., Zhang et al., 2007; Itambi et al.,
565 2009). Within the CMU, hematite shows cyclical fluctuations with a ~21 kyr periodicity, but other
566 terrigenous components (quartz and phyllosilicates) do not co-vary in abundance after a ~15% increase
567 at the onset of the CMU (**Fig. 3**). To explain the different abundance patterns, we interpret hematite as
568 wind-delivered, silicate minerals as runoff-delivered.

569 The hematite% peaks may be indicative of cyclical variability in wind-delivered material, rather
570 than the earlier prevailing consistently humid climate. The lithological anomaly of the CMU, the
571 fivefold increase in sedimentation rates and increase in reworked Cretaceous nannofossils (Agnini et
572 al., 2007; **Fig. 8**), as well as the silicate mineral and hematite% records all indicate marked fluctuations
573 in the hydrological regime throughout this interval. High hematite% may reflect the presence of high-
574 pressure cells over land, during an overall dry climate phase, with increased wind strength and dust
575 delivery to the sea (Larrasoña et al., 2003; Zhang et al., 2007; Itambi et al., 2009). In contrast, low
576 values of hematite% may indicate periods of greater humidity and enhanced precipitation. Such
577 alternation of wet and arid phases favored deeper soil erosion on the continental areas surrounding the
578 Belluno basin (Thiry, 2000; Schmitz and Pujalte, 2003), causing major washouts during the wet phases,
579 which may explain the fivefold increase in sedimentation rates and 15% increase in phyllosilicate
580 abundance in the CMU (**Fig. 3**).

581 The hematite% cycles are in phase with cycles in $\text{CaCO}_3\%$, radiolarian abundance, and bulk
582 carbonate $\delta^{13}\text{C}$, slightly preceding the others stratigraphically (**Fig. 3**). During the arid climate phase,
583 enhanced wind strength may have generated intense surface water mixing and offshore nutrient
584 upwelling, inducing increases in primary productivity and phytoplankton blooms. The blooms in
585 primary productivity resulted in deposition of abundant algal biomass, leading to the occurrence of
586 peaks of pleurostomellids, stiliostomellids and *Siphogenerinoides brevispinosa* in Assemblage E.
587 Productivity may have remained fairly high during the wet periods, as indicated by consistently high
588 biogenic barium throughout the CMU (Giusberti et al., 2007; Paytan et al., 2007). During the rainy

589 periods, upwelling rates may have been lower, with nutrients mostly supplied in river runoff. The
590 delivery of food to the seafloor may have been more continuous, but with more important input of
591 refractory organic matter from land.

592 In contrast to these proxies, which show cyclicity at precessional periods throughout the CMU,
593 higher plant *n*-alkane average chain length (ACL) and δD vary only in its lowermost 50 cm (Tipple et
594 al., 2011; [Fig. 9](#)). Possibly, the sedimentary *n*-alkanes were derived from a pool of plant material
595 produced during subsequent wet and dry phases, so that ACL and δD may represent averaged records
596 of leaf wax *n*-alkanes produced during different mean climate states in the upper CMU. Even so, the
597 δD values within the CMU are on average $\sim 15\text{\textperthousand}$ lower than above and below ([Fig. 9](#)), as reported for
598 the Cicogna section (10 km away; Krishnan et al., 2015), possibly reflecting more humid
599 conditions/higher precipitation during the PETM wet times (e.g., Sachse et al., 2006; Smith and
600 Freeman, 2006), or greater productivity of plant material during the wet phases. Alternatively, it may
601 reflect a primary change in the isotopic composition of meteoric waters (Krishnan et al., 2015).

602 In the following benthic foraminiferal Assemblage F (upper CMU, recovery phase),
603 *Siphogenerinoides brevispinosa* and *Tappanina selmensis* are less abundant, whereas *Bulimina*
604 *tuxpamensis*, *Abyssammina* spp., and *Nuttallides truempyi* increase in relative abundance ([Figs. 6, 7](#)).
605 These are typical deep-sea, open-ocean taxa which thrive under more oligotrophic conditions (e.g.,
606 Thomas, 1998), and might indicate progressively less intense or shorter primary productivity blooms
607 during the arid phases, and/or mark the return to fully oxygenated sea-floor and pore water conditions.
608 Less intense eutrophy at the transition from Assemblage E to F is further supported by calcareous
609 plankton data, showing a decrease in the planktic foraminiferal excursion species, and among
610 nannofossils, a decrease in *Ericsonia* (Agnini et al., 2007; Luciani et al., 2007; [Fig. 8](#)). Concluding with
611 the top of the CMU, there were marked changes in calcareous plankton assemblages, although benthic
612 foraminiferal Assemblage F persisted. Among calcareous nannofossils the abundance of *Zygrablithus*,
613 *Sphenolithus* and *Octolithus* increased, whereas that of reworked taxa decreased ([Fig. 8](#)). In the
614 planktic foraminiferal assemblage, *Acarinina* species declined in abundance, and the fauna became
615 more diverse, with fluctuations modulated by lithology in the marl-limestone couplets overlying the
616 CMU ([Fig. 8](#)).

617 The lithological unit above the CMU consists of an alternation of limestones and marls at
618 precessional frequencies (~ 21 kyrs; [Fig. 2](#)). These limestone-marl couplets persist for up to 8 meters

619 above the CMU (well beyond the top of the studied interval; Giusberti et al., 2007; Luciani et al.,
620 2007), then gradually become less clearly expressed, fading upwards. The marl-limestone couplets may
621 reflect the persistence of wet (marl)-arid (limestone) cycles for ~ 800 kyr after the end of the CMU
622 deposition, though at an amplitude declining over time. This persistence resembles the extended (650
623 kyr) humid period, starting at the onset of PETM, recognized in the sediment record at Site 401 of
624 eastern North Atlantic (Bornemann et al., 2014). Our benthic foraminiferal data agree with this
625 interpretation, showing substantially unchanged sea-floor conditions up to +650 cm (uppermost sample
626 analyzed).

627 **4.4 Clues from Forada on PETM climate change**

628 The integrated dataset collected at Forada supports the occurrence of enhanced climatic contrasts
629 and productivity changes in the western Tethys during the PETM, and agrees with previous studies
630 suggesting intense weather extremes at mid to subtropical latitudes (Fig. 10; Table S3). At the onset of
631 the PETM, middle to subtropical latitudes may have been characterized by intense, monsoonal-type
632 rainfall, followed by a succession of wet and arid phases, possibly precessionally paced, **during the core**
633 **of the PETM** (e.g., Collinson et al., 2007; Kraus and Rigging, 2007; Egger et al., 2009; Foreman et al.,
634 2014; Stassen et al., 2012a,b; 2015; **Fig. 10 and Table S3**). The Forada record allows to distinctly
635 recognize the temporal successions among these distinct climatic phases up to 800 kyr after the onset of
636 the PETM, and to directly relate them **to** the progression of the CIE, its recovery and termination. The
637 climatic conditions inferred from the Forada section and other records at similar latitudes differ from
638 those derived from the subtropical net evaporation zone (15°-35°N), (e.g., from the Tremp-Graus Basin
639 - Pyrenees), which document a generally much drier climate with a brief interval of increased
640 storminess and intense flash flood events at the onset of the PETM (Schmitz and Pujalte, 2007).
641 Records from subtropical to mid-latitudes also differ from records within the northern rain belt and into
642 the Arctic basin (>50°N), which suggest that humid conditions may have been more persistent there,
643 with increased rates of precipitation, and on average moister conditions during the PETM (Pagani et al.,
644 2006b; Sluijs et al., 2006; Harding et al., 2011; Dypvik et al., 2011; Kender et al., 2012; Wieczorek et
645 al., 2013; **Fig. 10; Table S3**).

646 The combination of all **these** climatic records (Fig. 10; Table S3) suggests **that** the net result of
647 increased weather extremes during peak-PETM might have been to decrease rainout at subtropical to
648 mid latitudes, and increase moisture transport toward the high latitudes, as originally suggested by

649 Pagani et al. (2006b). Few tropical records exist, so that precipitation changes here are less clear.
650 Rainfall in coastal Tanzania may have decreased during the early PETM, but combined with violent
651 precipitation events and floodings (Handley et al. 2008; 2012; Aze et al., 2014; **Table S3**). In Central
652 America, conditions **during the PETM** may have shifted to more continuously humid (Jaramillo et al.,
653 2010).

654 The long-lasting cyclity and precise chronology at Forada suggest that this enhanced climate
655 variability at subtropical to mid latitudes may have lasted for several hundred of thousand years after
656 the onset of the CIE. Despite **the possible decrease of net rainout**, these weather extremes persisting
657 over several 10^5 kyr may have significantly enhanced the rate of erosion and weathering, through the
658 occurrence of alternating wet-dry periods. The weathering may **have led to a decrease in** atmospheric
659 CO₂ levels, by consumption of CO₂ during weathering reactions. The increased supply of cations
660 through enhanced weathering-erosion would have driven ocean pH up, and **atmospheric** CO₂ down
661 (Broecker and Peng, 1982; Raymo et al., 1988; Zachos et al., 2005). Enhanced seasonal extremes
662 across large geographical areas (the subtropical to mid latitudinal belt) thus might have been a response
663 to the large CO₂ input at the Paleocene-Eocene transition, and may have had a primary role in restoring
664 the carbon cycle to steady state.

665

666 **6 Conclusions**

667 The continuous and expanded record of benthic foraminifera across the PETM at Forada,
668 integrated with the extensive datasets previously generated across this interval, may provide the most
669 complete reconstruction of ecological and climatic changes during the Paleocene/Eocene thermal
670 maximum in Europe. Coupled sedimentological, molecular and micropaleontological records highlight
671 a complex sequence of environmental and climatic changes during the time period across the CIE:

- 672 - Climatic and oceanographic conditions started to change ~30 kyr before the onset of the PETM, with
673 a possible precursor event.
- 674 - Our high-resolution benthic foraminiferal record combined with the established chronology lets us
675 infer that the BEE in the central-western Tethys occurred over a time interval of not more than 4 kyr.
676 At the onset of the PETM, combined de-oxygenation, acidification and environmental instability may
677 have synergistically impacted deep sea life.

678 -Four benthic foraminiferal assemblages occur (C-E and lower F) within the CMU (coinciding with the
679 main phase of CIE). Assemblage C is characterized by successive peaks of different agglutinated
680 recolonizers. Calcareous recolonizers return in the following Assemblage D, after calcium carbonate
681 saturation increased. The complex succession of peaks of agglutinated and hyaline recolonizers in these
682 two assemblages (C, D; 12.5 kyr), suggests multiple repopulation episodes. The benthic foraminiferal
683 data integrated with molecular and mineralogical data point to increased precipitation and strong
684 continental erosion during this short initial stage of the PETM.

685 - Within the core of the CIE, $\delta^{13}\text{C}$ and mineralogical properties such as hematite and calcium carbonate
686 wt % vary at precessional periodicity. Combined with data on radiolarian abundance and benthic
687 foraminiferal assemblage composition this variability suggests an alternation of overall wetter and drier
688 periods. Enhanced weather extremes during most of the PETM may have led to a decrease in total
689 precipitation over the central western Tethys.

690 - The benthic foraminiferal assemblage at Forada did not significantly change with the onset of the
691 deposition of marl-limestone couplets unit above the CMU (mid and upper third of Assemblage F).
692 This suggests that the enhanced climatic variability at precessional timescales persisted well after the
693 end of the CIE recovery. We argue that enhanced seasonal extremes at mid-latitudes might have been a
694 direct climate response to the huge CO_2 input at the Paleocene-Eocene transition, and may have had a
695 primary role in restoring carbon cycle steady state through links with the water cycle and weathering
696 rates.

697

698 Acknowledgments

699 This work was funded by the Italian Ministry of Education and Research (MIUR) funds (PRIN 2001,
700 2007 and 2010-2011 to Domenico Rio; n. prot. 2001048975_002; 2007W9B2WE_004;
701 2010X3PP8J_003). This manuscript benefited from constructive reviews of Robert Speijer and
702 Nicoletta Mancin. LG and FBG are deeply indebted to Domenico Rio for the original idea of the
703 "Paleogene Veneto Project", the financial and material support, and for fruitful discussions during all
704 these years. ET acknowledges financial support by the Leverhulme foundation (UK) and NSF Grant
705 OCE 1232413.

706

707 **References**

708 Agnini, C., Fornaciari, E., Rio, D., Tateo, F., Backman, J., and Giusberti, L.: Response to calcareous
709 nannofossil assemblages, mineralogy and geochemistry to the environmental perturbations across the
710 Paleocene/Eocene boundary in the Venetian Pre-Alps, *Mar. Micropaleont.*, 63, 19-38, 2007.

711 Agnini, C., Macrì, P., Backman, J., Brinkhuis, H., Fornaciari, E., Giusberti, G., Luciani, V., Rio, D.,
712 Sluijs, A., and Speranza, F.: An early Eocene carbon cycle perturbation at ~52.5 Ma in the Southern
713 Alps: chronology and biotic response, *Paleoceanography*, 24, PA2209, 2009.

714 Alegret, L., Molina, E., and Thomas, E.: Benthic foraminiferal faunal turnover across the
715 Cretaceous/Tertiary Boundary at Agost (Southeastern Spain), *Mar. Micropaleont.*, 48, 251-279, 2003.

716 Alegret, L., Ortiz, S., Arenillas, I., and Molina, E.: Palaeoenvironmental turnover across the
717 Palaeocene/Eocene boundary at the Stratotype section in Dababiya (Egypt) based on benthic
718 foraminifera, *Terra Nova*, 17, 526-536, 2005.

719 Alegret, L., Ortiz, N., and Molina, E.: Extinction and recovery of benthic foraminifera across the
720 Paleocene-Eocene Thermal Maximum at the Alamedilla section (Southern Spain), *Palaeogeogr.*
721 *Palaeocl. Palaeoecol.*, 279, 186-200, 2009a.

722 Alegret, L., Ortiz, S., Orue-Extebarria, X., Bernaola, G., Baceta, J. I., Monechi, S., Apellaniz, E.,
723 Pujalte, V.: The Paleocene-Eocene Thermal Maximum: New data on microfossil turnover at the
724 Zumaia section, Spain, *Palaios*, 24, 318-328, 2009b.

725 Alegret, L., Ortiz, S., Arenillas, I., and Molina, E.: What happens when the ocean is overheated? The
726 foraminiferal response across the Paleocene-Eocene Thermal Maximum at the Alamedilla section
727 (Spain), *Geol. Soc. Am. Bull.*, 122, 1616-1624, 2010.

728 Alve, E., and Goldstein, S. T.: Propagule transport as a key method of dispersal in benthic foraminifera
729 (Protists), *Limnol. Oceanogr.*, 48, 2163-2170, 2003.

730 Arndt, S., Jørgense, B. B., LaRowe, D. E., Middeburg, J. J., Pancost, R. D., and Regnier, P.:
731 Quantifying the degradation of organic matter in marine sediments: a review and synthesis, *Earth-
732 Science Reviews*, 123, 53-86, 2013.

733 Arreguín-Rodríguez, G. J., Alegret, L., and Ortiz, S.: *Glomospira* acme during the Paleocene–Eocene
734 Thermal Maximum: response to CaCO_3 dissolution or to ecological forces?, *J. Foramin. Res.*, 43, 37–
735 49, 2013.

736 Arreguín-Rodríguez, G. J., Alegret, L., Sepúlveda, J., Newman, S., and Summons, R. E.: Enhanced
737 terrestrial input supporting the *Glomospira* acme across the Paleocene-Eocene boundary in Southern
738 Spain, *Micropaleontology*, 60(1), 43-51, 2014.

739 Aubry, M.-P., Ouda, K., Dupuis, C., Berggren, W. A., Van Couvering, J. A., Ali, J., Brinkhuis, H.,
740 Gingerich, P. R., Heilmann-Clausen, C., Hooker, J., Kent, D. V., King, C., Knox, R. W. O. B., Laga,
741 P., Molina, E., Schmitz, B., Steurbaut, E., and Ward, D. R.: The Global Standard Stratotype-Section
742 and Point (GSSP) for the base of the Eocene Series in the Dababiya section (Egypt), *Episodes*, 30, 271–
743 286, 2007.

744 Aze, T., Pearson, P. N., Dickson, A. J., Badger, M. P. S., Bown, P. R., Pancost, R. D., Gibbs, S. J.,
745 Huber, B. T., Leng, M. J., Coe, A. L., Cohen, A. S., and Foster, G. L.: Extreme warming of tropical
746 waters during the Paleocene-Eocene Thermal Maximum, *Geology*, 42, 739-742, 2014.

747 Bains, S., Corfield, R. M., and Norris, R. D.: Mechanisms of climate warming at the end of the
748 Paleocene, *Science*, 285, 724–727, 1999.

749 Bąk, K.: Deep-water agglutinated foraminiferal changes across the Cretaceous/Tertiary and
750 Paleocene/Eocene transitions in the deep flysch environment; eastern part of Outer Carpathians
751 (Bieszczady Mts, Poland), in: *Proceedings of the Six International Workshop on Agglutinated*
752 *Foraminifera*, Prague, Czech Republic, September 1-7, 2001, edited by: Bubik, M., and Kaminski, M.
753 A., *Grzybowski Foundation Special Publication*, Drukarnia Narodowa, Kraków, 8, 1-56, 2004.

754 Barry, J. P., Buck, K. R, Lovera, C. F., Kuhnz, L., Whaling, P. J., Peltzer, E. T., Walz, P., and Brewer,
755 P. G.: Effects of Direct Ocean CO_2 Injection on Deep-Sea Meiofauna, *J. Oceanogr.*, 60, 759-766, 2004.

756 Beckmann, J. P.: Distribution of benthonic foraminifera at the Cretaceous-Tertiary boundary of
757 Trinidad (West Indies), in: *International Geological Congress Report*, 21 Session Norden, Copenhagen.
758 Part 5: The Cretaceous-Tertiary boundary, 57-59, 1960.

759 Benjamini, C.: The Paleocene-Eocene boundary in Israel. A candidate for the boundary stratotype,
760 *Neues Jahrb. Geol. P.-A.*, 186, 49-61, 1992.

761 Berggren, W. A., and Aubert, J.: Paleocene benthonic foraminiferal biostratigraphy, paleobiogeography
762 and paleoecology of Atlantic-Tethyan regions: Midway type fauna, *Palaeogeogr. Palaeocl. Palaeoecol.*,
763 18, 73–192, 1975.

764 Berggren, W. A., and Miller, K. G.: Cenozoic bathyal and abyssal calcareous benthic foraminiferal
765 zonation, *Micropaleontology*, 35, 308–320, 1989.

766 Bernhard, J. M., and Sen Gupta, B. K.: Foraminifera of oxygen deplete environments, in: Sen Gupta, B.
767 K. (Ed.), *Modern Foraminifera*, Dordrecht, Kluwer Academic Publishers, 201-216, 1999.

768 Boersma, A.: **Oligocene and Other Tertiary Benthic Foraminifers from a Depth Traverse Down Walvis**
769 **Ridge, Deep Sea Drilling Project Leg 74, Southeast Atlantic, Initial Rep. Deep Sea**, 75, 1273-1300,
770 1984.

771 Boltovskoy, E., Scott, D.B., and Medioli, F.S.: Morphological variations of benthic foraminiferal tests
772 in response to changes in ecological parameters; a review, *J. Palaeontol.*, 65, 175-185, 1991.

773 Bornemann, A., Norris, R. D., Lyman, J. A., D'haenens, S., Groeneveld, J., Röhl, U., Farley, K. A., and
774 Speijer, R.P.: Persistent environmental change after the Paleocene–Eocene Thermal Maximum in the
775 eastern North Atlantic, *Earth Planet. Sc. Lett.*, 394, 70–81, 2014.

776 Boscolo Galazzo, F., Giusberti, L., Luciani, V., and Thomas, E.: Paleoenvironmental changes during
777 the Middle Eocene Climatic Optimum (MECO) and its aftermath: the benthic foraminiferal record
778 from the Alano section (NE Italy), *Palaeogeogr. Palaeocl. Palaeoecol.*, 378, 22–35, 2013.

779 Boscolo Galazzo, F., Thomas, E., Pagani, M., Warren, C., Luciani, V., Giusberti, L.: The middle
780 Eocene climatic optimum (MECO): A multiproxy record of paleoceanographic changes in the
781 southeast Atlantic (ODP Site 1263, Walvis Ridge), *Paleoceanography*, 29, 1143-1161, 2014.

782 Boscolo-Galazzo, F., Thomas, E., Giusberti, L.: Benthic foraminiferal response to the Middle Eocene
783 Climatic Optimum (MECO) in the Southeastern Atlantic (ODP Site 1263). *Palaeogeogr. Palaeocl.*
784 *Palaeoecol.*, 417, 432-444, 2015.

785 Bowen, G. J., Beerling, D. J., Koch, P.L., Zachos, J.C, Quattlebaum, T.: A humid climate state during
786 the Palaeocene/Eocene thermal maximum, *Nature*, 432, 495–499, 2004.

787 Bowen, G. J., Maibauer, B. J., Kraus, M. J., **Röhl**, U., Westerhold. T., Steike, A., Gingerich, P. D.,
788 Wing, S. L., and Clyde, W. J.: Two massive, rapid release of carbon during the onset of the
789 Palaeocene-Eocene thermal maximum, *Nat. Geosci.*, 8, 44-47, 2015.

790 Braga, G., De Biase, R., Gruning, A., and Proto Decima, F.: Foraminiferi bentonici del Paleocene e
791 dell'Eocene della sezione di Possagno, in: *Monografia micropaleontogica sul Paleocene e l'Eocene di*
792 *Possagno, Provincia di Treviso, Italia*, edited by: Bolli, H. M., *Schweizerische Paläontologische*
793 *Abhandlungen*, Basel, 97, 85-111, 1975.

794 Bralower, T. J.: Evidence of surface water oligotrophy during the Paleocene-Eocene thermal
795 maximum: Nannofossil assemblage data from Ocean Drilling Program Site 690, Maud Rise, Weddell
796 Sea, *Paleoceanography*, 17, 1023, 2002.

797 Broecker, W. S., and Peng, T-H.: *Tracers in the sea*. Palisades, New York, Eldigio Press, 690 pp., 1982.

798 Buzas, M. A., Culver, S. J., and Jorissen, F. J.: A statistical evaluation of the microhabitats of living
799 (stained) infaunal benthic foraminifera, *Mar. Micropaleont.*, 29, 73–76, 1993.

800 Cetean, C., Setoyama, E., Kaminski, M. A., Neagu, T., Bubík, M., Filipescu, S., and Tyszka:
801 *Eobigenerina*, n. gen., a cosmopolitan deep-water agglutinated foraminifer, and remarks on species
802 formerly assigned to the genera *Pseudobolivina* and *Bigenerina*, in: *Eight International Workshop on*
803 *Agglutinated Foraminifera, Abstract Volume*, edited by: Filipescu, S., and Kaminski, M. A.,
804 *Grzybowski Foundation Special Publication*, Presa Universitară Clujeană, Romania, 14, 6-7, 2008a.

805 Cetean, C., Bălcăi, R., Kaminski, M. A., and Filipescu, S.: Biostratigraphy of the Cenomanian-Turonian
806 boundary in the Eastern Carpathians (Dâmbovița Valley): preliminary observations, *Stud. Univ. Babeș-*
807 *Bol., Geologia*, 53 (1), 11-23, 2008b.

808 Cetean, C., Setoyama, E., Kaminski, M. A., Neagu, T., Bubík, M., Filipescu, S. and Tyszka, J.:
809 *Eobigenerina*, a cosmopolitan deep-water agglutinated foraminifer, and remarks on late Paleozoic to
810 Mesozoic species formerly assigned to *Pseudobolivina* and *Bigenerina*, in: *Proceedings of the Eight*
811 *International Workshop on Agglutinated Foraminifera*, edited by: Filipescu, S. and Kaminski, M. A.

812 (Eds.), Grzybowski Foundation Special Publication, Presa Universitară Clujeană, Romania, 16, 19-27,
813 2011.

814 Chun, C. O. J., Delaney, M. L., and Zachos, J. C.: Paleoredox changes across the Paleocene-Eocene
815 thermal maximum, Walvis Ridge (ODP Sites 1262, 1263, and 1266): Evidence from Mn and U
816 enrichment factors, *Paleoceanography*, 25(4), PA4202, 2010.

817 Coccioni, R. and Galeotti, S.: Orbitally induced cycles in benthic foraminiferal morphogroups and
818 trophic structure distribution patterns from the *late Albian “Amadeus Segment”* (Central Italy), *J.*
819 *Micropalaeont.*, 12, 227–239, 1993.

820 Coccioni, R., Bancala, G., Catanzariti, R., Fornaciari, E., Frontalini, F., Giusberti, L., Jovane, L.,
821 Luciani, V., Savian, J., and Sprovieri, M.: An integrated stratigraphic record of the Palaeocene-lower
822 Eocene at Gubbio (Italy): new insights into the early Palaeogene hyperthermals and carbon isotope
823 excursions, *Terra Nova*, 45, 380-386, 2012.

824 Collinson, M. E., Steart, D. C., Scott, A. C., Glasspool, I. J., and Hooker, J. J.: Episodic fire, runoff and
825 deposition at the Palaeocene–Eocene boundary, *J. Geol. Soc. London*, 164, 87–97, 2007.

826 Corliss, B. H.: Microhabitats of Benthic Foraminifera within deep-sea sediments, *Nature*, 314, 435–
827 438, 1985.

828 Corliss, B. H. and Chen, C.: Morphotype patterns of Norwegian Sea deep-sea benthic foraminifera and
829 ecological implications, *Geology*, 16, 716–719, 1988.

830 ~~Colosimo, A. B., Bralower, T. J., and Zachos, J. C.: Evidence of lysocline shoaling at the
831 Paleocene/Eocene Thermal Maximum on Shatsky Rise, northwest Pacific, *Proceedings of the Ocean
832 Drilling Program, Scientific Results 198: College Station, Texas*, 1-36, 2006.~~

833 Cramer, B. S., Wright, J. D., Kent, D. V., and Aubry, M.-P.: Orbital climate forcing of $\delta^{13}\text{C}$ excursions
834 in the late Paleocene-early Eocene (chrons C24n-C25n), *Paleoceanography*, 18, 1097, 2003.

835 Crouch, E. M., Dickens, G. R., Brinkhuis, H., Aubry, M.-P., Hollis, C. J., Rogers, K. M., and Visscher,
836 H.: The *Apectodinium* acme and terrestrial discharge during the Paleocene-Eocene thermal maximum:

837 New palynological, geochemical and calcareous nannoplankton observations at Tawanui, New
838 Zealand, *Palaeogeogr. Palaeocl. Palaeoecol.*, 194, 387–403, 2003.

839 Dallanave, E., Tauxe, L., Muttoni, G., and Rio, D.: Silicate weathering machine at work: rock magnetic
840 data from the late Paleocene–early Eocene Cicogna section, Italy, *Geochem. Geophys. Geosy.*, 11(7),
841 Q07008, 2010.

842 Dallanave, E., Muttoni, G., Agnini, C., Tauxe, L., and Rio, D.: Is there a normal magnetic-polarity
843 event during the Palaeocene–Eocene thermal maximum (~55 Ma)? Insights from the palaeomagnetic
844 record of the Belluno Basin (Italy), *Geophys. J. Int.*, 191, 517-529, 2012.

845 DeConto, R. M., Galeotti, S., Pagani, M., Tracy, D., Schaefer, K., Zhang, T., Pollard, D., Beerling, D.
846 J.: Past extreme warming events linked to massive carbon release from thawing permafrost, *Nature*,
847 484, 87–91, 2012.

848 D'haenens, S., Bornemann, A., Stassen, P., and Speijer, R.: Multiple early Eocene benthic foraminiferal
849 assemblage and $\delta^{13}\text{C}$ fluctuations at DSDP Site 401 (Bay of Biscay-NE Atlantic), *Mar. Micropaleont.*,
850 88-89, 15-35, 2012.

851 Dickens, G. R., 2011: Down the rabbit hole, toward appropriate discussion of methane release from gas
852 hydrate systems during the Paleocene-Eocene thermal maximum and other past hyperthermal events,
853 *Clim. Past*, 7, 831-846, 2011.

854 Dickens, G. R., Castillo, M. M., and Walker, J. C. G.: A blast of gas in the latest Paleocene: Simulating
855 first-order effects of massive dissociation of oceanic methane hydrate, *Geology*, 25, 259-262, 1997.

856 Dickson, A. J., Rees-Owen, R. L., März, C., Coe, A. L., Cohen, A. S., Pancost, R. D., Taylor, K., and
857 Shcherbinina, E.: The spread of marine anoxia on the northern Tethys margin during the Paleocene-
858 Eocene Thermal Maximum, *Paleoceanography*, 29, 471-488, 2014.

859 Di Napoli Alliata, E., Proto Decima, F., and Pellegrini, G. B.: Studio geologico, stratigrafico e
860 micropaleontologico dei dintorni di Belluno, *Memorie della Società Geologica Italiana*, 9, 1-28, 1970.

861 Dunkley Jones, T., D. J. Lunt, D. N. Schmidt, A. Ridgwell, A. Sluijs, P. J. Valdez, and M. A. Maslin:
862 Climate model and proxy data constraints on ocean warming across the Paleocene–Eocene Thermal
863 Maximum, *Earth Science Reviews*, 125, 123–145, 2013.

864 Dypvik, H., Riber, L., Burca, F., Rüther, D., Jargvoll, D., Nagy, J., and Jochmann, M.: The Paleocene–
865 Eocene thermal maximum (PETM) in Svalbard — clay mineral and geochemical signals, *Palaeogeogr.*
866 *Palaeocl. Palaeoecol.*, 302, 156–169, 2011.

867 Egger, H., Fenner, J., Heilmann-Clausen, C., Roegl, F., Sachsenhofer, R. F., and Schmitz, B.:
868 Paleoproductivity of the northwestern Tethyan margin (Anthering section, Austria) across the
869 Paleocene–Eocene transition, in: *Causes and Consequences of Globally Warm Climates in the Early*
870 *Paleogene*, edited by: Wing, S.L., Gingerich, P. D., Schmitz, B., and Thomas, E., *Geol. S. Am. S.*,
871 Boulder, Colorado, The Geological Society of America, 369, 133–146, 2003.

872 Egger, H., Homayoun, M., Huber, H., Roegl, F., Schmitz, B.: Early Eocene climatic, volcanic, and
873 biotic events in the northwestern Tethyan Untersberg section, Austria, *Palaeogeogr. Palaeocl.*
874 *Palaeoecol.*, 217, 243– 264, 2005.

875 Egger, H., Heilmann-Clausen, C., Schmitz, B.: From shelf to abyss: Record of the Paleocene/Eocene-
876 boundary in the Eastern Alps (Austria), *Geol. Acta*, 7, 215–227, 2009.

877 Ernst, S. R., Guasti, E., Dupuis, C., and Speijer, R. P., Environmental perturbation in the southern
878 Tethys across the Paleocene/Eocene boundary (Dababyia, Egypt): Foraminiferal and clay minerals
879 record, *Mar. Micropaleont.*, 60, 89-111, 2006.

880 ~~Fenero, R., Thomas, E., Alegret, L., and Molina, E.: Oligocene benthic foraminifera in the Fuente~~
881 ~~Caldera section (Betic Cordillera, Spain): paleoenvironmental inferences. J. Foramin. Res.~~, 42, 286
882 ~~304, 2012.~~

883 Fontanier, C., Jorissen, F. J., Chaillou, G., Anschutz, P., Gremare, A., and Griveaud, C.: Live
884 foraminiferal faunas from a 2800 m deep lower canyon station from the Bay of Biscay: faunal response
885 to focusing of refractory organic matter, *Deep-Sea Res. I*, 52, 1189-1227, 2005.

886 ~~Fontanier, C., Jorissen, F. J., Anschutz, P., and Chaillou, G.: Seasonal variability of benthic~~
887 ~~foraminiferal faunas at 1000 m depth in the Bay of Biscay, J. Foramin. Res.~~, 36, 61-76, 2006a.

888 Fontanier, C., Mackensen, A., Jorissen, F. J., Anschutz, P., Licari, L., and Griveaud, C.: Stable oxygen
889 and carbon isotopes of live benthic foraminifera from the Bay of Biscay: Microhabitat impact and
890 seasonal variability, *Mar. Micropaleont.*, 58, 159-183, 2006b.

891 Fontanier, C., Duros, P., Toyofuku, T., Oguri, K., Koho, K. A., Buscail, R., Grémare, A., Radakovitch,
892 O., Deflandre, B., de Nooijer, L.J., Bichon, S., Goubet, S., Ivanovsky, A., Chabaud, G., Menniti, C.,
893 Reichart, G.-J., and Kitazato, H.: Living (stained) deep-sea foraminifera off Hachinohe (NE JAPAN,
894 Western Pacific): environmental interplay in oxygen-depleted ecosystems, *J. Foramin. Res.*, 44, 281-
895 299, 2014.

896 Foreman, B. Z., Heller, P. L., Clementz, M. T.: Fluvial response to abrupt global warming at the
897 Palaeocene/Eocene boundary, *Nature*, 491, 92-95, 2014.

898 Fornaciari, E., Giusberti, L., Luciani, V., Tateo, F., Agnini, C., Backman, J., Oddone, M., and Rio, D.:
899 An expanded Cretaceous–Tertiary transition in a pelagic setting of the Southern Alps (central–western
900 Tethys), *Palaeogeogr. Palaeocl. Palaeoecol.*, 255, 98–131, 2007.

901 Foster, L. C., Schmidt, D. N., Thomas, E., Arndt, S., Ridgwell, A.: Surviving rapid climate change in
902 the deep sea during the Paleogene hyperthermals, *Proc. Natl. Acad. Sci.*, 110(23), 9273-9276, 2013.

903 Frenzel, P.: Die benthischen Foraminiferen der Ruegener Schreibkreide (Unter Maastricht, NE
904 Deutschland), *Neue Palaeontologische Abhandlungen*, Dresden, Germany, CPress Verlag, Band 3,
905 2000.

906 Friedrich, O.: Benthic foraminifera and their role to decipher paleoenvironment during mid-Cretaceous
907 Oceanic Anoxic Events—"the anoxic benthic foraminifera" paradox, *Revue de Micropaléontologie*, 177,
908 2-18, 2009.

909 Friedrich, O., Nishi, H., Pross, J., Schmiedel, G., Hemleben, C.: Millennial-to centennial scale
910 interruptions of the Oceanic Anoxic Event 1b (early Albian, mid Cretaceous) inferred from benthic
911 foraminiferal repopulation events, *Palaios*, 20, 64-77, 2005.

912 ~~Galeotti, S., Bellagamba, M., Kaminski, M. A., and Montanari, A.: Deep sea benthic foraminiferal
913 recolonisation following a volcanielastic event in the lower Campanian of the Seaglia Rossa Formation
914 (Umbria-Marche Basin, central Italy), *Mar. Micropaleont.*, 44, 57-76, 2002.~~

915 Galeotti, S., Kaminski, M. A., Coccioni, R., and Speijer, R.: High resolution deep water agglutinated
916 foraminiferal record across the Paleocene/Eocene transition in the Contessa Road Section (central
917 Italy), in: Proceedings of the Sixth International Workshop on Agglutinated Foraminifera, edited by:
918 Bubik, M. and Kaminski, M. A. (Eds.), Grzybowski Foundation Special Publication, Drukarnia
919 Narodowa, Kraków, 8, 83–103, 2004.

920 Garel, S., Schnyder, J., Jacob, J., Dupuis, C., Boussafir, M., Le Milbeau, C., Storme, J.-Y., Iakovleva,
921 A. I., Yans, J., Baudin, F., Fléhoc C., and Quesnel, F.: Paleo hydrological and paleoenvironmental
922 changes recorded in terrestrial sediments of the Paleocene–Eocene boundary (Normandy, France),
923 *Palaeogeogr. Palaeoecol. Palaeoecol.*, 376, 184–199, 2013.

924 Gavrilov, Y. O., Kodina, L. A., Lubchenko, I. Y., and Muzylev, N. G.: The late Paleocene anoxic event
925 in epicontinental seas of Peri-Tethys and formation of the sapropelite unit; sedimentology and
926 geochemistry, *Lithol. Miner. Resour.*, 32, 427–450, 1997.

927 Gibbs, S. J., Bralower, T. J., Bown, P. R., Zachos, J. C., and Bybell, L.M.: Shelf and open-ocean
928 calcareous phytoplankton assemblages across the Paleocene-Eocene Thermal Maximum: Implications
929 for global productivity gradients, *Geology*, 34, 233-236, 2006.

930 Gibson, T. G., Bybell, L. M., and Owens, J. P.: Latest Paleocene lithologic and biotic events in neritic
931 deposits of southwestern New-Jersey, *Paleoceanography*, 8 (4), 495–514, 1993.

932 Gibson, T. G., Bybell, L. M., and Mason, D.B.: Stratigraphic and climatic implications of clay mineral
933 changes around the Paleocene/Eocene boundary of the northeastern US margin, *Sediment. Geol.*, 134,
934 65–92, 2000.

935 Gingerich, P. D.: Mammalian response to climate change at the Paleocene-Eocene boundary: Polecat
936 Bench record in the northern Bighorn Basin, Wyoming, in: Wing, S.L., Gingerich, P. D., Schmitz, B.,
937 and Thomas, E., *Geol. S. Am. S.*, Boulder, Colorado, The Geological Society of America, 369, 463–
938 478, 2003.

939 Giusberti, L., Rio, D., Agnini, C., Backman, J., Fornaciari, E., Tateo, F., and Oddone, M.: Mode and
940 tempo of the Paleocene-Eocene Thermal Maximum from the Venetian pre-Alps, *Geol. Soc. Am. Bull.*,
941 119, 391-412, 2007.

942 Giusberti, L., Coccioni, R., Sprovieri, M., and Tateo, F.: Perturbation at the sea floor during the
943 Paleocene–Eocene Thermal Maximum: evidence from benthic foraminifera at Contessa Road, Italy,
944 *Mar. Micropaleont.*, 70, 102–119, 2009.

945 Gooday, A. J.: Deep-sea benthic foraminiferal species which exploit phytodetritus: characteristic
946 features and controls on distribution, *Mar. Micropaleont.*, 22, 187-205, 1993.

947 Gooday, A. J.: The biology of deep-sea Foraminifera: a review of some advances and their applications
948 in paleoceanography, *Palaios*, 9, 14-31, 1994.

949 Gooday, A. J.: Benthic foraminifera (Protista) as tools in deep-water paleoceanography: Environmental
950 influences on faunal characteristics, *Adv. Mar. Biol.*, 46, 1-90, 2003.

951 Gooday, A. J., Hughes, J. A., and Levin, L. A.: The foraminiferan macrofauna from three North
952 Carolina (U.S.A.) slope sites with contrasting carbon flux: a comparison with the metazoan
953 macrofauna, *Deep-Sea Res. I*, 48, 1709-1739, 2001.

954 Gooday, A. J., Nomaki, H., and Kitazato, H.: Modern deep-sea benthic foraminifera: a brief review of
955 their morphology-based biodiversity and trophic diversity, in: *Biogeochemical Controls on*
956 *Palaeoceanographic Environmental Proxies*, edited by: Austin, W. E. N. and James, R. H., *Geol. Soc.*
957 *Spec. Publ.*, Bath, UK, The Geological Society Publishing House, 303, 97–119, 2008.

958 Guasti, E., and Speijer, R. P.: The Paleocene-Eocene Thermal Maximum in Egypt and Jordan: An
959 overview of the planktic foraminiferal record, in: *Large Ecosystem Perturbations: Causes and*
960 *Consequences*, edited by: Monechi, S., Coccioni, R., and Rampino, M., *Geol. S. Am. S.*, Boulder,
961 Colorado, The Geological Society of America, 424, 53–67, 2007.

962 Gupta, A. K. and Thomas, E.: Latest Miocene-Pleistocene productivity and deep-sea ventilation in the
963 northwestern Indian Ocean (Deep Sea Drilling Project Site 219), *Paleoceanography*, 14, 62-73, 1999.

964 Gupta, A. K., and Thomas, E.: Initiation of Northern Hemisphere glaciation and strengthening of the
965 northeast Indian monsoon: Ocean Drilling Program Site 758, eastern equatorial Indian Ocean, *Geology*,
966 31(1), 47-50, 2003.

967 Gupta, A. K., Sundar Raj, M., Mohan, K., De, S.: A major change in monsoon-driven productivity in
968 the tropical Indian Ocean during ca 1.2–0.9 Myr: Foraminiferal faunal and stable isotope data,
969 *Palaeogeogr. Palaeoocl. Palaeoecol.*, 261, 234–245, 2008.

970 Hammer, Ø., Harper, D. A. T., and Ryan, P. D.: PAST: Paleontological Statistics Software Package for
971 Education and Data Analysis, *Palaeontol. Electron.* 4 (1), 1–9, 2001.

972 Hancock, H. J. L., and Dickens, G. R.: Carbonate dissolution episodes in Paleocene and Eocene
973 sediment, Shatsky Rise, west-central Pacific, in: Bralower, T. J., Premoli Silva, I., and Malone, M. J.
974 (Eds.), *Proceedings of the Ocean Drilling Program, Scientific Results*, 198, http://www-odp.tamu.edu/publications/198_SR/116/116.htm, 2005.

975

976 Handley, L., Pearson, P. N., McMillan, I. K., and Pancost, R. D.: Large terrestrial and marine carbon
977 and hydrogen isotope excursions in a new Paleocene/Eocene boundary section from Tanzania, *Earth*
978 *Planet. Sc. Lett.*, 275, 17–25, 2008.

979 Handley, L., O'Halloran, A., Pearson, P. N., Hawkins, E., Nicholas, C. J., Schouten, S., McMillan, I.
980 K., and Pancost, R. D.: Changes in the hydrological cycle in tropical East Africa during the Paleocene–
981 Eocene Thermal Maximum, *Palaeogeogr. Palaeoocl. Palaeoecol.*, 329–330, 10–21, 2012.

982 Harding, I. C., Charles, A. J., Marshall, J. E. A., Pälike, H., Roberts, A. P., Wilson, P. A., Jarvis, E.,
983 Thorne, R., Morris, E., Moremon, R., Pearce, R. B., and Akbari, S.: Sea-level and salinity fluctuations
984 during the Paleocene–Eocene thermal maximum in Arctic Spitsbergen, *Earth Planet. Sc. Lett.*, 303, 97–
985 107, 2011.

986 Harries, P. J. and Kauffman, E. G.: Patterns of survival and recovery following the Cenomanian–
987 Turonian (Late Cretaceous) mass extinction in the Western Interior Basin, United States, in: *Extinction*
988 *events in Earth History*, edited by: Kauffman, E. G. and Walliser, O. H., *Lect. Notes Earth Sci.*
989 Heidelberg Germany, Springer-Verlag, 30, 277–298, 1990.

990 ~~990 Harries, P. J., Kauffman, E. G., and Hansen, T. A.: Models for biotic survival following mass~~
991 ~~extinction, in: Biotic Recovery from Mass Extinction Events, edited by: Hart, M. B., Geol. Soc. Spec.~~
992 ~~Publ., The Geological Society Publishing House, Bath, UK, 102, 41–60, 1996.~~

993 Hayward, B. W., Johnson, K., Sabaa, A.T., Kawagata, S., and Thomas, E.: Cenozoic record of
994 elongate, cylindrical, deep-sea benthic foraminifera in the North Atlantic and equatorial Pacific
995 Oceans, *Mar. Micropaleont.*, 62, 141-162, 2010a.

996 Hayward, B. W., Sabaa, A. T., Thomas, E., Kawagata, S., Nomura, R., Schroder Adams, C., Gupta, A.
997 K., and Johnson, K.: Cenozoic record of elongate, cylindrical, deep-sea benthic foraminifera in the
998 Indian Ocean (ODP Sites 722, 738, 744, 758, and 763), *J. Foramin. Res.*, 40, 113-133, 2010b.

999 Hayward, B. W., Kawagata, S., Sabaa, A. T., Grenfell, H. R., van Kerckhoven, L., Johnson, K., and
1000 Thomas, E.: The Last Global Extinction (Mid-Pleistocene) of Deep-Sea Benthic Foraminifera
1001 (Chrysogoniidae, Ellipsoidinidae, Glandulonodosariidae, Plectofrondiculariidae, Pleurostomellidae,
1002 Stilostomellidae), their Late Cretaceous-Cenozoic History and Taxonomy, Cushman Foundation for
1003 Foraminiferal Research Special Publication, 43, Allen Press, Lawrence, USA, 408 pp., 2012.

1004 ~~Hess, S. and Jorissen, F. J.: Distribution patterns of living benthic foraminifera from Cap Breton
1005 canyon, Bay of Biscay: Faunal response to sediment instability, Deep Sea Res. Part I: Oceanographic
1006 Research Papers 56(9), 1555-1578, 2009.~~

1007 Holbourn, A. and Kuhnt, W.: No extinctions during Oceanic Anoxic Event 1b: the Aptian-Albian
1008 benthic foraminiferal record of ODP Leg 171, edited by: Kroon, D., Norris, R. D., and Klaus, A., Geol.
1009 Soc. London, Spec. Publ., Bath, UK, The Geological Society Publishing House, 183, 73-92, 2001.

1010 Holbourn, A., Kuhnt, W., Erbacher, J.: Benthic foraminifers from lower Albian black shales (Site 1049,
1011 ODP Leg 171): evidence for a non “uniformitarian” record, *J. Foramin. Res.*, 31, 60–74, 2001.

1012 Hönisch, B., Ridgwell, A., Schmidt, D. N., Thomas, E., Gibbs, S. J., Sluijs, A., Zeebe, R., Kump, L.,
1013 Martindale, R. C., Greene, S. E., Kiessling, W., Ries, J., Zachos, J. C., Royer, D. L., Barker, S.,
1014 Marchitto, T. M., Moyer, R., Pelejero, C., Ziveri, P., Foster, G. L., and Williams, B.: The Geological
1015 Record of Ocean Acidification, *Science*, 335, 1058-1963, 2012.

1016 Ishman, S. E., and Domack, E. W.: Oceanographic controls on benthic foraminifers from the
1017 Bellingshausen margin of the Antarctic Peninsula, *Mar. Micropaleont.*, 24, 119-155, 1994.

1018 Itambi, A. C., von Dobeneck, T., Mulitza, S., Bickert, T., and Heslop D.: Millennial-scale northwest
1019 African droughts related to Heinrich events and Dansgaard-Oeschger cycles: Evidence in marine
1020 sediments from offshore Senegal, *Paleoceanography*, 24, PA1205, 2009.

1021 Jaramillo, C. A., Ochoa, D., Contreras, L., Pagani, M., Carvajal-Ortiz, H., Pratt, L. M., Krishnan, S.,
1022 Cardona, A., Romero, M., Quiroz, L., Rodriguez, G., Rueda, M. J., De la Parra, F., Morón, S., Green,
1023 W., Bayona, G., Montes, C., Quintero, O., Ramirez, R., Mora, G., Schouten, S., Bermudez, H.,
1024 Navarrete, R., Parra, F., Alvarán, M., Osorno, J., Crowley, J. L., Valencia, V., and Vervoort, J.: Effects
1025 of rapid global warming at the Paleocene-Eocene boundary on Neotropical vegetation, *Science*, 330,
1026 957–961, 2010.

1027 John, C. M., Bohaty, S. M., Zachos, J. C., Sluijs, A., Gibbs, S., Brinkhuis, H., and Bralower, T. J.:
1028 North American continental margin records of the Paleocene-Eocene thermal maximum: Implications
1029 for global carbon and hydrological cycling, *Paleoceanography*, 23, PA2217, 2008.

1030 ~~John, C. M., Banerjee, N. R., Longstaffe, F. J., Sica, C., Law, K. R., Zachos, J. C.: Clay assemblage
1031 and oxygen isotopic constraints on the weathering response to the Paleocene Eocene thermal
1032 maximum, east coast of North America, *Geology*, 40, 591–594, 2012.~~

1033 John, E. H., Pearson, P. N., Coxall, H. K., Birch, H., Wade, B. S., and Foster, G. L.: Warm ocean
1034 processes and carbon cycling in the Eocene, *Phil. T. Roy. Soc. A*, 371, 20130099, 2013.

1035 John, E. H., Wilson, J. D., Pearson, P. N., and Ridgwell, A.: Temperature-dependent remineralization
1036 and carbon cycling in the warm Eocene oceans, *Palaeogeogr. Palaeoecol. Palaeoecol.*, 413, 158–166,
1037 2014.

1038 Jones, R. W. and Charnock, M. A.: “Morphogroups” of agglutinated foraminifera. Their life positions
1039 and feeding habits and potential applicability in (paleo)ecological studies, *Revue de Paléobiologie*, 4,
1040 311–320, 1985.

1041 ~~Jones, B. and Manning, D. A. C.: Comparison of geochemical indices used for the interpretation of
1042 palaeoredox conditions in ancient mudstones, *Chem. Geol.*, 111, 111–194, 1994.~~

1043 Jorissen, F. J.: Benthic foraminiferal successions across late Quaternary Mediterranean sapropels, *Mar.
1044 Geol.*, 153, 91–101, 1999.

1045 Jorissen, F. J., De Stigter, H. C., and Widmark, J. G. V.: A conceptual model explaining benthic
1046 foraminiferal microhabitats, *Mar. Micropaleont.*, 26, 3–15, 1995.

1047 Jorissen, F. J., Fontanier, C., and Thomas, E.: Paleoceanographical proxies based on deep-sea benthic
1048 foraminiferal assemblage characteristics, in: *Proxies in Late Cenozoic Paleoceanography: Pt. 2:*
1049 *Biological tracers and biomarkers*, edited by: Hillaire-Marcel, C. and A. de Vernal, A., 1, Elsevier,
1050 Amsterdam, The Netherlands, 264–325, 2007.

1051 Kaiho, K.: Phylogeny of deep-sea calcareous trochospiral benthic foraminifera: evolution and
1052 diversification, *Micropalaeontology*, 44, 291–311, 1998.

1053 Kaiho, K., Arinobu, T., Ishiwatari, R., Morgans, H. E. G., Okada, H., Takeda, N., Tazaki, K., Zhou, G.
1054 P., Kajiwara, Y., Matsumoto, R., Hirai, A., Niitsuma, N., and Wada, H.: Latest Paleocene benthic
1055 foraminiferal extinction and environmental changes at Tawanui, New Zealand, *Paleoceanography*, 11,
1056 447–465, 1996.

1057 Kaminski M. A. and Gradstein, F. M.: An Atlas of Paleogene Cosmopolitan Deep-Water Agglutinated
1058 Foraminifera, Grzybowski Foundation Special Publication, Drukarnia Narodowa, Kraków, 10, 547 pp.,
1059 2005.

1060 Kaminski, M. A., Kuhnt, W., and Radley, J. D.: Paleocene–Eocene deep water agglutinated
1061 foraminifera from the Numidian Flysch (Rift, Northern Morocco): Their significance for the
1062 paleoceanography of the Gibraltar gateway, *J. Micropaleontol.*, 15, 1–19, 1996.

1063 Katz, M. E., Wright, J. D., Katz, D. R., Miller, K. G., Pak, D. K., Shackleton, N. J., and Thomas, E.:
1064 Early Cenozoic benthic foraminiferal isotopes: species reliability and interspecies correction factors,
1065 *Paleoceanography*, 18, 1024, 2003.

1066 ~~Kauffman, E. G. and Harries, P. J.: The importance of crisis progenitors in recovery from mass
1067 extinction, in: *Biotic Recovery from Mass Extinction Events*, edited by: Hart, M. B., Geol. Soc. Spec.
1068 Publ., The Geological Society Publishing House, Bath, UK, 102, 15–39, 1996.~~

1069 Kelly, D. C., Bralower, T. J., Zachos, J. C., Premoli Silva, I., and Thomas, E.: Rapid diversification of
1070 planktonic foraminifera in the tropical Pacific (ODP Site 865) during the late Paleocene thermal
1071 maximum, *Geology* 24, 423–426, 1996.

1072 Kelly, D. C., Bralower, T. J., and Zachos, J. C.: Evolutionary consequences of the latest Paleocene
1073 thermal maximum for tropical planktonic foraminifera, *Palaeogeogr. Palaeocl. Palaeoecol.*, 141, 139-
1074 161, 1998.

1075 Kelly, D. C., Nielsen, T. M. J., McCarren, H. K., Zachos, J. C., and Röhl, U.: Spatiotemporal patterns
1076 of carbonate sedimentation in the South Atlantic: Implications for carbon cycling during the
1077 Paleocene–Eocene thermal maximum, *Palaeogeogr. Palaeocl. Palaeoecol.*, 293, 30-40, 2010.

1078 Kennett, J. P., and Stott, L. D.: Abrupt deep-sea warming, palaeoceanographic changes and benthic
1079 extinctions at the end of the Palaeocene, *Nature*, 353, 225–229, 1991.

1080 Kender, S., Stephenson, M. H., Riding, J.,B., Leng, M. J., O'BKnox, R. W., Peck, V. L., Kendrick, C.
1081 P., Ellis, M. A., Vane, C. H., and Jamieson, R.: Marine and terrestrial environmental changes in NW
1082 Europe preceding carbon release at the Paleocene–Eocene transition, *Earth Planet. Sc. Lett.*, 353–354,
1083 108–120, 2012.

1084 Kirtland Turner, S., and Ridgwell, A.: Recovering the true size of an Eocene hyperthermal from the
1085 marine sedimentary record, *Paleoceanography*, 28(4), 700-712, 2013.

1086 Koutsoukos, E. A. M., Leary, P. M., and Hart, M. B.: Latest Cenomanian–earliest Turonian low-
1087 oxygen tolerant benthonic foraminifera: a case study from the Sergipe Basin (N.E. Brazil) and the
1088 western Anglo-Paris Basin (southern England), *Palaeogeogr. Palaeocl. Palaeoecol.*, 77, 145–177, 1990.

1089 Kraus, M. J. and Riggins, S.: Transient drying during the Paleocene–Eocene Thermal Maximum
1090 (PETM): analysis of paleosols in the Bighorn Basin, Wyoming, *Palaeogeogr. Palaeocl. Palaeoecol.*,
1091 245, 444–461, 2007.

1092 Kraus, M. J., McInerney, F. A., Wing, S. L., Secord, R., Baczyński, A. A., Bloch, J. I.: Paleohydrologic
1093 response to continental warming during the Paleocene–Eocene Thermal Maximum, Bighorn Basin,
1094 Wyoming, *Palaeogeogr. Palaeocl. Palaeoecol.*, 370, 196-208, 2013.

1095 Krishnan, S., Pagani, M., and Agnini, C.: Leaf waxes as recorders of paleoclimatic changes during the
1096 Paleocene–Eocene Thermal Maximum: Regional expressions from the Belluno Basin, *Org. Geochem.*,
1097 80, 8-17, 2015.

1098 Kuhnt, W.: Abyssal recolonization by benthic foraminifera after the Cenomanian/Turonian boundary
1099 anoxic event in the North Atlantic, *Mar. Micropaleont.*, 19, 257-274, 1992.

1100 Kuhnt, W.: Early Danian benthic foraminiferal community structures, *Geulhemmerberg*, SE
1101 Netherlands, *Geol. Mijnbouw*, 75, 163-172, 1996.

1102 Kuhnt, W. and Collins, E. S.: Cretaceous to Paleogene benthic foraminifers from the Iberia abyssal
1103 plain, in: *Proceedings of the ODP*, edited by: Whitmarsh, R. B., Sawyer, D. S., Klaus, A., and Masson,
1104 D. G., *Scientific Results*, 149, College Station, TX Ocean Drilling Program, 203-316, 1996.

1105 Kuhnt, W., Collins, E., and Scott, D. B.: Deep water agglutinated foraminiferal assemblages across the
1106 Gulf Stream: distribution pattern and taphonomy, in: *Proceedings of the Fifth International Workshop*
1107 on Agglutinated Foraminifera, edited by: Hart, M. B., Kaminski, M. A., and Smart, C.W., Grzybowski
1108 Foundation Special Publication, Drukarnia Narodowa, Kraków, 7, 261-298, 2000.

1109 Kuhnt, W. and Kaminski, M. A.: Changes in the community structure of deep-water agglutinated
1110 foraminifers across the K/T boundary in the Basque Basin (northern Spain), *Revista Española de*
1111 *Micropaleontologia*, 25, 57-92, 1993.

1112 Kuhnt, W. and Kaminski, M. A.: The reponse of benthic foraminifera to the K/T boundary event-a
1113 review, in: *Géologie de l'Afrique et de l'Atlantique Sud-Comptes Rendu des Colloques de géologie*
1114 *d'Angers*, 16-20 Juillet, 1994, edited by: Jardiné, S., de Klasz, I., and Debenay, J. P., B. Cent. Rech.
1115 Expl., *Memoire*, Pau, Société nationale Elf Aquitaine, 16, 433-442, 1996.

1116 Larrasoña, J. C., Roberts, A. P., Rohling, E. J., Winklhofer, M., and Wehausen, R.: Three million
1117 years of monsoon variability over the northern Sahara, *Clim. Dynam.*, 21, 689-698, 2003.

1118 Levin, L. A.: **Oxygen Minimum Zone Benthos: Adaptation and Community Response to Hypoxia**,
1119 *Oceanogr. Mar. Biol.*, 41, 1-45, 2003.

1120 Lirer, F.: A new technique for retrieving calcareous microfossils from lithified lime deposits,
1121 *Micropaleontology*, 46 (4), 365-369, 2000.

1122 Littler, K., Röhl, U., Westerhold, T., and Zachos, J. C.: A high-resolution benthic stable-isotope record
1123 for the South Atlantic: Implications for orbital-scale changes in Late Paleocene–Early Eocene climate
1124 and carbon cycling. *Palaeogeogr. Palaeocl. Palaeoecol.*, 401, 18-30, 2014.

1125 Luciani, V., Giusberti, L., Agnini, C., Backman, J., Fornaciari, E., and Rio, D.: The Paleocene-Eocene
1126 Thermal Maximum as recorded by Tethyan planktonic foraminifera in the Forada section (northern
1127 Italy), *Mar. Micropaleont.*, 64, 189-214, 2007.

1128 Ma, Z., Gray, E., Thomas, E., Murphy, B., Zachos, J. C., and Paytan, A.: Carbon sequestration during
1129 the Paleocene-Eocene Thermal maximum by an efficient biological pump. *Nat. Geosci.*, 7, 382-388,
1130 2014.

1131 Mancin, N., Hayward, B. W., Trattenero, I., Cobianchi, M., and Lupi, C.: Can the morphology of deep-
1132 sea benthic foraminifera reveal what caused their extinction during the mid-Pleistocene Climate
1133 Transition? *Mar. Micropaleont.*, 104, 53–70, 2013.

1134 McCarren, H., Thomas, E., Hasegawa, T., Röhl, U., and Zachos, J. C.: Depth dependency of the
1135 Paleocene-Eocene carbon isotope excursion: Paired benthic and terrestrial biomarker records (ODP
1136 Leg 208, Walvis Ridge), *Geochem. Geophys. Geosy.*, 9, Q10008, 2008.

1137 McInerney, F. A. and Wing, S. L.: The Paleocene-Eocene thermal maximum: A perturbation of carbon
1138 cycle, climate, and biosphere with implications for the future, *Annu. Rev. Earth Pl. Sc.*, 39, 489–516,
1139 2011.

1140 Meissner, K. J., Bralower, T. J., Alexander, K., Dunkley Jones, T., Sijp, W., and Ward, M.: The
1141 Paleocene-Eocene Thermal Maximum: how much carbon is enough?, *Paleoceanography*, 29, 946-963,
1142 2014.

1143 Mohan, K., Gupta, A. K., and Bhaumik, A. K.: Distribution of deep-sea benthic foraminifera in the
1144 Neogene of Blake Ridge, NW Atlantic Ocean, *J. Micropalaeontol.*, 30, 33-74, 2011.

1145 Murphy, B. H., Farley, K. A., and Zachos, J. C.: An extraterrestrial ^3He -based timescale for the
1146 Paleocene-Eocene thermal maximum (PETM) from Walvis Ridge, IODP Site 1266, *Geochim.
1147 Cosmochim. Ac.*, 74, 5098-5108, 2010.

1148 Murray, J. W.: *Ecology and palaeoecology of benthic foraminifera*. Longman, Harlow, 397 pp., 1991.

1149 Murray, J. W.: *Ecology and Applications of Benthic Foraminifera*, Cambridge University Press, USA,
1150 xi + 426 pp., 2006.

1151 Murray, J. W. and Pudsey, C. J.: Living (stained) and dead foraminifera from the newly ice-free Larsen
1152 Ice Shelf, Weddell Sea, Antarctica: ecology and taphonomy, *Mar. Micropal.*, 53, 67-81, 2004.

1153 Nagy, J., Jargvoll, D., Dypvik, H., Jochmann, M., and Riber, L.: *Environmental changes during the*
1154 *Paleocene-Eocene Thermal Maximum in Spitsbergen as reflected by benthic foraminifera*, *Polar Res.*,
1155 32, 19737, 2013.

1156 Nicolo, M. J., Dickens, G. R., and Hollis, C. J.: South Pacific intermediate water oxygen depletion at
1157 the onset of the Paleocene-Eocene thermal maximum as depicted in New Zealand margin sections,
1158 *Paleoceanography* 25, PA4210, 2010.

1159 Nomura, R.: Paleogene to Neogene deep-sea paleoceanography in the eastern Indian Ocean: benthic
1160 foraminifera from ODP Sites 747, 757 and 758, *Micropaleontology*, 41, 251-290, 1995.

1161 Ortiz, N.: Differential patterns of benthic foraminiferal extinctions near the Paleogene/Eocene
1162 boundary in the North Atlantic and western Tethys, *Mar. Micropaleont.*, 26, 341-359, 1995.

1163 ~~Ortiz, S., Alegret, L., Payros, A., Orue Extebarria, X., Apellaniz, E., Molina, E.: Distribution pattern of~~
1164 ~~benthic foraminifera across Ypresian Lutetian Gorronatxe section, Northern Spain: Response to~~
1165 ~~sedimentary disturbance~~. *Mar. Micropaleont.*, 78, 1-13, 2011.

1166 Pälike, C., Delaney, M. L., and Zachos, J. C.: Deep-sea redox across the Paleocene-Eocene thermal
1167 maximum, *Geochem. Geophys. Geosy.*, 15, 1038-1053, 2014.

1168 Pagani, M., Caldeira, K., Archer, D., and Zachos, J. C.: An ancient carbon mystery, *Science*, 314,
1169 1556-1557, 2006a.

1170 Pagani, M., Pedentchouk, N., Huber, M., Sluijs, A., Schouten, S., Brinkhuis, H., Sinninghe Damsté, J.
1171 S., Dickens, G. R., & the Expedition 302 Scientists: Arctic hydrology during global warming at the
1172 Palaeocene/Eocene Thermal Maximum, *Nature*, 442, 671-675, 2006b.

1173 Panchuk, K., Ridgwell, A., and Kump, L. R.: Sedimentary response to Paleocene-Eocene Thermal
1174 Maximum carbon release: A model-data comparison, *Geology*, 36 (4), 315–318, 2008.

1175 Panieri, G., Sen Gupta, B. K.: Benthic foraminifera of the Blake Ridge hydrate mound, Western North
1176 Atlantic Ocean, *Mar. Micropaleont.*, 66, 91-102, 2007.

1177 Paytan, A., Averyt, K., Faul, K., Gray, E., and Thomas, E.: Barite accumulation, ocean productivity,
1178 and Sr/Ba in barite across the Paleocene-Eocene Thermal Maximum, *Geology* 35, 1139–1142, 2007.

1179 ~~Pearson, P. N. and Thomas, E.: Drilling disturbance and constraints on the onset of the
1180 Palaeocene/Eocene boundary carbon isotope excursion in New Jersey, *Clim. Past*, 11: 95–104, 2015.~~

1181 Penman, D. E., Hönisch, B., Zeebe, R. E, Thomas, E., and Zachos, J. C., Rapid and sustained surface
1182 ocean acidification during the Paleocene-Eocene Thermal Maximum, *Paleoceanography*, 29, 357-369,
1183 2014.

1184 Pflum, C. E., and Frerichs, W. E.: Gulf of Mexico Deep-Water Foraminifers, Cushman Foundation for
1185 Foraminiferal Research, Special Publication, 14, 125 pp., 1976.

1186 Pierrehumbert, R. T.: The hydrologic cycle in deep-time climate problems, *Nature*, 419, 191–198,
1187 2002.

1188 ~~Post, J. E., Thomas, E., and Heaney, P. J.: Jianshuiite in oceanic manganese nodules at the Paleocene-
1189 Eocene Boundary, *Am. Mineral.*, 101, doi 10.2138/am-2016-5347 ,(2016).~~

1190 Raymo, M. E., Ruddiman, F., and Froelich, P. N.: Influence of late Cenozoic mountain building on
1191 ocean geochemical cycles, *Geology*, 16, 649-653, 1988.

1192 Ravizza, G. E., Norris, R. N., Blusztajn, J., and Aubry, M.-P.: An osmium isotope excursion associated
1193 with the Late Paleocene Thermal Maximum: evidence of intensified chemical weathering,
1194 *Paleoceanography*, 16, 155-163, 2001.

1195 Robert, C. and Chamley, H.: Development of early Eocene warm climates, as inferred from clay
1196 mineral variations in oceanic sediments, *Global Planet. Change*, 89, 315–331, 1991.

1197 Robert, C., and Kennett, J. P.: Antarctic subtropical humid episode at the Paleocene–Eocene boundary:
1198 clay–mineral evidence, *Geology*, 22, 211–214, 1994.

1199 Rodriguez-Tovar, F. J., Uchman, A., Alegret, L., Molina, E.: Impact of the Paleocene–Eocene Thermal
1200 Maximum on the macrobenthic community: Ichnological record from the Zumaia section, northern
1201 Spain, *Mar. Geol.*, 282, 178–187, 2011.

1202 Röhl, U., Westerhold, T., Bralower, T. J., and Zachos, J. C.: On the duration of the Paleocene-Eocene
1203 Thermal Maximum (PETM), *Geochem. Geophys. Geosy*, 8, Q12002, 2007.

1204 Sachse, D., Radke, J., and Gleixner, G.: δD values of individual n-alkanes from terrestrial plants along
1205 a climatic gradient-implications for the sedimentary biomarker record, *Org. Geochem.*, 37, 469–483,
1206 2006.

1207 Schmiedl, G.: Late Quaternary benthic foraminiferal assemblages from the eastern South Atlantic:
1208 Reconstruction of deep-water circulation and productivity changes, *Reports on Polar Research*, 160;
1209 207 pp. (in German), 1995.

1210 Schmiedl, G. and Mackensen, A.: Late Quaternary paleoproductivity and deep water circulation in the
1211 eastern South Atlantic Ocean: evidence from benthic foraminifera, *Palaeogeogr. Palaeocl. Palaeoecol.*
1212 130, 43–80, 1997.

1213 Schmiedl, G., De Bovee, F., Buscail, R., Charriere, B., Hemleben, C., Medernach, L., Picon, P.:
1214 Trophic control of benthic foraminiferal abundance and microhabitat in the bathyal Gulf of Lions,
1215 western Mediterranean Sea, *Mar. Micropaleont.*, 40, 167–188, 2000.

1216 Schmitz, B., and Pujalte, V.: Sea-level, humidity, and land-erosion records across the initial Eocene
1217 Thermal Maximum from a continental-marine transect in northern Spain, *Geology*, 31, 689–692, 2003.

1218 Schmitz, B., Pujalte, V.: Abrupt increase in seasonal extreme precipitation at the Paleocene–Eocene
1219 boundary, *Geology*, 35, 215–218, 2007.

1220 Schmitz, B., Asaro, F., Molina, E., Monechi, S., Von Salis, K., Speijer, R.: High resolution iridium,
1221 δ¹³C, δ¹⁸O, foraminifera and nannofossil profiles across the latest Paleocene benthic extinction event at
1222 Zumaya, *Palaeogeogr. Palaeocl. Palaeoecol.*, 133, 49–68, 1997.

1223 Schmitz, B., Pujalte, V., and Nùñez-Betelu, K.: Climate and sea level perturbations during the initial
1224 Eocene thermal maximum: Evidence from siliciclastic units in the Basque Basin (Ermua, Zumaia and
1225 Trabakua Pass), northern Spain, *Palaeogeogr. Palaeocl.*, 165, 299-320, 2001.

1226 Schoon, P. L., Heilmann-Clausen, C., Schultz, B. P., Sinninghe Damsté, J. S., Schouten, S.: Warming
1227 and environmental changes in the eastern North Sea Basin during the Palaeocene–Eocene Thermal
1228 Maximum as revealed by biomarker lipids, *Org. Geochem.*, 78, 79–88, 2015.

1229 Secord, R., Gingerich, P. D., Lohmann, K. C., and MacLeod, K. G.: Continental warming preceding
1230 the Palaeocene-Eocene thermal maximum, *Nature*, 467, 955–958, 2010.

1231 **Seibel, B. A., and Walsh, P. J.: Potential impacts of CO₂ injection on deep-sea biota, *Science*, 294, 319–**
1232 **320, 2001.**

1233 Sgarrella, F., Sprovieri, F., Di Stefano, E., and Caruso, S.: Paleoceanography conditions at the base of
1234 the Pliocene in the Southern Mediterranean Basin, *Riv. Ital. Paleontol. S.*, 103, 207-220, 1997.

1235 Sing, R. K., and Gupta, A. K.: Late Oligocene-Miocene paleoceanographic evolution of the
1236 southeastern Indian Ocean: evidence from deep-sea benthic foraminifera (ODP Site 757), *Mar.*
1237 *Micropaleont.*, 51, 153-170, 2004.

1238 **Sluijs, A., and Brinkhuis, H.: A dynamic climate and ecosystem state during the Paleocene-Eocene**
1239 **Thermal Maximum: inferences from dinoflagellate cyst assemblages on the New Jersey Shelf,**
1240 ***Biogeosciences*, 6, 1755–1781, 2009.**

1241 Sluijs, A., Schouten, S., Pagani, M., Woltering, M., Brinkhuis, H., Sinninghe Damsté, J. S., Dickens,
1242 G. R., Huber, M., Reichart, G.-J., Stein, R., Matthiessen, J., Lourens, L. J., Pedentchouk, N., Backman,
1243 J., Moran, K., and The Expedition 302 Scientists: Subtropical Arctic Ocean temperatures during the
1244 Palaeocene/Eocene Thermal Maximum, *Nature*, 441, 610–613, 2006.

1245 Sluijs, A., Bowen, G. J., Brinkhuis, H., Lourens, L. J., and Thomas, E.: The Paleocene-Eocene thermal
1246 maximum super greenhouse: Biotic and geochemical signatures, age models and mechanisms of global
1247 change, in: Deep-Time Perspectives on Climate Change: Marrying the Signal From Computer Models
1248 and Biological Proxies, edited by: Williams, M., Haywood, A.M., Gregory, F. J., and Schmidt, D. N.,

1249 The Micropalaeontological Society Special Publication, The Geological Society, London, 323–350,
1250 2007a.

1251 Sluijs, A., Brinkhuis, H., Schouten, S., Bohaty, S.M., John, C.M., Zachos, J.C., Reichart, G.-J.,
1252 Sinninghe Damsté, J.S., Crouch, E.M., and Dickens, G.R.: Environmental precursors to rapid light
1253 carbon injection at the Palaeocene/Eocene boundary, *Nature*, 450, 1218-1221, 2007b.

1254 ~~Sluijs, A., Brinkhuis, H., Crouch, E. M., John, C. M., Handley, L., Munsterman, D., Bohaty, S. M.,~~
1255 ~~Zachos, J. C., Reichart, G., Schouten, S., Pancost, R. D., Sinninghe Damste, J. S., Welters, N. L. D.,~~
1256 ~~Letter, A. F., and Dickens, G. R., Eustatic variations during the Paleocene Eocene greenhouse world.~~
1257 ~~Paleoceanography~~, 23, PA4216, 2008.

1258 Sluijs, A., Bijl, P. K., Schouten, S., Röhl, U., Reichart, G.-J., and Brinkhuis, H.: Southern Ocean
1259 warming, sea level and hydrological change during the Paleocene-Eocene thermal maximum, *Clim.*
1260 *Past*, 7 (1), 47-61, 2011.

1261 ~~Smith, F. A. and Freeman, K. H., 2006. Influence of physiology and climate on δD of leaf wax n-~~
1262 ~~alkanes from C3 and C4 grasses, *Geochim. Cosmochim. Ac.*, 70, 1172–1187, 2006.~~

1263 Smith, F. A., Wing, S. L., and Freeman, K. H.: Magnitude of the carbon isotope excursion at the
1264 Paleocene–Eocene Thermal Maximum: the role of plant community change, *Earth Planet. Sc. Lett.*,
1265 262, 50–65, 2007.

1266 Speijer, R. P. and Schmitz, B.: A benthic foraminiferal record of Paleocene sea level and trophic/redox
1267 conditions at Gebel Aweina, Egypt, *Palaeogeogr. Palaeocl. Palaeoecol.*, 137, 79–101, 1998.

1268 Speijer, R. P., Schmitz, B., Aubry, M.-P., and Charisi, S. D.: The latest Paleocene benthic extinction
1269 event: punctuated turnover in outer neritic foraminiferal faunas from Gebel Aweina, Egypt, in: Aubry,
1270 M.-P. and Benjamini, C. (Eds.): Paleocene/Eocene boundary events in space and time, *Israel J. Earth*
1271 *Sci.*, 44, 207–222, 1996.

1272 Speijer, R. P., Schmitz, B., and van der Zwaan, G. J.: Benthic foraminiferal extinction and repopulation
1273 in response to latest Paleocene Tethyan anoxia, *Geology*, 25, 683-686, 1997.

1274 Speijer, R. P., Scheibner, C., Stassen, P., and Morsi, A.-M.: Response of marine ecosystems to deep-
1275 time global warming: a synthesis of biotic patterns across the Paleocene-Eocene thermal maximum
1276 (PETM), *Austrian Journal of Earth Sciences*, 105, 6-16, 2012.

1277 Stassen, P., Thomas, E., and Speijer, R. P.: The progression of environmental changes during the onset
1278 of the Paleocene-Eocene Thermal Maximum (New Jersey Coastal Plain), *Austrian Journal of Earth
1279 Sciences* 105/1, 169-178, 2012a.

1280 Stassen, P., Thomas, E., and Speijer, R. P.: Integrated stratigraphy of the Paleocene-Eocene thermal
1281 maximum in the New Jersey Coastal Plain: Toward understanding the effects of global warming in a
1282 shelf environment, *Paleoceanography*, 27, PA4210, 2012b.

1283 Stassen, P., Thomas, E., Speijer, R. P.: Paleocene-Eocene Thermal Maximum environmental change in
1284 the New Jersey Coastal Plain: benthic foraminiferal biotic events, *Mar. Micropaleont.*, 115: 1-23, 2015.

1285 Steineck, P., Thomas, E.: The latest Paleocene crisis in the deep sea: ostracode succession at Maud
1286 Rise, *Southern Ocean, Geology*, 24, 583–586, 1996.

1287 Stoll, H. M., Shimizu, N., Archer, D., and Ziveri, P.: Coccolithophore productivity response to
1288 greenhouse event of the Paleocene-Eocene Thermal Maximum, *Earth Planet. Sc. Lett.*, 258, 192-206,
1289 2007.

1290 Suhr, S. B., Pond, D. W., Gooday, A. J., and Smith, C. R.: Selective feeding by foraminifera on
1291 phytodetritus on the western Antarctic Peninsula shelf: evidence from fatty acid biomarker analysis,
1292 *Mar. Ecol.-Prog. Ser.*, 262, 153–162, 2003.

1293 Takata, H., Nomura, R., and Khim, B.-K.: Response to abyssal benthic foraminifera to mid-Oligocene
1294 glacial events in the eastern Equatorial Pacific Ocean (ODP Leg 199), *Palaeogeogr. Palaeocl.
1295 Palaeoecol.*, 292, 1-11, 2010.

1296 Takeda, K., and Kaiho, K.: Faunal turnovers in central Pacific benthic foraminifera during the
1297 Paleocene-Eocene thermal maximum, *Palaeogeogr. Palaeocl. Palaeoecol.*, 251, 175–197, 2007.

1298 Thiry, M.: Palaeoclimatic interpretation of clay minerals in marine deposits: An outlook from the
1299 continental origin, *Earth-Science Reviews*, 49, 201–221, 2000.

1300 Thomas, D. J., Bralower, T. J., and Zachos, J. C.: New evidence for subtropical warming during the
1301 late Paleocene thermal maximum: Stable isotopes from Deep Sea Drilling Project Site 527: Walvis
1302 Ridge, *Paleoceanography*, 14, 561–570, 1999.

1303 Thomas, D. J., Zachos, J. C., Bralower, T. J., Thomas, E., and Bohaty, S.: Warming the fuel for the
1304 fire: Evidence for the thermal dissociation of methane hydrate during the Paleocene-Eocene thermal
1305 maximum, *Geology*, 30, 1067–1070, 2002.

1306 Thomas, E.: Late Eocene to Recent deep-sea benthic foraminifers from the central equatorial Pacific
1307 Ocean, in: *Initial Rep. Deep Sea*, edited by: Mayer, L., Theyer, F., Barron, J. A., Dunn, D. A.,
1308 Handyside, T., Hills, S., Jarvis, I., Nigrini, C. A., Pisias, N. C., Pujos, A., Saito, T., Stout, P., Thomas,
1309 E., Weinreich, N., and Wilkens, R. H., 85, US Government Printing Office, Washington, 655–656,
1310 1985.

1311 Thomas, E.: Development of Cenozoic deep-sea benthic foraminiferal faunas in Antarctic waters, *Geol.*
1312 *Soc. Spec. Publ.*, 47, 283–296, 1989.

1313 Thomas, E.: Late Cretaceous through Neogene deep-sea benthic foraminifers (Maud Rise, Weddell
1314 Sea, Antarctica), in: *Proceedings of the Ocean Drilling Program, Scientific Results*, edited by: Barker,
1315 P. F., Kennett, J. P., O'Connell, S., Berkowitz, S., Bryant, W. R., Burckle, L. H., Egeberg, P. K.,
1316 Fiitterer, D. K., Qersonde, R. E., Qolovchenko, X., Hamilton, N., Lawver, L., Lazarus, D. B., Lonsdale,
1317 M., Mohr, B., Nagao, T., Pereira, C. P. Q., Pudsey, C. J., Robert, C. M., Schandl, E., SpiejJ, V., Stott,
1318 L. D., Thomas, E., Thompson, K. F. M., and Wise, S. W. Jr., 113, College Station, TX (Ocean Drilling
1319 Program), 571–594, 1990.

1320 Thomas, E.: Biogeography of the late Paleocene benthic foraminiferal extinction, in: *Late Paleocene-*
1321 *Early Eocene Climatic and Biotic Events in the Marine and Terrestrial Records*, edited by: Aubry, M.
1322 P., Lucas, S., and Berggren, W., A., Columbia University Press, New York, 214–243, 1998.

1323 Thomas, E.: Extinction and food at the seafloor: A high-resolution benthic foraminiferal record across
1324 the Initial Eocene Thermal Maximum, Southern Ocean Site 690, in: *Causes and Consequences of*
1325 *Globally Warm Climates in the Early Paleogene*, edited by: Wing, S. L., Gingerich, P. D., Schmitz, B.,
1326 and Thomas, E., *Geol. S. Am. S.*, Boulder, Colorado, The Geological Society of America, 369, 319–
1327 332, 2003.

1328 Thomas, E.: Cenozoic mass extinctions in the deep sea: What perturbs the largest habitat on Earth?, in:
1329 Large Ecosystem Perturbations: Causes and Consequences, edited by: Monechi, S., Coccioni, R., and
1330 Rampino, M., Geol. S. Am. S., Boulder, Colorado, The Geological Society of America, 424, 1–23,
1331 2007.

1332 Thomas, E. and Gooday, A. W.: Cenozoic deep-sea benthic foraminifers: Tracers for changes in
1333 oceanic productivity?, *Geology*, 24, 355-358, 1996.

1334 Thomas, E. and Shackleton, N. J.: The Paleocene-Eocene benthic foraminiferal extinction and stable
1335 isotopes anomalies, *Geol. Soc. Spec. Publ.*, 101, 401-441, 1996.

1336 Thomas, E., Zachos, J. C., and Bralower, T. J.: Deep-Sea Environments on a Warm Earth: latest
1337 Paleocene-early Eocene, in: *Warm Climates in Earth History*, edited by: Huber, B., MacLeod, K., and
1338 Wing, S., Cambridge University Press, Cambridge, UK, 132–160, 2000.

1339 Tipple, B. J., Pagani, M., Krishnan, S., Dirghangi, S. S., Galeotti, S., Agnini, C., Giusberti, L., Rio, D.:
1340 Coupled high-resolution marine and terrestrial records of carbon and hydrologic cycles variations
1341 during the Paleocene-Eocene Thermal Maximum (PETM), *Earth Planet. Sc. Lett.*, 311, 82-92, 2011.

1342 Tjalsma, R. C. and Lohmann, G. P.: Paleocene-Eocene bathyal and abyssal benthic foraminifera from
1343 the Atlantic Ocean, *Micropaleontology Special Publication*, 4, 1–90, 1983.

1344 Torrent, J., Barro, V., and Liu, Q.: Magnetic enhancement is linked to and precedes hematite formation
1345 in aerobic soil, *Geophysical Res. Lett.*, 33, L02401, 2006.

1346 Van Morkhoven, F. P. C. M., Berggren, W. A., and Edwards, A. S.: Cenozoic cosmopolitan deep-water
1347 benthic foraminifera. *B. Cent. Rech. Expl., Mèmoire*, 11, 1-421, 1986.

1348 Von Hillebrandt, A.: Das Paläozän und seine Foraminiferenfauna im Becken von Reichenhall und
1349 Salzburg, *Bayerische Akademie der Wissenschaften, Mathematisch-Naturwissenschaftliche Klasse*,
1350 *Abhandlungen, neue folge*, München, 108, 9-180, 1962.

1351 Waśkowska, A.: Response of Early Eocene deep-water benthic foraminifera to volcanic ash falls in the
1352 Polish Outer Carpathians: Palaeoecological implications, *Palaeogeogr. Palaeocl. Palaeoecol.*, 305, 50-64,
1353 2011.

1354 Wendler, I., Huber, B. T., MacLeod, K. G., and Wendler, J. E.: Stable oxygen and carbon isotope
1355 systematics of exquisitely preserved Turonian foraminifera from Tanzania - understanding isotopic
1356 signatures in fossils, *Mar. Micropaleont.*, 102, 1-33, 2013.

1357 Westerhold, T., Röhl, U., Laskar, J., Raffi, I., Bowles, J., Lourens, L. J., and Zachos, J. C.: On the
1358 duration of Magnetochrons C24r and C25n, and the timing of early Eocene global warming events:
1359 Implications from the ODP Leg 208 Walvis Ridge depth transect, *Paleoceanography*, 22, PA2201,
1360 2007.

1361 Wieczorek, R., Fantle, M. S., Kump, L. R., Ravizza, G.: Geochemical evidence for volcanic activity
1362 prior to and enhanced terrestrial weathering during the Paleocene Eocene Thermal maximum,
1363 *Geochim. Cosmochim. Ac.*, 119, 391-410, 2013.

1364 Wing, S. L., Harrington, G. J., Smith, F. A., Bloch, J. I., Boyer, D. M., and Freeman, K. H.: Transient
1365 floral change and rapid global warming at the Paleocene-Eocene boundary, *Science* 310, 993–996,
1366 2005.

1367 Winguth, A. M. E., Thomas, E., Winguth, C.: Global decline in ocean ventilation, oxygenation, and
1368 productivity during the Paleocene-Eocene Thermal Maximum: Implications for the benthic extinction,
1369 *Geology*, 40, 263-266, 2012.

1370 ~~Winguth, A. M. E., Shellito, C., Shields, C., and Winguth, C.: Climate response at the Paleocene-
1371 Eocene Thermal Maximum to greenhouse gas forcing – A model study with CCSM3, *J. Climate*, 23,
1372 2562–2584, 2010.~~

1373 Zachos, J. C., Pagani, M., Sloan, L. C., Thomas, E., and Billups, K.: Trends, rhythms, and aberrations
1374 in global climate 65 Ma to present, *Science* 292, 686–693, 2001.

1375 Zachos, J. C., Schouten, S., Bohaty, S., Quattlebaum, T., Sluijs, A., Brinkhuis, H., Gibbs, S. J., and
1376 Bralower, T. J.: Extreme warming of mid latitude coastal ocean during the Paleocene-Eocene thermal
1377 maximum: inferences from TEX86 and isotope data, *Geology*, 34, 737–740, 2006.

1378 Zachos, J. C., Röhl, U., Schellenberg, S. A., Sluijs, A., Hodell, D. A., Kelly, D. C., Thomas, E., Nicolo,
1379 M., Raffi, I., Lourens, L. J., Mccarren, H. and Kroon, D.: Rapid acidification of the ocean during the
1380 Paleocene-Eocene Thermal Maximum, *Science*, 308, 1611-1615, 2005.

1381 Zeebe, R. E., Zachos, J. C., and Dickens, G. R.: Carbon dioxide forcing alone insufficient to explain
1382 Paleocene-Eocene Thermal Maximum warming, *Nat. Geosci.*, 2, 576-580, 2009.

1383 Zeebe, R. E., Dickens, G. R., Ridgwell, A., Sluijs, A., and Thomas, E.: Onset of carbon isotope
1384 excursion at the Paleocene-Eocene Thermal Maximum took millennia, not 13 years (Comment), *P.*
1385 *Natl. Acad. Sci. USA*, 111, E1062-E1063, 2014.

1386 Zhang, Y., Ji, J., Balsam, W. L., Liu L., Chen J.: High resolution hematite and goethite records from
1387 ODP 1143, South China Sea: Co-evolution of monsoonal precipitation and El Niño over the past
1388 600,000 years, *Earth Planet. Sc. Lett.*, 264, 136–150, 2007.

1389 Zhou, X., Thomas, E., Rickaby, R. E. M., Winguth, A. M. E., and Lu, Z.: I/Ca evidence for global
1390 upper ocean deoxygenation during the Paleocene-Eocene Thermal Maximum (PETM),
1391 *Paleoceanography*, 29(10), 964-975, 2014.

1392

1393 **Figures captions**

1394 **Figure 1.** Location of the Forada section in the context of the Piave River Valley in the Belluno
1395 Province (the “Valbelluna”), northeastern Italy.

1396 **Figure 2.** Faunal and geochemical variations across the PETM at Forada section plotted against
1397 chronostratigraphy, precessional cycles, lithology, recognized benthic foraminiferal assemblages (A to
1398 G) and isotopic intervals. % agglutinated=agglutinated to agglutinated and calcareous hyaline ratio; %
1399 infaunal taxa=infaunal to infaunal and epifaunal ratio; simple diversity and Fisher- α diversity index;
1400 N/g=number of benthic foraminifera per gram (faunal density) in the >63 mm size fraction; coarse
1401 fraction (CF) calculated according to Hancock and Dickens (2005) **as the weight percent of the >63 μ m**
1402 **size fraction relative to the weight of the bulk sample**; Fragmentation index (F-Index) is from Luciani
1403 et al. (2007). The gray bands indicate intervals of carbonate dissolution. α = pre-CIE dissolution,
1404 β =burndown layer, BFDI=benthic foraminiferal dissolution interval. Modified from Giusberti et al.
1405 (2007).

1406 **Figure 3.** Summary of the main mineralogical, geochemical and cyclostratigraphic features recognized
1407 across the Paleocene-Eocene boundary and in the clay marl unit (CMU) of the Forada section and
1408 radiolarian abundance plotted against isotopic intervals and recognized benthic foraminiferal
1409 assemblages (A to F). **N/g for the radiolarians refers to the number of radiolarians (>125 μ m fraction)**
1410 **per gram of dry sediment**. F-Index from Luciani et al. (2007). VPDB—Vienna PeeDee belemnite
1411 standard. Modified from Giusberti et al. (2007).

1412 **Fig. 4.** Stratigraphic distribution of benthic foraminiferal extinction taxa (CET) across the
1413 Paleocene/Eocene boundary in the Forada section plotted against lithology, $\delta^{13}\text{C}$ bulk record, CaCO_3
1414 percentage, isotopic intervals and recognized benthic foraminiferal assemblages (A to F), based on data
1415 from the >63 μ m size fraction integrated with data from >125 micron fraction. The gray bands indicate
1416 intervals of carbonate dissolution. Question marks: doubtful identification. Triangle: post BEE
1417 occurrence of one specimen of *Coryphostoma midwayensis* has been recorded in the sample BRI 300
1418 (295 cm above the base of CMU).

1419 **Figure 5.** Relative abundance of the most abundant benthic foraminiferal taxa across the PETM at
1420 Forada plotted against biostratigraphy, precessional cycles, lithology, $\delta^{13}\text{C}$ bulk record, recognized

1421 benthic foraminiferal assemblages (A to F) and isotopic intervals. Benthic foraminiferal biozonation
1422 after Berggren and Miller (1989). The gray bands indicate intervals of carbonate dissolution. α = pre-
1423 CIE dissolution, β =burndown layer, BFDI=benthic foraminiferal dissolution interval. "Other
1424 buliminids" group includes only representatives of the families Buliminidae, Buliminellidae and
1425 Turrilinidae (*Bulimina*, *Buliminella*, *Quadratobuliminella*, *Sitella* and *Turrilina*).

1426 Figure 6. Relative abundance of selected benthic foraminifera across the PETM at Forada plotted
1427 against biostratigraphy, precessional cycles, lithology, $\delta^{13}\text{C}$ bulk record, recognized benthic
1428 foraminiferal assemblages (A to F) and isotopic intervals. Benthic foraminiferal biozonation after
1429 Berggren and Miller (1989). The gray bands indicate intervals of carbonate dissolution. α = pre-CIE
1430 dissolution, β =burndown layer, BFDI=benthic foraminiferal dissolution interval.

1431 Figure 7. Enlargement of the interval from -1m to +2m across the P/E boundary at Forada showing the
1432 relative abundance of selected benthic foraminifera plotted against biostratigraphy, precessional cycles,
1433 lithology, $\delta^{13}\text{C}$ bulk record, recognized benthic foraminiferal assemblages (A to F) and isotopic
1434 intervals. Benthic foraminiferal biozonation after Berggren and Miller (1989). The gray bands indicate
1435 intervals of carbonate dissolution. α =Pre-CIE dissolution interval; β =burndown layer, BFDI=benthic
1436 foraminiferal dissolution interval.

1437 Figure 8. Summary of main calcareous plankton (calcareous nannofossils and planktonic foraminifera)
1438 and benthic foraminiferal events and inferred environmental conditions (from Agnini et al., 2007;
1439 Luciani et al., 2007 and present work), isotopic intervals, thickness, precessional cycles and benthic
1440 foraminiferal assemblages (A to F) recognized in this work. The stratigraphic intervals containing
1441 assemblages A and B, C and D to F are considered as pre-extinction, extinction and repopulation
1442 intervals, respectively. Benthic foraminiferal zonation after Berggren and Miller (1989).

1443 Figure 9. Stable carbon isotope ratios of higher plant n-alkanes (a), stable hydrogen isotope ratios of
1444 higher plant n-alkanes (b) with higher plant average chain length values (c) for Forada PETM plotted
1445 against isotopic intervals and recognized benthic foraminiferal assemblages (A to F). Terrestrial higher
1446 plant n-C27, n-C29, and n-C31 δD values are shown as crosses, closed circles, and triangles,
1447 respectively. Redrawn from data of Tipple et al. (2011).

1448 Figure 10. Paleogeographic map (from <http://www.odsн.de/odsн/services/paleomap/paleomap.html>) at
1449 55 Ma showing sites where paleohydrological reconstructions for the PETM are available. Numbers
1450 follow a north to south paleolatitudinal order. Blue dots indicate areas where an increase in
1451 precipitation has been inferred; Green dots indicate areas where an increase in climatic contrasts or a
1452 fluctuating precipitation regime have been inferred; Orange dots indicate areas where an increase in
1453 aridity has been inferred; Purple dots indicate areas where hydrological changes have been inferred but
1454 the pattern not specified. 1. Lomonosov Ridge, Arctic Sea; 2, 3. Spitsbergen Central Basin and
1455 Svalbard archipelago; 4. Central North Sea Basin; 5. Eastern North Sea Basin; 6. Williston Basin,
1456 western North Dakota, (USA) 7. Bighorn Basin, Wyoming (USA); 8. Rhenodanubian Basin, Austria; 9.
1457 Belluno Basin, northeastern Italy; 10. Aktumsuk and Kaurtakapy sections, Uzbekistan and Kazakhstan;
1458 11. Dieppe-Hampshire Basin, France; 12. London Basin; 13. DSDP Site 401 Bay of Biscay, North-
1459 eastern Atlantic Ocean; 14. Western Colorado (USA); 15. New Jersey Coastal Plain (USA); 16. Central
1460 Valley of California (USA); 17. Basque Basin, northern Spain; 18. Tremp Basin, northern Spain; 19.
1461 Alamedilla section, southern Spain; 20. Tornillo Basin, Texas (USA); 21. Salisbury embayment, mid-
1462 Atlantic coastal plain (USA); 22. Gafsa Basin, Tunisia; 23. Zin Valley of Negev, Israel; 24. Dababiya
1463 section, Egypt; 25. Northern Neotropics, (Colombia and Venezuela); 26. TDP Site 14, Tanzania; 27.
1464 Tawanui section, North Island (New Zealand); 28. Clarence River valley, South Island (New Zealand);
1465 29. Central Westland, South Island (New Zealand); 30. ODP Site 1172, East Tasman Plateau; 31. ODP
1466 Site 690 Weddell Sea, Southern Ocean. See Supplement Table S3 for references and additional
1467 information.

1468 **Table caption**

1469 Table 1. Summary of the known ecological preferences of selected benthic foraminifera, as evaluated
1470 from the literature, common at Forada.

1471 **Plates captions**

1472 Plate 1. SEM micrographs of the most representative Paleocene cosmopolitan extinction taxa (CET)
1473 occurring at Forada. 1. *Angulogavelinella avnimelechi*, spiral view (BRI-25.5); 2. *Angulogavelinella*
1474 *avnimelechi*, lateral view (BRI-185.5); 3. *Gavelinella beccariiformis*, umbilical view (BRI-75); 4.
1475 *Osangularia velascoensis*, spiral view (BRI-50,5); 5. *Anomalinoides rubiginosus* (BRI-9); 6.
1476 *Cibicidoides dayi* (BRI-37); 7. *Cibicidoides velascoensis*, spiral view (BRI-75,5); 8. *Cibicidoides*

1477 *velascoensis*, lateral view (BRI-135.5); 9. *Cibicidoides hyphalus* (BRI-50,5); 10. "Neoeponides"
1478 *megastoma* (BRI-135); 11. *Gyroidinoides globosus* (BRI-50.5); 12. *Gyroidinoides quadratus* (BRI-
1479 185,5); 13. *Coryphostoma midwayensis* (BRI-50,5); 14. *Aragonina velascoensis* (BRI-50.5); 15.
1480 *Bolivinoides delicatulus* (BRI-135.5); 16. *Neoflabellina semireticulata* (BRI-365); 17. *Pullenia coryelli*
1481 (BRI-50,5); 18. *Remesella varians* (BRI-310.5); 19. *Clavulinoides globulifera* (BRI-25.5); 20.
1482 *Clavulinoides trilatera* (BRI-33); 21. *Clavulinoides amorpha*; 22. *Marssonella indentata* (BRI-25.5);
1483 23. *Dorothia beloides* (BRI-260); 24. *Dorothia pupa* (BRI-105).

1484 Plate 2. SEM micrographs of the most representative species of the Eocene postextinction faunas
1485 occurring at Forada. 1. *Ammobaculites agglutinans* (BRI+10); 2. *Eobigenerina variabilis* (BRI+50); 3.
1486 *Eobigenerina variabilis* (BRI+50); 4. *Karrerulina conversa* (BRI+50); 5. *Karrerulina horrida* (BRI-
1487 25.5); 6. *Spiroplectammina navarroana* (BRI-33/7); 7. *Spiroplectammina spectabilis* (BRI+50); 8.
1488 *Rashnovammina munda* (BRI-50,5); 9. *Haplophragmoides* cf. *kirki*. (BRI+5); 10. *Saccammina*
1489 *placenta* (BRI-25.5); 11. *Glomospira irregularis* (BRI+35); 12. *Glomospira charoides* (BRI-75.5); 13.
1490 *Osangularia* sp. (BRI+15); 14. *Globocassidulina subglobosa* (BRI+15); 15. *Tappanina selmensis*
1491 (BRI+15); 16. *Tappanina selmensis* (BRI-9); 17. *Siphogenerinoides brevispinosa* (BRI-11); 18.
1492 *Siphogenerinoides brevispinosa* (BRI-365); 19. *Bulimina tuxpamensis* (BRI+150); 20. *Bulimina*
1493 *tuxpamensis* (BRI+150); 21. *Pleurostomella* sp. (BRI+150); 22. *Bolivina* sp. costate (BRI+385); 23.
1494 *Nuttallides truempyi* (BRI+150); 24. *Oridorsalis umbonatus* (BRI-135.5); 25. *Aragonina aragonensis*
1495 (BRI-105); 26. *Abyssammina poagi* (TAL7B).

1496 Plate 3. SEM micrographs of the most representative taxa of the upper Paleocene-lower Eocene of
1497 Forada section. 1. *Quadratobuliminella pyramidalis* (BRI-75.5); 2. *Buliminella grata* (BRI-591); 3.
1498 *Bulimina midwayensis* (BRI+35); 4. *Bulimina alazanensis* (BRI +150); 5,6. *Bulimina trinitatensis*
1499 (BRI-9); 7. *Bolivinoides crenulata* (BRI-9); 8. *Bolivinoides crenulata* (BRI-25.5); 9. *Bolivinoides*
1500 *floridana* (BRI-410); 10 *Bolivina* sp. smooth (BRI-410); 11. *Bolivina* sp. smooth (BRI-410); 12.
1501 *Reussella* sp. (BRI-365); 13. *Angulogerina muralis* (BRI-75.5); 14. *Angulogerina muralis* (BRI-75.5);
1502 15. *Angulogerina?* sp. (BRI-9); 16. *Angulogerina?* sp.(BRI-35.5); 17. *Rectobulimina carpentierae*
1503 (BRI-466); 18. *Allomorphina trochoides* (BRI-25.5); 19. *Quadriflorina allomorphinoides* (TAL
1504 7B); 20. *Cibicidoides eocaenus* (BRI-9); 21. *Anomalinoides* sp. 2 (BRI-135); 22. *Cibicides* sp. (BRI-
1505 591); 23. *Cibicidoides praemundulus* (BRI+150); 24. *Nonion havanense* (BRI-591).

1506 Plate 4. SEM micrographs of some taxa of the upper Paleocene-lower Eocene of Forada section. 1.
1507 *Ammodiscus cretaceus* (BRI-29.5); 2. *Ammodiscus peruvianus* (BRI-9); 3. *Haplophragmoides walteri*
1508 (BRI-75.5); 4. *Haplophragmoides horridus* (BRI +35); 5. *Recurvoides* sp. (BRI -33/-37); 6.
1509 *Glomospira serpens* (BRI-260); 7. *Trochamminoides proteus* (BRI-25.5); 8. *Paratrochamminoides*
1510 *heteromorphus* (BRI+40); 9. *Glomospira* cf. *gordialis* (BRI +35); 10. *Gaudryina* sp. (BRI +15); 11.
1511 *Karrerulina coniformis* (BRI -135); 12. *Caudammina ovuloides* (BRI-260); 13. *Gaudryina pyramidata*
1512 (BRI-17.5); 14. Big-sized lituolid, apertural view (BRI-9); 15. *Hormosina velascoensis* (BRI-33/37);
1513 16. *Pseudonodosinella troyeri* (BRI-260); 17. "Pseudobolivina" sp. 2 in Galeotti et al. (2004)
1514 (BRI+35); 18. *Pseudoclavulina trinitatensis* (BRI+150); 19. *Spiroplectammina spectabilis* (BRI-50.5);
1515 20. Big-sized lituolid, lateral view (BRI-9).

1516

Fig. 1

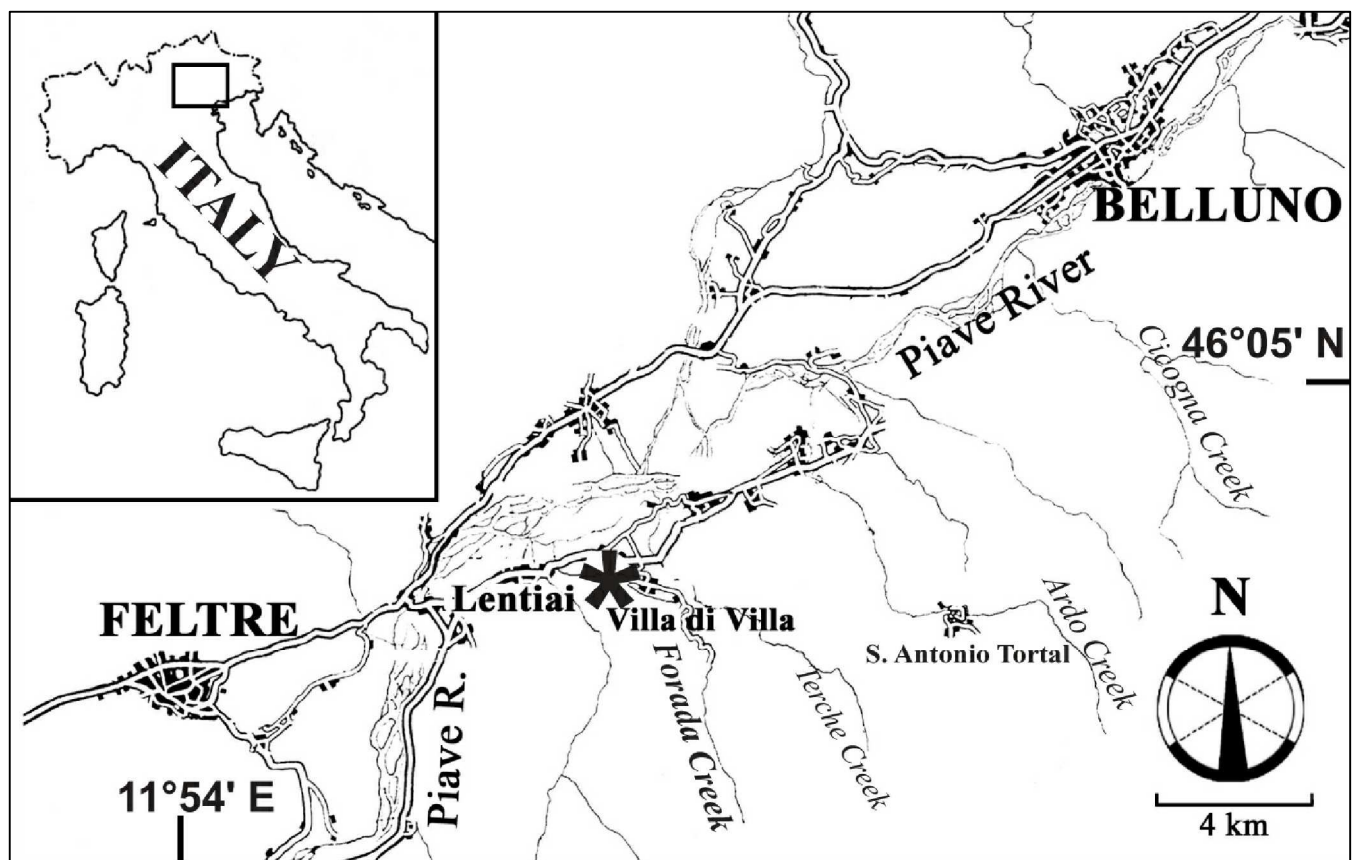


Fig. 2

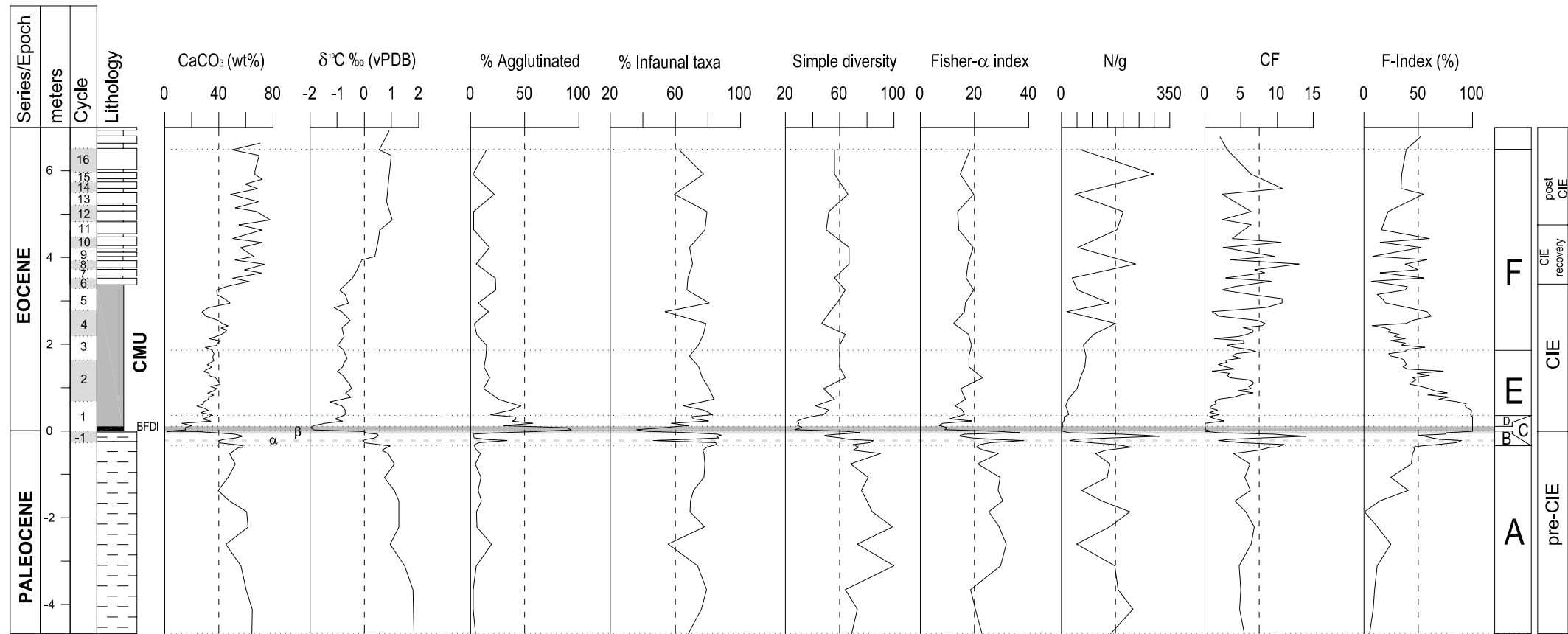


Fig. 3

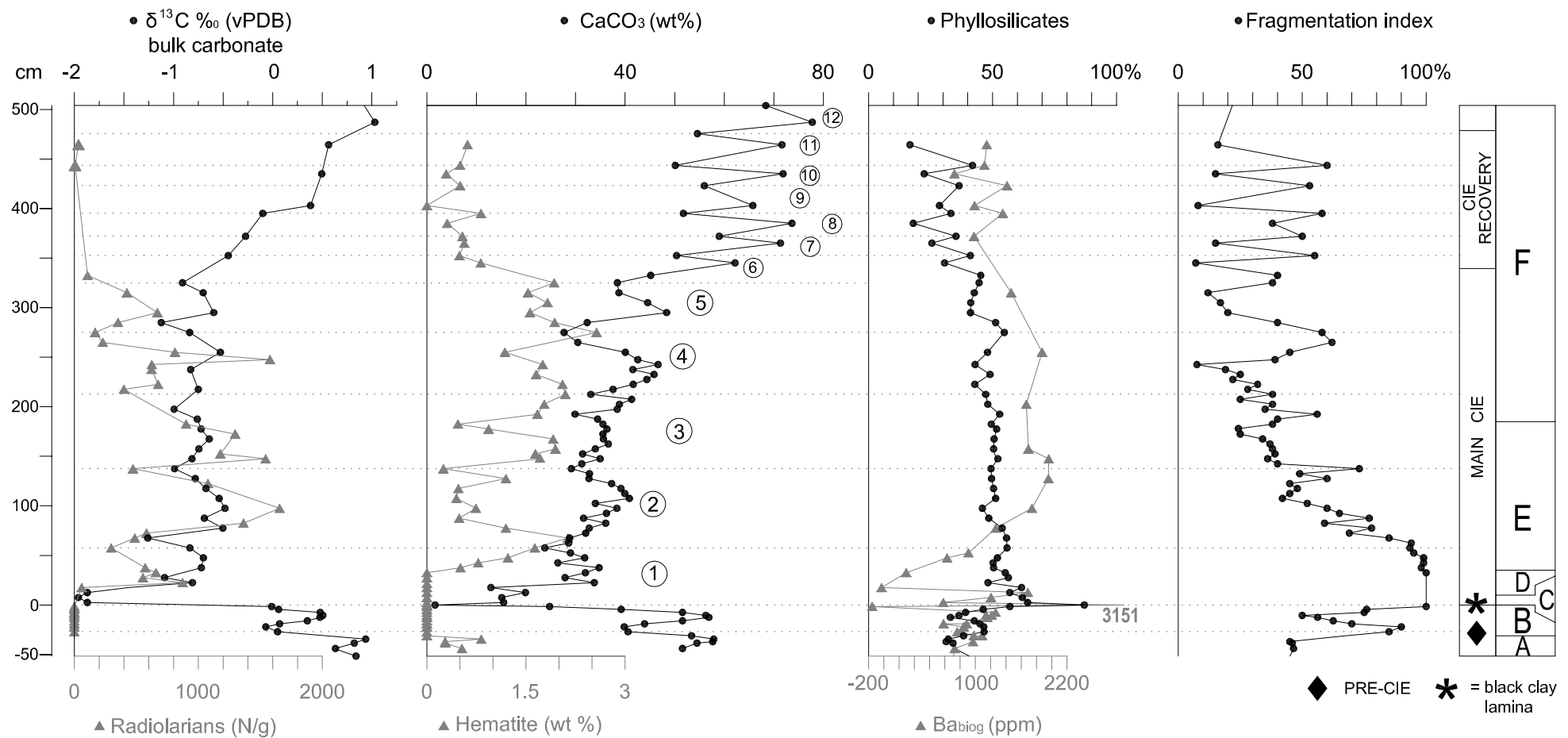


Fig. 4

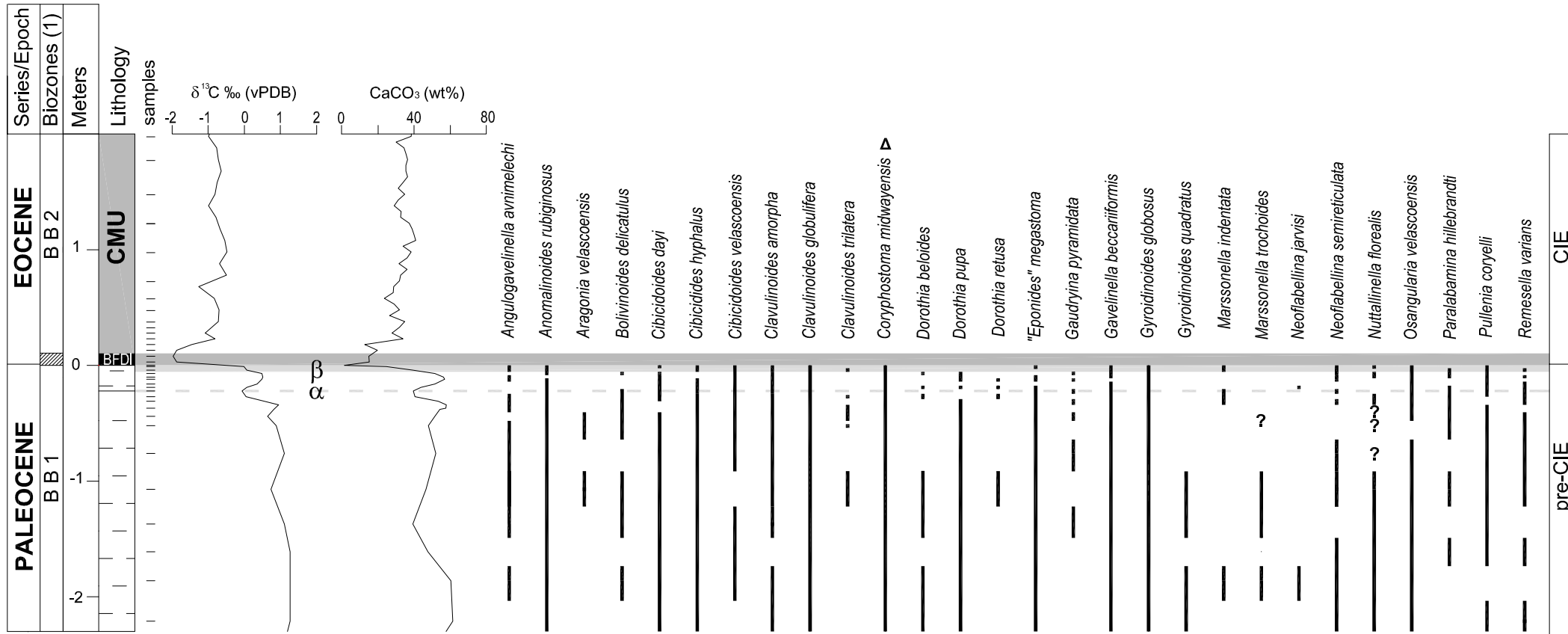


Fig. 5

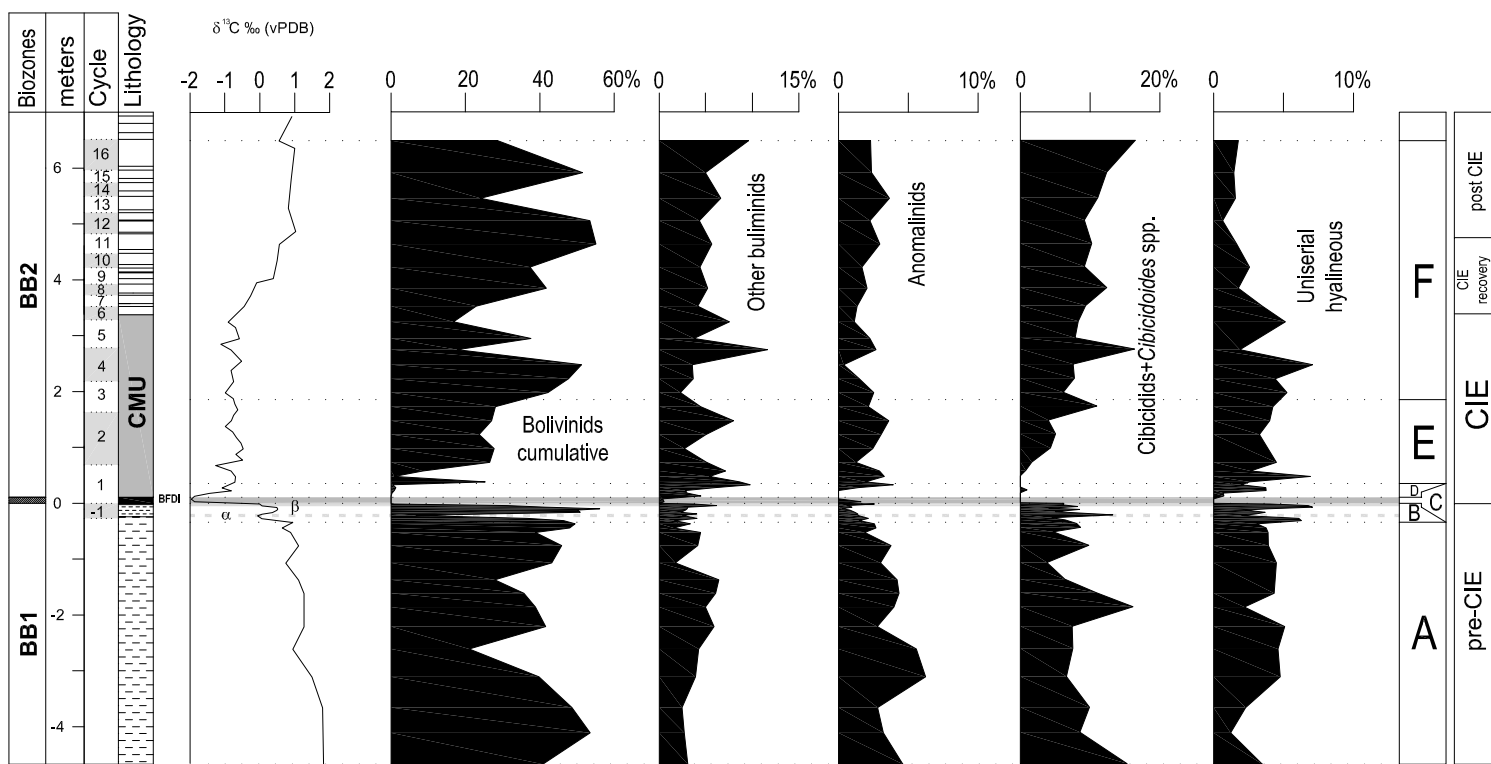


Fig. 6

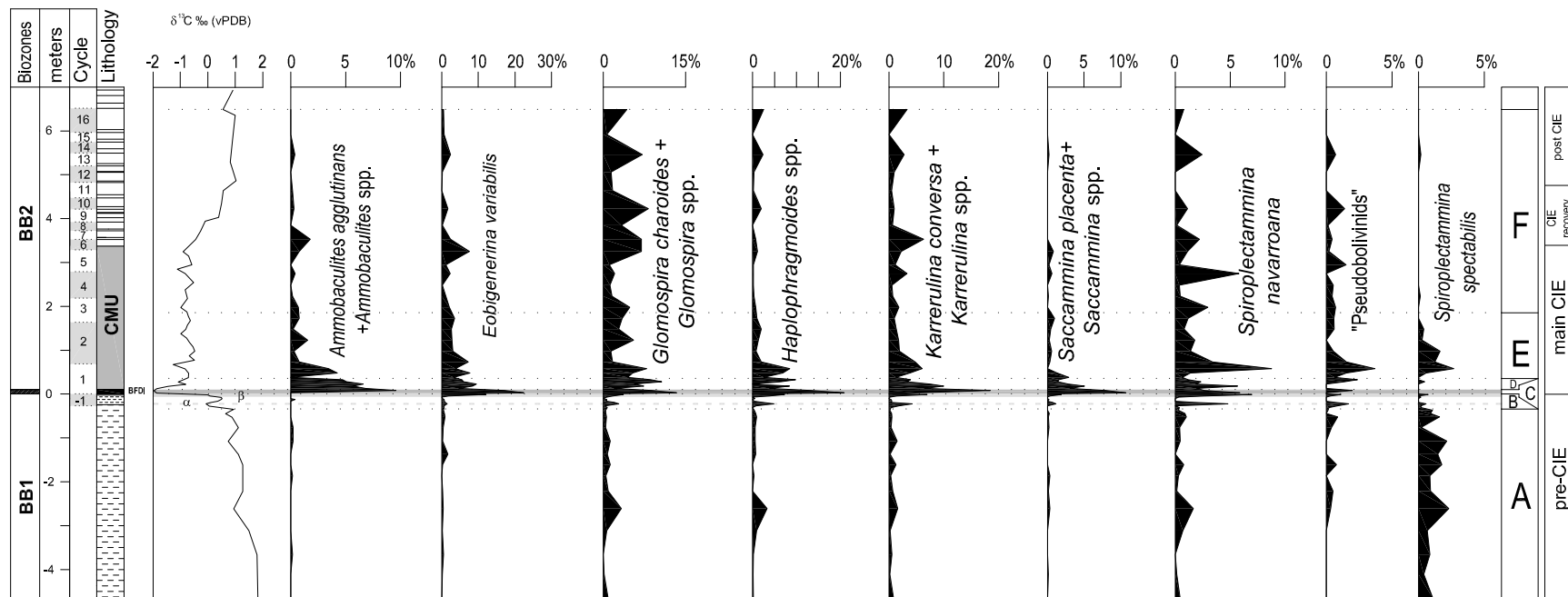
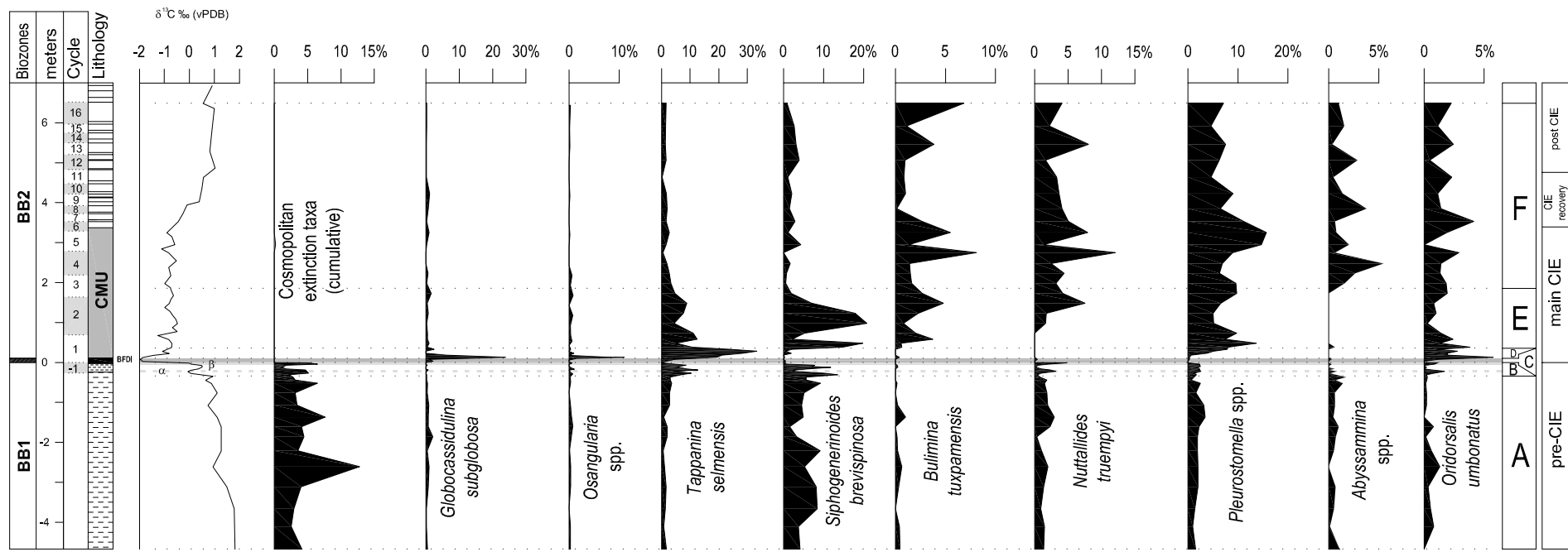


Fig. 7

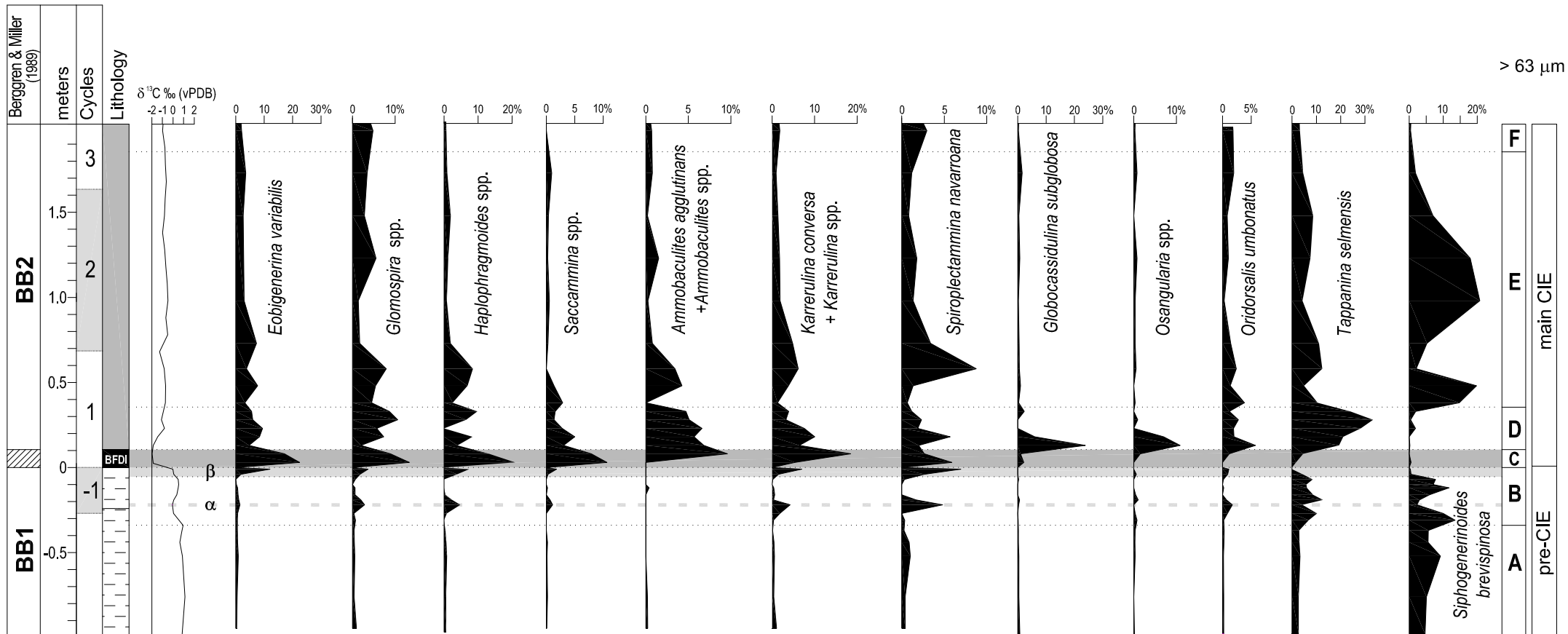


Fig. 8

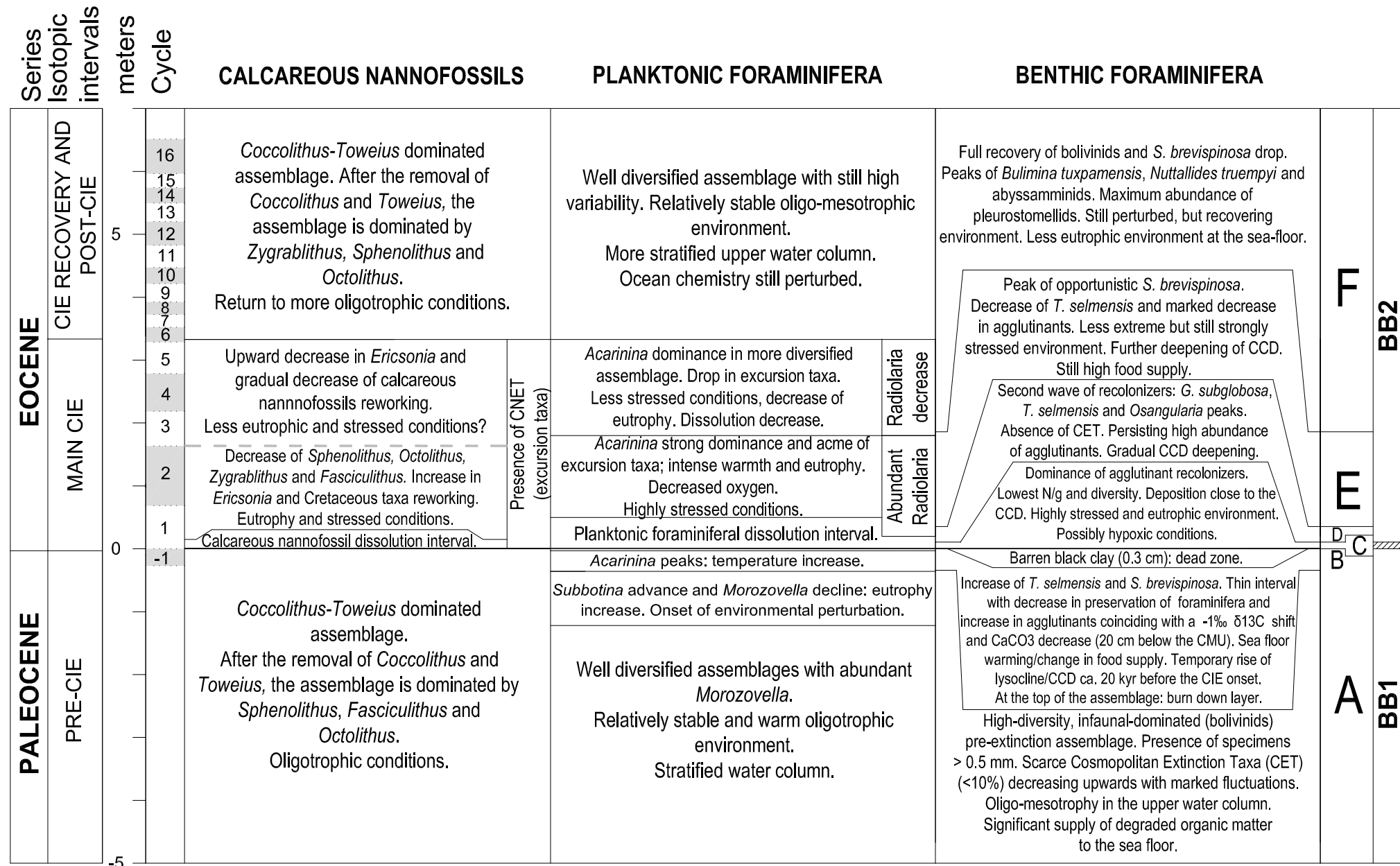


Fig. 9

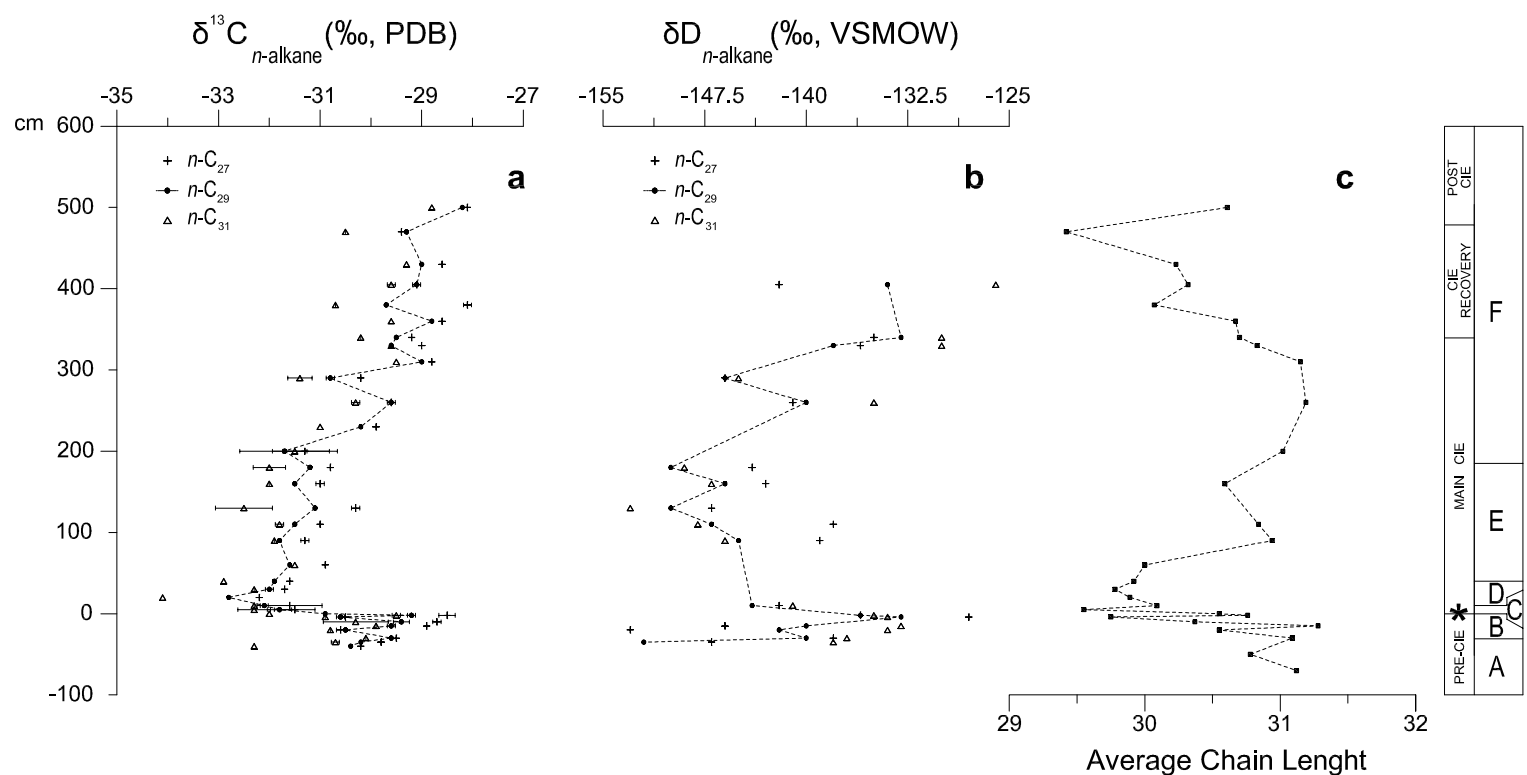
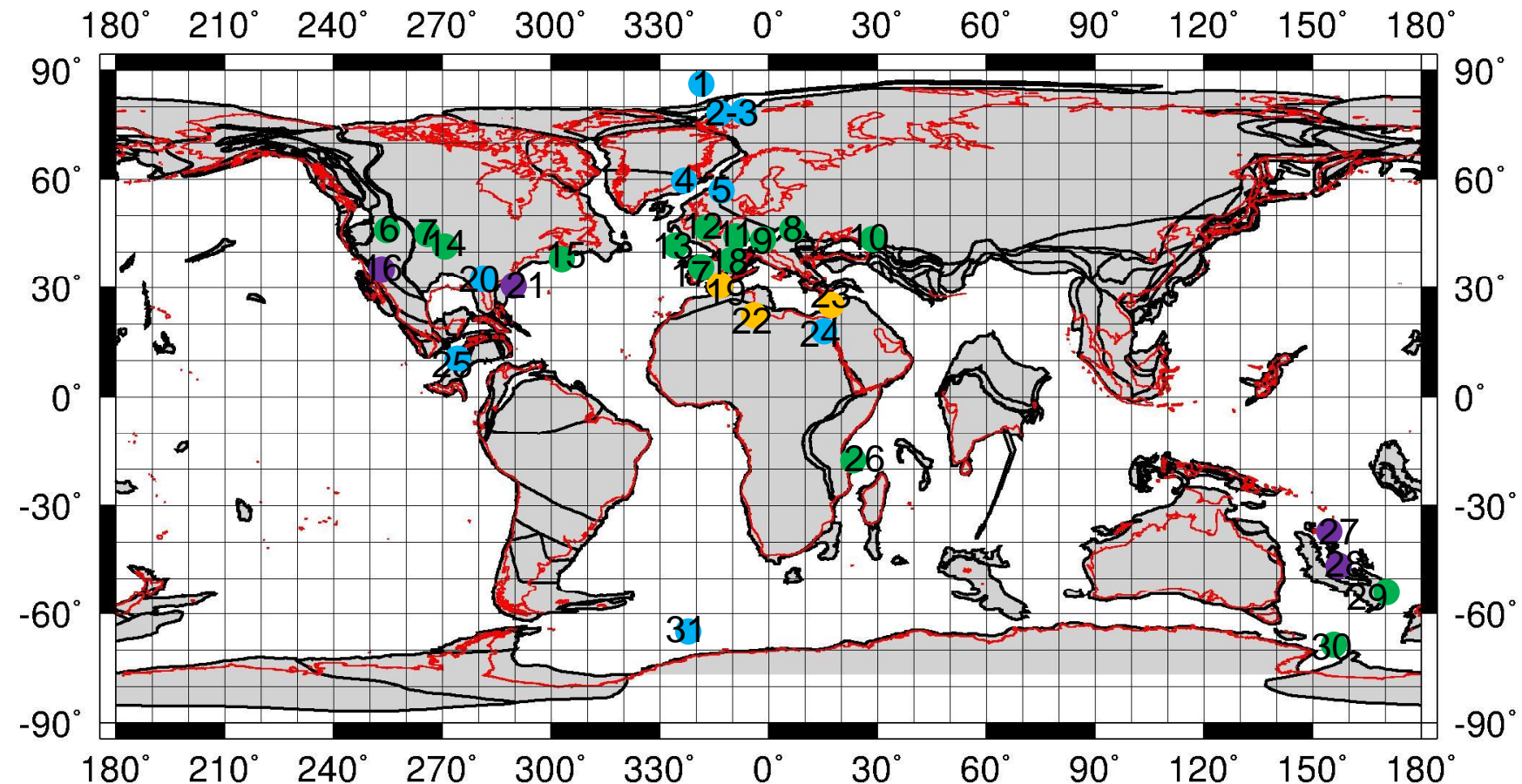
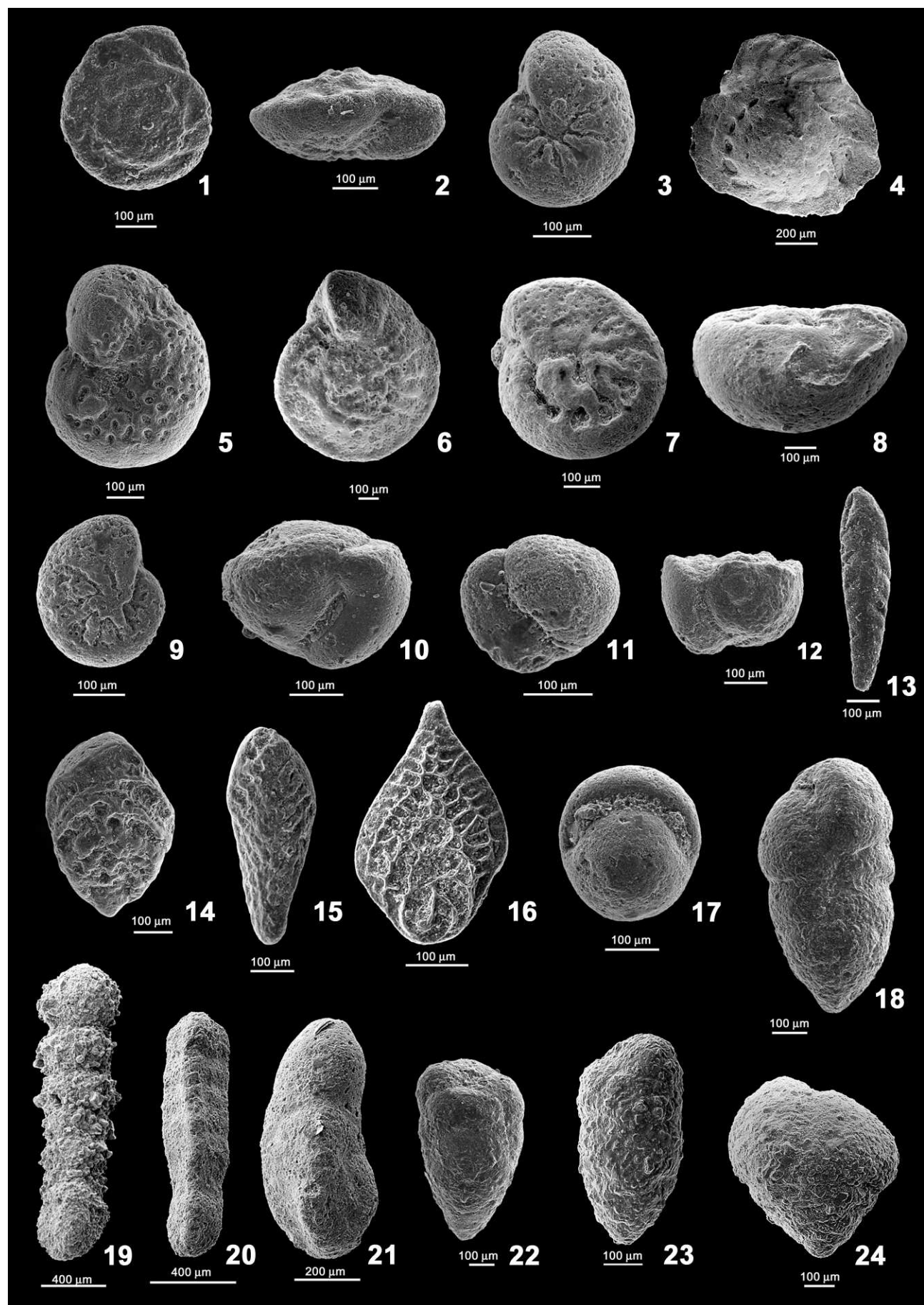


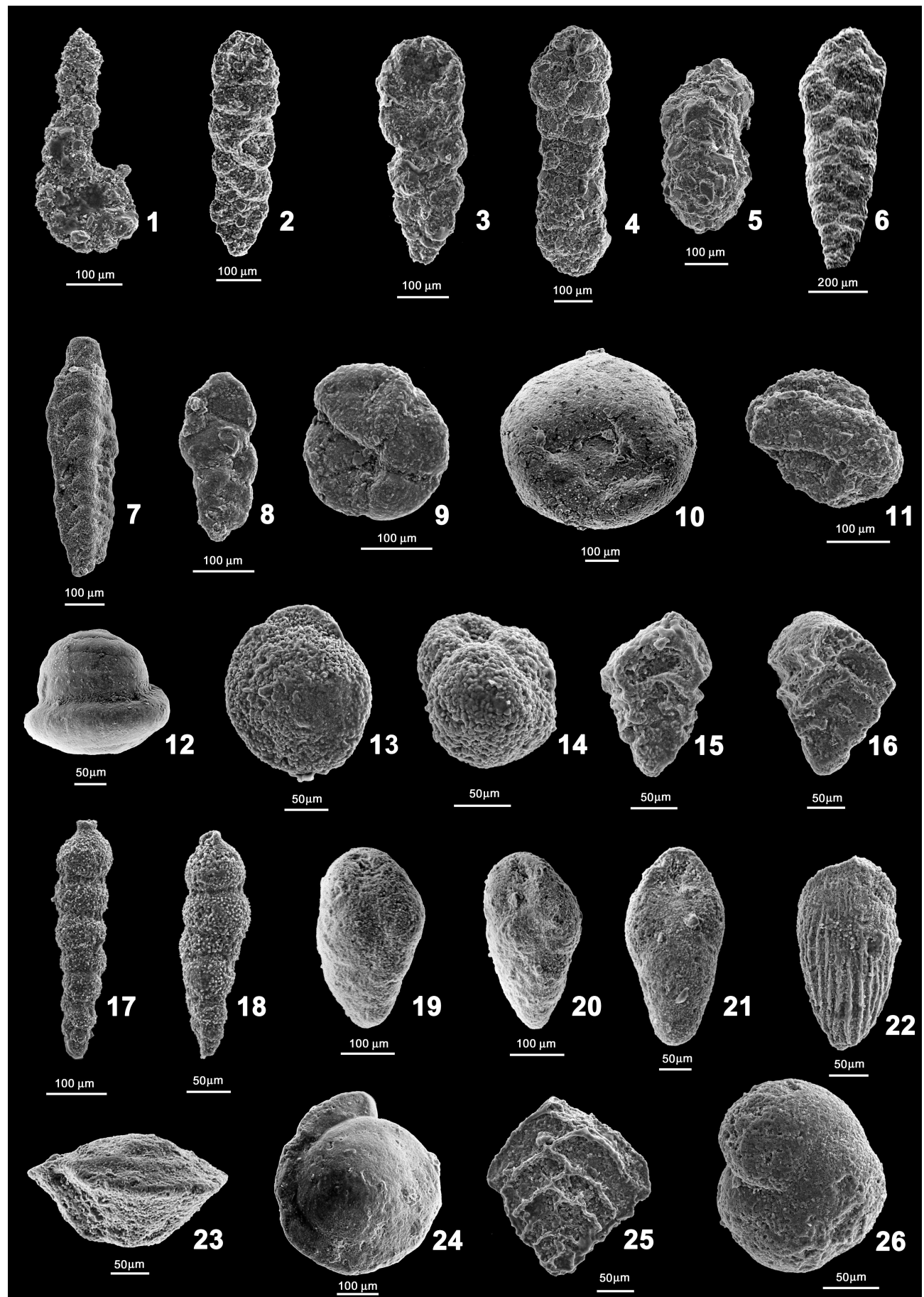
Fig. 10



55.0 Ma Reconstruction

Plate 1





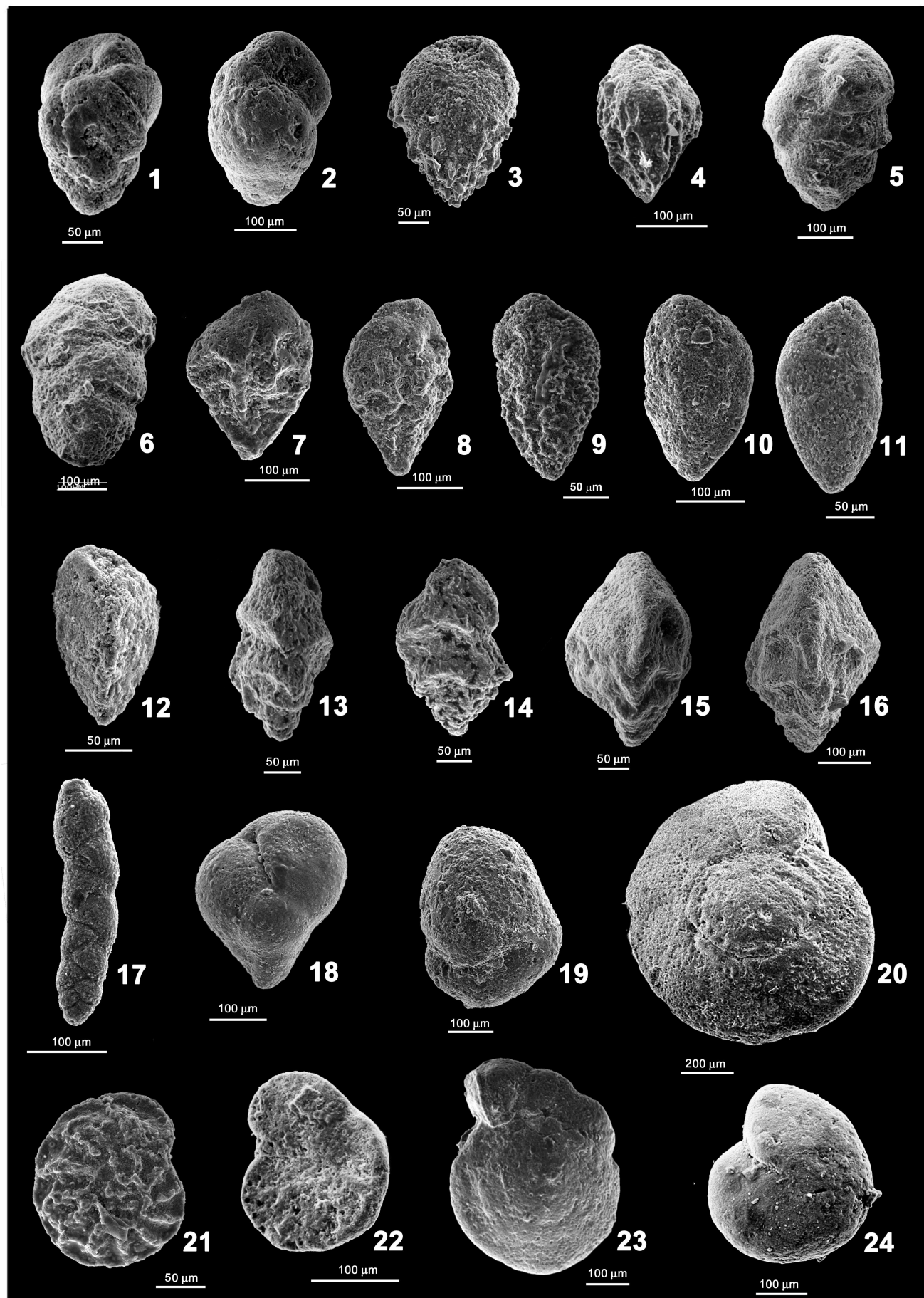


Plate 4

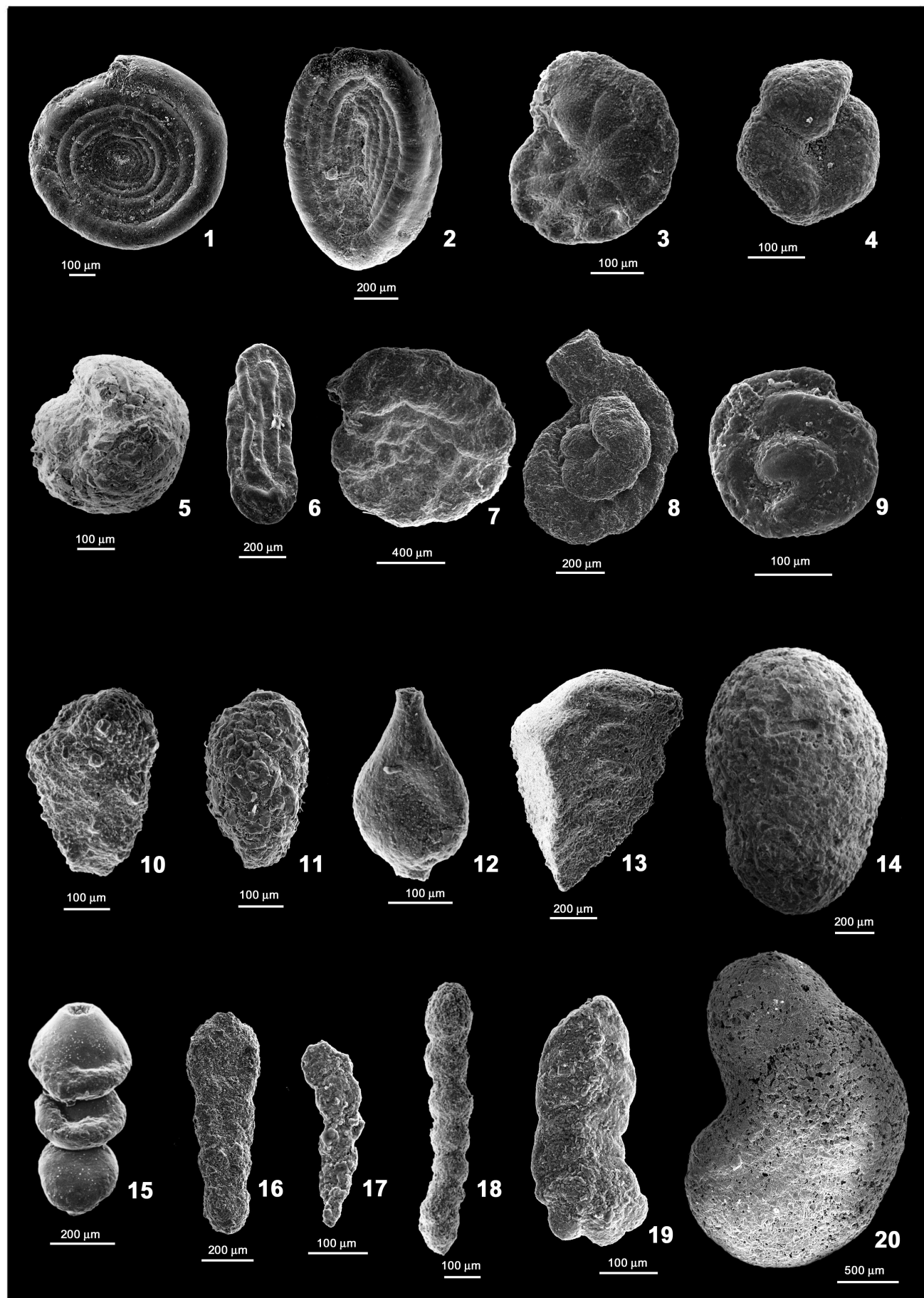


Table 1.

<i>Ammobaculites agglutinans</i>	Deep-infaunal recoloniser within the K/Pg boundary clay at Sopelana section (Spain). Adapted to low carbonate availability with high capability for dispersal and colonisation of abiotic substrates. Reported in present day slope high productivity areas.	Gooday, 2003; Gooday et al., 2001; Kuhnt and Kaminski, 1993.
<i>Eobigenerina variabilis</i>	Opportunist, able to live under low oxygen conditions. Dominant in the recovery faunas after the Cretaceous OAE2.	Cetean et al., 2008a,b. See also text.
<i>Globocassidulina subglobosa</i>	Cosmopolitan, highly adaptable, long-ranging opportunistic species. Modern representatives of this species described from a wide variety of environmental settings, including hydrate mounds. Possibly feeding on phytodetritus and reflecting pulsed food supply to the sea floor in oxygenated deepwater settings. Abundant at high southern latitudes where seasonality is extreme. At many sites it appears after the BEE and blooms as an opportunist.	Ernst et al., 2006; Gooday, 1993, 1994; Gupta and Thomas, 2003; Gooday et al., 2008; Ishman and Domack, 1994; Jorissen et al., 2007; Mohan et al., 2011; Murray and Pudsey, 2004; Nomura, 1995; Panieri and Sen Gupta, 2007; Sgarrella et al., 1997; Singh and Gupta, 2004; Suhr et al., 2003; Takata et al., 2010; Takeda and Kaiho, 2007.
<i>Glomospira</i> spp.	Very abundant in the lowermost Eocene at several deep-water locations (the "Glomospira acme"). Generally oligotrophic indicators, they though could be indicative of an abundant supply of terrigenous, refractory organic matter, independent from local primary productivity. Resistant to carbonate dissolution and able to live in environments with low carbonate supply. High ecological tolerance: occur in environments subjected to rapid changes with fluctuating ecological conditions.	Arreguín-Rodríguez et al., 2013, 2014; Galeotti et al., 2004; Kaminski and Gradstein, 2005; Kaminski et al., 1996; Kuhnt and Collins, 1996; Ortiz, 1995; Waśkowska, 2011.
<i>Haplophragmoides</i> spp.	Representatives of the genus pioneer sediments just above anoxic OAE2 black shales in the abyssal North Atlantic that contain no benthic foraminifera. Commonly documented in the basal PETM dissolution interval of shelfal and bathyal Tethyan sections.	Alegret et al., 2005; Ernst et al., 2006; Friedrich, 2009; Kuhnt, 1992; Ortiz, 1995.
<i>Karrerulina conversa</i>	Deep infaunal taxon peaking in the basal PETM at Zumaya (Spain). Resistant to carbonate dissolution and able to live in environments with low carbonate supply. Modern representatives are part of the oligotrophic biofacies on abyssal plains with well-oxygenated bottom and interstitial waters. Recognized in the lowermost Eocene of the Iberia Abyssal Plain.	Bak, 2004; Kaminski and Gradstein, 2005; Kuhnt and Collins, 1996; Kuhnt et al. 2000; Ortiz, 1995; See text.
<i>Oridorsalis umbonatus</i>	Very long-ranging, extant taxon (since the Turonian-Coniacian). Opportunistic lifestyle. Reported both in oligotrophic and eutrophic environments. It may feed on phytodetritus. Shallow infaunal dweller, with very small tests but increased calcification just above the base of the PETM at Site 1263 (Walvis Ridge, SE Atlantic), where it dominates the assemblage.	Foster et al., 2013; Kaiho, 1998; Katz et al., 2003; Gooday, 1993, 1994; Gupta and Thomas, 1999; Gupta et al., 2008; Schmiedl, 1995; Schmiedl and Mackensen, 1997; Thomas and Shackleton, 1996; Wendler et al., 2013.
<i>Osangularia</i> spp.	Opportunistically repopulate the sea floor during short-term re-oxygenation phases of Cretaceous OAEs. Opportunistic phytodetritus feeders during OAE1b, thriving on an enhanced carbon flux to the sea floor and tolerating some degree of oxygen depletion. Peak of <i>Osangularia</i> spp. are reported across the PETM of the Alamedilla section (Spain).	Alegret et al., 2009a; Friedrich, 2009; Friedrich et al., 2005; Holbourn and Kuhnt, 2001; Holbourn et al., 2001. See also text.
<i>Saccammina</i> spp.	Recolonizer within the K/Pg boundary clay of the Sopelana section (Spain). Adapted to low carbonate availability with high capability for dispersal and colonisation of abiotic substrates. Common on modern productive continental margins.	Gooday et al., 2008; Kuhnt and Kaminski, 1993.
<i>Siphogenerinoides brevispinosa</i>	Typical of many open ocean sites in the aftermath of the peak CIE. Opportunist capable to rapidly colonize the sediment when productivity increases during environmental instability. At some locations it bloomed during the PETM and other hyperthermals, at others it had its highest occurrence in the lowermost part of the PETM.	Giusberti et al., 2009; Thomas, 1998, 2003, 2007; Thomas and Shackleton, 1996.
<i>Spiroplectammina navarroana</i>	Minor component of PETM postextinction faunas. At some locations common just after the K/Pg boundary.	Alegret et al., 2003; Alegret et al., 2009b; Ortiz, 1995.
Stilostomellids and pleurostomellids	Infaunal taxa widely distributed in oligotrophic and eutrophic regions with sustained or highly seasonal phytoplankton productivity. Tolerated warm, locally oxygen-depleted, carbonate-corrosive bottom waters, as demonstrated by their survival across the PETM. Across Cretaceous OAEs, pleurostomellids were found within black-shales. Possibly adapted to low-oxygen conditions, or able to rapidly recolonize the sea-floor during brief intervals of reoxygenation.	Coccioni and Galeotti, 1993; Friedrich, 2009; Friedrich et al., 2005; Hayward et al., 2010a,b, 2012; Holbourn and Kuhnt, 2001; Mancin et al., 2013.
<i>Tappanina selmensis</i>	Upper bathyal to outer shelf species in the Campanian and throughout the Paleocene. High-productivity, stress-tolerant and opportunistic species possibly thriving in continuously stressed, dysoxic sea bottom conditions. Common in the deep-sea only just before and especially following the BEE.	Alegret et al., 2009a; Boersma, 1984; D'haenens et al., 2012; Frenzel, 2000; Giusberti et al., 2009; Kuhnt, 1996; Kuhnt and Kaminski, 1996; Stassen et al., 2012a,b, 2015; Steineck and Thomas, 1996; Thomas, 1989, 1990, 1998; Thomas and Shackleton, 1996; van Morkhoven et al., 1986.

1 **Variability in climate and productivity during the**
2 **Paleocene/Eocene Thermal Maximum in the western Tethys**
3 **(Forada section)**

4
5 **L. Giusberti¹, F. Boscolo Galazzo¹, and E. Thomas^{2,3}**
6

7 [1] Department of Geosciences, University of Padova, Via Gradenigo 6, 35131 Padova, Italy;

8 [2] Department of Geology and Geophysics, Yale University, 210 Whitney Avenue, New Haven CT
9 06511, USA

10 [3] Department of Earth and Environmental Sciences, Earth and Environmental Sciences, Wesleyan
11 University, 265 Church Street, Middletown, CT 06459, USA

12
13 Correspondence to: L. Giusberti (luca.giusberti@unipd.it)

14
15 **Abstract**

16
17 The Forada section (northeastern Italy) provides a continuous, expanded deep-sea record of the
18 Paleocene/Eocene thermal maximum (PETM) in the central-western Tethys. We combine a new, high
19 resolution, benthic foraminiferal assemblage record with published calcareous plankton, mineralogical
20 and biomarker data to document climatic and environmental changes across the PETM, highlighting
21 the benthic foraminiferal extinction event (BEE). The onset of the PETM, occurring ~30 kyr after a
22 precursor event, is marked by a thin, black, barren clay layer, possibly representing a brief pulse of
23 anoxia and carbonate dissolution. The BEE occurred within the 10 cm interval including this layer.
24 During the first 3.5 kyr of the PETM, several agglutinated recolonizing taxa show rapid species
25 turnover, indicating a highly unstable, CaCO_3 -corrosive environment. Calcareous taxa reappeared after
26 this interval, and the next ~ 9 kyr were characterized by rapid alternation of peaks in abundance of
27 various calcareous and agglutinated recolonizers. These observations suggest that synergistic stressors,
28 including deep water CaCO_3 -corrosiveness, low oxygenation, and high environmental instability
29 caused the extinction. Combined faunal and biomarker data (BIT index, higher plant *n*-alkane average
30 chain length) and the high abundance of the mineral chlorite suggest that erosion and weathering

increased strongly at the onset of the PETM, due to an overall wet climate with invigorated hydrological cycle, which led to storm flood-events carrying massive sediment discharge into the Belluno Basin. This interval was followed by the core of the PETM, characterized by four precessionally paced cycles in $\text{CaCO}_3\%$, hematite%, $\delta^{13}\text{C}$, abundant occurrence of opportunistic benthic foraminiferal taxa, as well as calcareous nannofossil and planktonic foraminiferal taxa typical of high productivity environments, radiolarians, and lower $\delta\text{D}_{n\text{-alkanes}}$. We interpret these cycles as reflecting alternation between an overall arid climate, characterized by strong winds and intense upwelling, and an overall humid climate, with abundant rains and high sediment delivery (including refractory organic carbon) from land. Precessionally paced marl-limestone couplets occur throughout the recovery interval of the CIE and up to ten meters above it, suggesting that these wet-dry cycles persisted, though at declining intensity, after the peak PETM. Enhanced climate extremes at mid-latitudes might have been a direct response to the massive CO_2 input in the ocean atmosphere system at the Paleocene-Eocene transition, and may have had a primary role in restoring the Earth system to steady state.

45

46 1 Introduction

47 The Paleocene-Eocene Thermal Maximum (PETM) has over the last twenty four years attracted
48 intensive study by the scientific community, as one of the most dramatic and rapid climatic disruptions
49 of the Cenozoic (e.g., Kennett and Stott, 1991; Zachos et al., 2001; Sluijs et al., 2007a; McInerney and
50 Wing, 2011; Littler et al., 2014). During the PETM (~55.6 Ma), the Earth's surface temperature
51 increased by ~5°C in a few thousand years (McInerney and Wing, 2011; Dunkley-Jones et al., 2013;
52 Zeebe et al., 2014; Bowen et al., 2015), and remained high for 100 to 170-200 kyr (e.g., Röhl et al.,
53 2007; Giusberti et al., 2007; Murphy et al., 2010). The PETM is recognized in terrestrial and marine
54 settings by a negative carbon isotope excursion (CIE; e.g., Kennett and Stott, 1991; Bowen et al.,
55 2004), with variable magnitude ranging from ~2-4.5‰ in marine carbonates (e.g., Thomas and
56 Shackleton, 1996; Bains et al., 1999; Thomas et al., 2002; Zachos et al., 2006; Handley et al., 2008;
57 McCarren et al., 2008) to 4-7‰ in marine and terrestrial organic carbon and leaf waxes (e.g., Kaiho et
58 al., 1996; Bowen et al., 2004, 2015; Pagani et al., 2006a; Smith et al., 2007; Handley et al., 2008;
59 McCarren et al., 2008). This CIE is attributed to a massive, rapid input of isotopically light carbon into
60 the ocean-atmosphere system, which destabilized the global carbon cycle and led to rapid and extreme

61 global warming (e.g., Dickens et al., 1997; Thomas and Shackleton, 1996; Pagani et al., 2006b;
62 Panchuk et al., 2008; Dickens, 2011; DeConto et al., 2012). Both the source(s) of the carbon and the
63 triggering mechanism(s) of the emissions are still strongly debated (e.g., Meissner et al., 2014), in part
64 because the pattern and size of the CIE does not necessarily simply reflect the size and isotopic
65 signature of the carbon input, but is affected by biotic and sedimentary processes (e.g., Kirtland Turner
66 and Ridgwell, 2013). Despite these debates, the onset of the CIE is an outstanding global correlation
67 tool (McInerney and Wing, 2011; Stassen et al., 2012b), formally used to define the base of the Eocene
68 (Aubry et al., 2007).

69 The carbon cycle perturbation of the PETM led to acidification of surface ocean waters (Penman
70 et al., 2014) and severe shallowing of the calcite compensation depth (CCD; Zachos et al., 2005; Kelly
71 et al., 2010; Hönisch et al., 2012). Widespread carbonate dissolution coincided with the base of the CIE
72 (e.g., Thomas and Shackleton, 1996; Thomas, 1998; Hancock and Dickens, 2005; McCarren et al.,
73 2008). The profound paleoceanographic changes affected primary and export productivity (e.g.,
74 Thomas, 2007; Winguth et al., 2012; Ma et al., 2014), which in general increased in marginal basins
75 and along continental margins, but decreased in open oceans (e.g., Gibbs et al., 2006; Stoll et al., 2007;
76 Speijer et al., 2012). The higher ocean temperatures may have led to increased remineralization of
77 organic matter in the oceans due to increased metabolic rates (John et al., 2013, 2014; Boscolo Galazzo
78 et al., 2014; Ma et al., 2014). The combination of increased remineralization, higher temperatures and
79 increased ocean stratification led to a decrease of oxygen levels in bottom waters regionally, especially
80 along continental margins (including the Arctic Ocean) and in the Atlantic Ocean (e.g., Beniamini,
81 1992; Speijer et al., 1992; Gavrilov et al., 1997; Thomas, 2007; Chun et al., 2010; Speijer et al., 2012;
82 Winguth et al., 2012; Nagy et al., 2013; Wieczorek et al., 2013; Dickson et al., 2014; Pälike et al.,
83 2014; Post et al., 2016), while Oxygen Minimum Zones in open oceans expanded globally (Zhou et al.,
84 2014), including at Forada (Luciani et al., 2007).

85 The increased primary productivity in marginal basins has been linked to increased influx of nutrients
86 from the continents, caused by increased erosion and weathering due to intensification of the
87 hydrological cycle, because precipitation is correlated to globally-averaged surface temperatures (e.g.,
88 Pierrehumbert, 2002). A widespread increase in kaolinite in PETM sediments has been related to the
89 global increase in precipitation and intensity of chemical weathering (e.g., Robert and Chamley, 1991;
90 Robert and Kennett, 1994; Kaiho et al., 1996; Gibson et al., 2000), as also suggested by Os-isotope
91 evidence (Ravizza et al., 2001; Wieczorek et al., 2013). However, reconstruction of hydrological

92 changes from clay mineral assemblages is complex, and additional evidence is needed (Thiry, 2000;
93 Schmitz and Pujalte 2003; 2007; Egger et al., 2003; 2005; Handley et al., 2012).

94 The severe climatic perturbations of the PETM profoundly affected terrestrial and marine
95 ecosystems, triggering faunal and floral radiations and migrations (e.g., Kelly et al., 1996; Bralower,
96 2002; Gingerich, 2003; Wing et al., 2005; Sluijs et al., 2007a; Jaramillo et al., 2010; McInerney and
97 Wing, 2011). Deep-sea benthic foraminifera experienced the most severe extinction of the Cenozoic,
98 the benthic foraminiferal extinction event (BEE) (Thomas, 1989, 1990, 1998; Kennett and Stott, 1991;
99 Thomas and Shackleton, 1996; Alegret et al., 2009a, b; 2010). The BEE was rapid (<10 kyr; Thomas,
100 1989, 2003, 2007), and wiped out the Cretaceous bathyal and abyssal “Velasco-type fauna” (Berggren
101 and Aubert, 1975; Tjalsma and Lohmann, 1983; Thomas, 1998, 2007), marking a significant step
102 towards the establishment of modern benthic foraminiferal fauna (Thomas, 2007). The extinction was
103 far less severe in shelf environments (Gibson et al., 1993; Speijer, 2012; Stassen et al., 2015).

104 The cause of this global extinction remains under debate, because neither anoxia nor higher or
105 lower productivity, nor carbonate dissolution occurred globally at bathyal to abyssal depths in the deep
106 sea, the largest habitat on Earth (e.g., Thomas, 2003, 2007; Alegret et al., 2010), and benthic
107 foraminifera are highly efficient dispersers (Alve and Goldstein, 2003). The link between the
108 environmental changes during the PETM and the benthic foraminiferal extinction event thus remains
109 poorly understood. A common obstacle to perform detailed high-resolution studies of the PETM in
110 deep-sea sediments is the fact that many records are condensed or discontinuous, especially across the
111 few thousand years (Zeebe et al., 2014) of the onset of the carbon isotope excursion. The Forada
112 section (northeastern Italy) represents an outstanding exception in that it contains an expanded deep-sea
113 record of the PETM, which has been extensively studied because of its continuity and cyclostratigraphy
114 (Agnini et al., 2007; Giusberti et al., 2007; Luciani et al., 2007; Tipple et al., 2011; Dallanave et al.,
115 2012). Carbonate dissolution is less severe at Forada than in many other sections, with calcareous
116 benthic foraminifera present for most of the interval characterized by the CIE (> 4 m; Giusberti et al.,
117 2007). Given the limited number globally of complete and expanded deep-sea PETM sections, the
118 Forada section represents an invaluable opportunity to investigate the environmental impacts of the
119 PETM and repercussions on deep-sea fauna.

120 We provide a high-resolution benthic foraminiferal record for the Forada section, in order to
121 reconstruct the progression (tempo and mode) of environmental and biotic changes during the PETM.
122 These data allow us to reconstruct the environmental disruption and the benthic foraminiferal response

123 to PETM warming in detail, and document the community recovery. Benthic foraminiferal data are
124 integrated with sedimentological and geochemical data (Giusberti et al., 2007; Tipple et al., 2011), and
125 data on calcareous plankton communities (Agnini et al., 2007; Luciani et al., 2007), providing perhaps
126 the most complete reconstruction across the PETM in Europe to date.

127 We pay homage to research by Italian researchers (Di Napoli Alliata et al., 1970; Braga et al.,
128 1975), who first described the benthic foraminiferal turnover across the Paleocene-Eocene transition in
129 Italy.

130

131 **2 Materials and methods**

132 **2.1 The Forada section**

133 The Forada section (46.036083°N, 12.063975°E) is exposed along the Forada creek, ~ 2 km east of
134 the village of Lentiai (Fig. 1) in the Venetian Pre-Alps (NE Italy). It consists of ca. 62 m of Scaglia
135 Rossa, pink-reddish limestones and marly limestones, locally rhythmically bedded, and encompassing
136 the Upper Cretaceous through the lower Eocene (Fornaciari et al., 2007; Giusberti et al., 2007). The
137 upper Paleocene–lower Eocene succession is interrupted by the clay marl unit (CMU; Giusberti et al.,
138 2007), which marks the PETM and correlates with clay-rich units on other continental margins (e.g.,
139 Schmitz et al., 2001; Crouch et al., 2003; John et al., 2008; Nicolo et al., 2010). The investigated
140 interval has been subdivided into four sub-intervals based on the $\delta^{13}\text{C}$ record in bulk rock (Giusberti et
141 al., 2007). From bottom to top, these are the pre-CIE, the main CIE, the CIE recovery and post-CIE
142 (Fig. 2). The main CIE (Giusberti et al., 2007; Figs. 2, 3) occurs in the >3 m-thick CMU, within which
143 are recorded the short-lived occurrences of the calcareous plankton “excursion taxa” (Kelly et al., 1996,
144 1998) and the BEE (Agnini et al., 2007; Giusberti et al., 2007; Luciani et al., 2007). Sedimentation
145 rates in the CMU were five times higher than in the upper Paleocene, indicating increased continental
146 weathering and run-off, which led to increased sediment influx in the Belluno Basin (Giusberti et al.,
147 2007).

148

149 **2.2 Benthic foraminifera**

150 Benthic foraminiferal assemblages were studied in 54 samples from the same set studied by
151 Luciani et al. (2007) across an ~11 meter-thick interval straddling the PETM (-467 to +591.5 cm; Fig.

152 2), which reflects \sim 800 kyr (Giusberti et al., 2007). In this study the planktic foraminifera
153 fragmentation index (F Index) of Luciani et al. (2007) is used as a proxy for dissolution (Figs. 2, 3)
154 (Hancock and Dickens, 2005). The sample spacing for benthic foraminiferal assemblage analysis was
155 determined based on biostratigraphic and cyclostratigraphic data (Agnini et al., 2007; Giusberti et al.,
156 2007; Luciani et al., 2007). A sampling interval of 3–5 cm was used across the onset of the CIE (-42.5
157 to + 50 cm interval), a 25 cm sample interval over the main CIE (from +75 to 335 cm). Below -42.5 cm
158 and above 335 cm we adopted a spacing between 20 and 50 cm. Samples were collected excluding, to
159 the extent possible, bioturbated material. Further selection and removal of bioturbated material was
160 carried out in the laboratory before sample processing. Data previously collected from the Forada
161 section indicate that significant bioturbation effects are not present (e.g., Agnini et al., 2007; Giusberti
162 et al., 2007; Luciani et al., 2007).

163 Foraminifera were extracted from the indurated marls and limestones using the “cold acetolysis”
164 technique of Lirer (2000), following Luciani et al. (2007). Soft marly and clayey samples (mostly from
165 the CMU interval) were disaggregated using a 10–30% solution of hydrogen peroxide. The samples
166 with the lowest content of CaCO_3 (e.g., clays of basal CMU) were treated with diluted hydrogen
167 peroxide (10%), in order to prevent possible additional breakage of tests (especially of planktic
168 foraminifera). For more details on the comparison between the two methods of preparation (cold
169 acetolysis versus hydrogen peroxide), we refer to Luciani et al. (2007).

170 The quantitative study of benthic foraminifera was based on representative splits (using a micro-
171 splitter Jones, Geneq Inc.) of approximately 200–400 individuals $>63 \mu\text{m}$ and $<500 \mu\text{m}$ (Table S1). The
172 use of the small-size fraction is time-consuming and presents difficulties in taxonomic determination,
173 but we preferred to avoid the loss of small taxa, which are important for paleoecological investigations
174 (e.g., Thomas 1985; Boscolo Galazzo et al., 2013; 2015), especially directly after the BEE when small
175 species are dominant (Thomas, 1998; Foster et al., 2013). Between 0 and -222 cm (uppermost
176 Paleocene), the fraction $\geq 125 \mu\text{m}$ of at least 1/4 of the residue was carefully scanned for large
177 specimens of the extinction taxa, here labeled “Cosmopolitan Extinction Taxa” (CET) (see Thomas,
178 1998, 2003). These CET records have been treated qualitatively (Fig. 4). The extinction taxa include:
179 *Anomalinoides rubiginosus*, *Angulogavelinella avnimelechi*, *Aragonia velascoensis*, *Bolivinoides*
180 *delicatulus*, *Cibicidoides dayi*, *C. hyphalus*, *C. velascoensis*, *Clavulina amorpha*, *Clavulinoides*
181 *trilatera*, *Clavulinoides globulifera*, *Coryphostoma midwayensis*, *Dorothia beloides*, *D. bulletta*, *D.*
182 *pupa*, *D. retusa*, *Neoeponides megastoma*, *Gavelinella beccariiformis*, *Gyroidinoides globosus*, *G.*

183 *quadratus*, *Marsonella indentata*, *Neoflabellina jarvisi*, *N. semireticulata*, *Nuttallinella florealis*,
184 *Osangularia velascoensis*, *Paralabamina hillebrandti*, *Pullenia coryelli*, *Remesella varians* (e.g.,
185 Beckmann, 1960; Von Hillebrandt, 1962; Tjalsma and Lohmann, 1983; Speijer et al., 1996; Thomas,
186 1998), each of which is present at Forada.

187 We identified most common taxa at the species level (Table S2). Taxa with high morphological
188 variability and/or variable preservation were identified at generic or higher taxonomic level. Specimens
189 of the most representative taxa were imaged using the SEM at the C.U.G.A.S. (Centro Universitario
190 Grandi Apparecchiature Scientifiche) of Padova University (Plates 1-4). Relative abundances of the
191 taxa and taxon-groups, along with faunal indices such as the calcareous-agglutinated ratio, the infaunal-
192 epifaunal ratio, and bi-triserial percentage were calculated (Figs. 2, 5-7 and Fig. S1). The absolute
193 abundance (N/g: number of benthic foraminifera per gram-bulk dried sediment) was calculated for both
194 the ≥ 63 and ≥ 500 μm fractions. Faunal diversity indices (Species diversity and Fisher- α ; Fig. 2) were
195 calculated using the PAST package (Hammer et al., 2001). Segments belonging to tubular/branched
196 agglutinated forms (e.g., *Rhizammina*, *Rhabdammina*, *Bathysiphon*) were counted, but excluded from
197 calculations because there is no reliable method to convert the abundance of multiple fragments into
198 that of single individuals (Ernst et al., 2006).

199 We assigned species to epifaunal and infaunal morphotypes by comparing their test morphology to
200 the morphotypes in Corliss (1985), Jones and Charnock (1985), Corliss and Chen (1988), Kaminski
201 and Gradstein, (2005), Hayward et al. (2012), and Mancin et al. (2013). However, caution is needed in
202 applying taxonomic uniformitarianism due to our limited knowledge of the biology and ecology of the
203 highly diverse living species. Even for many living species, the relation between test morphology and
204 microhabitat has not been directly observed, but is extrapolated from data on other taxa (e.g., Jorissen,
205 1999). The assignment of modern foraminifera to microhabitats based on their morphology may be
206 accurate only about 75% (Buzas et al., 1993): comparisons between past and recent environments thus
207 need careful evaluation, and cross correlation between benthic foraminiferal and other proxy data. The
208 ecology as evaluated from the literature (Table 1) is shown for selected benthic foraminiferal taxa from
209 the PETM interval at Forada.

210

211 2.3 Age model

212 The age model used for calculating the longevity of benthic foraminiferal assemblages (see below)
213 follows Luciani et al. (2007), with the lower Eocene chronology based on the cyclostratigraphic age
214 model of Giusberti et al. (2007; Fig. 3). The duration of each precessional cycle has been assumed to be
215 21 kyr. Sedimentological and geochemical parameters oscillate cyclically within the main CIE, in at
216 least five complete precessional cycles (Figs. 2, 3). The CIE recovery interval is composed of six
217 distinct, precessional marly-limestone couplet cycles (Fig. 3). The recognition of eleven cycles in the
218 combined CIE and recovery interval implies an estimate of the total duration of the CIE of ca. 230 kyr
219 (Fig. 3). Giusberti et al. (2007) and Röhl et al. (2007) disagree on the duration of the main CIE and
220 recovery interval (179±17 kyr and 231±22 kyr, respectively). The main difference between these two
221 chronologies is the assignment of different numbers of precessional cycles within the main body and
222 recovery interval (Tipple et al. 2011). A ${}^3\text{He}$ -based chronology for Site 1266 (Walvis Ridge) suggests a
223 total PETM duration of 234 +48/-34 kyr (Murphy et al., 2010), in line with the age model of Giusberti
224 et al. (2007).

225 Lithological cycles have not been firmly identified in the Paleocene part of the section, and
226 sedimentation rates are interpolated between the base of the PETM at ± 0 cm and the lowest occurrence
227 of the calcareous nannofossil *Discoaster multiradiatus* at ca.-12.5 m (Giusberti et al., 2007), using a
228 duration of the time between these events of 1.238 Myr (Westerhold et al., 2007). In this age model, the
229 investigated portion of Forada section spans ca. 800 kyr.

230

231 3 Results

232 Benthic foraminiferal assemblages are generally dominated by calcareous hyaline taxa (85-90%;
233 Fig. 2), but agglutinated taxa significantly increase in abundance within the CMU (25-90%; Fig. 2).
234 Infaunal taxa strongly dominate the assemblage throughout the studied interval (~80%). Faunal
235 diversity is fairly high, particularly in the upper Paleocene (Fig. 2), and preservation is generally
236 moderate, though poor within the lowermost centimeters of the Eocene. Most foraminiferal tests at
237 Forada are recrystallized, and totally or partially filled with calcite.

238 Composition and abundance of the assemblages change prominently across the ca. 11 m-thick
239 interval investigated (Figs. 2, 5-7) coeval with the geochemical signature of the PETM, and broadly
240 coincident with the main lithological changes. We recognized six successive benthic foraminiferal

241 assemblages (labeled A to F; Figs. 2, 5-8), mainly based on changes in abundance of the taxa listed in
242 Table 1. Assemblages A and B are characteristic of the dominantly reddish calcareous marls mottled by
243 greenish "flames" of the uppermost Paleocene, separated by the thin, barren clay layer from
244 Assemblages C, D and E, which occur in the first half of the main excursion of the CIE (lowermost
245 Eocene), within the CMU (basal green laminated clays overlaid by mottled reddish clays, marly clays
246 and marls). Assemblage F characterizes the marls of the upper half of the CMU, as well as the CIE
247 recovery interval and the overlying post-excursion interval of reddish limestone–marl couplets
248 (Giusberti et al., 2007).

249 **3.1.1 Assemblage A: the upper Paleocene fauna**

250 Assemblage A (-467.5 to -37.5 cm, estimated duration >430 kyr) has a high diversity, with
251 abundant infaunal taxa (ca. 70-80%; Fig. 2). Small bolivinids (<125 μ m) of the *Bolivinoides crenulata*
252 group (Plate 3, Figs. 7-9), and smooth-walled *Bolivina* spp. together comprise 50-60% of the > 63 μ m
253 fauna (Fig. 5), with *Siphogenerinoides brevispinosa* (~10%) and other buliminids less common (Figs.
254 5, 6). Epifaunal morphotypes are mainly represented by small cibicidids (10%), *Anomalinoides* spp.
255 (5%) and *Cibicidoides* spp. (usually <5%; Fig. 5). Rare taxa include reussellids, angulogerinids,
256 nodosariids, dentalinids, gyroidinids, valvalabaminids and unilocular hyaline taxa (Fig. S1).
257 Agglutinated taxa are mainly represented by *Spiroplectammina spectabilis*, *Trochamminoides* spp.,
258 *Paratrocchamminoides* spp., *Reophax* spp. and *Subreophax* spp. The Paleocene Cosmopolitan
259 Extinction Taxa (CET; Plate 1) are not a major component of the assemblage >63 μ m (<10%; Fig. 6),
260 but are common to abundant in the size fraction >125 μ m (>20%). Many of these have large, heavily
261 calcified tests. The most common taxa include *Gavelinella beccariiformis*, *Pullenia coryelli* and
262 *Coryphostoma midwayensis* (Table S1). CET such as *Clavulinoides globulifera*, *Cibicidoides dayi* and
263 *Cibicidoides velascoensis* are common in the >500 μ m size fraction, together with trochamminids and
264 large lituolids (Plate 1, Figs. 19, 6-8; Plate 4, Figs. 7, 8, 14, 20). The latter occur up to the top of the
265 Paleocene, but are absent in the Eocene. At -261.5 cm, the Cosmopolitan Extinction Taxa (CET) peak
266 at 15%, their maximum abundance in the studied section (Fig. 6). At the same level, peaks of large,
267 stout, heavily calcified taxa (e.g., *Cibicidoides* and anomalinids) co-occur with agglutinated taxa
268 (*Glomospira*, *Spiroplectammina* and *Haplophragmoides*, Figs. 6, 7), whereas small, thin-walled forms
269 such as bolivinids, *Siphogenerinoides brevispinosa* and cibicids decline markedly in relative abundance

270 (Figs. 5-7). Faunal density (N/g), diversity and the percentage abundance of infaunal morphotypes
271 decrease (Fig. 2), as do $\delta^{13}\text{C}$ and $\text{CaCO}_3\%$, whereas the planktonic foraminiferal fragmentation index
272 (F Index) increases significantly (Fig. 2). The upper boundary of this assemblage is defined by the
273 increase in abundance of the opportunistic taxa *Tappanina selmensis* and *Siphogenerinoides*
274 *brevispinosa*, marking the onset of Assemblage B.

275 **3.1.2 Assemblage B: the pre-CIE Paleocene fauna**

276 Assemblage B occurs at -31 to 0 cm, estimated duration ~ 34 kyr. At about -20 cm the lithology
277 shifts from reddish to greenish marls with *Zoophycos* and *Chondrites* (intervals Pa I and II of Giusberti
278 et al., 2007). In this assemblage, *Siphogenerinoides brevispinosa* and *Tappanina selmensis* increase in
279 relative abundance compared to Assemblage A (>10% at ~ 27 and -12 cm; Figs. 6, 7). Between the
280 two peaks of *S. brevispinosa* (at about ~ 20 cm; Figs. 6, 7), there is a transient negative carbon isotope
281 excursion of about 1‰, a drop in CaCO_3 from 60 to 40%, a decline in the coarse fraction to 2%, and a
282 peak in the F-Index (85-90%; Figs. 2, 3). Small and thin-walled taxa such as bolivinids, cibicidids and
283 *S. brevispinosa* decrease markedly in relative abundance, whereas big, heavily calcified taxa (e.g.,
284 Cosmopolitan Extinction Taxa, *Cibicidoides* spp., *Nuttallides truempyi*) and agglutinated forms
285 increase (Figs. 5-7). In addition, faunal density drops, as does the percentage of infaunal taxa (from
286 90% to 50%), and diversity increases (Fig. 2). From -4.5 cm upwards, the preservation of benthic
287 foraminifera deteriorates, while the F Index reaches 100% (Figs. 2, 3). At -1.5 cm preservation worsens
288 and most bi-triserial taxa decline in abundance drastically, whereas benthic foraminiferal absolute
289 abundance and $\text{CaCO}_3\%$ both decrease (Fig. 2). Faunal diversity peaks, and anomalinids, *Cibicidoides*
290 spp., *N. truempyi*, *O. umbonatus* as well as agglutinated forms increase markedly in relative abundance
291 (Figs. 2, 5, 6). In the uppermost Paleocene sample, we see the highest occurrence of most CET (Figs. 4,
292 6). Few CET (e.g., *Aragonina velascoensis*) disappear below this sample (Fig. 4). These are generally
293 rare, occurring discontinuously throughout the Paleocene, even in large samples of residue $>125 \mu\text{m}$
294 (Fig. 4). The uppermost occurrence of the CET defines the upper boundary of this assemblage, at the
295 base of the black clay layer.

296 **3.1.3 The black clay**

297 The lowermost Eocene is a thin, black clay layer (0 to +0.3 cm), slightly enriched in organic
298 carbon, and carbonate-free (Giusberti et al., 2007; Figs. 3, 8). This clay marks the base of the CMU,
299 and contains a few specimens only, agglutinated benthic foraminifera of the genera *Haplophragmoides*
300 and *Recurvoides* (10 specimens in 22 g washed sediment). It probably was deposited over less than a
301 millennium, in view of its small thickness and place within the precessionally paced cycles in the
302 PETM.

303 **3.1.4 Assemblage C: basal CIE agglutinated fauna**

304 We label this lowermost Eocene interval (lowermost 10 cm of laminated green clays of CMU;
305 estimated duration ~3.5 kyr) the BFDI (i.e., benthic foraminiferal dissolution interval), sediment with
306 low CaCO₃ wt % (~15%), and the most negative $\delta^{13}\text{C}$ values in bulk carbonate (-2‰). Assemblage C is
307 dominated by agglutinated taxa (about 90%; Fig. 2) with badly preserved and deformed tests. Tests of
308 calcareous-hyaline forms are rare, partially dissolved and fragmented. Assemblage C has minimum
309 values of faunal density (<5), diversity, and wt% coarse fraction (Fig. 2). Infaunal morphotypes have
310 their lowest abundance (ca. 36%; Figs. 2, 6). Agglutinated foraminifera are mainly represented by
311 *Eobigenerina variabilis* (25%; Plate 1, Figs. 2, 3), *Haplophragmoides* spp. (20%), *Glomospira* spp.
312 (15%), *Saccamina* spp. (10%) and *Spiroplectammina navarroana* (~ 8%; Plate 2, Fig. 6). In its upper
313 part, Assemblage C has high abundances of *Karrerulina* spp. (~20%; *K. conversa*; Plate 2, Fig. 4) and
314 *Ammobaculites agglutinans* (10%; Plate 2, Fig. 1). The latter taxa occur at relatively high abundance in
315 the overlying assemblages, up to ~+50-70 cm (Figs. 6, 7). The upper boundary of this assemblage is
316 defined by the first substantial recovery of hyaline taxa (>50%).

317 **3.1.5 Assemblage D: lowermost CIE fauna**

318 In Assemblage D (+10 to +35 cm, lithologically characterized by laminated green clays; estimated
319 duration ~9 kyr), calcareous-hyaline forms are consistently present and badly preserved, with dominant
320 taxa having dwarfed and thin-walled tests, e.g., *Globocassidulina subglobosa* (25%), *Tappanina*
321 *selmensis* (20%), and *Osangularia* spp. (~11%; Figs. 6, 7; Plate 2, Figs. 13-16). A specific assignment
322 of basal PETM osangulariids at Forada is not possible because of their very small size and poor state of
323 preservation. From +30 cm upwards, relative abundances of *G. subglobosa* and *Osangularia* spp.
324 drastically decline, whereas *T. selmensis* reaches its maximum abundance (ca. 33%; Figs. 6, 7). Minor
325 components are "other buliminids" group (up to 10% at the top of the Assemblage; see Fig. 5 and Fig.

326 5-related caption), *Pleurostomella* spp., *Oridorsalis umbonatus*, anomalinids and stilostomellids (Figs.
327 5, 6 and Fig. S1). Agglutinated forms remain abundant, up to 50%. At +20 cm, calcified radiolarians
328 become abundant, dominating the microfossil association up to +2 m above the base of CMU (Luciani
329 et al., 2007; Figs. 3, 8). Within the interval of Assemblage D, $\delta^{13}\text{C}$ shifts from -2 to -1‰, and the
330 CaCO_3 wt% recovers to ~40%, despite strong dilution with terrigenous sediments (Fig. 3). The upper
331 boundary of this assemblage is defined by the consistent decrease of *T. selmensis* (to <5%).

332 **3.1.6 Assemblage E: main CIE fauna I**

333 In this interval (+35 to +185 cm; lithologically characterized by green and reddish clays and marls;
334 estimated duration ca. 42 kyr) benthic foraminiferal preservation improves, and calcareous-hyaline
335 forms dominate the assemblages again (Fig. 2). *Siphogenerinoides brevispinosa* is consistently present
336 again, with two peaks up to 20% (Figs. 6, 7). *Pleurostomella* spp. increase to up to >10%, and
337 *Bolivinoides crenulata* and smooth-walled *Bolivina* spp. to up to 30 - 40% (Figs. 5, 6). Calcareous-
338 hyaline epifauna such as cibicids and anomalinids reappear at <5% (Fig. 5). Faunal density and
339 diversity gradually increase upwards, whereas agglutinated taxa markedly decrease in abundance
340 (<20%) at ~+70 cm (Fig. 2). The upper boundary of this assemblage is defined by the marked drop in
341 relative abundance of *S. brevispinosa* (to <5%).

342 **3.1.7 Assemblage F: main CIE fauna II, CIE recovery and post CIE fauna**

343 Assemblage F characterizes the upper half of the CMU (reddish marls), from about +185 cm up to
344 its top (+337.5 cm), and the overlying interval (red marly limestone couplets) up to +649 cm; estimated
345 total duration > 281 kyr). The relative abundance of *Siphogenerinoides brevispinosa* is low (<5%),
346 whereas *Bulimina tuxpamensis* and *Nuttallides truempyi* increase in abundance, respectively to 5 and
347 10%, and show cyclical variations in relative abundance (Figs. 6, 7). Pleurostomellids (~10%), "other
348 buliminids" group (~10%; Fig. 5), cibicids (~10%), *Oridorsalis umbonatus* (~5%), stilostomellids
349 (~5%) and *Abyssammina* spp. (~5%) are common (Figs. 5, 6). Relative abundance of infaunal taxa
350 (mostly bolivinids) and faunal density (N/g) returns to their Paleocene values (75-80%; Fig. 2).
351 Diversity increases (simple diversity up to 60, Fisher- α diversity up to 20; Fig. 2) but remains lower
352 than in the Paleocene. All faunal indices show cyclical variation (Fig. 2), as do the relative abundance
353 of benthic foraminifera, and planktic foraminiferal and calcareous nannofossil assemblages (Agnini et

354 al., 2007; Luciani et al., 2007). In the lower third of the interval in which this assemblage occurs, just
355 above the CMU (ca. +337.5 cm), the relative and absolute abundance of radiolarians decrease markedly
356 and agglutinated taxa such as *Glomospira* spp., *Eobigenerina variabilis* and *Karrerulina* spp. slightly
357 increase in relative abundance (~+2-3%) (Figs. 2, 3, 6, 7).

358

359 4 Discussion

360 4.1 Paleodepth of the Forada section

361 Based on benthic foraminifera in the >125 μ m size fraction, Giusberti et al. (2007) suggested a
362 paleodepth between 600 and 1000 meters for the Forada section. Our data on the >63 μ m size fraction
363 suggest a somewhat greater paleodepth, i.e., upper lower bathyal, between 1000 and 1500 meters (van
364 Morkhoven et al., 1986). Representatives of the bathyal and abyssal Velasco-type fauna (Berggren and
365 Aubert, 1975), such as *Aragonia velascoensis*, *Cibicidoides velascoensis*, *Gyroidinoides globosus*,
366 *Nuttallides truempyi*, *Nuttallinella florealis*, *Osangularia velascoensis* and *Gavelinella beccariiformis*
367 are common at Forada. The faunas across the uppermost PETM interval and higher are similar to the
368 PETM-fauna in the upper abyssal Alamedilla section (Souther Spain; Alegret et al., 2009a) and at
369 Walvis Ridge at 1500 m paleodepth (Thomas and Shackleton, 1996; Thomas, 1998). *Abyssammina*
370 spp. and *Nuttallides truempyi* (upper depth limit at 1000 and 300 m respectively; Van Morkhoven et
371 al., 1986; Speijer and Schmitz, 1998) increase in abundance by more than a factor of 2 during the
372 PETM at Forada, as typical for PETM deep-sea benthic foraminiferal records (e.g., Thomas, 1998;
373 Thomas and Shackleton, 1996; Thomas, 2007; Alegret et al., 2009a, 2011; Giusberti et al., 2009). In
374 these deliberations we excluded the bolivinids, because we consider that their high abundance is due to
375 the “delta depression effect” (see below).

376 4.2 Environmental reconstruction during the late Paleocene

377 4.2.1 The Belluno Basin Paleocene deep-sea environment (Assemblage A)

378 Throughout most of the investigated section, infauna strongly dominate over epifauna, mainly
379 due to the high abundances of bolivinids (Figs. 2, 5). Such dominance of bolivinids is common in
380 lower and middle Eocene hemipelagic Scaglia sediments in the Belluno basin (Agnini et al., 2009;
381 Boscolo Galazzo et al., 2013). Presently, bolivinids are common along continental margins, and at

382 bathyal depths, at the interception of the oxygen minimum zone (OMZ) with the seafloor, typically
383 between 200 and 1000 m in modern oceans (Levin, 2003). High abundances of bolivinids commonly
384 correlate with high organic matter flux and/or oxygen depletion (e.g., Murray, 1991; Gooday, 1994;
385 Bernhard and Sen Gupta, 1999; Schmiedl et al., 2000; Thomas et al., 2000; Jorissen et al., 1995, 2007;
386 Thomas, 2007). We see high abundances of such taxa typically at greater depths than usual in regions
387 with significant organic matter input from rivers, the so-called “delta-depression” effect first described
388 in the Gulf of Mexico (Pflum and Frerichs, 1976; Jorissen et al., 2007). Such lateral inputs of organic
389 matter thus result in (partial) decoupling between the food supply to the benthos and local primary
390 productivity (e.g., Fontanier et al., 2005; Arndt et al., 2013).

391 At Forada, there is neither geochemical nor sedimentological evidence for persistent suboxic
392 conditions at the sea-floor (Giusberti et al., 2007), and the high benthic foraminiferal faunal diversity
393 likewise does not indicate low oxygen conditions. The upper Paleocene calcareous plankton is
394 dominated by morozovellids indicating oligotrophic surface water conditions (Luciani et al., 2007; Fig.
395 8). The calcareous nannofossil assemblage is dominated by the generalist taxa *Toweius* and
396 *Coccolithus*, with high percentages of *Sphenolithus* and *Fasciculithus* (Agnini et al., 2007; Fig. 8),
397 supporting that surface waters were oligotrophic. We thus think that environments in the Belluno
398 Basin, close to a continental margin (Agnini et al., 2007), were characterized by the “delta depression
399 effect”, in which hemipelagic sedimentation incorporated significant laterally transported terrigenous
400 organic matter to serve as food for the benthos (e.g., Fontanier et al., 2008; Arndt et al., 2013).
401 The occurrence of large, epifaunal (> 500 µm) species (Assemblage A and B), has been related to an
402 optimum food supply, but also to very low food supply, since a lack of food keeps individuals from
403 reproducing successfully and leads to continued test-growth (Boltovskoy et al., 1991; Thomas and
404 Gooday, 1996).

405 Overall, Assemblage A, indicates oligo-mesotrophic surface waters, with bolivinids probably
406 exploiting refractory, laterally advected organic matter. The high faunal diversity suggests that seasonal
407 to periodical increases in primary productivity may have occurred (e.g., Gooday, 2003; Fontanier et al.,
408 2006a, 2006b, 2014), allowing a species-rich, highly diverse infauna and epifauna to inhabit the sea-
409 floor, and co-occur with the bolivinids in the sedimentary record.

410 At Forada, the relative abundance of Paleocene Cosmopolitan Extinction Taxa (CET) is low
411 (average <10%; Fig. 6), due to the large number of Bolivinacea dominating the fine size fraction used

412 for this study (>63 μ m). Many CET (Plate 1) are epifaunal morphotypes, commonly larger than 125
413 μ m, as also noted elsewhere (e.g., Giusberti et al., 2009). Similarly low percentages (12-15%) of CET
414 have been recorded in Scaglia sediments of the Contessa section (Giusberti et al., 2009) and at ODP
415 Site 690 by Thomas (2003), where infaunal morphotypes (buliminids and uniserial calcareous taxa) are
416 abundant in the >63 μ m fraction.

417

418 **4.2.2 The precursor warming event (Assemblage B)**

419 The onset of Assemblage B, about 34 kyr before the onset of the CIE (~30 cm), is marked by
420 increase in relative abundance of opportunistic taxa such as *Tappanina selmensis* and
421 *Siphogenerinoides brevispinosa* (Figs. 6, 7; Table 1). The arrival of *Tappanina selmensis*, an upper
422 bathyal to outer shelf species in the Maastrichtian (Frenzel, 2000), at greater depths might indicate
423 warming of deep waters before the beginning of the PETM, as also reflected in the migration of warm-
424 water planktonic species to high southern latitudes (Thomas and Shackleton, 1996; Table 1). The
425 benthic foraminiferal changes roughly coincided with a significant increase in acarininids% (planktonic
426 foraminifera, >50%), likely indicating warming of surface waters (Luciani et al., 2007; Fig. 8). The
427 foraminiferal assemblages hence suggest warming throughout the water column, and increased surface
428 nutrient availability and deep-water food availability, whereas no changes in productivity in calcareous
429 nannofossils are recorded (Agnini et al., 2007; Luciani et al., 2007; Fig. 8). The foraminiferal evidence
430 for warming is associated with an increase in $\delta D_{n\text{-alkanes}}$ and TEX_{86} values (Fig. 9), suggesting increased
431 aridity and sea surface temperature prior to the onset of the CIE (Tipple et al., 2011).

432 Multiple proxies thus indicate that climatic and oceanographic conditions started to change ~30
433 kyr before the onset of the CIE, pointing to a PETM precursor event, reflected by a <5-cm thick
434 dissolution interval at ~22 cm, coinciding with a negative shift in bulk $\delta^{13}\text{C}$ (-1‰; Figs. 2, 3). Within
435 this interval dissolution-sensitive benthic foraminifera (e.g., *S. brevispinosa* and small bolivinids)
436 markedly decrease in abundance, while more robust and agglutinated taxa increase (Figs. 2, 5-8), as
437 does the F-Index of planktic foraminifera (to ~ 85-90%; Luciani et al., 2007; Fig. 3). This dissolution
438 level may thus reflect a brief episode of rising lysocline/CCD (<5 kyr) in response to a precursory
439 emission of isotopically light carbon (Bowen et al., 2015). Similar precursor events have been observed
440 worldwide (e.g., Sluijs et al., 2007b; 2011; Secord et al., 2010; Kraus et al., 2013; Garel et al., 2013;

441 Bornemann et al., 2014; Bowen et al., 2015), indicating that disturbance of the global carbon cycle
442 started before the PETM, as potentially also reflected in the occurrence of hyperthermals in the
443 Paleocene (Thomas et al., 2000; Cramer et al., 2003; Coccioni et al., 2012).

444 At the top of Assemblage B (uppermost 4.5 cm), just prior to the onset of the CIE, carbonate
445 preservation declined markedly, as reflected in F-Index, $\text{CaCO}_3\%$, and foraminiferal preservation. In
446 this interval, representing the “burndown” layer (BL; e.g., Thomas and Shackleton, 1996; Thomas et
447 al., 1999; Giusberti et al., 2007; Figs. 4, 7, 8), CET remained present. Dissolution in the upper BL
448 removed most thin, dissolution-prone calcareous tests (e.g., *Siphogenerinoides brevispinosa* and small
449 bolivinids), concentrating the more heavily calcified and the agglutinated taxa (included CET; Fig. 5-
450 7). Benthic foraminiferal assemblages in the topmost Paleocene at Forada thus cannot be interpreted
451 with confidence due to the severe dissolution.

452 **4.3 Climate and marine life during the PETM**

453 **4.3.1 The black clay: a desert below the CCD**

454 This very thin, carbonate-free interval is somewhat enigmatic. The virtually barren sediment may
455 have been deposited during the maximum rise of the CCD, under environmental conditions so
456 unfavorable that benthic life was excluded, a "dead-zone" (*sensu* Harries and Kauffman, 1990) during
457 the earliest phase of the PETM. Geochemical redox indices in the black clay and the underlying and
458 overlying samples suggest persistently oxygenated bottom waters (Giusberti et al., 2007), but may
459 reflect diagenesis during re-oxygenation of bottom waters after a short period of anoxia, as commonly
460 observed for Mediterranean sapropels (Higgs et al., 1994; van Santvoort et al., 1996). The presence of the
461 thin black clay without microfossils thus is highly suggestive of a brief pulse of anoxia, as supported by
462 a single peak value of organic carbon (0.6 wt %; Giusberti et al., 2007). The high value of biogenic
463 barium (3151 ppm) in the black clay (Fig. 3), despite the fact that barite is generally not preserved
464 under anoxic conditions (Paytan and Griffith, 2007; Paytan et al., 2007) may represent reprecipitation at
465 the oxic/anoxic sediment interface after dissolution under anoxic conditions (Giusberti et al., 2007),
466 and/or high rates of organic remineralization in the water column, during which the barite forms (Ma et
467 al., 2014).

468 **4.3.2 The early peak PETM (Assemblages C and D)**

469 The 10 cm of sediment directly overlying the Paleocene/Eocene boundary (i.e. the base of the CIE;
470 Figs. 7, 8) was deposited in strongly CaCO_3 –corrosive waters, below the lysocline and close to or
471 below the CCD. The rapid rise of the CCD/lysocline during the PETM is a predicted consequence of
472 massive input of carbon (CO_2 or CH_4) in the ocean-atmosphere system on a millennial timescale (e.g.,
473 Dickens et al., 1997; Thomas, 1998; Zachos et al., 2005; Zeebe et al., 2009, 2014; Hoenisch et al.,
474 2012). The carbonate dissolution at Forada is consistent with observations at many other deep-sea sites
475 (e.g., Schmitz et al., 1997; Thomas, 1998; Zachos et al., 2005; Kelly et al., 2010). The benthic
476 foraminiferal extinction event (BEE) at Forada (i.e., corresponding to the the BB1/BB2 zonal boundary
477 of Berggren and Miller, 1989) occurs within this 10 cm-thick interval, between the top of the CET-
478 bearing burndown layer and the base of Assemblage D, where benthic calcareous taxa reappear (Figs.
479 4, 7, 8). The concentration of CET in the burndown layer, and the reappearance of calcareous hyaline
480 taxa only 10 cm above the onset of the PETM at Forada, confirms that the CET extinction occurred
481 over 3.5 kyr or less in the central western Tethys, similar to evaluations of this timing from carbon
482 cycle modeling (Zeebe et al., 2014).

483 Sediment just above the black clay, reflecting a first slight deepening of the CCD, contains a low
484 diversity, fauna of mostly agglutinated, dwarfed (close to 63 μm in diameter) benthic foraminifera, and
485 calcareous nannofossils with signs of dissolution, with planktic foraminifera virtually absent (Agnini et
486 al., 2007; Luciani et al., 2007; Fig. 8). This first wave of benthic pioneers recolonized the sea-floor
487 during the peak-CIE, in CaCO_3 -undersaturated waters, and reflects a highly stressed environment
488 (Assemblage C; Figs. 6-8). Among the pioneers, *Eobigenerina variabilis* is peculiar of the PETM of
489 the Forada section (Figs. 6, 7). *Eobigenerina* is a recently erected genus in the Textulariopsidae,
490 including non-calcareous species previously assigned to *Bigenerina* (Cetean et al., 2011), and it is
491 known to behave opportunistically during Cretaceous Oceanic Anoxic Event 2 (OAE2; Table 1). A
492 major component of the upper part of Assemblage C is *Karrerulina conversa* (Fig. 7). The species
493 dominates the lowermost Eocene deposits in the Polish Carpathians (Bąk, 2004), commonly occurring in
494 the Paleocene-Eocene of the Central North Sea and Labrador margin, and in Morocco (Kaminski and
495 Gradstein, 2005). Modern *Karrerulina* (e.g., *K. apicularis*=*K. conversa*) live in oligotrophic abyssal
496 plains, with well-oxygenated bottom and interstitial waters (Table 1). However, the test morphology of
497 *Karrerulina*, combined with its abundant occurrence in the doubtless stressed environment of the basal
498 PETM at Forada and Zumaia (Table 1), suggests that this genus may also act opportunistically.

499 After ca. 4 kyr, a further deepening of CCD allowed a consistent increase in abundance of benthic
500 calcareous taxa (ca. 50%; Assemblage D; Fig. 2), coinciding with the lowermost recovery of bulk
501 carbonate $\delta^{13}\text{C}$ values, from $-2\text{\textperthousand}$ to $-1\text{\textperthousand}$ (Giusberti et al., 2007; Tipple et al., 2011; Fig. 7). These
502 calcareous recolonizers included dwarfed and thin-walled forms of *G. subglobosa*, *Tappanina*
503 *selmensis*, *Osangularia* spp. and *Oridorsalis umbonatus* (Figs. 6, 7). A similar peak in small
504 *Osangularia* also occurs in the basal PETM at Contessa Section, as documented for the first time in the
505 present paper (Fig. S2). Representatives of the genus *Osangularia* (*Osangularia* spp.) behaved
506 opportunistically in the PETM of the Tethyan Alamedilla section (Alegret et al., 2009a). Moreover,
507 Boscolo Galazzo et al. (2013) found small-size *Osangularia* within organic-rich levels immediately
508 following the Middle Eocene Climatic Optimum in the Alano section (in northeastern Italy). During the
509 Cretaceous OAEs *Osangularia* spp. opportunistically repopulated the sea floor during short-term re-
510 oxygenation phases (see references in Table 1). Although *Osangularia* is generally referred to as
511 preferring stable well oxygenated environments (e.g., Murray, 2006; Alegret et al., 2003), we suggest
512 that some extinct species of this genus could actually behave as opportunist and recolonizer.

513 Assemblage D contains almost equal abundances of calcareous and agglutinated taxa, indicating
514 that factors other than bottom water CaCO_3 concentration were controlling faunal variability within this
515 assemblage (Figs. 6, 7). Possibly, strongly enhanced runoff and sediment delivery can explain the
516 abundance of agglutinated taxa (40-60%), such as *Glomospira* spp. (e.g., Arreguín-Rodríguez et al.,
517 2013, 2014), above the first 10 cm of the CMU. We thus recognize a rapid succession of recolonizer
518 taxa during the first 12 kyr of the CIE (Assemblages C-D). The small size of both the agglutinated and
519 hyaline recolonizers is indicative of r-strategist species which reproduce quickly and can thus quickly
520 repopulate stressed environments, as soon as conditions improve slightly (e.g., Koutsoukos et al., 1990;
521 Thomas, 2003). The rapid pace at which different populations of recolonizers succeeded each other
522 indicates a highly unstable environment, with marked fluctuations in the amount, timing and quality of
523 the food reaching the sea floor. Sediment deposition during this interval may have occurred in rapid
524 pulses, e.g., following intense rainstorms, carrying refractory organic matter to the deep-sea
525 environment. Pauses between events may have allowed the benthic foraminifera to recolonize the
526 sediment, profiting of the abundance of food. This is consistent with calcareous nannofossil
527 assemblages showing an increase in *Ericsonia* and declines in abundance of *Sphenolithus*, *Octolithus*,
528 *Zygrablithus* and *Fasciculithus*, indicating an unstable and nutrient rich upper water column (Agnini et

529 al., 2007; Fig. 8). Archaeal biomarkers show a large influx of terrestrial, soil-derived organic matter
530 (Branched and Isoprenoid Tetraethers or BIT Index) from the onset of the PETM up to ~+10 cm
531 (Tipple et al., 2011). Higher plant *n*-alkane average chain length (ACL) decreased immediately after
532 the onset of the CIE, consistent with increased humidity (Fig. 9; Tipple et al., 2011). The abundance of
533 the clay mineral chlorite indicates enhanced physical erosion (Robert and Kennett, 1994) during
534 deposition of the lower 50 cm of the CMU, rapidly decreasing upward (Fig. S3).

535 The greenish marly clays containing Assemblages C and D show primary lamination, indicating
536 that macrobenthic invertebrates were absent, as at Dee and Mead Stream sections (New Zealand;
537 Nicolo et al., 2010), and Zumaya (Spain; Rodriguez-Tovar et al., 2011). The presence of benthic
538 foraminifera, however, indicates that bottom and pore waters were not permanently anoxic. Pore waters
539 may have become dysoxic periodically due to high temperatures, decomposing organic matter and
540 possibly enhanced water column stratification, leading to the absence of metazoans and stressed
541 benthic foraminiferal assemblages. Low-pH sea-floor conditions may have also played a significant
542 role in excluding macrobenthic fauna in this early phase of PETM at Forada. Deep-sea animals are
543 highly sensitive to even modest but rapid pH changes (Seibel and Walsh, 2001), which are harmful
544 even for infaunal deep-sea communities (Barry et al., 2004).

545 4.3.3 The core of the CIE and Recovery (Assemblages E, F)

546 The benthic foraminiferal assemblage changes significantly from Assemblage D to assemblage E,
547 coinciding with the gradual reappearing of mottling (as thin reddish “flames” in the green sediment).
548 Bolivinids return as a major faunal component (50%), and agglutinated taxa decrease in abundance.
549 Peaks of tapered elongate calcareous forms, including *Siphogenerinoides brevispinosa*, “other
550 buliminids” group, pleurostomellids and stiliostomellids, replace the recolonizers (Figs. 5, 6). These
551 groups could have been functioned as opportunistic taxa, able to flourish when food supply was
552 periodically high (e.g., Table 1). Coinciding with Assemblage E, planktic foraminifera return to be a
553 significant component of the microfossil assemblage (e.g., Luciani et al., 2007; Fig. 8), while
554 radiolarians remain abundant throughout the CMU (Giusberti et al., 2007; Luciani et al., 2007). The
555 planktic foraminiferal assemblage is dominated by acarininids, with a double peak of the excursion
556 species *Acarinina sibaiyaensis* and *A. africana*, which, combined with the high percentages of the
557 nannofossil *Ericsonia*, indicate warm and eutrophic surface waters (e.g., Ernst et al., 2006; Guasti and
558 Speijer, 2007; Agnini et al., 2007; Luciani et al., 2007; Fig. 8).

559 Detrital hematite sharply increased in concentration at the onset of Assemblage E (Giusberti et al.,
560 2007; Dallanave et al., 2010; 2012; Fig. 3). Hematite forms in soils under warm and dry conditions, and
561 an increase of hematite in marine sediments is considered indicative of an arid climate over the
562 adjoining land, with increased wind strength (Larrasoña et al., 2003; Zhang et al., 2007; Itambi et al.,
563 2009), or humid to subhumid climates with seasonal drying (Torrent et al., 2006). It is delivered to the
564 deep-sea environment through river runoff or as aeolian dust (e.g., Zhang et al., 2007; Itambi et al.,
565 2009). Within the CMU, hematite shows cyclical fluctuations with a ~21 kyr periodicity, but other
566 terrigenous components (quartz and phyllosilicates) do not co-vary in abundance after a ~15% increase
567 at the onset of the CMU (Fig. 3). To explain the different abundance patterns, we interpret hematite as
568 wind-delivered, silicate minerals as runoff-delivered.

569 The hematite% peaks may be indicative of cyclical variability in wind-delivered material, rather
570 than the earlier prevailing consistently humid climate. The lithological anomaly of the CMU, the
571 fivefold increase in sedimentation rates and increase in reworked Cretaceous nannofossils (Agnini et
572 al., 2007; Fig. 8), as well as the silicate mineral and hematite% records all indicate marked fluctuations
573 in the hydrological regime throughout this interval. High hematite% may reflect the presence of high-
574 pressure cells over land, during an overall dry climate phase, with increased wind strength and dust
575 delivery to the sea (Larrasoña et al., 2003; Zhang et al., 2007; Itambi et al., 2009). In contrast, low
576 values of hematite% may indicate periods of greater humidity and enhanced precipitation. Such
577 alternation of wet and arid phases favored deeper soil erosion on the continental areas surrounding the
578 Belluno basin (Thiry, 2000; Schmitz and Pujalte, 2003), causing major washouts during the wet phases,
579 which may explain the fivefold increase in sedimentation rates and 15% increase in phyllosilicate
580 abundance in the CMU (Fig. 3).

581 The hematite% cycles are in phase with cycles in $\text{CaCO}_3\%$, radiolarian abundance, and bulk
582 carbonate $\delta^{13}\text{C}$, slightly preceding the others stratigraphically (Fig. 3). During the arid climate phase,
583 enhanced wind strength may have generated intense surface water mixing and offshore nutrient
584 upwelling, inducing increases in primary productivity and phytoplankton blooms. The blooms in
585 primary productivity resulted in deposition of abundant algal biomass, leading to the occurrence of
586 peaks of pleurostomellids, stiliostomellids and *Siphogenerinoides brevispinosa* in Assemblage E.
587 Productivity may have remained fairly high during the wet periods, as indicated by consistently high
588 biogenic barium throughout the CMU (Giusberti et al., 2007; Paytan et al., 2007). During the rainy

589 periods, upwelling rates may have been lower, with nutrients mostly supplied in river runoff. The
590 delivery of food to the seafloor may have been more continuous, but with more important input of
591 refractory organic matter from land.

592 In contrast to these proxies, which show cyclicity at precessional periods throughout the CMU,
593 higher plant *n*-alkane average chain length (ACL) and δD vary only in its lowermost 50 cm (Tipple et
594 al., 2011; Fig. 9). Possibly, the sedimentary *n*-alkanes were derived from a pool of plant material
595 produced during subsequent wet and dry phases, so that ACL and δD may represent averaged records
596 of leaf wax *n*-alkanes produced during different mean climate states in the upper CMU. Even so, the
597 δD values within the CMU are on average $\sim 15\text{\textperthousand}$ lower than above and below (Fig. 9), as reported for
598 the Cicogna section (10 km away; Krishnan et al., 2015), possibly reflecting more humid
599 conditions/higher precipitation during the PETM wet times (e.g., Sachse et al., 2006; Smith and
600 Freeman, 2006), or greater productivity of plant material during the wet phases. Alternatively, it may
601 reflect a primary change in the isotopic composition of meteoric waters (Krishnan et al., 2015).

602 In the following benthic foraminiferal Assemblage F (upper CMU, recovery phase),
603 *Siphogenerinoides brevispinosa* and *Tappanina selmensis* are less abundant, whereas *Bulimina*
604 *tuxpamensis*, *Abyssammina* spp., and *Nuttallides truempyi* increase in relative abundance (Figs. 6, 7).
605 These are typical deep-sea, open-ocean taxa which thrive under more oligotrophic conditions (e.g.,
606 Thomas, 1998), and might indicate progressively less intense or shorter primary productivity blooms
607 during the arid phases, and/or mark the return to fully oxygenated sea-floor and pore water conditions.
608 Less intense eutrophy at the transition from Assemblage E to F is further supported by calcareous
609 plankton data, showing a decrease in the planktic foraminiferal excursion species, and among
610 nannofossils, a decrease in *Ericsonia* (Agnini et al., 2007; Luciani et al., 2007; Fig. 8). Concluding with
611 the top of the CMU, there were marked changes in calcareous plankton assemblages, although benthic
612 foraminiferal Assemblage F persisted. Among calcareous nannofossils the abundance of *Zygrablithus*,
613 *Sphenolithus* and *Octolithus* increased, whereas that of reworked taxa decreased (Fig. 8). In the
614 planktic foraminiferal assemblage, *Acarinina* species declined in abundance, and the fauna became
615 more diverse, with fluctuations modulated by lithology in the marl-limestone couplets overlying the
616 CMU (Fig. 8).

617 The lithological unit above the CMU consists of an alternation of limestones and marls at
618 precessional frequencies (~ 21 kyrs; Fig. 2). These limestone-marl couplets persist for up to 8 meters

619 above the CMU (well beyond the top of the studied interval; Giusberti et al., 2007; Luciani et al.,
620 2007), then gradually become less clearly expressed, fading upwards. The marl-limestone couplets may
621 reflect the persistence of wet (marl)-arid (limestone) cycles for ~ 800 kyr after the end of the CMU
622 deposition, though at an amplitude declining over time. This persistence resembles the extended (650
623 kyr) humid period, starting at the onset of PETM, recognized in the sediment record at Site 401 of
624 eastern North Atlantic (Bornemann et al., 2014). Our benthic foraminiferal data agree with this
625 interpretation, showing substantially unchanged sea-floor conditions up to +650 cm (uppermost sample
626 analyzed).

627 **4.4 Clues from Forada on PETM climate change**

628 The integrated dataset collected at Forada supports the occurrence of enhanced climatic contrasts
629 and productivity changes in the western Tethys during the PETM, and agrees with previous studies
630 suggesting intense weather extremes at mid to subtropical latitudes (Fig. 10; Table S3). At the onset of
631 the PETM, middle to subtropical latitudes may have been characterized by intense, monsoonal-type
632 rainfall, followed by a succession of wet and arid phases, possibly precessionally paced, during the core
633 of the PETM (e.g., Collinson et al., 2007; Kraus and Rigging, 2007; Egger et al., 2009; Foreman et al.,
634 2014; Stassen et al., 2012a,b; 2015; Fig. 10 and Table S3). The Forada record allows to distinctly
635 recognize the temporal successions among these distinct climatic phases up to 800 kyr after the onset of
636 the PETM, and to directly relate them to the progression of the CIE, its recovery and termination. The
637 climatic conditions inferred from the Forada section and other records at similar latitudes differ from
638 those derived from the subtropical net evaporation zone (15°-35°N), (e.g., from the Tremp-Graus Basin
639 - Pyrenees), which document a generally much drier climate with a brief interval of increased
640 storminess and intense flash flood events at the onset of the PETM (Schmitz and Pujalte, 2007).
641 Records from subtropical to mid-latitudes also differ from records within the northern rain belt and into
642 the Arctic basin (>50°N), which suggest that humid conditions may have been more persistent there,
643 with increased rates of precipitation, and on average moister conditions during the PETM (Pagani et al.,
644 2006b; Sluijs et al., 2006; Harding et al., 2011; Dypvik et al., 2011; Kender et al., 2012; Wieczorek et
645 al., 2013; Fig. 10; Table S3).

646 The combination of all these climatic records (Fig. 10; Table S3) suggests that the net result of
647 increased weather extremes during peak-PETM might have been to decrease rainout at subtropical to
648 mid latitudes, and increase moisture transport toward the high latitudes, as originally suggested by

649 Pagani et al. (2006b). Few tropical records exist, so that precipitation changes here are less clear.
650 Rainfall in coastal Tanzania may have decreased during the early PETM, but combined with violent
651 precipitation events and floodings (Handley et al. 2008; 2012; Aze et al., 2014; Table S3). In Central
652 America, conditions during the PETM may have shifted to more continuously humid (Jaramillo et al.,
653 2010).

654 The long-lasting cyclity and precise chronology at Forada suggest that this enhanced climate
655 variability at subtropical to mid latitudes may have lasted for several hundred of thousand years after
656 the onset of the CIE. Despite the possible decrease of net rainout, these weather extremes persisting
657 over several 10^5 kyr may have significantly enhanced the rate of erosion and weathering, through the
658 occurrence of alternating wet-dry periods. The weathering may have led to a decrease in atmospheric
659 CO_2 levels, by consumption of CO_2 during weathering reactions. The increased supply of cations
660 through enhanced weathering-erosion would have driven ocean pH up, and atmospheric CO_2 down
661 (Broecker and Peng, 1982; Raymo et al., 1988; Zachos et al., 2005). Enhanced seasonal extremes
662 across large geographical areas (the subtropical to mid latitudinal belt) thus might have been a response
663 to the large CO_2 input at the Paleocene-Eocene transition, and may have had a primary role in restoring
664 the carbon cycle to steady state.

665

666 **6 Conclusions**

667 The continuous and expanded record of benthic foraminifera across the PETM at Forada,
668 integrated with the extensive datasets previously generated across this interval, may provide the most
669 complete reconstruction of ecological and climatic changes during the Paleocene/Eocene thermal
670 maximum in Europe. Coupled sedimentological, molecular and micropaleontological records highlight
671 a complex sequence of environmental and climatic changes during the time period across the CIE:

672 - Climatic and oceanographic conditions started to change ~30 kyr before the onset of the PETM, with
673 a possible precursor event.

674 - Our high-resolution benthic foraminiferal record combined with the established chronology lets us
675 infer that the BEE in the central-western Tethys occurred over a time interval of not more than 4 kyr.
676 At the onset of the PETM, combined de-oxygenation, acidification and environmental instability may
677 have synergistically impacted deep sea life.

678 -Four benthic foraminiferal assemblages occur (C-E and lower F) within the CMU (coinciding with the
679 main phase of CIE). Assemblage C is characterized by successive peaks of different agglutinated
680 recolonizers. Calcareous recolonizers return in the following Assemblage D, after calcium carbonate
681 saturation increased. The complex succession of peaks of agglutinated and hyaline recolonizers in these
682 two assemblages (C, D; 12.5 kyr), suggests multiple repopulation episodes. The benthic foraminiferal
683 data integrated with molecular and mineralogical data point to increased precipitation and strong
684 continental erosion during this short initial stage of the PETM.

685 - Within the core of the CIE, $\delta^{13}\text{C}$ and mineralogical properties such as hematite and calcium carbonate
686 wt % vary at precessional periodicity. Combined with data on radiolarian abundance and benthic
687 foraminiferal assemblage composition this variability suggests an alternation of overall wetter and drier
688 periods. Enhanced weather extremes during most of the PETM may have led to a decrease in total
689 precipitation over the central western Tethys.

690 - The benthic foraminiferal assemblage at Forada did not significantly change with the onset of the
691 deposition of marl-limestone couplets unit above the CMU (mid and upper third of Assemblage F).
692 This suggests that the enhanced climatic variability at precessional timescales persisted well after the
693 end of the CIE recovery. We argue that enhanced seasonal extremes at mid-latitudes might have been a
694 direct climate response to the huge CO_2 input at the Paleocene-Eocene transition, and may have had a
695 primary role in restoring carbon cycle steady state through links with the water cycle and weathering
696 rates.

697

698 **Acknowledgments**

699 This work was funded by the Italian Ministry of Education and Research (MIUR) funds (PRIN 2001,
700 2007 and 2010-2011 to Domenico Rio; n. prot. 2001048975_002; 2007W9B2WE_004;
701 2010X3PP8J_003). This manuscript benefited from constructive reviews of Robert Speijer and
702 Nicoletta Mancin. LG and FBG are deeply indebted to Domenico Rio for the original idea of the
703 "Paleogene Veneto Project", the financial and material support, and for fruitful discussions during all
704 these years. ET acknowledges financial support by the Leverhulme foundation (UK) and NSF Grant
705 OCE 1232413.

706

707 **References**

708 Agnini, C., Fornaciari, E., Rio, D., Tateo, F., Backman, J., and Giusberti, L.: Response to calcareous
709 nannofossil assemblages, mineralogy and geochemistry to the environmental perturbations across the
710 Paleocene/Eocene boundary in the Venetian Pre-Alps, *Mar. Micropaleont.*, 63, 19-38, 2007.

711 Agnini, C., Macrì, P., Backman, J., Brinkhuis, H., Fornaciari, E., Giusberti, G., Luciani, V., Rio, D.,
712 Sluijs, A., and Speranza, F.: An early Eocene carbon cycle perturbation at ~52.5 Ma in the Southern
713 Alps: chronology and biotic response, *Paleoceanography*, 24, PA2209, 2009.

714 Alegret, L., Molina, E., and Thomas, E.: Benthic foraminiferal faunal turnover across the
715 Cretaceous/Tertiary Boundary at Agost (Southeastern Spain), *Mar. Micropaleont.*, 48, 251-279, 2003.

716 Alegret, L., Ortiz, S., Arenillas, I., and Molina, E.: Palaeoenvironmental turnover across the
717 Palaeocene/Eocene boundary at the Stratotype section in Dababiya (Egypt) based on benthic
718 foraminifera, *Terra Nova*, 17, 526-536, 2005.

719 Alegret, L., Ortiz, N., and Molina, E.: Extinction and recovery of benthic foraminifera across the
720 Paleocene-Eocene Thermal Maximum at the Alamedilla section (Southern Spain), *Palaeogeogr.*
721 *Palaeocl. Palaeoecol.*, 279, 186-200, 2009a.

722 Alegret, L., Ortiz, S., Orue-Extebarria, X., Bernaola, G., Baceta, J. I., Monechi, S., Apellaniz, E.,
723 Pujalte, V.: The Paleocene-Eocene Thermal Maximum: New data on microfossil turnover at the
724 Zumaia section, Spain, *Palaios*, 24, 318-328, 2009b.

725 Alegret, L., Ortiz, S., Arenillas, I., and Molina, E.: What happens when the ocean is overheated? The
726 foraminiferal response across the Paleocene-Eocene Thermal Maximum at the Alamedilla section
727 (Spain), *Geol. Soc. Am. Bull.*, 122, 1616-1624, 2010.

728 Alve, E., and Goldstein, S. T.: Propagule transport as a key method of dispersal in benthic foraminifera
729 (Protists), *Limnol. Oceanogr.*, 48, 2163-2170, 2003.

730 Arndt, S., Jørgense, B. B., LaRowe, D. E., Middeburg, J. J., Pancost, R. D., and Regnier, P.:
731 Quantifying the degradation of organic matter in marine sediments: a review and synthesis, *Earth-
732 Science Reviews*, 123, 53-86, 2013.

733 Arreguín-Rodríguez, G. J., Alegret, L., and Ortiz, S.: *Glomospira* acme during the Paleocene–Eocene
734 Thermal Maximum: response to CaCO_3 dissolution or to ecological forces?, *J. Foramin. Res.*, 43, 37–
735 49, 2013.

736 Arreguín-Rodríguez, G. J., Alegret, L., Sepúlveda, J., Newman, S., and Summons, R. E.: Enhanced
737 terrestrial input supporting the *Glomospira* acme across the Paleocene-Eocene boundary in Southern
738 Spain, *Micropaleontology*, 60(1), 43-51, 2014.

739 Aubry, M.-P., Ouda, K., Dupuis, C., Berggren, W. A., Van Couvering, J. A., Ali, J., Brinkhuis, H.,
740 Gingerich, P. R., Heilmann-Clausen, C., Hooker, J., Kent, D. V., King, C., Knox, R. W. O. B., Laga,
741 P., Molina, E., Schmitz, B., Steurbaut, E., and Ward, D. R.: The Global Standard Stratotype-Section
742 and Point (GSSP) for the base of the Eocene Series in the Dababiya section (Egypt), *Episodes*, 30, 271–
743 286, 2007.

744 Aze, T., Pearson, P. N., Dickson, A. J., Badger, M. P. S., Bown, P. R., Pancost, R. D., Gibbs, S. J.,
745 Huber, B. T., Leng, M. J., Coe, A. L., Cohen, A. S., and Foster, G. L.: Extreme warming of tropical
746 waters during the Paleocene-Eocene Thermal Maximum, *Geology*, 42, 739-742, 2014.

747 Bains, S., Corfield, R. M., and Norris, R. D.: Mechanisms of climate warming at the end of the
748 Paleocene, *Science*, 285, 724–727, 1999.

749 Bąk, K.: Deep-water agglutinated foraminiferal changes across the Cretaceous/Tertiary and
750 Paleocene/Eocene transitions in the deep flysch environment; eastern part of Outer Carpathians
751 (Bieszczady Mts, Poland), in: *Proceedings of the Six International Workshop on Agglutinated*
752 *Foraminifera*, Prague, Czech Republic, September 1-7, 2001, edited by: Bubik, M., and Kaminski, M.
753 A., Grzybowski Foundation Special Publication, Drukarnia Narodowa, Kraków, 8, 1-56, 2004.

754 Barry, J. P., Buck, K. R, Lovera, C. F., Kuhn, L., Whaling, P. J., Peltzer, E. T., Walz, P., and Brewer,
755 P. G.: Effects of Direct Ocean CO_2 Injection on Deep-Sea Meiofauna, *J. Oceanogr.*, 60, 759-766, 2004.

756 Beckmann, J. P.: Distribution of benthonic foraminifera at the Cretaceous-Tertiary boundary of
757 Trinidad (West Indies), in: *International Geological Congress Report*, 21 Session Norden, Copenhagen.
758 Part 5: The Cretaceous-Tertiary boundary, 57-59, 1960.

759 Benjamini, C.: The Paleocene-Eocene boundary in Israel. A candidate for the boundary stratotype,
760 Neues Jahrb. Geol. P.-A., 186, 49-61, 1992.

761 Berggren, W. A., and Aubert, J.: Paleocene benthonic foraminiferal biostratigraphy, paleobiogeography
762 and paleoecology of Atlantic-Tethyan regions: Midway type fauna, *Palaeogeogr. Palaeocl. Palaeoecol.*,
763 18, 73–192, 1975.

764 Berggren, W. A., and Miller, K. G.: Cenozoic bathyal and abyssal calcareous benthic foraminiferal
765 zonation, *Micropaleontology*, 35, 308–320, 1989.

766 Bernhard, J. M., and Sen Gupta, B. K.: Foraminifera of oxygen deplete environments, in: Sen Gupta, B.
767 K. (Ed.), *Modern Foraminifera*, Dordrecht, Kluwer Academic Publishers, 201-216, 1999.

768 Boersma, A.: Oligocene and Other Tertiary Benthic Foraminifers from a Depth Traverse Down Walvis
769 Ridge, Deep Sea Drilling Project Leg 74, Southeast Atlantic, Initial Rep. Deep Sea, 75, 1273-1300,
770 1984.

771 Boltovskoy, E., Scott, D.B., and Medioli, F.S.: Morphological variations of benthic foraminiferal tests
772 in response to changes in ecological parameters; a review, *J. Palaeontol.*, 65, 175-185, 1991.

773 Bornemann, A., Norris, R. D., Lyman, J. A., D'haenens, S., Groeneveld, J., Röhl, U., Farley, K. A., and
774 Speijer, R.P.: Persistent environmental change after the Paleocene–Eocene Thermal Maximum in the
775 eastern North Atlantic, *Earth Planet. Sc. Lett.*, 394, 70–81, 2014.

776 Boscolo Galazzo, F., Giusberti, L., Luciani, V., and Thomas, E.: Paleoenvironmental changes during
777 the Middle Eocene Climatic Optimum (MEO) and its aftermath: the benthic foraminiferal record
778 from the Alano section (NE Italy), *Palaeogeogr. Palaeocl. Palaeoecol.*, 378, 22–35, 2013.

779 Boscolo Galazzo, F., Thomas, E., Pagani, M., Warren, C., Luciani, V., Giusberti, L.: The middle
780 Eocene climatic optimum (MEO): A multiproxy record of paleoceanographic changes in the
781 southeast Atlantic (ODP Site 1263, Walvis Ridge), *Paleoceanography*, 29, 1143-1161, 2014.

782 Boscolo-Galazzo, F., Thomas, E., Giusberti, L.: Benthic foraminiferal response to the Middle Eocene
783 Climatic Optimum (MEO) in the Southeastern Atlantic (ODP Site 1263). *Palaeogeogr. Palaeocl.*
784 *Palaeoecol.*, 417, 432-444, 2015.

785 Bowen, G. J., Beerling, D. J., Koch, P.L., Zachos, J.C, Quattlebaum, T.: A humid climate state during
786 the Palaeocene/Eocene thermal maximum, *Nature*, 432, 495–499, 2004.

787 Bowen, G. J., Maibauer, B. J., Kraus, M. J., Röhl, U., Westerhold. T., Steike, A., Gingerich, P. D.,
788 Wing, S. L., and Clyde, W. J.: Two massive, rapid release of carbon during the onset of the
789 Palaeocene-Eocene thermal maximum, *Nat. Geosci.*, 8, 44-47, 2015.

790 Braga, G., De Biase, R., Gruning, A., and Proto Decima, F.: Foraminiferi bentonici del Paleocene e
791 dell'Eocene della sezione di Possagno, in: *Monografia micropaleontogica sul Paleocene e l'Eocene di*
792 *Possagno, Provincia di Treviso, Italia*, edited by: Bolli, H. M., *Schweizerische Paläontologische*
793 *Abhandlungen*, Basel, 97, 85-111, 1975.

794 Bralower, T. J.: Evidence of surface water oligotrophy during the Paleocene-Eocene thermal
795 maximum: Nannofossil assemblage data from Ocean Drilling Program Site 690, Maud Rise, Weddell
796 Sea, *Paleoceanography*, 17, 1023, 2002.

797 Broecker, W. S., and Peng, T-H.: *Tracers in the sea*. Palisades, New York, Eldigio Press, 690 pp., 1982.

798 Buzas, M. A., Culver, S. J., and Jorissen, F. J.: A statistical evaluation of the microhabitats of living
799 (stained) infaunal benthic foraminifera, *Mar. Micropaleont.*, 29, 73–76, 1993.

800 Cetean, C., Setoyama, E., Kaminski, M. A., Neagu, T., Bubík, M., Filipescu, S., and Tyszka:
801 *Eobigenerina*, n. gen., a cosmopolitan deep-water agglutinated foraminifer, and remarks on species
802 formerly assigned to the genera *Pseudobolivina* and *Bigenerina*, in: *Eight International Workshop on*
803 *Agglutinated Foraminifera, Abstract Volume*, edited by: Filipescu, S., and Kaminski, M. A.,
804 *Grzybowski Foundation Special Publication*, Presa Universitară Clujeană, Romania, 14, 6-7, 2008a.

805 Cetean, C., Bălcăi, R., Kaminski, M. A., and Filipescu, S.: Biostratigraphy of the Cenomanian-Turonian
806 boundary in the Eastern Carpathians (Dâmbovița Valley): preliminary observations, *Stud. Univ. Babeș-*
807 *Bol., Geologia*, 53 (1), 11-23, 2008b.

808 Cetean, C., Setoyama, E., Kaminski, M. A., Neagu, T., Bubík, M., Filipescu, S. and Tyszka, J.:
809 *Eobigenerina*, a cosmopolitan deep-water agglutinated foraminifer, and remarks on late Paleozoic to
810 Mesozoic species formerly assigned to *Pseudobolivina* and *Bigenerina*, in: *Proceedings of the Eight*
811 *International Workshop on Agglutinated Foraminifera*, edited by: Filipescu, S. and Kaminski, M. A.

812 (Eds.), Grzybowski Foundation Special Publication, Presa Universitară Clujeană, Romania, 16, 19-27,
813 2011.

814 Chun, C. O. J., Delaney, M. L., and Zachos, J. C.: Paleoredox changes across the Paleocene-Eocene
815 thermal maximum, Walvis Ridge (ODP Sites 1262, 1263, and 1266): Evidence from Mn and U
816 enrichment factors, *Paleoceanography*, 25(4), PA4202, 2010.

817 Coccioni, R. and Galeotti, S.: Orbitally induced cycles in benthic foraminiferal morphogroups and
818 trophic structure distribution patterns from the late Albian “Amadeus Segment” (Central Italy), *J.*
819 *Micropalaeont.*, 12, 227–239, 1993.

820 Coccioni, R., Bancala, G., Catanzariti, R., Fornaciari, E., Frontalini, F., Giusberti, L., Jovane, L.,
821 Luciani, V., Savian, J., and Sprovieri, M.: An integrated stratigraphic record of the Palaeocene-lower
822 Eocene at Gubbio (Italy): new insights into the early Palaeogene hyperthermals and carbon isotope
823 excursions, *Terra Nova*, 45, 380-386, 2012.

824 Collinson, M. E., Steart, D. C., Scott, A. C., Glasspool, I. J., and Hooker, J. J.: Episodic fire, runoff and
825 deposition at the Palaeocene–Eocene boundary, *J. Geol. Soc. London*, 164, 87–97, 2007.

826 Corliss, B. H.: Microhabitats of Benthic Foraminifera within deep-sea sediments, *Nature*, 314, 435–
827 438, 1985.

828 Corliss, B. H. and Chen, C.: Morphotype patterns of Norwegian Sea deep-sea benthic foraminifera and
829 ecological implications, *Geology*, 16, 716–719, 1988.

830 ~~Colosimo, A. B., Bralower, T. J., and Zachos, J. C.: Evidence of lysocline shoaling at the
831 Paleocene/Eocene Thermal Maximum on Shatsky Rise, northwest Pacific, Proceedings of the Ocean
832 Drilling Program, Scientific Results 198: College Station, Texas, 1-36, 2006.~~

833 Cramer, B. S., Wright, J. D., Kent, D. V., and Aubry, M.-P.: Orbital climate forcing of $\delta^{13}\text{C}$ excursions
834 in the late Paleocene-early Eocene (chrons C24n-C25n), *Paleoceanography*, 18, 1097, 2003.

835 Crouch, E. M., Dickens, G. R., Brinkhuis, H., Aubry, M.-P., Hollis, C. J., Rogers, K. M., and Visscher,
836 H.: The *Apectodinium* acme and terrestrial discharge during the Paleocene-Eocene thermal maximum:

837 New palynological, geochemical and calcareous nannoplankton observations at Tawanui, New
838 Zealand, *Palaeogeogr. Palaeocl. Palaeoecol.*, 194, 387–403, 2003.

839 Dallanave, E., Tauxe, L., Muttoni, G., and Rio, D.: Silicate weathering machine at work: rock magnetic
840 data from the late Paleocene–early Eocene Cicogna section, Italy, *Geochem. Geophys. Geosy.*, 11(7),
841 Q07008, 2010.

842 Dallanave, E., Muttoni, G., Agnini, C., Tauxe, L., and Rio, D.: Is there a normal magnetic-polarity
843 event during the Palaeocene–Eocene thermal maximum (~55 Ma)? Insights from the palaeomagnetic
844 record of the Belluno Basin (Italy), *Geophys. J. Int.*, 191, 517-529, 2012.

845 DeConto, R. M., Galeotti, S., Pagani, M., Tracy, D., Schaefer, K., Zhang, T., Pollard, D., Beerling, D.
846 J.: Past extreme warming events linked to massive carbon release from thawing permafrost, *Nature*,
847 484, 87–91, 2012.

848 D'haenens, S., Bornemann, A., Stassen, P., and Speijer, R.: Multiple early Eocene benthic foraminiferal
849 assemblage and $\delta^{13}\text{C}$ fluctuations at DSDP Site 401 (Bay of Biscay-NE Atlantic), *Mar. Micropaleont.*,
850 88-89, 15-35, 2012.

851 Dickens, G. R., 2011: Down the rabbit hole, toward appropriate discussion of methane release from gas
852 hydrate systems during the Paleocene-Eocene thermal maximum and other past hyperthermal events,
853 *Clim. Past*, 7, 831-846, 2011.

854 Dickens, G. R., Castillo, M. M., and Walker, J. C. G.: A blast of gas in the latest Paleocene: Simulating
855 first-order effects of massive dissociation of oceanic methane hydrate, *Geology*, 25, 259-262, 1997.

856 Dickson, A. J., Rees-Owen, R. L., März, C., Coe, A. L., Cohen, A. S., Pancost, R. D., Taylor, K., and
857 Shcherbinina, E.: The spread of marine anoxia on the northern Tethys margin during the Paleocene-
858 Eocene Thermal Maximum, *Paleoceanography*, 29, 471-488, 2014.

859 Di Napoli Alliata, E., Proto Decima, F., and Pellegrini, G. B.: Studio geologico, stratigrafico e
860 micropaleontologico dei dintorni di Belluno, *Memorie della Società Geologica Italiana*, 9, 1-28, 1970.

861 Dunkley Jones, T., D. J. Lunt, D. N. Schmidt, A. Ridgwell, A. Sluijs, P. J. Valdez, and M. A. Maslin:
862 Climate model and proxy data constraints on ocean warming across the Paleocene–Eocene Thermal
863 Maximum, *Earth Science Reviews*, 125, 123–145, 2013.

864 Dypvik, H., Riber, L., Burca, F., Rüther, D., Jargvoll, D., Nagy, J., and Jochmann, M.: The Paleocene–
865 Eocene thermal maximum (PETM) in Svalbard — clay mineral and geochemical signals, *Palaeogeogr.*
866 *Palaeocl. Palaeoecol.*, 302, 156–169, 2011.

867 Egger, H., Fenner, J., Heilmann-Clausen, C., Roegl, F., Sachsenhofer, R. F., and Schmitz, B.:
868 Paleoproductivity of the northwestern Tethyan margin (Anthering section, Austria) across the
869 Paleocene–Eocene transition, in: *Causes and Consequences of Globally Warm Climates in the Early*
870 *Paleogene*, edited by: Wing, S.L., Gingerich, P. D., Schmitz, B., and Thomas, E., *Geol. S. Am. S.*,
871 Boulder, Colorado, The Geological Society of America, 369, 133–146, 2003.

872 Egger, H., Homayoun, M., Huber, H., Roegl, F., Schmitz, B.: Early Eocene climatic, volcanic, and
873 biotic events in the northwestern Tethyan Untersberg section, Austria, *Palaeogeogr. Palaeocl.*
874 *Palaeoecol.*, 217, 243– 264, 2005.

875 Egger, H., Heilmann-Clausen, C., Schmitz, B.: From shelf to abyss: Record of the Paleocene/Eocene-
876 boundary in the Eastern Alps (Austria), *Geol. Acta*, 7, 215–227, 2009.

877 Ernst, S. R., Guasti, E., Dupuis, C., and Speijer, R. P., Environmental perturbation in the southern
878 Tethys across the Paleocene/Eocene boundary (Dababyia, Egypt): Foraminiferal and clay minerals
879 record, *Mar. Micropaleont.*, 60, 89-111, 2006.

880 ~~Fenero, R., Thomas, E., Alegret, L., and Molina, E.: Oligocene benthic foraminifera in the Fuente~~
881 ~~Caldera section (Betic Cordillera, Spain): paleoenvironmental inferences. J. Foramin. Res.~~, 42, 286–
882 304, 2012.

883 Fontanier, C., Jorissen, F. J., Chaillou, G., Anschutz, P., Gremare, A., and Griveaud, C.: Live
884 foraminiferal faunas from a 2800 m deep lower canyon station from the Bay of Biscay: faunal response
885 to focusing of refractory organic matter, *Deep-Sea Res. I*, 52, 1189-1227, 2005.

886 Fontanier, C., Jorissen, F. J., Anschutz, P., and Chaillou, G.: Seasonal variability of benthic
887 foraminiferal faunas at 1000 m depth in the Bay of Biscay, *J. Foramin. Res.*, 36, 61-76, 2006a.

888 Fontanier, C., Mackensen, A., Jorissen, F. J., Anschutz, P., Licari, L., and Griveaud, C.: Stable oxygen
889 and carbon isotopes of live benthic foraminifera from the Bay of Biscay: Microhabitat impact and
890 seasonal variability, *Mar. Micropaleont.*, 58, 159-183, 2006b.

891 Fontanier, C., Duros, P., Toyofuku, T., Oguri, K., Koho, K. A., Buscail, R., Grémare, A., Radakovitch,
892 O., Deflandre, B., de Nooijer, L.J., Bichon, S., Goubet, S., Ivanovsky, A., Chabaud, G., Menniti, C.,
893 Reichart, G.-J., and Kitazato, H.: Living (stained) deep-sea foraminifera off Hachinohe (NE JAPAN,
894 Western Pacific): environmental interplay in oxygen-depleted ecosystems, *J. Foramin. Res.*, 44, 281-
895 299, 2014.

896 Foreman, B. Z., Heller, P. L., Clementz, M. T.: Fluvial response to abrupt global warming at the
897 Palaeocene/Eocene boundary, *Nature*, 491, 92-95, 2014.

898 Fornaciari, E., Giusberti, L., Luciani, V., Tateo, F., Agnini, C., Backman, J., Oddone, M., and Rio, D.:
899 An expanded Cretaceous–Tertiary transition in a pelagic setting of the Southern Alps (central–western
900 Tethys), *Palaeogeogr. Palaeocl. Palaeoecol.*, 255, 98–131, 2007.

901 Foster, L. C., Schmidt, D. N., Thomas, E., Arndt, S., Ridgwell, A.: Surviving rapid climate change in
902 the deep sea during the Paleogene hyperthermals, *Proc. Natl. Acad. Sci.*, 110(23), 9273-9276, 2013.

903 Frenzel, P.: Die benthischen Foraminiferen der Ruegener Schreibkreide (Unter Maastricht, NE
904 Deutschland), *Neue Palaeontologische Abhandlungen*, Dresden, Germany, CPress Verlag, Band 3,
905 2000.

906 Friedrich, O.: Benthic foraminifera and their role to decipher paleoenvironment during mid-Cretaceous
907 Oceanic Anoxic Events—"the anoxic benthic foraminifera" paradox, *Revue de Micropaléontologie*, 177,
908 2-18, 2009.

909 Friedrich, O., Nishi, H., Pross, J., Schmiedel, G., Hemleben, C.: Millennial-to centennial scale
910 interruptions of the Oceanic Anoxic Event 1b (early Albian, mid Cretaceous) inferred from benthic
911 foraminiferal repopulation events, *Palaios*, 20, 64-77, 2005.

912 Galeotti, S., Bellagamba, M., Kaminski, M. A., and Montanari, A.: Deep sea benthic foraminiferal
913 recolonisation following a volcanielastic event in the lower Campanian of the Seaglia Rossa Formation
914 (Umbria-Marche Basin, central Italy), *Mar. Micropaleont.*, 44, 57-76, 2002.

915 Galeotti, S., Kaminski, M. A., Coccioni, R., and Speijer, R.: High resolution deep water agglutinated
916 foraminiferal record across the Paleocene/Eocene transition in the Contessa Road Section (central
917 Italy), in: Proceedings of the Sixth International Workshop on Agglutinated Foraminifera, edited by:
918 Bubik, M. and Kaminski, M. A. (Eds.), Grzybowski Foundation Special Publication, Drukarnia
919 Narodowa, Kraków, 8, 83–103, 2004.

920 Garel, S., Schnyder, J., Jacob, J., Dupuis, C., Boussafir, M., Le Milbeau, C., Storme, J.-Y., Iakovleva,
921 A. I., Yans, J., Baudin, F., Fléhoc C., and Quesnel, F.: Paleo hydrological and paleoenvironmental
922 changes recorded in terrestrial sediments of the Paleocene–Eocene boundary (Normandy, France),
923 *Palaeogeogr. Palaeoecol. Palaeoecol.*, 376, 184–199, 2013.

924 Gavrilov, Y. O., Kodina, L. A., Lubchenko, I. Y., and Muzylev, N. G.: The late Paleocene anoxic event
925 in epicontinental seas of Peri-Tethys and formation of the sapropelite unit; sedimentology and
926 geochemistry, *Lithol. Miner. Resour.*, 32, 427–450, 1997.

927 Gibbs, S. J., Bralower, T. J., Bown, P. R., Zachos, J. C., and Bybell, L.M.: Shelf and open-ocean
928 calcareous phytoplankton assemblages across the Paleocene-Eocene Thermal Maximum: Implications
929 for global productivity gradients, *Geology*, 34, 233-236, 2006.

930 Gibson, T. G., Bybell, L. M., and Owens, J. P.: Latest Paleocene lithologic and biotic events in neritic
931 deposits of southwestern New-Jersey, *Paleoceanography*, 8 (4), 495–514, 1993.

932 Gibson, T. G., Bybell, L. M., and Mason, D.B.: Stratigraphic and climatic implications of clay mineral
933 changes around the Paleocene/Eocene boundary of the northeastern US margin, *Sediment. Geol.*, 134,
934 65–92, 2000.

935 Gingerich, P. D.: Mammalian response to climate change at the Paleocene-Eocene boundary: Polecat
936 Bench record in the northern Bighorn Basin, Wyoming, in: Wing, S.L., Gingerich, P. D., Schmitz, B.,
937 and Thomas, E., *Geol. S. Am. S.*, Boulder, Colorado, The Geological Society of America, 369, 463–
938 478, 2003.

939 Giusberti, L., Rio, D., Agnini, C., Backman, J., Fornaciari, E., Tateo, F., and Oddone, M.: Mode and
940 tempo of the Paleocene-Eocene Thermal Maximum from the Venetian pre-Alps, *Geol. Soc. Am. Bull.*,
941 119, 391-412, 2007.

942 Giusberti, L., Coccioni, R., Sprovieri, M., and Tateo, F.: Perturbation at the sea floor during the
943 Paleocene–Eocene Thermal Maximum: evidence from benthic foraminifera at Contessa Road, Italy,
944 *Mar. Micropaleont.*, 70, 102–119, 2009.

945 Gooday, A. J.: Deep-sea benthic foraminiferal species which exploit phytodetritus: characteristic
946 features and controls on distribution, *Mar. Micropaleont.*, 22, 187-205, 1993.

947 Gooday, A. J.: The biology of deep-sea Foraminifera: a review of some advances and their applications
948 in paleoceanography, *Palaios*, 9, 14-31, 1994.

949 Gooday, A. J.: Benthic foraminifera (Protista) as tools in deep-water paleoceanography: Environmental
950 influences on faunal characteristics, *Adv. Mar. Biol.*, 46, 1-90, 2003.

951 Gooday, A. J., Hughes, J. A., and Levin, L. A.: The foraminiferan macrofauna from three North
952 Carolina (U.S.A.) slope sites with contrasting carbon flux: a comparison with the metazoan
953 macrofauna, *Deep-Sea Res. I*, 48, 1709-1739, 2001.

954 Gooday, A. J., Nomaki, H., and Kitazato, H.: Modern deep-sea benthic foraminifera: a brief review of
955 their morphology-based biodiversity and trophic diversity, in: *Biogeochemical Controls on*
956 *Palaeoceanographic Environmental Proxies*, edited by: Austin, W. E. N. and James, R. H., *Geol. Soc.*
957 *Spec. Publ.*, Bath, UK, The Geological Society Publishing House, 303, 97–119, 2008.

958 Guasti, E., and Speijer, R. P.: The Paleocene-Eocene Thermal Maximum in Egypt and Jordan: An
959 overview of the planktic foraminiferal record, in: *Large Ecosystem Perturbations: Causes and*
960 *Consequences*, edited by: Monechi, S., Coccioni, R., and Rampino, M., *Geol. S. Am. S.*, Boulder,
961 Colorado, The Geological Society of America, 424, 53–67, 2007.

962 Gupta, A. K. and Thomas, E.: Latest Miocene-Pleistocene productivity and deep-sea ventilation in the
963 northwestern Indian Ocean (Deep Sea Drilling Project Site 219), *Paleoceanography*, 14, 62-73, 1999.

964 Gupta, A. K., and Thomas, E.: Initiation of Northern Hemisphere glaciation and strengthening of the
965 northeast Indian monsoon: Ocean Drilling Program Site 758, eastern equatorial Indian Ocean, *Geology*,
966 31(1), 47-50, 2003.

967 Gupta, A. K., Sundar Raj, M., Mohan, K., De, S.: A major change in monsoon-driven productivity in
968 the tropical Indian Ocean during ca 1.2–0.9 Myr: Foraminiferal faunal and stable isotope data,
969 *Palaeogeogr. Palaeoocl. Palaeoecol.*, 261, 234–245, 2008.

970 Hammer, Ø., Harper, D. A. T., and Ryan, P. D.: PAST: Paleontological Statistics Software Package for
971 Education and Data Analysis, *Palaeontol. Electron.* 4 (1), 1–9, 2001.

972 Hancock, H. J. L., and Dickens, G. R.: Carbonate dissolution episodes in Paleocene and Eocene
973 sediment, Shatsky Rise, west-central Pacific, in: Bralower, T. J., Premoli Silva, I., and Malone, M. J.
974 (Eds.), *Proceedings of the Ocean Drilling Program, Scientific Results*, 198, http://www-odp.tamu.edu/publications/198_SR/116/116.htm, 2005.

975

976 Handley, L., Pearson, P. N., McMillan, I. K., and Pancost, R. D.: Large terrestrial and marine carbon
977 and hydrogen isotope excursions in a new Paleocene/Eocene boundary section from Tanzania, *Earth*
978 *Planet. Sc. Lett.*, 275, 17–25, 2008.

979 Handley, L., O'Halloran, A., Pearson, P. N., Hawkins, E., Nicholas, C. J., Schouten, S., McMillan, I.
980 K., and Pancost, R. D.: Changes in the hydrological cycle in tropical East Africa during the Paleocene–
981 Eocene Thermal Maximum, *Palaeogeogr. Palaeoocl. Palaeoecol.*, 329–330, 10–21, 2012.

982 Harding, I. C., Charles, A. J., Marshall, J. E. A., Pälike, H., Roberts, A. P., Wilson, P. A., Jarvis, E.,
983 Thorne, R., Morris, E., Moremon, R., Pearce, R. B., and Akbari, S.: Sea-level and salinity fluctuations
984 during the Paleocene–Eocene thermal maximum in Arctic Spitsbergen, *Earth Planet. Sc. Lett.*, 303, 97–
985 107, 2011.

986 Harries, P. J. and Kauffman, E. G.: Patterns of survival and recovery following the Cenomanian–
987 Turonian (Late Cretaceous) mass extinction in the Western Interior Basin, United States, in: *Extinction*
988 *events in Earth History*, edited by: Kauffman, E. G. and Walliser, O. H., *Lect. Notes Earth Sci.*
989 Heidelberg Germany, Springer-Verlag, 30, 277–298, 1990.

990 ~~991 Harries, P. J., Kauffman, E. G., and Hansen, T. A.: Models for biotic survival following mass~~
991 ~~extinction, in: Biotic Recovery from Mass Extinction Events, edited by: Hart, M. B., Geol. Soc. Spec.~~
992 ~~Publ., The Geological Society Publishing House, Bath, UK, 102, 41–60, 1996.~~

993 Hayward, B. W., Johnson, K., Sabaa, A.T., Kawagata, S., and Thomas, E.: Cenozoic record of
994 elongate, cylindrical, deep-sea benthic foraminifera in the North Atlantic and equatorial Pacific
995 Oceans, *Mar. Micropaleont.*, 62, 141-162, 2010a.

996 Hayward, B. W., Sabaa, A. T., Thomas, E., Kawagata, S., Nomura, R., Schroder Adams, C., Gupta, A.
997 K., and Johnson, K.: Cenozoic record of elongate, cylindrical, deep-sea benthic foraminifera in the
998 Indian Ocean (ODP Sites 722, 738, 744, 758, and 763), *J. Foramin. Res.*, 40, 113-133, 2010b.

999 Hayward, B. W., Kawagata, S., Sabaa, A. T., Grenfell, H. R., van Kerckhoven, L., Johnson, K., and
1000 Thomas, E.: The Last Global Extinction (Mid-Pleistocene) of Deep-Sea Benthic Foraminifera
1001 (Chrysogoniidae, Ellipsoidinidae, Glandulonodosariidae, Plectofrondiculariidae, Pleurostomellidae,
1002 Stilostomellidae), their Late Cretaceous-Cenozoic History and Taxonomy, Cushman Foundation for
1003 Foraminiferal Research Special Publication, 43, Allen Press, Lawrence, USA, 408 pp., 2012.

1004 ~~Hess, S. and Jorissen, F. J.: Distribution patterns of living benthic foraminifera from Cap Breton~~
1005 ~~canyon, Bay of Biscay: Faunal response to sediment instability, Deep Sea Res. Part I: Oceanographic~~
1006 ~~Research Papers 56(9), 1555-1578, 2009.~~

1007 Holbourn, A. and Kuhnt, W.: No extinctions during Oceanic Anoxic Event 1b: the Aptian-Albian
1008 benthic foraminiferal record of ODP Leg 171, edited by: Kroon, D., Norris, R. D., and Klaus, A., Geol.
1009 Soc. London, Spec. Publ., Bath, UK, The Geological Society Publishing House, 183, 73-92, 2001.

1010 Holbourn, A., Kuhnt, W., Erbacher, J.: Benthic foraminifers from lower Albian black shales (Site 1049,
1011 ODP Leg 171): evidence for a non “uniformitarian” record, *J. Foramin. Res.*, 31, 60–74, 2001.

1012 Hönisch, B., Ridgwell, A., Schmidt, D. N., Thomas, E., Gibbs, S. J., Sluijs, A., Zeebe, R., Kump, L.,
1013 Martindale, R. C., Greene, S. E., Kiessling, W., Ries, J., Zachos, J. C., Royer, D. L., Barker, S.,
1014 Marchitto, T. M., Moyer, R., Pelejero, C., Ziveri, P., Foster, G. L., and Williams, B.: The Geological
1015 Record of Ocean Acidification, *Science*, 335, 1058-1963, 2012.

1016 Ishman, S. E., and Domack, E. W.: Oceanographic controls on benthic foraminifers from the
1017 Bellingshausen margin of the Antarctic Peninsula, *Mar. Micropaleont.*, 24, 119-155, 1994.

1018 Itambi, A. C., von Dobeneck, T., Mulitza, S., Bickert, T., and Heslop D.: Millennial-scale northwest
1019 African droughts related to Heinrich events and Dansgaard-Oeschger cycles: Evidence in marine
1020 sediments from offshore Senegal, *Paleoceanography*, 24, PA1205, 2009.

1021 Jaramillo, C. A., Ochoa, D., Contreras, L., Pagani, M., Carvajal-Ortiz, H., Pratt, L. M., Krishnan, S.,
1022 Cardona, A., Romero, M., Quiroz, L., Rodriguez, G., Rueda, M. J., De la Parra, F., Morón, S., Green,
1023 W., Bayona, G., Montes, C., Quintero, O., Ramirez, R., Mora, G., Schouten, S., Bermudez, H.,
1024 Navarrete, R., Parra, F., Alvarán, M., Osorno, J., Crowley, J. L., Valencia, V., and Vervoort, J.: Effects
1025 of rapid global warming at the Paleocene-Eocene boundary on Neotropical vegetation, *Science*, 330,
1026 957–961, 2010.

1027 John, C. M., Bohaty, S. M., Zachos, J. C., Sluijs, A., Gibbs, S., Brinkhuis, H., and Bralower, T. J.:
1028 North American continental margin records of the Paleocene-Eocene thermal maximum: Implications
1029 for global carbon and hydrological cycling, *Paleoceanography*, 23, PA2217, 2008.

1030 ~~John, C. M., Banerjee, N. R., Longstaffe, F. J., Sica, C., Law, K. R., Zachos, J. C.: Clay assemblage
1031 and oxygen isotopic constraints on the weathering response to the Paleocene Eocene thermal
1032 maximum, east coast of North America, *Geology*, 40, 591–594, 2012.~~

1033 John, E. H., Pearson, P. N., Coxall, H. K., Birch, H., Wade, B. S., and Foster, G. L.: Warm ocean
1034 processes and carbon cycling in the Eocene, *Phil. T. Roy. Soc. A*, 371, 20130099, 2013.

1035 John, E. H., Wilson, J. D., Pearson, P. N., and Ridgwell, A.: Temperature-dependent remineralization
1036 and carbon cycling in the warm Eocene oceans, *Palaeogeogr. Palaeoecol. Palaeoecol.*, 413, 158–166,
1037 2014.

1038 Jones, R. W. and Charnock, M. A.: “Morphogroups” of agglutinated foraminifera. Their life positions
1039 and feeding habits and potential applicability in (paleo)ecological studies, *Revue de Paléobiologie*, 4,
1040 311–320, 1985.

1041 ~~Jones, B. and Manning, D. A. C.: Comparison of geochemical indices used for the interpretation of
1042 palaeoredox conditions in ancient mudstones, *Chem. Geol.*, 111, 111–194, 1994.~~

1043 Jorissen, F. J.: Benthic foraminiferal successions across late Quaternary Mediterranean sapropels, *Mar.
1044 Geol.*, 153, 91–101, 1999.

1045 Jorissen, F. J., De Stigter, H. C., and Widmark, J. G. V.: A conceptual model explaining benthic
1046 foraminiferal microhabitats, *Mar. Micropaleont.*, 26, 3–15, 1995.

1047 Jorissen, F. J., Fontanier, C., and Thomas, E.: Paleoceanographical proxies based on deep-sea benthic
1048 foraminiferal assemblage characteristics, in: *Proxies in Late Cenozoic Paleoceanography: Pt. 2:*
1049 *Biological tracers and biomarkers*, edited by: Hillaire-Marcel, C. and A. de Vernal, A., 1, Elsevier,
1050 Amsterdam, The Netherlands, 264–325, 2007.

1051 Kaiho, K.: Phylogeny of deep-sea calcareous trochospiral benthic foraminifera: evolution and
1052 diversification, *Micropalaeontology*, 44, 291–311, 1998.

1053 Kaiho, K., Arinobu, T., Ishiwatari, R., Morgans, H. E. G., Okada, H., Takeda, N., Tazaki, K., Zhou, G.
1054 P., Kajiwara, Y., Matsumoto, R., Hirai, A., Niitsuma, N., and Wada, H.: Latest Paleocene benthic
1055 foraminiferal extinction and environmental changes at Tawanui, New Zealand, *Paleoceanography*, 11,
1056 447–465, 1996.

1057 Kaminski M. A. and Gradstein, F. M.: An Atlas of Paleogene Cosmopolitan Deep-Water Agglutinated
1058 Foraminifera, Grzybowski Foundation Special Publication, Drukarnia Narodowa, Kraków, 10, 547 pp.,
1059 2005.

1060 Kaminski, M. A., Kuhnt, W., and Radley, J. D.: Paleocene–Eocene deep water agglutinated
1061 foraminifera from the Numidian Flysch (Rift, Northern Morocco): Their significance for the
1062 paleoceanography of the Gibraltar gateway, *J. Micropaleontol.*, 15, 1–19, 1996.

1063 Katz, M. E., Wright, J. D., Katz, D. R., Miller, K. G., Pak, D. K., Shackleton, N. J., and Thomas, E.:
1064 Early Cenozoic benthic foraminiferal isotopes: species reliability and interspecies correction factors,
1065 *Paleoceanography*, 18, 1024, 2003.

1066 ~~Kauffman, E. G. and Harries, P. J.: The importance of crisis progenitors in recovery from mass
1067 extinction, in: *Biotic Recovery from Mass Extinction Events*, edited by: Hart, M. B., Geol. Soc. Spec.
1068 Publ., The Geological Society Publishing House, Bath, UK, 102, 15–39, 1996.~~

1069 Kelly, D. C., Bralower, T. J., Zachos, J. C., Premoli Silva, I., and Thomas, E.: Rapid diversification of
1070 planktonic foraminifera in the tropical Pacific (ODP Site 865) during the late Paleocene thermal
1071 maximum, *Geology* 24, 423–426, 1996.

1072 Kelly, D. C., Bralower, T. J., and Zachos, J. C.: Evolutionary consequences of the latest Paleocene
1073 thermal maximum for tropical planktonic foraminifera, *Palaeogeogr. Palaeocl. Palaeoecol.*, 141, 139-
1074 161, 1998.

1075 Kelly, D. C., Nielsen, T. M. J., McCarren, H. K., Zachos, J. C., and Röhl, U.: Spatiotemporal patterns
1076 of carbonate sedimentation in the South Atlantic: Implications for carbon cycling during the
1077 Paleocene–Eocene thermal maximum, *Palaeogeogr. Palaeocl. Palaeoecol.*, 293, 30-40, 2010.

1078 Kennett, J. P., and Stott, L. D.: Abrupt deep-sea warming, palaeoceanographic changes and benthic
1079 extinctions at the end of the Palaeocene, *Nature*, 353, 225–229, 1991.

1080 Kender, S., Stephenson, M. H., Riding, J.,B., Leng, M. J., O'BKnox, R. W., Peck, V. L., Kendrick, C.
1081 P., Ellis, M. A., Vane, C. H., and Jamieson, R.: Marine and terrestrial environmental changes in NW
1082 Europe preceding carbon release at the Paleocene–Eocene transition, *Earth Planet. Sc. Lett.*, 353–354,
1083 108–120, 2012.

1084 Kirtland Turner, S., and Ridgwell, A.: Recovering the true size of an Eocene hyperthermal from the
1085 marine sedimentary record, *Paleoceanography*, 28(4), 700-712, 2013.

1086 Koutsoukos, E. A. M., Leary, P. M., and Hart, M. B.: Latest Cenomanian–earliest Turonian low-
1087 oxygen tolerant benthonic foraminifera: a case study from the Sergipe Basin (N.E. Brazil) and the
1088 western Anglo-Paris Basin (southern England), *Palaeogeogr. Palaeocl. Palaeoecol.*, 77, 145–177, 1990.

1089 Kraus, M. J. and Riggins, S.: Transient drying during the Paleocene–Eocene Thermal Maximum
1090 (PETM): analysis of paleosols in the Bighorn Basin, Wyoming, *Palaeogeogr. Palaeocl. Palaeoecol.*,
1091 245, 444–461, 2007.

1092 Kraus, M. J., McInerney, F. A., Wing, S. L., Secord, R., Baczyński, A. A., Bloch, J. I.: Paleohydrologic
1093 response to continental warming during the Paleocene–Eocene Thermal Maximum, Bighorn Basin,
1094 Wyoming, *Palaeogeogr. Palaeocl. Palaeoecol.*, 370, 196-208, 2013.

1095 Krishnan, S., Pagani, M., and Agnini, C.: Leaf waxes as recorders of paleoclimatic changes during the
1096 Paleocene–Eocene Thermal Maximum: Regional expressions from the Belluno Basin, *Org. Geochem.*,
1097 80, 8-17, 2015.

1098 Kuhnt, W.: Abyssal recolonization by benthic foraminifera after the Cenomanian/Turonian boundary
1099 anoxic event in the North Atlantic, *Mar. Micropaleont.*, 19, 257-274, 1992.

1100 Kuhnt, W.: Early Danian benthic foraminiferal community structures, *Geulhemmerberg*, SE
1101 Netherlands, *Geol. Mijnbouw*, 75, 163-172, 1996.

1102 Kuhnt, W. and Collins, E. S.: Cretaceous to Paleogene benthic foraminifers from the Iberia abyssal
1103 plain, in: *Proceedings of the ODP*, edited by: Whitmarsh, R. B., Sawyer, D. S., Klaus, A., and Masson,
1104 D. G., *Scientific Results*, 149, College Station, TX Ocean Drilling Program, 203-316, 1996.

1105 Kuhnt, W., Collins, E., and Scott, D. B.: Deep water agglutinated foraminiferal assemblages across the
1106 Gulf Stream: distribution pattern and taphonomy, in: *Proceedings of the Fifth International Workshop*
1107 on Agglutinated Foraminifera, edited by: Hart, M. B., Kaminski, M. A., and Smart, C.W., Grzybowski
1108 Foundation Special Publication, Drukarnia Narodowa, Kraków, 7, 261-298, 2000.

1109 Kuhnt, W. and Kaminski, M. A.: Changes in the community structure of deep-water agglutinated
1110 foraminifers across the K/T boundary in the Basque Basin (northern Spain), *Revista Española de*
1111 *Micropaleontologia*, 25, 57-92, 1993.

1112 Kuhnt, W. and Kaminski, M. A.: The reponse of benthic foraminifera to the K/T boundary event-a
1113 review, in: *Géologie de l'Afrique et de l'Atlantique Sud-Comptes Rendu des Colloques de géologie*
1114 *d'Angers*, 16-20 Juillet, 1994, edited by: Jardiné, S., de Klasz, I., and Debenay, J. P., B. Cent. Rech.
1115 Expl., *Memoire*, Pau, Société nationale Elf Aquitaine, 16, 433-442, 1996.

1116 Larrasoña, J. C., Roberts, A. P., Rohling, E. J., Winklhofer, M., and Wehausen, R.: Three million
1117 years of monsoon variability over the northern Sahara, *Clim. Dynam.*, 21, 689-698, 2003.

1118 Levin, L. A.: Oxygen Minimum Zone Benthos: Adaptation and Community Response to Hypoxia,
1119 *Oceanogr. Mar. Biol.*, 41, 1-45, 2003.

1120 Lirer, F.: A new technique for retrieving calcareous microfossils from lithified lime deposits,
1121 *Micropaleontology*, 46 (4), 365-369, 2000.

1122 Littler, K., Röhl, U., Westerhold, T., and Zachos, J. C.: A high-resolution benthic stable-isotope record
1123 for the South Atlantic: Implications for orbital-scale changes in Late Paleocene–Early Eocene climate
1124 and carbon cycling. *Palaeogeogr. Palaeocl. Palaeoecol.*, 401, 18-30, 2014.

1125 Luciani, V., Giusberti, L., Agnini, C., Backman, J., Fornaciari, E., and Rio, D.: The Paleocene-Eocene
1126 Thermal Maximum as recorded by Tethyan planktonic foraminifera in the Forada section (northern
1127 Italy), *Mar. Micropaleont.*, 64, 189-214, 2007.

1128 Ma, Z., Gray, E., Thomas, E., Murphy, B., Zachos, J. C., and Paytan, A.: Carbon sequestration during
1129 the Paleocene-Eocene Thermal maximum by an efficient biological pump. *Nat. Geosci.*, 7, 382-388,
1130 2014.

1131 Mancin, N., Hayward, B. W., Trattenero, I., Cobianchi, M., and Lupi, C.: Can the morphology of deep-
1132 sea benthic foraminifera reveal what caused their extinction during the mid-Pleistocene Climate
1133 Transition? *Mar. Micropaleont.*, 104, 53–70, 2013.

1134 McCarren, H., Thomas, E., Hasegawa, T., Röhl, U., and Zachos, J. C.: Depth dependency of the
1135 Paleocene-Eocene carbon isotope excursion: Paired benthic and terrestrial biomarker records (ODP
1136 Leg 208, Walvis Ridge), *Geochem. Geophys. Geosy.*, 9, Q10008, 2008.

1137 McInerney, F. A. and Wing, S. L.: The Paleocene-Eocene thermal maximum: A perturbation of carbon
1138 cycle, climate, and biosphere with implications for the future, *Annu. Rev. Earth Pl. Sc.*, 39, 489–516,
1139 2011.

1140 Meissner, K. J., Bralower, T. J., Alexander, K., Dunkley Jones, T., Sijp, W., and Ward, M.: The
1141 Paleocene-Eocene Thermal Maximum: how much carbon is enough?, *Paleoceanography*, 29, 946-963,
1142 2014.

1143 Mohan, K., Gupta, A. K., and Bhaumik, A. K.: Distribution of deep-sea benthic foraminifera in the
1144 Neogene of Blake Ridge, NW Atlantic Ocean, *J. Micropalaeontol.*, 30, 33-74, 2011.

1145 Murphy, B. H., Farley, K. A., and Zachos, J. C.: An extraterrestrial ^3He -based timescale for the
1146 Paleocene-Eocene thermal maximum (PETM) from Walvis Ridge, IODP Site 1266, *Geochim.
1147 Cosmochim. Ac.*, 74, 5098-5108, 2010.

1148 Murray, J. W.: *Ecology and palaeoecology of benthic foraminifera*. Longman, Harlow, 397 pp., 1991.

1149 Murray, J. W.: *Ecology and Applications of Benthic Foraminifera*, Cambridge University Press, USA,
1150 xi + 426 pp., 2006.

1151 Murray, J. W. and Pudsey, C. J.: Living (stained) and dead foraminifera from the newly ice-free Larsen
1152 Ice Shelf, Weddell Sea, Antarctica: ecology and taphonomy, *Mar. Micropal.*, 53, 67-81, 2004.

1153 Nagy, J., Jargvoll, D., Dypvik, H., Jochmann, M., and Riber, L.: Environmental changes during the
1154 Paleocene-Eocene Thermal Maximum in Spitsbergen as reflected by benthic foraminifera, *Polar Res.*,
1155 32, 19737, 2013.

1156 Nicolo, M. J., Dickens, G. R., and Hollis, C. J.: South Pacific intermediate water oxygen depletion at
1157 the onset of the Paleocene-Eocene thermal maximum as depicted in New Zealand margin sections,
1158 *Paleoceanography* 25, PA4210, 2010.

1159 Nomura, R.: Paleogene to Neogene deep-sea paleoceanography in the eastern Indian Ocean: benthic
1160 foraminifera from ODP Sites 747, 757 and 758, *Micropaleontology*, 41, 251-290, 1995.

1161 Ortiz, N.: Differential patterns of benthic foraminiferal extinctions near the Paleogene/Eocene
1162 boundary in the North Atlantic and western Tethys, *Mar. Micropaleont.*, 26, 341-359, 1995.

1163 ~~Ortiz, S., Alegret, L., Payros, A., Orue Extebarria, X., Apellaniz, E., Molina, E.: Distribution pattern of
1164 benthic foraminifera across Ypresian Lutetian Gorrondatxe section, Northern Spain: Response to
1165 sedimentary disturbance. Mar. Micropaleont.~~, 78, 1-13, 2011.

1166 Pälike, C., Delaney, M. L., and Zachos, J. C.: Deep-sea redox across the Paleocene-Eocene thermal
1167 maximum, *Geochem. Geophys. Geosy.*, 15, 1038-1053, 2014.

1168 Pagani, M., Caldeira, K., Archer, D., and Zachos, J. C.: An ancient carbon mystery, *Science*, 314,
1169 1556-1557, 2006a.

1170 Pagani, M., Pedentchouk, N., Huber, M., Sluijs, A., Schouten, S., Brinkhuis, H., Sinninghe Damsté, J.
1171 S., Dickens, G. R., & the Expedition 302 Scientists: Arctic hydrology during global warming at the
1172 Palaeocene/Eocene Thermal Maximum, *Nature*, 442, 671-675, 2006b.

1173 Panchuk, K., Ridgwell, A., and Kump, L. R.: Sedimentary response to Paleocene-Eocene Thermal
1174 Maximum carbon release: A model-data comparison, *Geology*, 36 (4), 315–318, 2008.

1175 Panieri, G., Sen Gupta, B. K.: Benthic foraminifera of the Blake Ridge hydrate mound, Western North
1176 Atlantic Ocean, *Mar. Micropaleont.*, 66, 91-102, 2007.

1177 Paytan, A., Averyt, K., Faul, K., Gray, E., and Thomas, E.: Barite accumulation, ocean productivity,
1178 and Sr/Ba in barite across the Paleocene-Eocene Thermal Maximum, *Geology* 35, 1139–1142, 2007.

1179 ~~Pearson, P. N. and Thomas, E.: Drilling disturbance and constraints on the onset of the
1180 Palaeocene/Eocene boundary carbon isotope excursion in New Jersey, *Clim. Past*, 11: 95–104, 2015.~~

1181 Penman, D. E., Hönisch, B., Zeebe, R. E, Thomas, E., and Zachos, J. C., Rapid and sustained surface
1182 ocean acidification during the Paleocene-Eocene Thermal Maximum, *Paleoceanography*, 29, 357-369,
1183 2014.

1184 Pflum, C. E., and Frerichs, W. E.: Gulf of Mexico Deep-Water Foraminifers, Cushman Foundation for
1185 Foraminiferal Research, Special Publication, 14, 125 pp., 1976.

1186 Pierrehumbert, R. T.: The hydrologic cycle in deep-time climate problems, *Nature*, 419, 191–198,
1187 2002.

1188 Post, J. E., Thomas, E., and Heaney, P. J.: Jianshuiite in oceanic manganese nodules at the Paleocene-
1189 Eocene Boundary, *Am. Mineral.*, 101, doi 10.2138/am-2016-5347 ,(2016).

1190 Raymo, M. E., Ruddiman, F., and Froelich, P. N.: Influence of late Cenozoic mountain building on
1191 ocean geochemical cycles, *Geology*, 16, 649-653, 1988.

1192 Ravizza, G. E., Norris, R. N., Blusztajn, J., and Aubry, M.-P.: An osmium isotope excursion associated
1193 with the Late Paleocene Thermal Maximum: evidence of intensified chemical weathering,
1194 *Paleoceanography*, 16, 155-163, 2001.

1195 Robert, C. and Chamley, H.: Development of early Eocene warm climates, as inferred from clay
1196 mineral variations in oceanic sediments, *Global Planet. Change*, 89, 315–331, 1991.

1197 Robert, C., and Kennett, J. P.: Antarctic subtropical humid episode at the Paleocene–Eocene boundary:
1198 clay–mineral evidence, *Geology*, 22, 211–214, 1994.

1199 Rodriguez-Tovar, F. J., Uchman, A., Alegret, L., Molina, E.: Impact of the Paleocene–Eocene Thermal
1200 Maximum on the macrobenthic community: Ichnological record from the Zumaia section, northern
1201 Spain, *Mar. Geol.*, 282, 178–187, 2011.

1202 Röhl, U., Westerhold, T., Bralower, T. J., and Zachos, J. C.: On the duration of the Paleocene-Eocene
1203 Thermal Maximum (PETM), *Geochem. Geophys. Geosy*, 8, Q12002, 2007.

1204 Sachse, D., Radke, J., and Gleixner, G.: δD values of individual n-alkanes from terrestrial plants along
1205 a climatic gradient-implications for the sedimentary biomarker record, *Org. Geochem.*, 37, 469–483,
1206 2006.

1207 Schmiedl, G.: Late Quaternary benthic foraminiferal assemblages from the eastern South Atlantic:
1208 Reconstruction of deep-water circulation and productivity changes, *Reports on Polar Research*, 160;
1209 207 pp. (in German), 1995.

1210 Schmiedl, G. and Mackensen, A.: Late Quaternary paleoproductivity and deep water circulation in the
1211 eastern South Atlantic Ocean: evidence from benthic foraminifera, *Palaeogeogr. Palaeocl. Palaeoecol.*
1212 130, 43–80, 1997.

1213 Schmiedl, G., De Bovee, F., Buscail, R., Charriere, B., Hemleben, C., Medernach, L., Picon, P.:
1214 Trophic control of benthic foraminiferal abundance and microhabitat in the bathyal Gulf of Lions,
1215 western Mediterranean Sea, *Mar. Micropaleont.*, 40, 167–188, 2000.

1216 Schmitz, B., and Pujalte, V.: Sea-level, humidity, and land-erosion records across the initial Eocene
1217 Thermal Maximum from a continental-marine transect in northern Spain, *Geology*, 31, 689–692, 2003.

1218 Schmitz, B., Pujalte, V.: Abrupt increase in seasonal extreme precipitation at the Paleocene–Eocene
1219 boundary, *Geology*, 35, 215–218, 2007.

1220 Schmitz, B., Asaro, F., Molina, E., Monechi, S., Von Salis, K., Speijer, R.: High resolution iridium,
1221 δ¹³C, δ¹⁸O, foraminifera and nannofossil profiles across the latest Paleocene benthic extinction event at
1222 Zumaya, *Palaeogeogr. Palaeocl. Palaeoecol.*, 133, 49–68, 1997.

1223 Schmitz, B., Pujalte, V., and Nùñez-Betelu, K.: Climate and sea level perturbations during the initial
1224 Eocene thermal maximum: Evidence from siliciclastic units in the Basque Basin (Ermua, Zumaia and
1225 Trabakua Pass), northern Spain, *Palaeogeogr. Palaeocl.*, 165, 299-320, 2001.

1226 Schoon, P. L., Heilmann-Clausen, C., Schultz, B. P., Sinninghe Damsté, J. S., Schouten, S.: Warming
1227 and environmental changes in the eastern North Sea Basin during the Palaeocene–Eocene Thermal
1228 Maximum as revealed by biomarker lipids, *Org. Geochem.*, 78, 79–88, 2015.

1229 Secord, R., Gingerich, P. D., Lohmann, K. C., and MacLeod, K. G.: Continental warming preceding
1230 the Palaeocene-Eocene thermal maximum, *Nature*, 467, 955–958, 2010.

1231 Seibel, B. A., and Walsh, P. J.: Potential impacts of CO₂ injection on deep-sea biota, *Science*, 294, 319–
1232 320, 2001.

1233 Sgarrella, F., Sprovieri, F., Di Stefano, E., and Caruso, S.: Paleoceanography conditions at the base of
1234 the Pliocene in the Southern Mediterranean Basin, *Riv. Ital. Paleontol. S.*, 103, 207-220, 1997.

1235 Sing, R. K., and Gupta, A. K.: Late Oligocene-Miocene paleoceanographic evolution of the
1236 southeastern Indian Ocean: evidence from deep-sea benthic foraminifera (ODP Site 757), *Mar.
1237 Micropaleont.*, 51, 153-170, 2004.

1238 ~~Sluijs, A., and Brinkhuis, H.: A dynamic climate and ecosystem state during the Paleocene-Eocene
1239 Thermal Maximum: inferences from dinoflagellate cyst assemblages on the New Jersey Shelf,
1240 Biogeosciences, 6, 1755–1781, 2009.~~

1241 Sluijs, A., Schouten, S., Pagani, M., Woltering, M., Brinkhuis, H., Sinninghe Damsté, J. S., Dickens,
1242 G. R., Huber, M., Reichart, G.-J., Stein, R., Matthiessen, J., Lourens, L. J., Pedentchouk, N., Backman,
1243 J., Moran, K., and The Expedition 302 Scientists: Subtropical Arctic Ocean temperatures during the
1244 Palaeocene/Eocene Thermal Maximum, *Nature*, 441, 610–613, 2006.

1245 Sluijs, A., Bowen, G. J., Brinkhuis, H., Lourens, L. J., and Thomas, E.: The Paleocene-Eocene thermal
1246 maximum super greenhouse: Biotic and geochemical signatures, age models and mechanisms of global
1247 change, in: Deep-Time Perspectives on Climate Change: Marrying the Signal From Computer Models
1248 and Biological Proxies, edited by: Williams, M., Haywood, A.M., Gregory, F. J., and Schmidt, D. N.,

1249 The Micropalaeontological Society Special Publication, The Geological Society, London, 323–350,
1250 2007a.

1251 Sluijs, A., Brinkhuis, H., Schouten, S., Bohaty, S.M., John, C.M., Zachos, J.C., Reichart, G.-J.,
1252 Sinninghe Damsté, J.S., Crouch, E.M., and Dickens, G.R.: Environmental precursors to rapid light
1253 carbon injection at the Palaeocene/Eocene boundary, *Nature*, 450, 1218-1221, 2007b.

1254 ~~Sluijs, A., Brinkhuis, H., Crouch, E. M., John, C. M., Handley, L., Munsterman, D., Bohaty, S. M.,~~
1255 ~~Zachos, J. C., Reichart, G., Schouten, S., Pancost, R. D., Sinninghe Damste, J. S., Welters, N. L. D.,~~
1256 ~~Letter, A. F., and Dickens, G. R., Eustatic variations during the Paleocene Eocene greenhouse world.~~
1257 ~~Paleoceanography~~, 23, PA4216, 2008.

1258 Sluijs, A., Bijl, P. K., Schouten, S., Röhl, U., Reichart, G.-J., and Brinkhuis, H.: Southern Ocean
1259 warming, sea level and hydrological change during the Paleocene-Eocene thermal maximum, *Clim.*
1260 *Past*, 7 (1), 47-61, 2011.

1261 ~~Smith, F. A. and Freeman, K. H., 2006. Influence of physiology and climate on δD of leaf wax n-~~
1262 ~~alkanes from C3 and C4 grasses, *Geochim. Cosmochim. Ae.*, 70, 1172–1187, 2006.~~

1263 Smith, F. A., Wing, S. L., and Freeman, K. H.: Magnitude of the carbon isotope excursion at the
1264 Paleocene–Eocene Thermal Maximum: the role of plant community change, *Earth Planet. Sc. Lett.*,
1265 262, 50–65, 2007.

1266 Speijer, R. P. and Schmitz, B.: A benthic foraminiferal record of Paleocene sea level and trophic/redox
1267 conditions at Gebel Aweina, Egypt, *Palaeogeogr. Palaeocl. Palaeoecol.*, 137, 79–101, 1998.

1268 Speijer, R. P., Schmitz, B., Aubry, M.-P., and Charisi, S. D.: The latest Paleocene benthic extinction
1269 event: punctuated turnover in outer neritic foraminiferal faunas from Gebel Aweina, Egypt, in: Aubry,
1270 M.-P. and Benjamini, C. (Eds.): Paleocene/Eocene boundary events in space and time, *Israel J. Earth*
1271 *Sci.*, 44, 207–222, 1996.

1272 Speijer, R. P., Schmitz, B., and van der Zwaan, G. J.: Benthic foraminiferal extinction and repopulation
1273 in response to latest Paleocene Tethyan anoxia, *Geology*, 25, 683-686, 1997.

1274 Speijer, R. P., Scheibner, C., Stassen, P., and Morsi, A.-M.: Response of marine ecosystems to deep-
1275 time global warming: a synthesis of biotic patterns across the Paleocene-Eocene thermal maximum
1276 (PETM), *Austrian Journal of Earth Sciences*, 105, 6-16, 2012.

1277 Stassen, P., Thomas, E., and Speijer, R. P.: The progression of environmental changes during the onset
1278 of the Paleocene-Eocene Thermal Maximum (New Jersey Coastal Plain), *Austrian Journal of Earth
1279 Sciences* 105/1, 169-178, 2012a.

1280 Stassen, P., Thomas, E., and Speijer, R. P.: Integrated stratigraphy of the Paleocene-Eocene thermal
1281 maximum in the New Jersey Coastal Plain: Toward understanding the effects of global warming in a
1282 shelf environment, *Paleoceanography*, 27, PA4210, 2012b.

1283 Stassen, P., Thomas, E., Speijer, R. P.: Paleocene-Eocene Thermal Maximum environmental change in
1284 the New Jersey Coastal Plain: benthic foraminiferal biotic events, *Mar. Micropaleont.*, 115: 1-23, 2015.

1285 Steineck, P., Thomas, E.: The latest Paleocene crisis in the deep sea: ostracode succession at Maud
1286 Rise, *Southern Ocean, Geology*, 24, 583–586, 1996.

1287 Stoll, H. M., Shimizu, N., Archer, D., and Ziveri, P.: Coccolithophore productivity response to
1288 greenhouse event of the Paleocene-Eocene Thermal Maximum, *Earth Planet. Sc. Lett.*, 258, 192-206,
1289 2007.

1290 Suhr, S. B., Pond, D. W., Gooday, A. J., and Smith, C. R.: Selective feeding by foraminifera on
1291 phytodetritus on the western Antarctic Peninsula shelf: evidence from fatty acid biomarker analysis,
1292 *Mar. Ecol.-Prog. Ser.*, 262, 153–162, 2003.

1293 Takata, H., Nomura, R., and Khim, B.-K.: Response to abyssal benthic foraminifera to mid-Oligocene
1294 glacial events in the eastern Equatorial Pacific Ocean (ODP Leg 199), *Palaeogeogr. Palaeocl.
1295 Palaeoecol.*, 292, 1-11, 2010.

1296 Takeda, K., and Kaiho, K.: Faunal turnovers in central Pacific benthic foraminifera during the
1297 Paleocene-Eocene thermal maximum, *Palaeogeogr. Palaeocl. Palaeoecol.*, 251, 175–197, 2007.

1298 Thiry, M.: Palaeoclimatic interpretation of clay minerals in marine deposits: An outlook from the
1299 continental origin, *Earth-Science Reviews*, 49, 201–221, 2000.

1300 Thomas, D. J., Bralower, T. J., and Zachos, J. C.: New evidence for subtropical warming during the
1301 late Paleocene thermal maximum: Stable isotopes from Deep Sea Drilling Project Site 527: Walvis
1302 Ridge, *Paleoceanography*, 14, 561–570, 1999.

1303 Thomas, D. J., Zachos, J. C., Bralower, T. J., Thomas, E., and Bohaty, S.: Warming the fuel for the
1304 fire: Evidence for the thermal dissociation of methane hydrate during the Paleocene-Eocene thermal
1305 maximum, *Geology*, 30, 1067–1070, 2002.

1306 Thomas, E.: Late Eocene to Recent deep-sea benthic foraminifers from the central equatorial Pacific
1307 Ocean, in: *Initial Rep. Deep Sea*, edited by: Mayer, L., Theyer, F., Barron, J. A., Dunn, D. A.,
1308 Handyside, T., Hills, S., Jarvis, I., Nigrini, C. A., Pisias, N. C., Pujos, A., Saito, T., Stout, P., Thomas,
1309 E., Weinreich, N., and Wilkens, R. H., 85, US Government Printing Office, Washington, 655–656,
1310 1985.

1311 Thomas, E.: Development of Cenozoic deep-sea benthic foraminiferal faunas in Antarctic waters, *Geol.*
1312 *Soc. Spec. Publ.*, 47, 283–296, 1989.

1313 Thomas, E.: Late Cretaceous through Neogene deep-sea benthic foraminifers (Maud Rise, Weddell
1314 Sea, Antarctica), in: *Proceedings of the Ocean Drilling Program, Scientific Results*, edited by: Barker,
1315 P. F., Kennett, J. P., O'Connell, S., Berkowitz, S., Bryant, W. R., Burckle, L. H., Egeberg, P. K.,
1316 Fiitterer, D. K., Qersonde, R. E., Qolovchenko, X., Hamilton, N., Lawver, L., Lazarus, D. B., Lonsdale,
1317 M., Mohr, B., Nagao, T., Pereira, C. P. Q., Pudsey, C. J., Robert, C. M., Schandl, E., SpiejJ, V., Stott,
1318 L. D., Thomas, E., Thompson, K. F. M., and Wise, S. W. Jr., 113, College Station, TX (Ocean Drilling
1319 Program), 571–594, 1990.

1320 Thomas, E.: Biogeography of the late Paleocene benthic foraminiferal extinction, in: *Late Paleocene-*
1321 *Early Eocene Climatic and Biotic Events in the Marine and Terrestrial Records*, edited by: Aubry, M.
1322 P., Lucas, S., and Berggren, W., A., Columbia University Press, New York, 214–243, 1998.

1323 Thomas, E.: Extinction and food at the seafloor: A high-resolution benthic foraminiferal record across
1324 the Initial Eocene Thermal Maximum, Southern Ocean Site 690, in: *Causes and Consequences of*
1325 *Globally Warm Climates in the Early Paleogene*, edited by: Wing, S. L., Gingerich, P. D., Schmitz, B.,
1326 and Thomas, E., *Geol. S. Am. S.*, Boulder, Colorado, The Geological Society of America, 369, 319–
1327 332, 2003.

1328 Thomas, E.: Cenozoic mass extinctions in the deep sea: What perturbs the largest habitat on Earth?, in:
1329 Large Ecosystem Perturbations: Causes and Consequences, edited by: Monechi, S., Coccioni, R., and
1330 Rampino, M., Geol. S. Am. S., Boulder, Colorado, The Geological Society of America, 424, 1–23,
1331 2007.

1332 Thomas, E. and Gooday, A. W.: Cenozoic deep-sea benthic foraminifers: Tracers for changes in
1333 oceanic productivity?, *Geology*, 24, 355-358, 1996.

1334 Thomas, E. and Shackleton, N. J.: The Paleocene-Eocene benthic foraminiferal extinction and stable
1335 isotopes anomalies, *Geol. Soc. Spec. Publ.*, 101, 401-441, 1996.

1336 Thomas, E., Zachos, J. C., and Bralower, T. J.: Deep-Sea Environments on a Warm Earth: latest
1337 Paleocene-early Eocene, in: *Warm Climates in Earth History*, edited by: Huber, B., MacLeod, K., and
1338 Wing, S., Cambridge University Press, Cambridge, UK, 132–160, 2000.

1339 Tipple, B. J., Pagani, M., Krishnan, S., Dirghangi, S. S., Galeotti, S., Agnini, C., Giusberti, L., Rio, D.:
1340 Coupled high-resolution marine and terrestrial records of carbon and hydrologic cycles variations
1341 during the Paleocene-Eocene Thermal Maximum (PETM), *Earth Planet. Sc. Lett.*, 311, 82-92, 2011.

1342 Tjalsma, R. C. and Lohmann, G. P.: Paleocene-Eocene bathyal and abyssal benthic foraminifera from
1343 the Atlantic Ocean, *Micropaleontology Special Publication*, 4, 1–90, 1983.

1344 Torrent, J., Barro, V., and Liu, Q.: Magnetic enhancement is linked to and precedes hematite formation
1345 in aerobic soil, *Geophysical Res. Lett.*, 33, L02401, 2006.

1346 Van Morkhoven, F. P. C. M., Berggren, W. A., and Edwards, A. S.: Cenozoic cosmopolitan deep-water
1347 benthic foraminifera. *B. Cent. Rech. Expl., Mèmoire*, 11, 1-421, 1986.

1348 Von Hillebrandt, A.: Das Paläozän und seine Foraminiferenfauna im Becken von Reichenhall und
1349 Salzburg, *Bayerische Akademie der Wissenschaften, Mathematisch-Naturwissenschaftliche Klasse*,
1350 *Abhandlungen, neue folge*, München, 108, 9-180, 1962.

1351 Waśkowska, A.: Response of Early Eocene deep-water benthic foraminifera to volcanic ash falls in the
1352 Polish Outer Carpathians: Palaeoecological implications, *Palaeogeogr. Palaeocl. Palaeoecol.*, 305, 50-64,
1353 2011.

1354 Wendler, I., Huber, B. T., MacLeod, K. G., and Wendler, J. E.: Stable oxygen and carbon isotope
1355 systematics of exquisitely preserved Turonian foraminifera from Tanzania - understanding isotopic
1356 signatures in fossils, *Mar. Micropaleont.*, 102, 1-33, 2013.

1357 Westerhold, T., Röhl, U., Laskar, J., Raffi, I., Bowles, J., Lourens, L. J., and Zachos, J. C.: On the
1358 duration of Magnetochrons C24r and C25n, and the timing of early Eocene global warming events:
1359 Implications from the ODP Leg 208 Walvis Ridge depth transect, *Paleoceanography*, 22, PA2201,
1360 2007.

1361 Wieczorek, R., Fantle, M. S., Kump, L. R., Ravizza, G.: Geochemical evidence for volcanic activity
1362 prior to and enhanced terrestrial weathering during the Paleocene Eocene Thermal maximum,
1363 *Geochim. Cosmochim. Ac.*, 119, 391-410, 2013.

1364 Wing, S. L., Harrington, G. J., Smith, F. A., Bloch, J. I., Boyer, D. M., and Freeman, K. H.: Transient
1365 floral change and rapid global warming at the Paleocene-Eocene boundary, *Science* 310, 993–996,
1366 2005.

1367 Winguth, A. M. E., Thomas, E., Winguth, C.: Global decline in ocean ventilation, oxygenation, and
1368 productivity during the Paleocene-Eocene Thermal Maximum: Implications for the benthic extinction,
1369 *Geology*, 40, 263-266, 2012.

1370 ~~Winguth, A. M. E., Shellito, C., Shields, C., and Winguth, C.: Climate response at the Paleocene-~~
1371 ~~Eocene Thermal Maximum to greenhouse gas forcing – A model study with CCSM3, *J. Climate*, 23,~~
1372 ~~2562–2584, 2010.~~

1373 Zachos, J. C., Pagani, M., Sloan, L. C., Thomas, E., and Billups, K.: Trends, rhythms, and aberrations
1374 in global climate 65 Ma to present, *Science* 292, 686–693, 2001.

1375 Zachos, J. C., Schouten, S., Bohaty, S., Quattlebaum, T., Sluijs, A., Brinkhuis, H., Gibbs, S. J., and
1376 Bralower, T. J.: Extreme warming of mid latitude coastal ocean during the Paleocene-Eocene thermal
1377 maximum: inferences from TEX86 and isotope data, *Geology*, 34, 737–740, 2006.

1378 Zachos, J. C., Röhl, U., Schellenberg, S. A., Sluijs, A., Hodell, D. A., Kelly, D. C., Thomas, E., Nicolo,
1379 M., Raffi, I., Lourens, L. J., McCarren, H. and Kroon, D.: Rapid acidification of the ocean during the
1380 Paleocene-Eocene Thermal Maximum, *Science*, 308, 1611-1615, 2005.

1381 Zeebe, R. E., Zachos, J. C., and Dickens, G. R.: Carbon dioxide forcing alone insufficient to explain
1382 Paleocene-Eocene Thermal Maximum warming, *Nat. Geosci.*, 2, 576-580, 2009.

1383 Zeebe, R. E., Dickens, G. R., Ridgwell, A., Sluijs, A., and Thomas, E.: Onset of carbon isotope
1384 excursion at the Paleocene-Eocene Thermal Maximum took millennia, not 13 years (Comment), *P.*
1385 *Natl. Acad. Sci. USA*, 111, E1062-E1063, 2014.

1386 Zhang, Y., Ji, J., Balsam, W. L., Liu L., Chen J.: High resolution hematite and goethite records from
1387 ODP 1143, South China Sea: Co-evolution of monsoonal precipitation and El Niño over the past
1388 600,000 years, *Earth Planet. Sc. Lett.*, 264, 136–150, 2007.

1389 Zhou, X., Thomas, E., Rickaby, R. E. M., Winguth, A. M. E., and Lu, Z.: I/Ca evidence for global
1390 upper ocean deoxygenation during the Paleocene-Eocene Thermal Maximum (PETM),
1391 *Paleoceanography*, 29(10), 964-975, 2014.

1392

1393 **Figures captions**

1394 Figure 1. Location of the Forada section in the context of the Piave River Valley in the Belluno
1395 Province (the “Valbelluna”), northeastern Italy.

1396 Figure 2. Faunal and geochemical variations across the PETM at Forada section plotted against
1397 chronostratigraphy, precessional cycles, lithology, recognized benthic foraminiferal assemblages (A to
1398 G) and isotopic intervals. % agglutinated=agglutinated to agglutinated and calcareous hyaline ratio; %
1399 infaunal taxa=infaunal to infaunal and epifaunal ratio; simple diversity and Fisher- α diversity index;
1400 N/g=number of benthic foraminifera per gram (faunal density) in the >63 mm size fraction; coarse
1401 fraction (CF) calculated according to Hancock and Dickens (2005) as the weight percent of the >63 μm
1402 size fraction relative to the weight of the bulk sample; Fragmentation index (F-Index) is from Luciani
1403 et al. (2007). The gray bands indicate intervals of carbonate dissolution. α = pre-CIE dissolution,
1404 β =burndown layer, BFDI=benthic foraminiferal dissolution interval. Modified from Giusberti et al.
1405 (2007).

1406 Figure 3. Summary of the main mineralogical, geochemical and cyclostratigraphic features recognized
1407 across the Paleocene-Eocene boundary and in the clay marl unit (CMU) of the Forada section and
1408 radiolarian abundance plotted against isotopic intervals and recognized benthic foraminiferal
1409 assemblages (A to F). N/g for the radiolarians refers to the number of radiolarians (>125 μm fraction)
1410 per gram of dry sediment. F-Index from Luciani et al. (2007). VPDB—Vienna Peepee belemnite
1411 standard. Modified from Giusberti et al. (2007).

1412 Fig. 4. Stratigraphic distribution of benthic foraminiferal extinction taxa (CET) across the
1413 Paleocene/Eocene boundary in the Forada section plotted against lithology, $\delta^{13}\text{C}$ bulk record, CaCO_3
1414 percentage, isotopic intervals and recognized benthic foraminiferal assemblages (A to F), based on data
1415 from the >63 μm size fraction integrated with data from >125 micron fraction. The gray bands indicate
1416 intervals of carbonate dissolution. Question marks: doubtful identification. Triangle: post BEE
1417 occurrence of one specimen of *Coryphostoma midwayensis* has been recorded in the sample BRI 300
1418 (295 cm above the base of CMU).

1419 Figure 5. Relative abundance of the most abundant benthic foraminiferal taxa across the PETM at
1420 Forada plotted against biostratigraphy, precessional cycles, lithology, $\delta^{13}\text{C}$ bulk record, recognized

1421 benthic foraminiferal assemblages (A to F) and isotopic intervals. Benthic foraminiferal biozonation
1422 after Berggren and Miller (1989). The gray bands indicate intervals of carbonate dissolution. α = pre-
1423 CIE dissolution, β =burndown layer, BFDI=benthic foraminiferal dissolution interval. "Other
1424 buliminids" group includes only representatives of the families Buliminidae, Buliminellidae and
1425 Turrilinidae (*Bulimina*, *Buliminella*, *Quadratobuliminella*, *Sitella* and *Turrilina*).

1426 Figure 6. Relative abundance of selected benthic foraminifera across the PETM at Forada plotted
1427 against biostratigraphy, precessional cycles, lithology, $\delta^{13}\text{C}$ bulk record, recognized benthic
1428 foraminiferal assemblages (A to F) and isotopic intervals. Benthic foraminiferal biozonation after
1429 Berggren and Miller (1989). The gray bands indicate intervals of carbonate dissolution. α = pre-CIE
1430 dissolution, β =burndown layer, BFDI=benthic foraminiferal dissolution interval.

1431 Figure 7. Enlargement of the interval from -1m to +2m across the P/E boundary at Forada showing the
1432 relative abundance of selected benthic foraminifera plotted against biostratigraphy, precessional cycles,
1433 lithology, $\delta^{13}\text{C}$ bulk record, recognized benthic foraminiferal assemblages (A to F) and isotopic
1434 intervals. Benthic foraminiferal biozonation after Berggren and Miller (1989). The gray bands indicate
1435 intervals of carbonate dissolution. α =Pre-CIE dissolution interval; β =burndown layer, BFDI=benthic
1436 foraminiferal dissolution interval.

1437 Figure 8. Summary of main calcareous plankton (calcareous nannofossils and planktonic foraminifera)
1438 and benthic foraminiferal events and inferred environmental conditions (from Agnini et al., 2007;
1439 Luciani et al., 2007 and present work), isotopic intervals, thickness, precessional cycles and benthic
1440 foraminiferal assemblages (A to F) recognized in this work. The stratigraphic intervals containing
1441 assemblages A and B, C and D to F are considered as pre-extinction, extinction and repopulation
1442 intervals, respectively. Benthic foraminiferal zonation after Berggren and Miller (1989).

1443 Figure 9. Stable carbon isotope ratios of higher plant n-alkanes (a), stable hydrogen isotope ratios of
1444 higher plant n-alkanes (b) with higher plant average chain length values (c) for Forada PETM plotted
1445 against isotopic intervals and recognized benthic foraminiferal assemblages (A to F). Terrestrial higher
1446 plant n-C27, n-C29, and n-C31 δD values are shown as crosses, closed circles, and triangles,
1447 respectively. Redrawn from data of Tipple et al. (2011).

1448 Figure 10. Paleogeographic map (from <http://www.odsн.de/odsн/services/paleomap/paleomap.html>) at
1449 55 Ma showing sites where paleohydrological reconstructions for the PETM are available. Numbers
1450 follow a north to south paleolatitudinal order. Blue dots indicate areas where an increase in
1451 precipitation has been inferred; Green dots indicate areas where an increase in climatic contrasts or a
1452 fluctuating precipitation regime have been inferred; Orange dots indicate areas where an increase in
1453 aridity has been inferred; Purple dots indicate areas where hydrological changes have been inferred but
1454 the pattern not specified. 1. Lomonosov Ridge, Arctic Sea; 2, 3. Spitsbergen Central Basin and
1455 Svalbard archipelago; 4. Central North Sea Basin; 5. Eastern North Sea Basin; 6. Williston Basin,
1456 western North Dakota, (USA) 7. Bighorn Basin, Wyoming (USA); 8. Rhenodanubian Basin, Austria; 9.
1457 Belluno Basin, northeastern Italy; 10. Aktumsuk and Kaurtakapy sections, Uzbekistan and Kazakhstan;
1458 11. Dieppe-Hampshire Basin, France; 12. London Basin; 13. DSDP Site 401 Bay of Biscay, North-
1459 eastern Atlantic Ocean; 14. Western Colorado (USA); 15. New Jersey Coastal Plain (USA); 16. Central
1460 Valley of California (USA); 17. Basque Basin, northern Spain; 18. Tremp Basin, northern Spain; 19.
1461 Alamedilla section, southern Spain; 20. Tornillo Basin, Texas (USA); 21. Salisbury embayment, mid-
1462 Atlantic coastal plain (USA); 22. Gafsa Basin, Tunisia; 23. Zin Valley of Negev, Israel; 24. Dababiya
1463 section, Egypt; 25. Northern Neotropics, (Colombia and Venezuela); 26. TDP Site 14, Tanzania; 27.
1464 Tawanui section, North Island (New Zealand); 28. Clarence River valley, South Island (New Zealand);
1465 29. Central Westland, South Island (New Zealand); 30. ODP Site 1172, East Tasman Plateau; 31. ODP
1466 Site 690 Weddell Sea, Southern Ocean. See Supplement Table S3 for references and additional
1467 information.

1468 **Table caption**

1469 Table 1. Summary of the known ecological preferences of selected benthic foraminifera, as evaluated
1470 from the literature, common at Forada.

1471 **Plates captions**

1472 Plate 1. SEM micrographs of the most representative Paleocene cosmopolitan extinction taxa (CET)
1473 occurring at Forada. 1. *Angulogavelinella avnimelechi*, spiral view (BRI-25.5); 2. *Angulogavelinella*
1474 *avnimelechi*, lateral view (BRI-185.5); 3. *Gavelinella beccariiformis*, umbilical view (BRI-75); 4.
1475 *Osangularia velascoensis*, spiral view (BRI-50,5); 5. *Anomalinoides rubiginosus* (BRI-9); 6.
1476 *Cibicidoides dayi* (BRI-37); 7. *Cibicidoides velascoensis*, spiral view (BRI-75,5); 8. *Cibicidoides*

1477 *velascoensis*, lateral view (BRI-135.5); 9. *Cibicidoides hyphalus* (BRI-50,5); 10. "Neoeponides"
1478 *megastoma* (BRI-135); 11. *Gyroidinoides globosus* (BRI-50.5); 12. *Gyroidinoides quadratus* (BRI-
1479 185,5); 13. *Coryphostoma midwayensis* (BRI-50,5); 14. *Aragonina velascoensis* (BRI-50.5); 15.
1480 *Bolivinoides delicatulus* (BRI-135.5); 16. *Neoflabellina semireticulata* (BRI-365); 17. *Pullenia coryelli*
1481 (BRI-50,5); 18. *Remesella varians* (BRI-310.5); 19. *Clavulinoides globulifera* (BRI-25.5); 20.
1482 *Clavulinoides trilatera* (BRI-33); 21. *Clavulinoides amorpha*; 22. *Marssonella indentata* (BRI-25.5);
1483 23. *Dorothia beloides* (BRI-260); 24. *Dorothia pupa* (BRI-105).

1484 Plate 2. SEM micrographs of the most representative species of the Eocene postextinction faunas
1485 occurring at Forada. 1. *Ammobaculites agglutinans* (BRI+10); 2. *Eobigenerina variabilis* (BRI+50); 3.
1486 *Eobigenerina variabilis* (BRI+50); 4. *Karrerulina conversa* (BRI+50); 5. *Karrerulina horrida* (BRI-
1487 25.5); 6. *Spiroplectammina navarroana* (BRI-33/7); 7. *Spiroplectammina spectabilis* (BRI+50); 8.
1488 *Rashnovammina munda* (BRI-50,5); 9. *Haplophragmoides* cf. *kirki*. (BRI+5); 10. *Saccammina*
1489 *placenta* (BRI-25.5); 11. *Glomospira irregularis* (BRI+35); 12. *Glomospira charoides* (BRI-75.5); 13.
1490 *Osangularia* sp. (BRI+15); 14. *Globocassidulina subglobosa* (BRI+15); 15. *Tappanina selmensis*
1491 (BRI+15); 16. *Tappanina selmensis* (BRI-9); 17. *Siphogenerinoides brevispinosa* (BRI-11); 18.
1492 *Siphogenerinoides brevispinosa* (BRI-365); 19. *Bulimina tuxpamensis* (BRI+150); 20. *Bulimina*
1493 *tuxpamensis* (BRI+150); 21. *Pleurostomella* sp. (BRI+150); 22. *Bolivina* sp. costate (BRI+385); 23.
1494 *Nuttallides truempyi* (BRI+150); 24. *Oridorsalis umbonatus* (BRI-135.5); 25. *Aragonina aragonensis*
1495 (BRI-105); 26. *Abyssammina poagi* (TAL7B).

1496 Plate 3. SEM micrographs of the most representative taxa of the upper Paleocene-lower Eocene of
1497 Forada section. 1. *Quadratobuliminella pyramidalis* (BRI-75.5); 2. *Buliminella grata* (BRI-591); 3.
1498 *Bulimina midwayensis* (BRI+35); 4. *Bulimina alazanensis* (BRI +150); 5,6. *Bulimina trinitatensis*
1499 (BRI-9); 7. *Bolivinoides crenulata* (BRI-9); 8. *Bolivinoides crenulata* (BRI-25.5); 9. *Bolivinoides*
1500 *floridana* (BRI-410); 10 *Bolivina* sp. smooth (BRI-410); 11. *Bolivina* sp. smooth (BRI-410); 12.
1501 *Reussella* sp. (BRI-365); 13. *Angulogerina muralis* (BRI-75.5); 14. *Angulogerina muralis* (BRI-75.5);
1502 15. *Angulogerina?* sp. (BRI-9); 16. *Angulogerina?* sp.(BRI-35.5); 17. *Rectobulimina carpentierae*
1503 (BRI-466); 18. *Allomorphina trochoides* (BRI-25.5); 19. *Quadriflorina allomorphinoides* (TAL
1504 7B); 20. *Cibicidoides eocaenus* (BRI-9); 21. *Anomalinoides* sp. 2 (BRI-135); 22. *Cibicides* sp. (BRI-
1505 591); 23. *Cibicidoides praemundulus* (BRI+150); 24. *Nonion havanense* (BRI-591).

1506 Plate 4. SEM micrographs of some taxa of the upper Paleocene-lower Eocene of Forada section. 1.
1507 *Ammodiscus cretaceus* (BRI-29.5); 2. *Ammodiscus peruvianus* (BRI-9); 3. *Haplophragmoides walteri*
1508 (BRI-75.5); 4. *Haplophragmoides horridus* (BRI +35); 5. *Recurvoides* sp. (BRI -33/-37); 6.
1509 *Glomospira serpens* (BRI-260); 7. *Trochamminoides proteus* (BRI-25.5); 8. *Paratrochamminoides*
1510 *heteromorphus* (BRI+40); 9. *Glomospira* cf. *gordialis* (BRI +35); 10. *Gaudryina* sp. (BRI +15); 11.
1511 *Karrerulina coniformis* (BRI -135); 12. *Caudammina ovuloides* (BRI-260); 13. *Gaudryina pyramidata*
1512 (BRI-17.5); 14. Big-sized lituolid, apertural view (BRI-9); 15. *Hormosina velascoensis* (BRI-33/37);
1513 16. *Pseudonodosinella troyeri* (BRI-260); 17. "Pseudobolivina" sp. 2 in Galeotti et al. (2004)
1514 (BRI+35); 18. *Pseudoclavulina trinitatensis* (BRI+150); 19. *Spiroplectammina spectabilis* (BRI-50.5);
1515 20. Big-sized lituolid, lateral view (BRI-9).

1516

Fig. 1

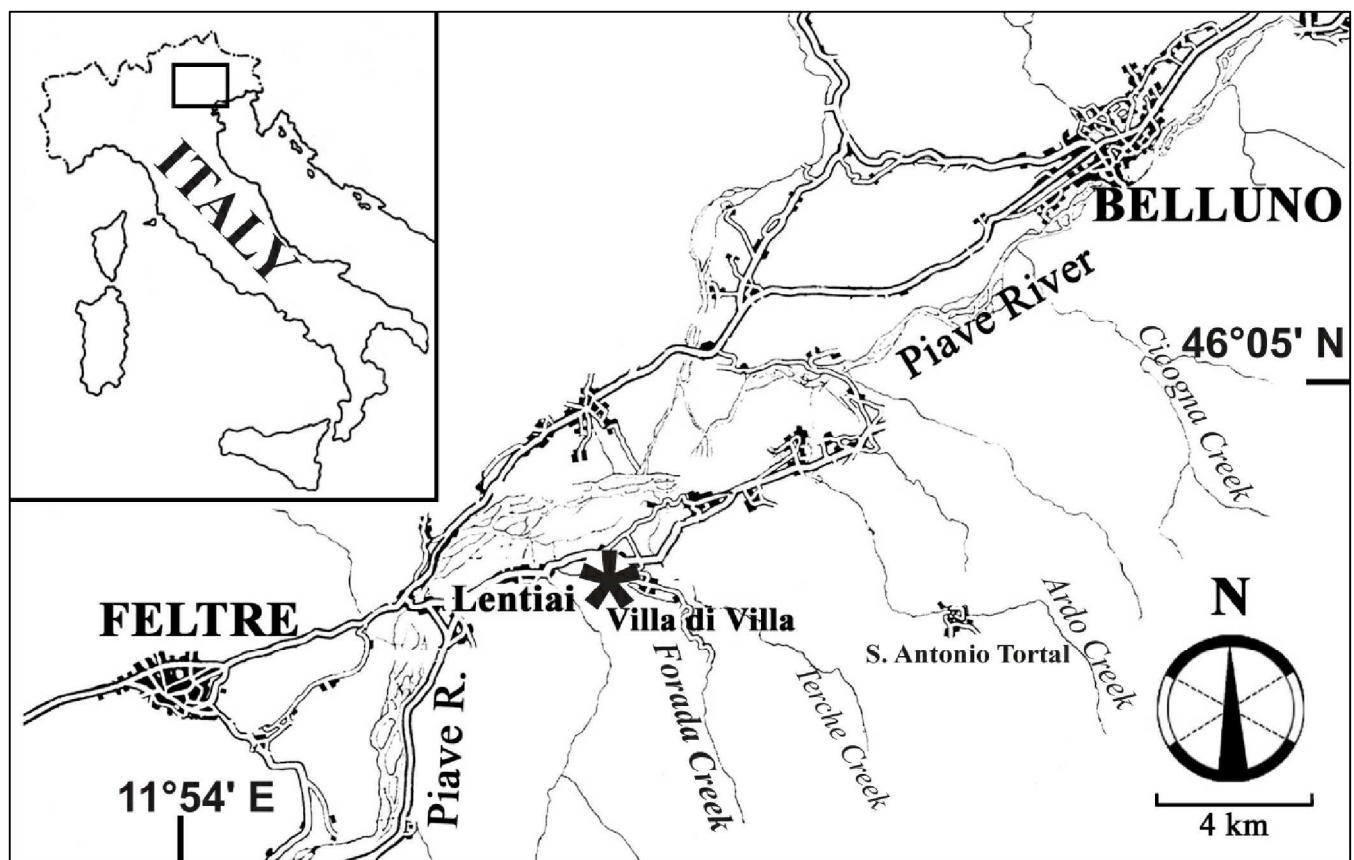


Fig. 2

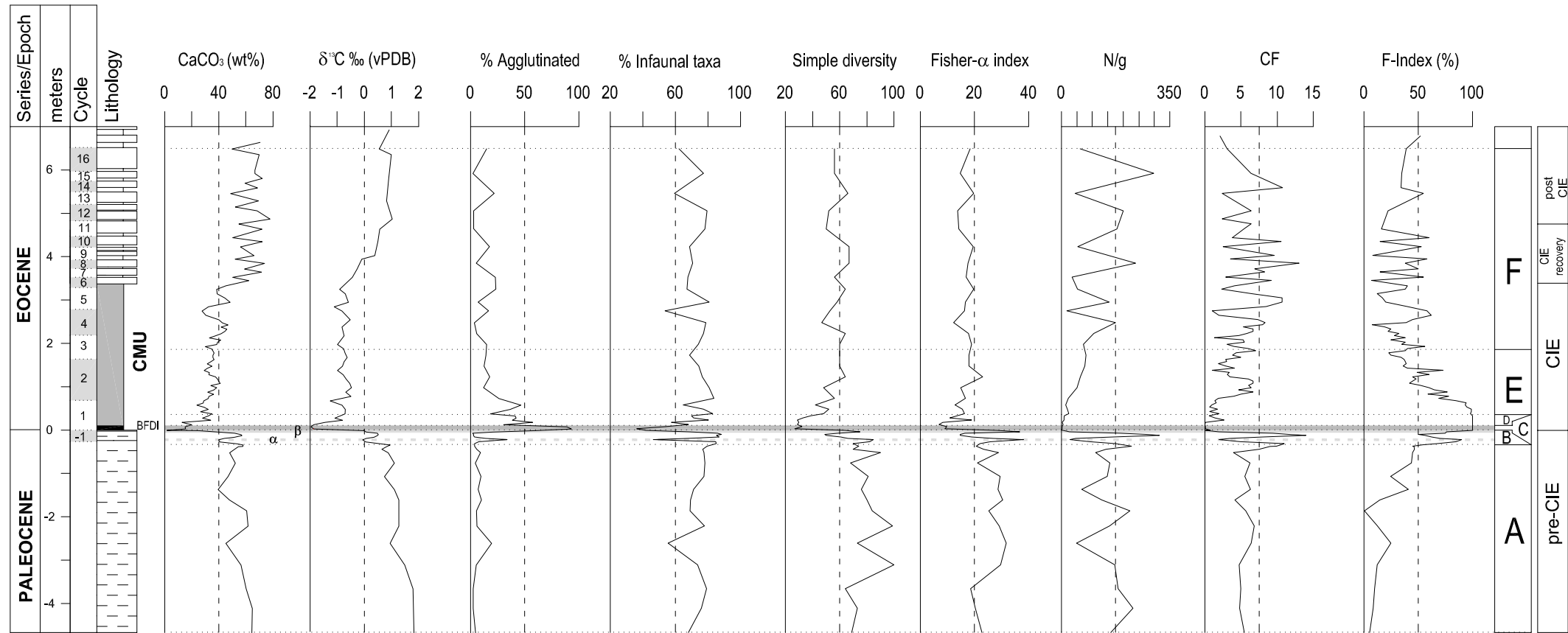


Fig. 3

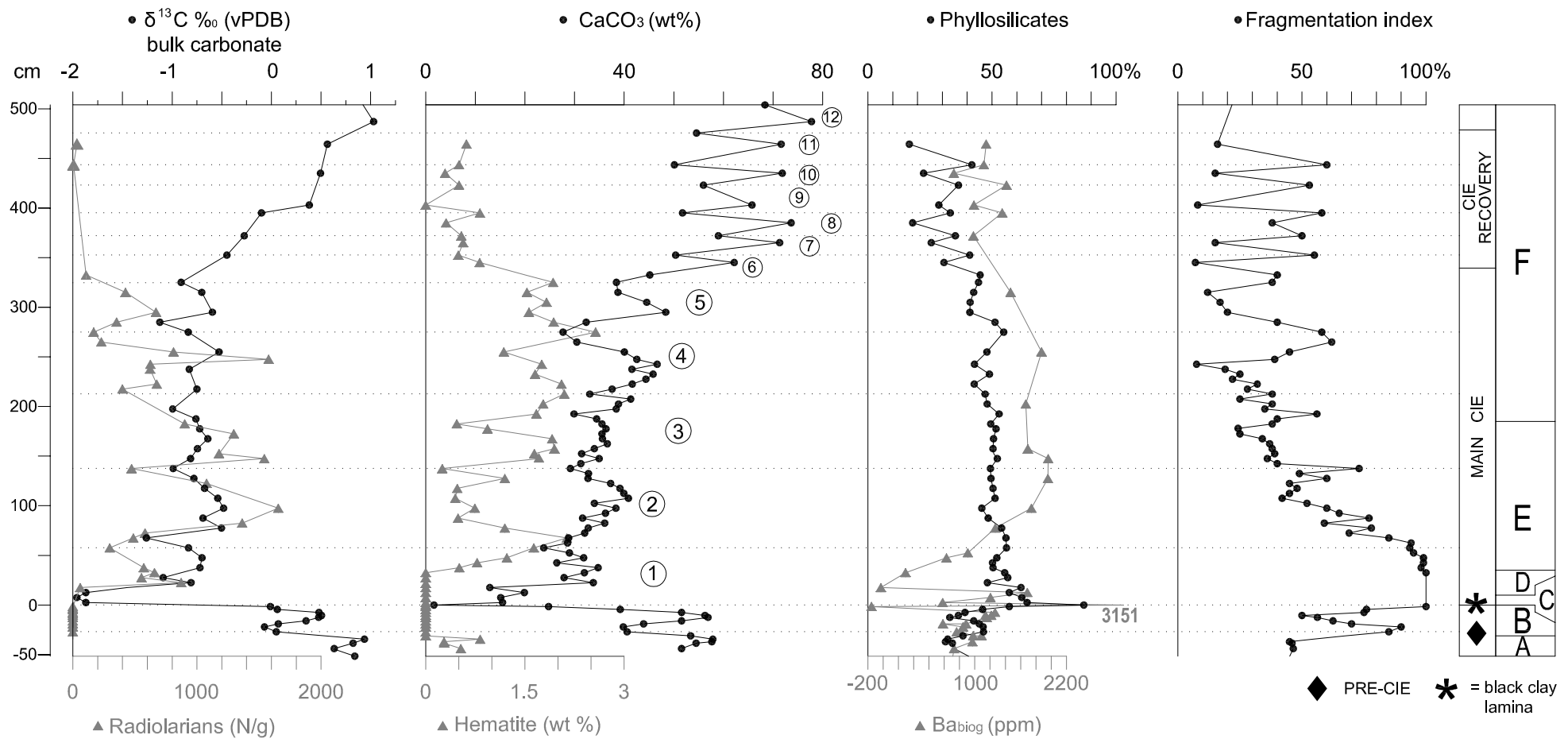


Fig. 4

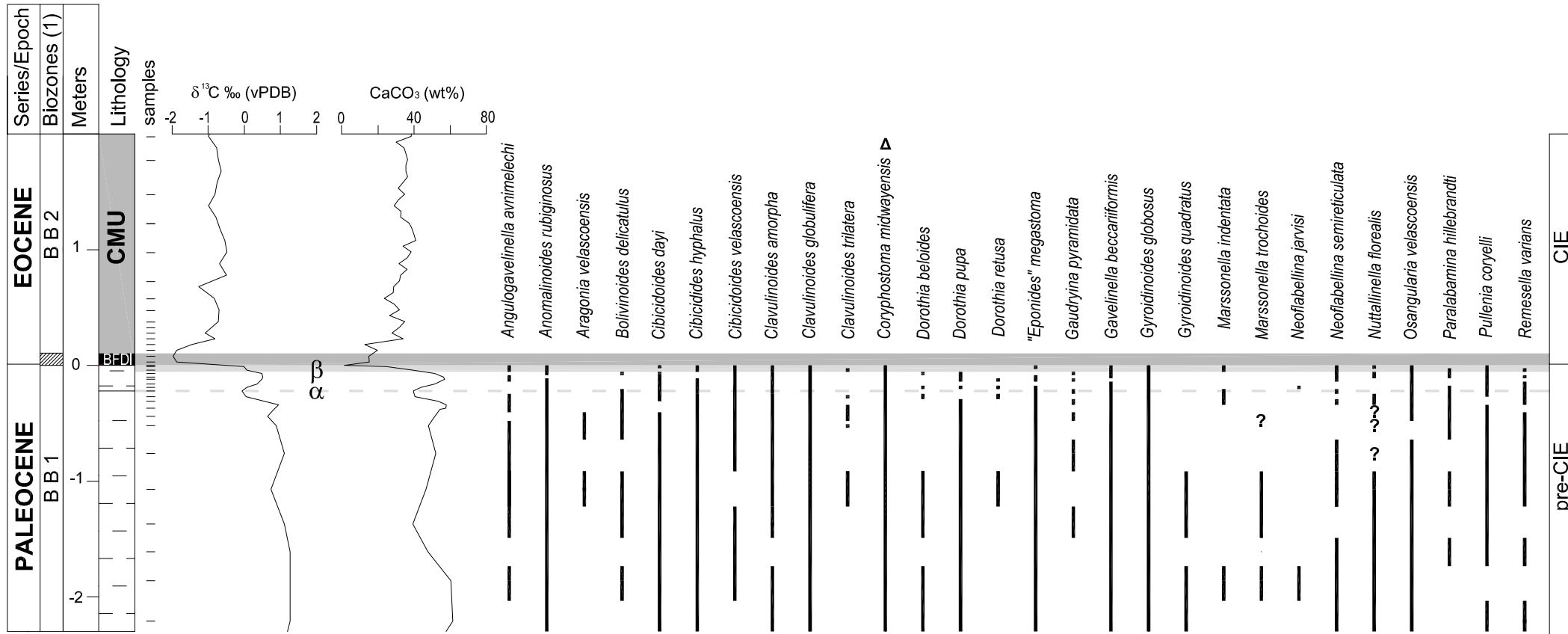


Fig. 5

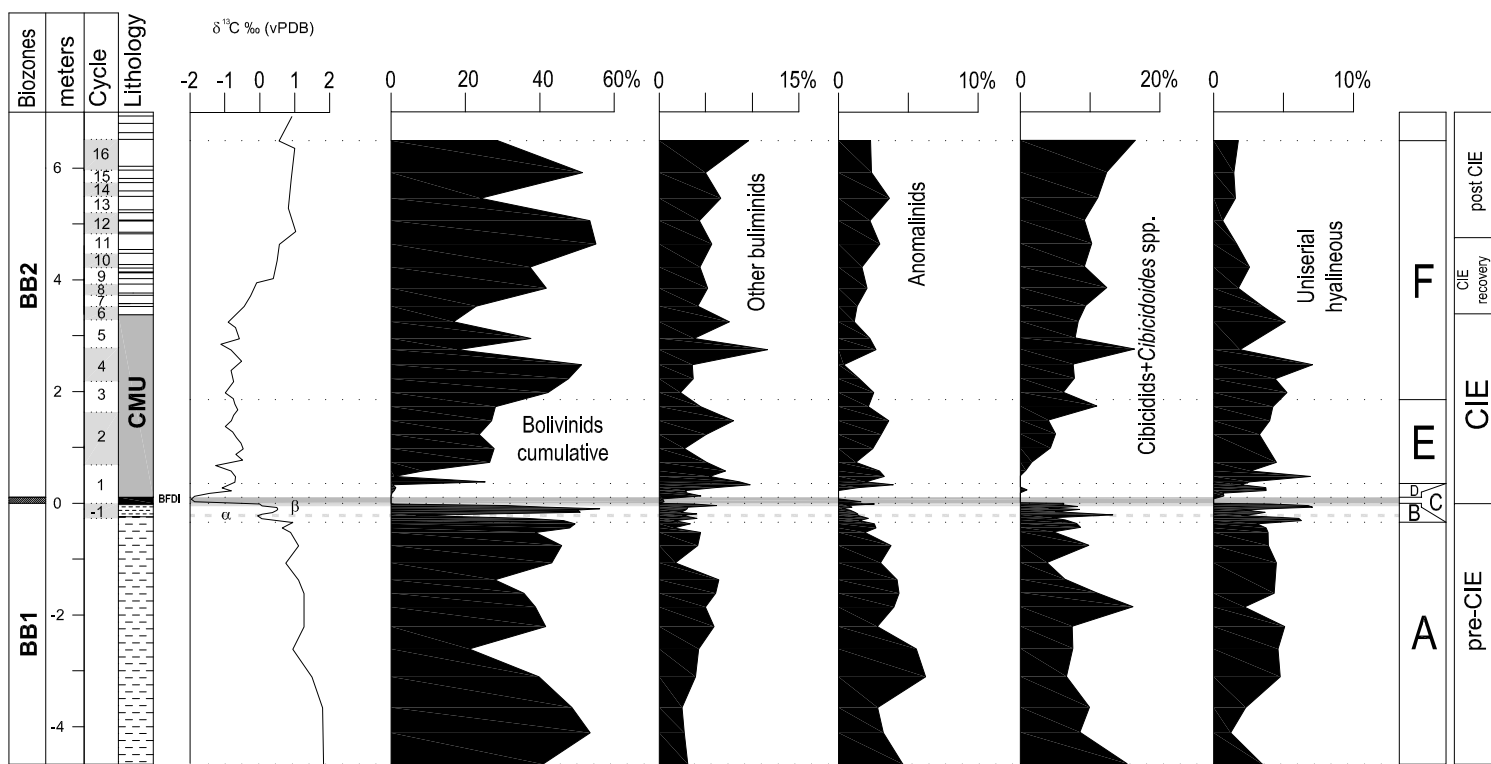


Fig. 6

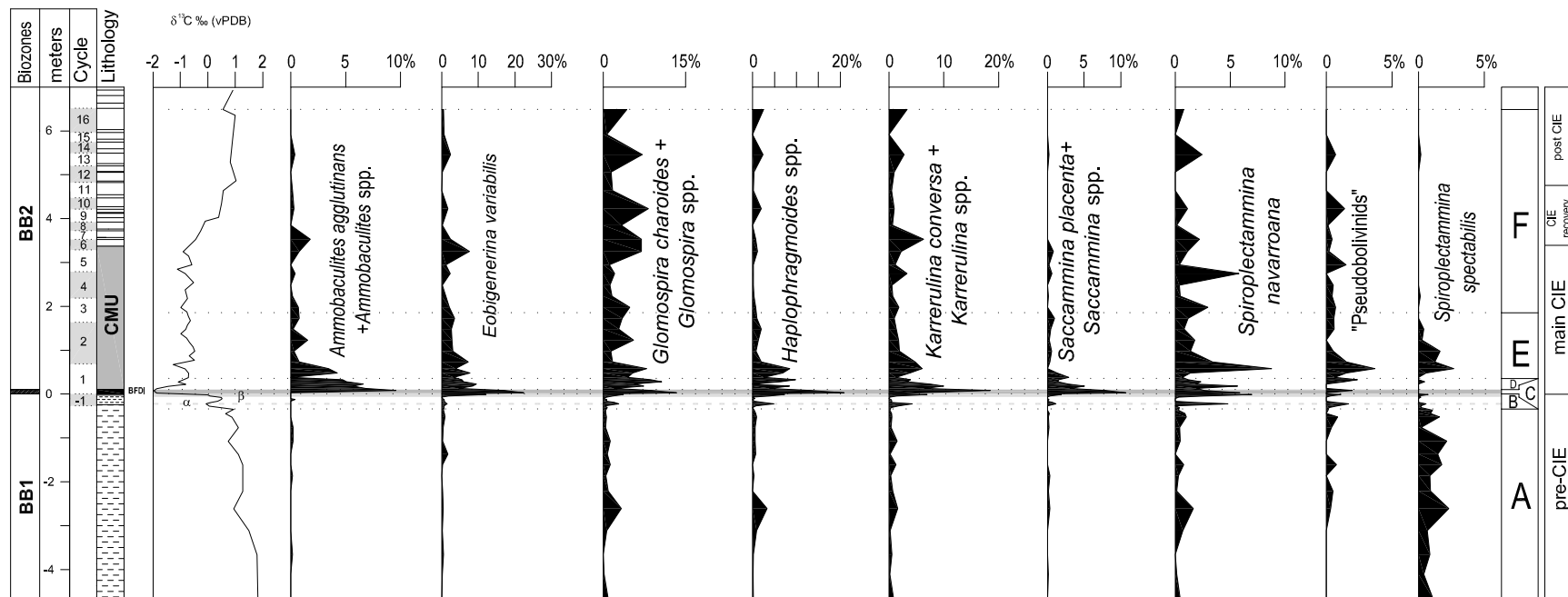
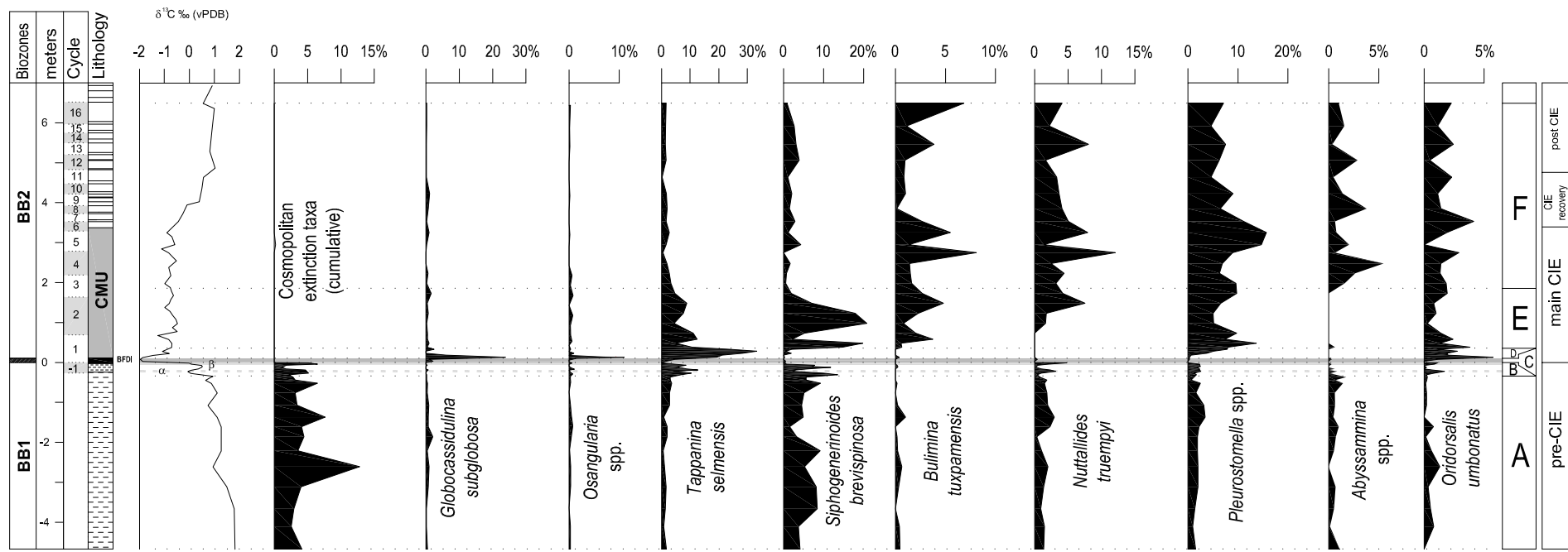


Fig. 7

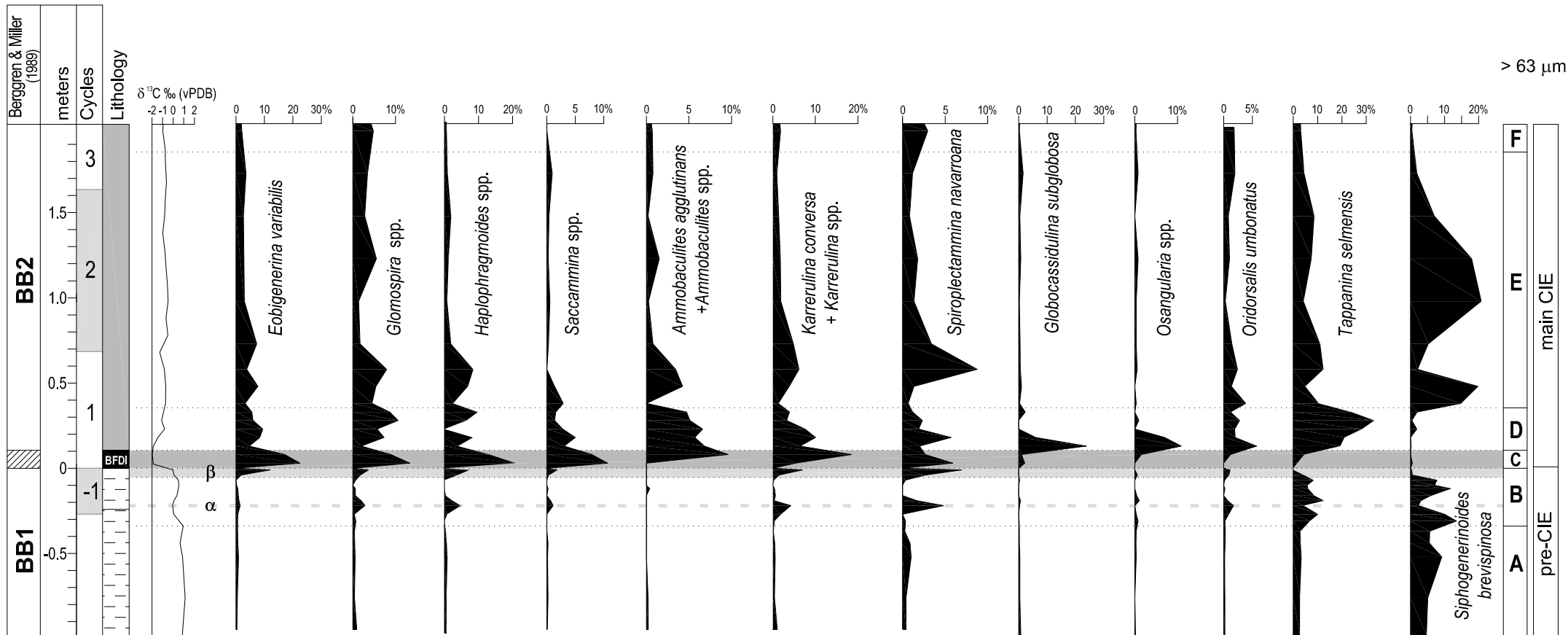


Fig. 8

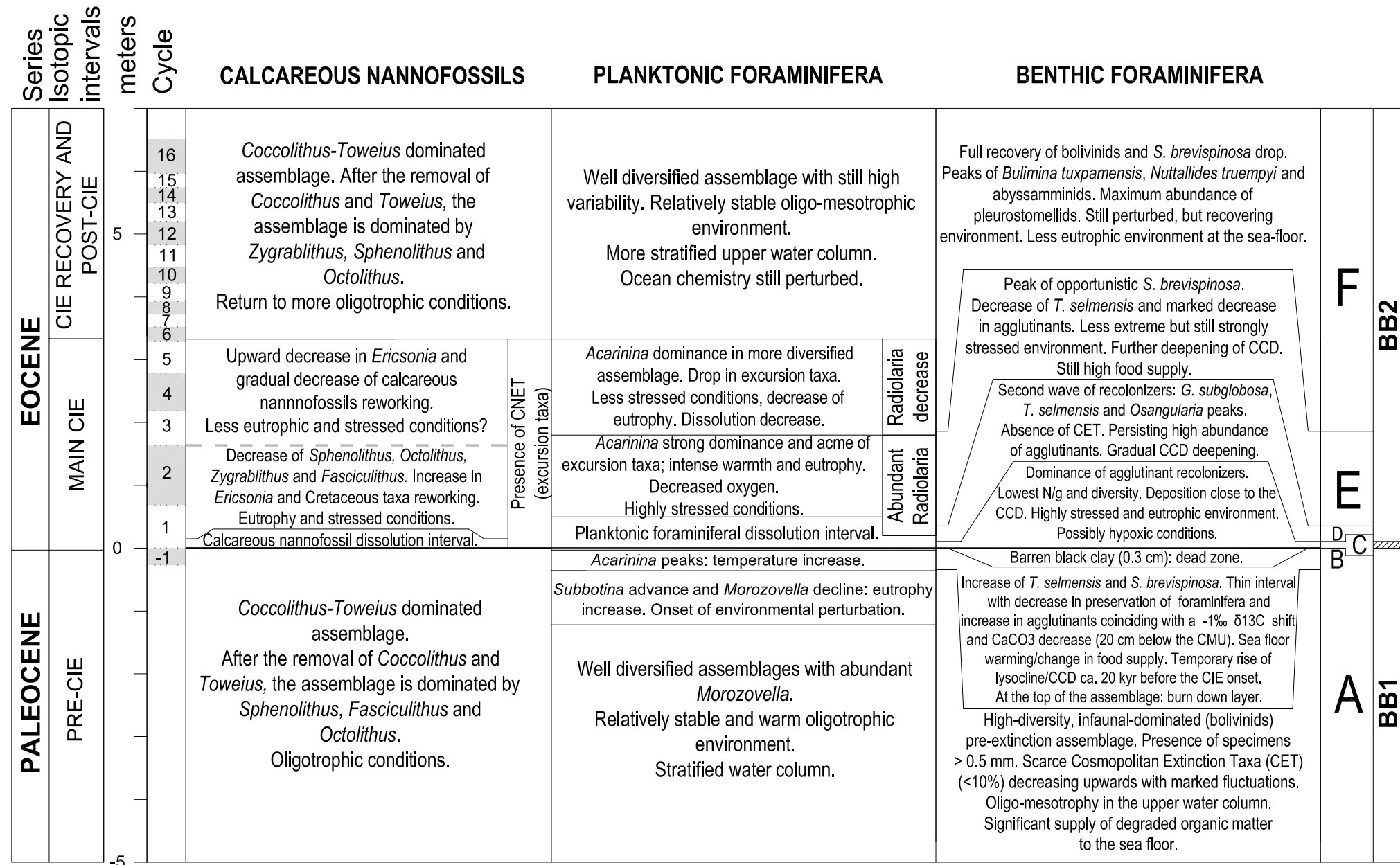


Fig. 9

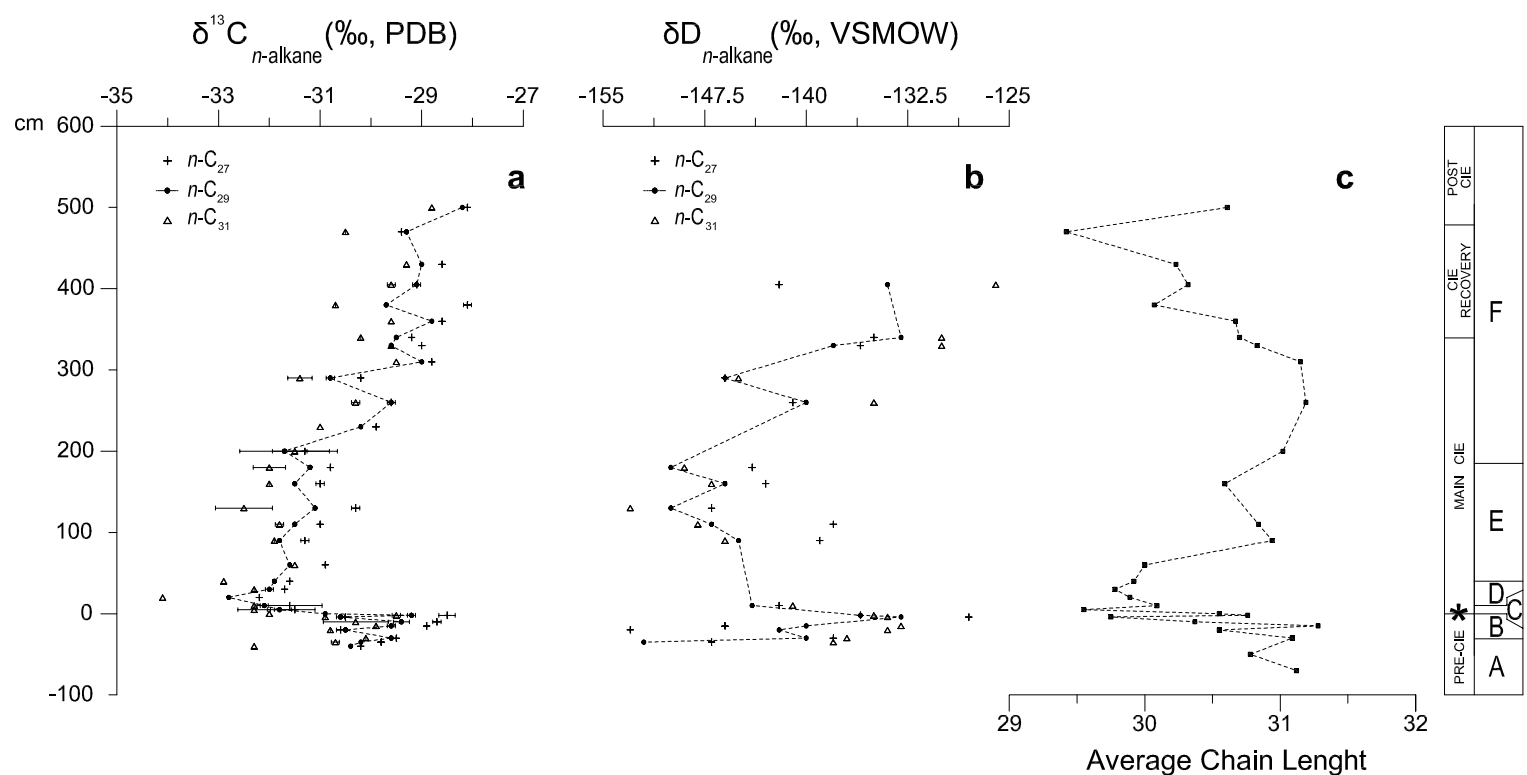
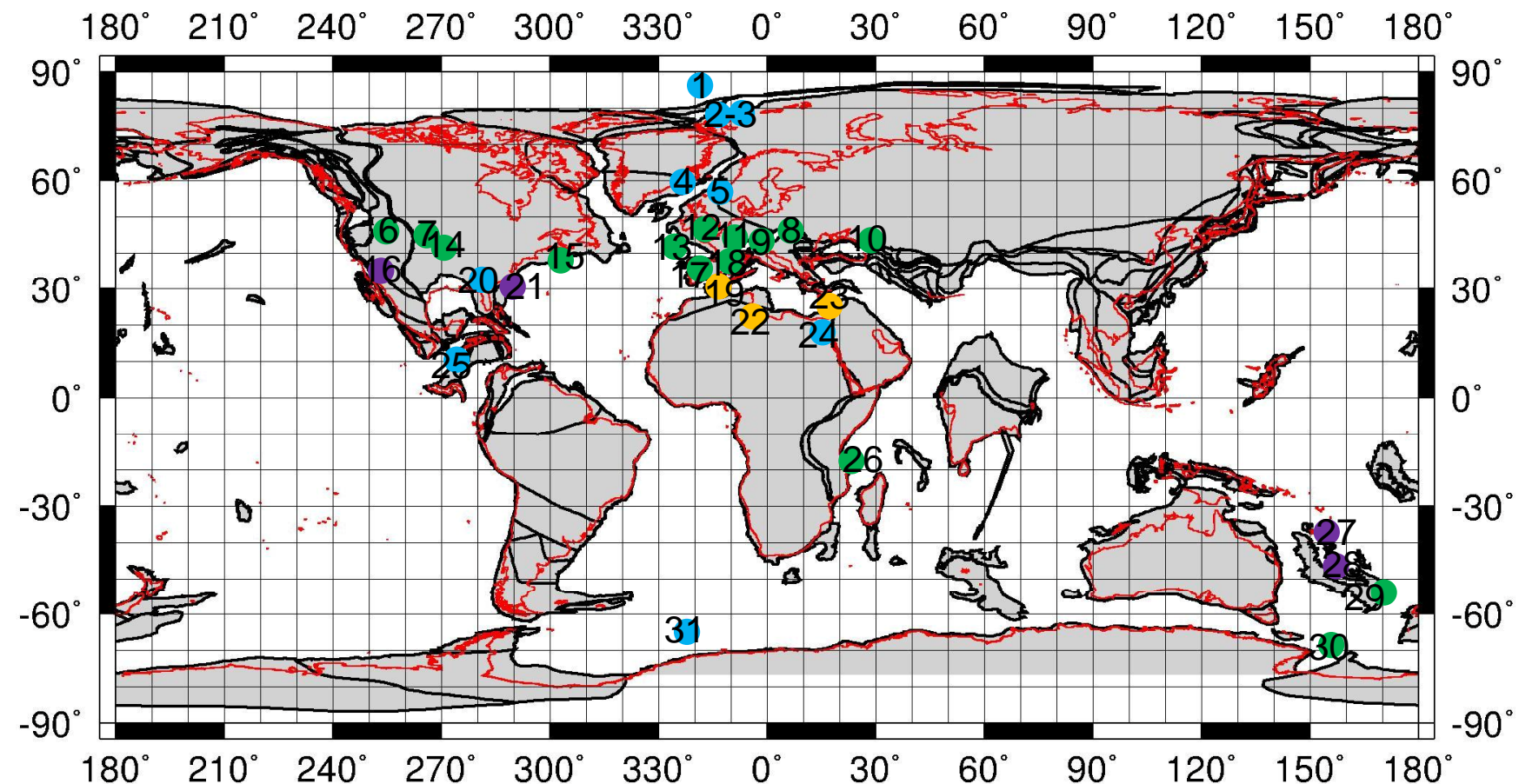


Fig. 10

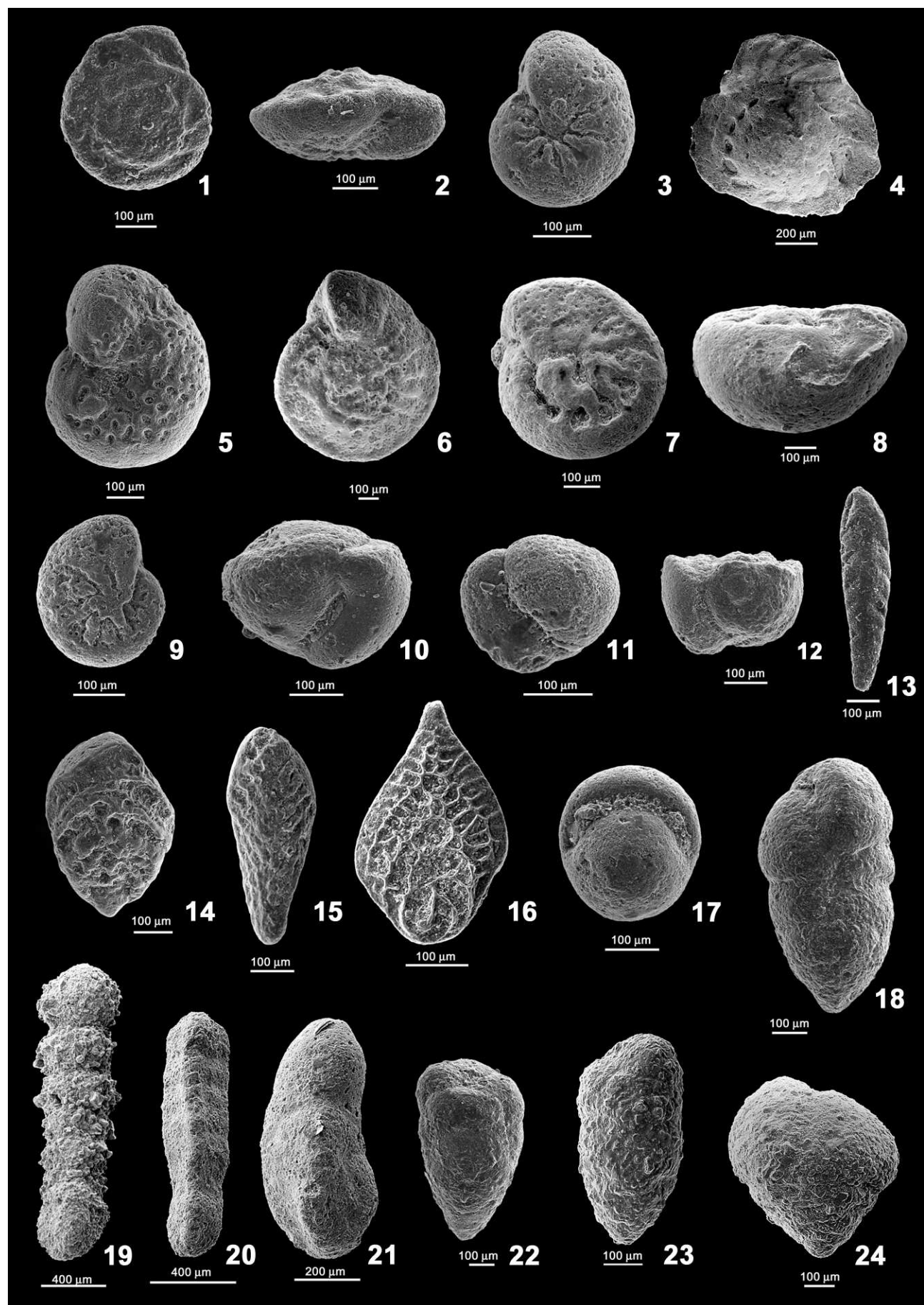


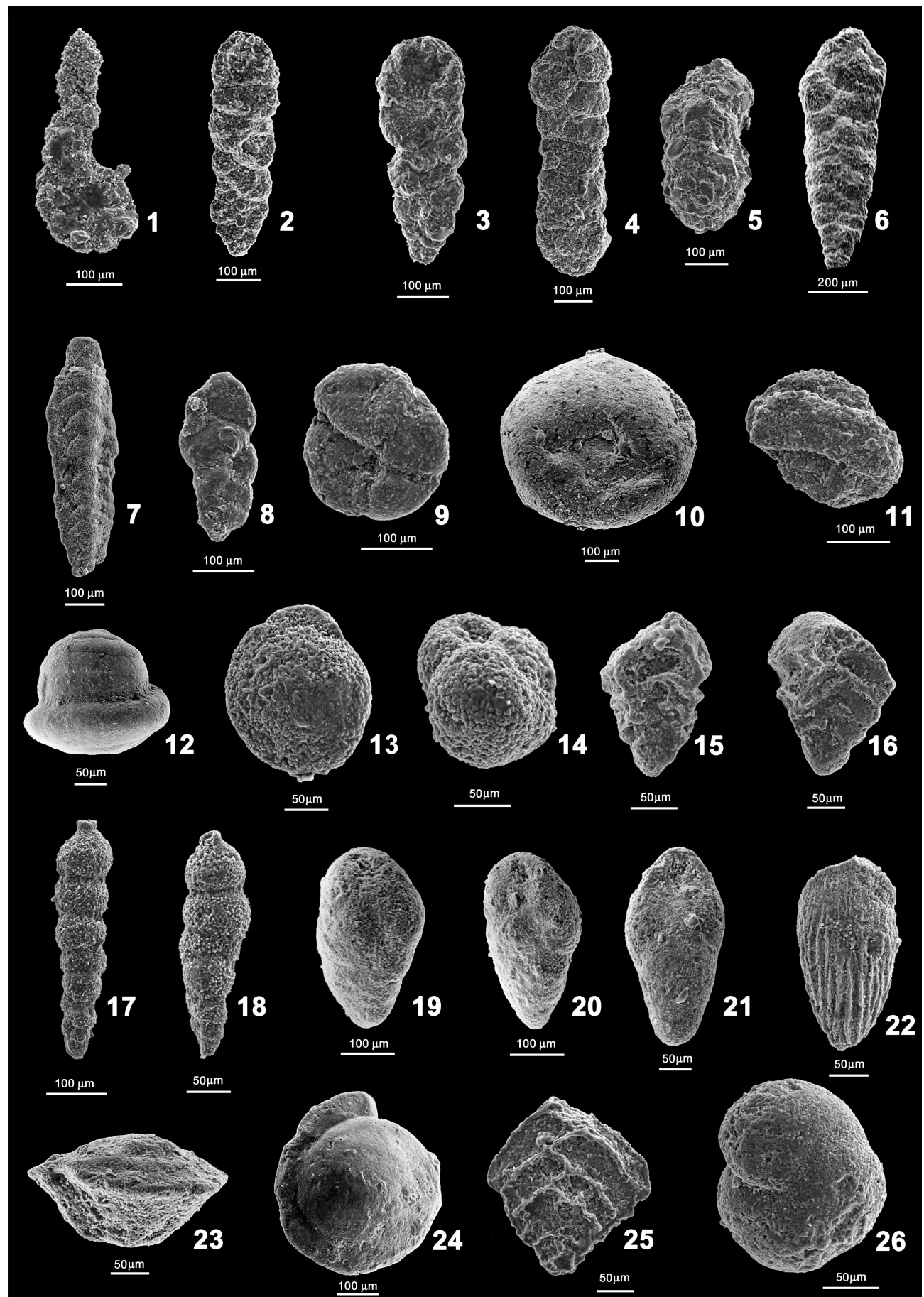
55.0 Ma Reconstruction

Table 1.

<i>Ammobaculites agglutinans</i>	Deep-infaunal recoloniser within the K/Pg boundary clay at Sopelana section (Spain). Adapted to low carbonate availability with high capability for dispersal and colonisation of abiotic substrates. Reported in present day slope high productivity areas.	Gooday, 2003; Gooday et al., 2001; Kuhnt and Kaminski, 1993.
<i>Eobigenerina variabilis</i>	Opportunist, able to live under low oxygen conditions. Dominant in the recovery faunas after the Cretaceous OAE2.	Cetean et al., 2008a,b. See also text.
<i>Globocassidulina subglobosa</i>	Cosmopolitan, highly adaptable, long-ranging opportunistic species. Modern representatives of this species described from a wide variety of environmental settings, including hydrate mounds. Possibly feeding on phytodetritus and reflecting pulsed food supply to the sea floor in oxygenated deepwater settings. Abundant at high southern latitudes where seasonality is extreme. At many sites it appears after the BEE and blooms as an opportunist.	Ernst et al., 2006; Gooday, 1993, 1994; Gupta and Thomas, 2003; Gooday et al., 2008; Ishman and Domack, 1994; Jorissen et al., 2007; Mohan et al., 2011; Murray and Pudsey, 2004; Nomura, 1995; Panieri and Sen Gupta, 2007; Sgarrella et al., 1997; Singh and Gupta, 2004; Suhr et al., 2003; Takata et al., 2010; Takeda and Kaiho, 2007.
<i>Glomospira</i> spp.	Very abundant in the lowermost Eocene at several deep-water locations (the "Glomospira acme"). Generally oligotrophic indicators, they though could be indicative of an abundant supply of terrigenous, refractory organic matter, independent from local primary productivity. Resistant to carbonate dissolution and able to live in environments with low carbonate supply. High ecological tolerance: occur in environments subjected to rapid changes with fluctuating ecological conditions.	Arreguín-Rodríguez et al., 2013, 2014; Galeotti et al., 2004; Kaminski and Gradstein, 2005; Kaminski et al., 1996; Kuhnt and Collins, 1996; Ortiz, 1995; Waśkowska, 2011.
<i>Haplophragmoides</i> spp.	Representatives of the genus pioneer sediments just above anoxic OAE2 black shales in the abyssal North Atlantic that contain no benthic foraminifera. Commonly documented in the basal PETM dissolution interval of shelfal and bathyal Tethyan sections.	Alegret et al., 2005; Ernst et al., 2006; Friedrich, 2009; Kuhnt, 1992; Ortiz, 1995.
<i>Karrerulina conversa</i>	Deep infaunal taxon peaking in the basal PETM at Zumaya (Spain). Resistant to carbonate dissolution and able to live in environments with low carbonate supply. Modern representatives are part of the oligotrophic biofacies on abyssal plains with well-oxygenated bottom and interstitial waters. Recognized in the lowermost Eocene of the Iberia Abyssal Plain.	Bak, 2004; Kaminski and Gradstein, 2005; Kuhnt and Collins, 1996; Kuhnt et al. 2000; Ortiz, 1995; See text.
<i>Oridorsalis umbonatus</i>	Very long-ranging, extant taxon (since the Turonian-Coniacian). Opportunistic lifestyle. Reported both in oligotrophic and eutrophic environments. It may feed on phytodetritus. Shallow infaunal dweller, with very small tests but increased calcification just above the base of the PETM at Site 1263 (Walvis Ridge, SE Atlantic), where it dominates the assemblage.	Foster et al., 2013; Kaiho, 1998; Katz et al., 2003; Gooday, 1993, 1994; Gupta and Thomas, 1999; Gupta et al., 2008; Schmiedl, 1995; Schmiedl and Mackensen, 1997; Thomas and Shackleton, 1996; Wendler et al., 2013.
<i>Osangularia</i> spp.	Opportunistically repopulate the sea floor during short-term re-oxygenation phases of Cretaceous OAEs. Opportunistic phytodetritus feeders during OAE1b, thriving on an enhanced carbon flux to the sea floor and tolerating some degree of oxygen depletion. Peak of <i>Osangularia</i> spp. are reported across the PETM of the Alamedilla section (Spain).	Alegret et al., 2009a; Friedrich, 2009; Friedrich et al., 2005; Holbourn and Kuhnt, 2001; Holbourn et al., 2001. See also text.
<i>Saccammina</i> spp.	Recolonizer within the K/Pg boundary clay of the Sopelana section (Spain). Adapted to low carbonate availability with high capability for dispersal and colonisation of abiotic substrates. Common on modern productive continental margins.	Gooday et al., 2008; Kuhnt and Kaminski, 1993.
<i>Siphogenerinoides brevispinosa</i>	Typical of many open ocean sites in the aftermath of the peak CIE. Opportunist capable to rapidly colonize the sediment when productivity increases during environmental instability. At some locations it bloomed during the PETM and other hyperthermals, at others it had its highest occurrence in the lowermost part of the PETM.	Giusberti et al., 2009; Thomas, 1998, 2003, 2007; Thomas and Shackleton, 1996.
<i>Spiroplectammina navarroana</i>	Minor component of PETM postextinction faunas. At some locations common just after the K/Pg boundary.	Alegret et al., 2003; Alegret et al., 2009b; Ortiz, 1995.
Stilostomellids and pleurostomellids	Infaunal taxa widely distributed in oligotrophic and eutrophic regions with sustained or highly seasonal phytoplankton productivity. Tolerated warm, locally oxygen-depleted, carbonate-corrosive bottom waters, as demonstrated by their survival across the PETM. Across Cretaceous OAEs, pleurostomellids were found within black-shales. Possibly adapted to low-oxygen conditions, or able to rapidly recolonize the sea-floor during brief intervals of reoxygenation.	Coccioni and Galeotti, 1993; Friedrich, 2009; Friedrich et al., 2005; Hayward et al., 2010a,b, 2012; Holbourn and Kuhnt, 2001; Mancin et al., 2013.
<i>Tappanina selmensis</i>	Upper bathyal to outer shelf species in the Campanian and throughout the Paleocene. High-productivity, stress-tolerant and opportunistic species possibly thriving in continuously stressed, dysoxic sea bottom conditions. Common in the deep-sea only just before and especially following the BEE.	Alegret et al., 2009a; Boersma, 1984; D'haenens et al., 2012; Frenzel, 2000; Giusberti et al., 2009; Kuhnt, 1996; Kuhnt and Kaminski, 1996; Stassen et al., 2012a,b, 2015; Steineck and Thomas, 1996; Thomas, 1989, 1990, 1998; Thomas and Shackleton, 1996; van Morkhoven et al., 1986.

Plate 1





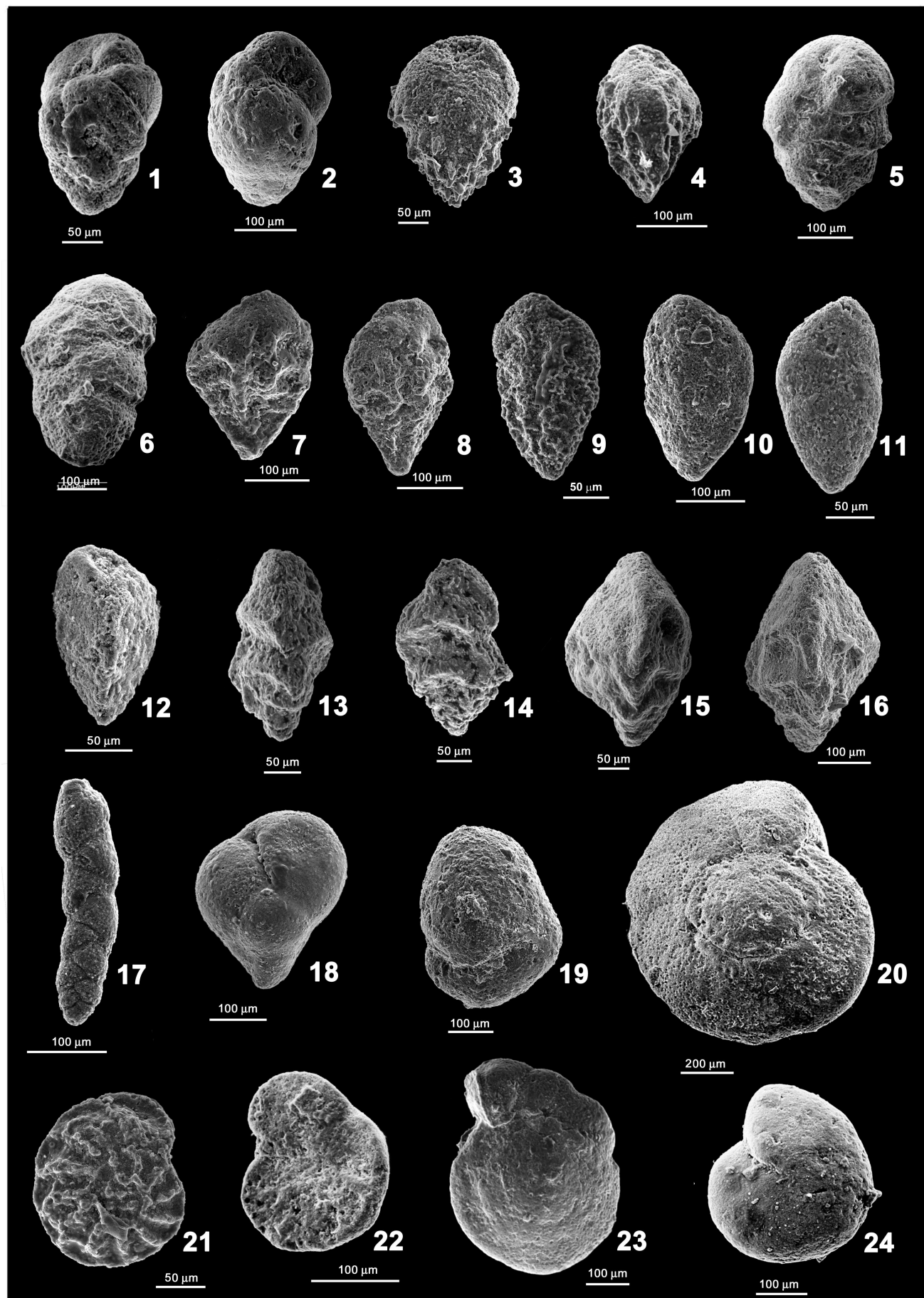


Plate 4

